End moraines and ice-marginal processes of surge-type glaciers

- Brúarjökull and Eyjabakkajökull, Iceland

Ívar Örn Benediktsson

"*Work expands so as to fill the time available for its completion*."
Cyril Northcote Parkinson (1909-1993)

End moraines and ice-marginal processes of surge-type glaciers

- Brúarjökull and Eyjabakkajökull, Iceland

Ívar Örn Benediktsson

A thesis submitted to the Faculty of Earth Sciences,
University of Iceland for the degree of Doctor of Philosophy in Geology

Thesis supervisors

Professor Ólafur Ingólfsson
Faculty of Earth Sciences, University of Iceland

Associate professor Kurt H. Kjær
Natural History Museum of Denmark, University of Copenhagen

Doctoral committee

Professor Ólafur Ingólfsson
Faculty of Earth Sciences, University of Iceland

Associate professor Kurt H. Kjær
Natural History Museum of Denmark, University of Copenhagen

Dr. Hreggviður Norðdahl, research scientist
Institute of Earth Sciences, University of Iceland

Opponents

Dr. Emrys Phillips, principal research scientist
British Geological Survey, Edinburgh

Professor Arjen P. Stroeven
Department of Physical Geography and Quaternary Geology,
Stockholm University

End moraines and ice-marginal processes of surge-type glaciers -
Brúarjökull and Eyjabakkajökull, Iceland

A thesis submitted to the Faculty of Earth Sciences, University of Iceland for the degree of Doctor of Philosophy in Geology

Faculty of Earth Sciences
School of Engineering and Natural Sciences
University of Iceland
Askja, Sturlugata 7
IS-101 Reykjavík
Iceland

ISBN 978-9979-9914-7-2

Printed by Leturprent
Reykjavík, December 2009

Contents

Preface

This thesis is the result of four years of research at the Institute of Earth Sciences, University of Iceland. Initially, investigations were planned on the end moraines of three surge-type glaciers in Iceland; Brúarjökull in 2005, Eyjabakkajökull in 2006 and 2007, and Múlajökull in 2008. Because the end moraines at Eyjabakkajökull turned out to be a larger research task than initially thought, the third field season was added in 2008. Consequently, fieldwork was not carried out on the end moraines at Múlajökull for this thesis.

The thesis is based on the four papers listed below as Appendices I-IV. The papers are either published or 'in press' in peer-reviewed international journals, and reproduced with the permission of Elsevier Science Ltd. and John Wiley and Sons, Inc. In the following, the papers are referred to by their roman numerals.

Appendix I

Kjær, K.H., Larsen, E., van der Meer, J.J.M., Ingólfsson, Ó., Benediktsson, Í.Ö., Knudsen, C.G., Schomacker, A., 2006. Subglacial decoupling at the sediment/bedrock interface: a new mechanism for rapid flowing ice. *Quaternary Science Reviews 25*, 2704-2712.

Appendix II

Benediktsson, Í.Ö., Möller, P., Ingólfsson, Ó., van der Meer, J.J.M., Kjær, K.H., Krüger, J., 2008. Instantaneous end moraine and sediment wedge formation during the 1890 glacier surge of Brúarjökull, Iceland. *Quaternary Science Reviews 27*, 209-234.

Appendix III

Benediktsson, Í.Ö., Ingólfsson, Ó., Schomacker, A., Kjær, K.H., (2009). Formation of submarginal and proglacial end moraines: implications of ice-flow mechanism during the 1963-64 surge of Brúarjökull, Iceland. *Boreas 38*, 440-457.

Appendix IV

Benediktsson, Í.Ö., Schomacker, A., Lokrantz, H., Ingólfsson, Ó., (in press). The 1890 surge end moraine at Eyjabakkajökull, Iceland: a re-assessment of a classic glaciotectonic locality. *Quaternary Science Reviews (2009)*, doi:10.1016/j.quascirev.2009.10.004.

Abstract

The present thesis describes the end moraines and ice-marginal processes of two surge-type glaciers in Iceland, Brúarjökull and Eyjabakkajökull. The aim of the research was to increase current understanding of fast flowing ice, and to identify causal links between glaciotectonics and glaciodynamics.

The results show that a mosaic of coupled and decoupled spots existed under the glaciers during surges, leading to variations in ice-flow mechanism and ice-marginal formations. At Brúarjökull, decoupling at the sediment/bedrock interface was the dominating mechanism behind the rapid ice-flow. This resulted in downglacier dislocation of the sediment and the formation of marginal sediment wedges on which proglacial, single-crested, and fold-dominated moraines formed instantaneously on the last day of the surge. Where deformation of the bed contributed most to the increased ice flow, the end moraines formed by thrusting in the submarginal zone.

The end moraines at Eyjabakkajökull are characterised by lateral variability in morphology and internal architecture. Large moraines with multiple symmetric crests are composed of overturned and overthrusted anticlines, while moraines with multiple asymmetric crests indicate imbricate thrust sheets. Both types of moraines formed where the foreland wedge was thick and the subglacial ice-flow mechanism was most likely dominated by deformation of the bed. In contrast, small, single-crested moraines formed in relation to sediment/bedrock decoupling where the foreland wedge was thin. The time frame for the formation of the end moraines was two to six days.

This study implies that surge end moraines are integrally related to the mechanism of ice flow. Future studies should, therefore, not only focus on the internal architecture of the moraines but also on the subglacial bed for relating their structural evolution to the glacier dynamics. Such an approach would increase current understanding of the dynamics and marginal formations of fast flowing ice masses, whether they are modern or ancient surge-type glaciers or ice streams.

Ágrip (abstract in Icelandic)

Í ritgerð þessari er fjallað um rannsóknir á jökulgörðum tveggja framhlaupsjökla á Íslandi, Brúarjökuls og Eyjabakkajökuls. Markmið rannsóknanna var að auka þekkingu á hegðun hraðfara jökla og kanna tengsl milli hreyfinga þeirra og aflögunar setlaga. Niðurstöður rannsóknanna sýna að stamir og sleipir blettir eru í undirlagi jöklanna við framhlaup. Þessir blettir hafa áhrif á flæði jöklanna og myndanir við jökuljaðrana. Stamir blettir myndast þar sem vatnsþrýstingur í setlögum undir jöklunum er lágur, en það gerist einkum þar sem grófkornótt setlög mynda meginhluta undirlagsins. Á slíkum blettum myndast spenna á mótum íss og sets, sem leiðir til aflögunar setlaga undir jöklunum. Sú aflögun á stóran þátt í skriði jöklanna. Jökulgarðar á þessum svæðum eru myndaðir úr setfleygum sem hafa þrýst upp undir jökuljaðrinum. Sleipir blettir myndast þar sem vatnsþrýstingur er hár í fínkornóttum setlögum undir jöklunum. Afleiðing þessa er að jöklarnir og undirlag þeirra lyftast frá berggrunninum við framhlaup. Þetta stuðluði að miklum skriðhraða í framhlaupum Brúarjökuls. Setið sem fluttist áfram með jöklinum þjappaðist saman og myndaði setfleyg undir sporðinum. Á ytri og hærri enda setfleygsins mynduðust einkamba jökulgarðar á síðasta degi framhlaupsins. Slíkir jökulgarðar einkennast af rótföstum fellingum sem eru skornar af sig- og þrýstimisgengjum.

Lögun og innri bygging jökulgarðanna við Eyjabakkajökul er breytileg. Stórir jökulgarðar með fjölda samhverfra kamba, eru myndaðir úr yfirsnúnum og brotnum fellingum. Jökulgarðar með fjölda ósamhverfra kamba, eru úr stöfluðum setfleygum. Þessir jökulgarðar myndast þar sem setlög voru þykk og skriðhraði jökulsins réðist af aflögun undirlagsins. Smærri, einkamba jökulgarðar mynduðust á ytri enda setfleygs þar sem setlög voru þunn og vatnsþrýstingur hár. Jökulgarðarnir við Eyjabakkajökul mynduðust á tveimur til sex dögum.

Þessi rannsókn sýnir að myndun jökulgarða er nátengd ferlum í undirlagi jöklanna á meðan á framhlaupum stendur. Breytileiki í lögun og innri byggingu orsakast af eiginleikum setlaga og skriðferlum jöklanna. Rannsóknir á jökulgörðum ættu ekki eingöngu að beinast að innri byggingu heldur einnig að undirlagi jöklanna svo tengja megi myndun garðanna við hreyfingar jöklanna. Slík nálgun myndi auka skilning á virkni og jaðarmyndunum hraðfara jökla, hvort sem um væri að ræða gamla eða samtíma framhlaupsjökla eða ísstrauma.

Acknowledgements

There are many people who have helped me along the way during the past four years. First of all, I want to thank my main supervisor, Ólafur Ingólfsson, for excellent guidance, support, and friendship, and for always deliberating carefully all sorts of professional, practical and financial problems. I'm also indebted to Ólafur for giving me the opportunity to teach and supervise undergraduate students at the University of Iceland and, indirectly, at the Agricultural University of Iceland. I thank my other supervisor, Kurt H. Kjær, for great support and constructive criticism, and for providing accommodation at the Geological Museum during my visits to Copenhagen. Thanks also to Hreggviður Norðdahl for keeping track of my research and for always being friendly and positive on my behalf.

Various funds and intitutions generously provided financial support for the fieldwork at Brúarjökull and Eyjabakkajökull. These include: the University of Iceland Research Fund, the Icelandic Research Council (RANNÍS), the Swedish National Research Council (VR), the Danish National Research Council, the Energy Research Fund of Landsvirkjun, the Royal Physiographic Society in Lund, the Crafoord Foundation, the Research Fund of Fljótsdalshreppur municipality, the Royal Swedish Academy of Sciences and Christian and Ottilia Brorsons travel fund for young scientists. Scholarships from the University of Iceland Research Fund, the Icelandic Research Fund for Graduate Students, and Landsvirkjun are also gratefully acknowledged. Thanks are furthermore due to the former Faculty of Science and the University of Iceland Research Fund for conference travel grants.

Many thanks to all the people who helped me in the field with the cleaning of big and small sections, measuring structures, running the Georadar, surveying cross-profiles, carrying equipment and just for being great company. These people are: Anders Schomacker, Ólafur Ingólfsson, Johannes Krüger, Kurt H. Kjær, Per Möller, Jaap van der Meer, Carita Grindvik Knudsen, Ida H.E.O. Jönsson, Lilja Rún Bjarnadóttir, Eiliv Larsen, Svante Björck, Louise Ravn, Silvana Correa Kjær, Hanna Lokrantz, Mark Johnson, Torbjörn Andersson, Amanda Ferguson, Eygló Ólafsdóttir, Skafti Brynjólfsson, Susie Ebmeier, Antje Herbrich, and Jón Björn Ólafsson. Without your help this research would not have been possible. Thanks are also due to Rúnar Ingi Hjartarson, Þórir Gíslason, Björn Oddson, and Jón Heiðar Frímannsson for logistical assistance and excellent monster-jeep driving in an absolutely hopeless terrain on the way to Brúarjökull and Eyjabakkajökull. I'm also grateful to the people at the University of Copenhagen and Lund University for a warm and a stimulating atmosphere during my visits there. Special thanks to Anders for great collaboration and friendship through the years.

Many good friends and colleagues at the Institute of Earth Sciences stimulated my research and enriched my life as a student through all kinds of chats and discussions. A few of them are Anders, Ólafur, Hreggviður, Friðgeir, Gabrielle, Esther, Hrafnhildur, Bergrún, Sæmundur, Skafti, Eygló, Bjarki, Sverrir, Ulf, Kristín, Sædís, Eydís, Guðrún, Jón and Leifur. My apologies to others whose names should have been included. Thanks to my friend, Davíð, for being interested in what I do, and for asking all sorts of questions that are both necessary and challenging, e.g: "Why is this important? Why should a part of my taxes be used to fund your research? Are there any breakthrough results in your thesis?"

Thanks to Anders Schomacker, Mark Johnson, Svanhildur Þorsteinsdóttir and Þorsteinn Sæmundsson for comments on the text and help with the layout.

I'm indebted to my parents-in-law, Þorsteinn and Guðný, for allowing me and my wife, Svanhildur, with our son, Þorsteinn Jökull, to live in their basement apartment, but also for babysitting, frequent dinner invitations and for being such good and supportive company just one floor above.

I am grateful to my mother, Friðgerður, and my late father, Benedikt Rúnar, for endless support in everything I do, but also for introducing me to the wonderful Icelandic nature when I was a child, especially during frequent visits to Skaftafell with all its glaciers and natural wonders. Thanks, mum, also for always being willing to help with what you can.

And Svanhildur – what can I say and where to begin? Thanks for being my best friend, for criticizing and encouraging me when needed, and calming me down and making me laugh when I was stressed, for letting me know when I was working too much, for proof-reading this thesis, for your endless care, and last but not least, for taking such good care of Þorsteinn Jökull, who has brought so much happiness into our lives. I love you both!

1 Introduction

1.1 Background

Glaciotectonic end moraines form at glacier margins during sustained advances, still-stands or small (winter) re-advances. They display wide varieties of morphologies, sediments and architectures, and are reliable indicators of sedimentary and glaciotectonic processes at work in glacial environments. They are typically formed due to deformation of proglacial or submarginal sediments, chiefly as a result of ice pushing, thrusting or gravity spreading, and signify the process of glaciotectonism beneath, at, or in front of ice margins (Aber et al., 1989; van der Wateren 1995a, b; Benn and Evans, 1998; Bennett, 2001; Aber and Ber, 2007). Glaciotectonism is an essential component of glacier dynamics and consequently, studies of glaciotectonic end moraines provide important information on fluctuations of ice margins, ice-flow mechanism, sediment shear strength, basal drainage, water pressure and hydrofracturing, subglacial and ice-marginal stresses, thermal regime of the glacier and the foreland, sediment transport, history of deformation events, and the overall interplay of glaciers with their forelands (Boulton and Hindmarsh, 1987; van der Wateren 1995a, b; Bennett, 2001; McCarrol and Rijsdijk, 2003; Motyka and Echelmeyer, 2003; Pedersen 2005; Kuriger et al., 2006; Phillips et al., 2008; Roberts et al., 2009). Consequently, end moraines are among the most important landforms of glacial landsystems as they outline the configuration of glaciers and provide valuable information for palaeoglaciological reconstructions.

End moraines at contemporary glacier margins have increasingly been investigated to serve as analogues to Pleistocene end moraines. Most of this research has concentrated on end moraines of non-surging glaciers (e.g. Kälin, 1971; Humlum, 1985; Krüger, 1985, 1993, 1994, 1996; Boulton, 1986; Shakesby, 1989; Hambrey and Huddart, 1995; Möller, 1995; Matthews et al., 1995; Bennett et al., 1996; Winkler and Nesje, 1999; Lyså and Lønne, 2001; Krüger et al., 2002, 2010; Motyka and Echelmeyer, 2003; Kuriger et al., 2006), but end moraines of surging glaciers, which periodically flow at increased rates, have attracted increased attention in recent years as a means of gaining information on the behaviour and mechanics of fast-flowing ice (e.g. Sharp 1985a; Croot, 1987, 1988a, b; Boulton et al., 1996, 1999; Huddart and Hambrey, 1996; Lønne and Lauritsen, 1996; Hart and Watts, 1997; Bennett et al., 1999, 2004a, b; Roberts et al., 2009). These studies have primarily focused on the structural properties of the moraines and the evolution of deformation within them, and thus yielded a large variety of models to explain glaciotectonic processes. However, less focus has been on finding causal links between the glaciotectonics and the dynamics of surging glaciers. This relation remains to be fully understood, but is essential for our understanding of fast-flowing glaciers. Many outlets of Pleistocene ice sheets are considered to have been fast flowing, either as temporary surging glaciers or ice streams with more constant fast flow, depositing end moraines that provide information on the dynamics of the former ice sheets (e.g. Bennett, 2003; van der Wateren, 2003; Stokes and Clark, 2001; Houmark-Nielsen and Kjær, 2003; Evans et al., 1999; 2008; Jennings, 2006). However, the interpretation of Pleistocene end moraines depends on the modern analogues used. Surging glaciers are thought to provide a suitable analogue to the fast-flowing terrestrial ice streams that controlled the discharge and regulated the stability and configuration of Pleistocene ice sheets (Gripp, 1929; Bennett, 2001; Stokes and Clark, 2001; Evans and Rea, 2003; Dowdeswell et al., 2004; Rignot and Kanagaratnam, 2006). Similarly, end moraines of surging glaciers should provide the best analogues to end moraines and ice-marginal sediment wedges of fast-flowing Pleistocene ice masses. Furthermore, end moraines of surge-type glaciers may also provide a small-scale analogue to ice-marginal processes and landforms of modern marine-based ice streams with inaccessible terminal zones. Increased understanding of the dynamics of modern fast-flowing ice is therefore a key to reconstructing palaeo-ice sheets.

1.2 Research aims

The Brúarjökull and Eyjabakkajökull surge-type glaciers in Iceland were selected for this study as their surges since the 19th century caused significant deformation of ice-marginal and proglacial sediments, resulting in prominent end moraine complexes in their forefields. The surges of Brúarjökull and Eyjabakkajökull were not described or studied in detail when they were in progress, thereby leaving open questions about the mechanism of ice flow, the processes of erosion and deposition, and the formation of landforms. The main purpose of this study is to investigate the end moraines and other ice-marginal features associated with the surges of Brúarjökull and Eyjabakkajökull, with the aim of understanding the processes responsible for their formation and their relation to surge dynamics. Important parameters, which are often unknown in the studies of end moraines, are known for the surges of Brúarjökull and Eyjabakkajökull, facilitating interpretation of landforms and structures resulting from the surges. These include the duration of the active and quiescent phases of the surge cycle, the ice-flow velocity and the extent of the surge advances, the geometry of the surging ice front (length, gradient, height), and the original thickness of the foreland wedge.

Brúarjökull and Eyjabakkajökull are highly different in dynamics, geometry and topographic setting. Brúarjökull covers an area of 1500 km2 and terminates with a 55 km long and unconstrained glacier margin. It advances 8-10 km during its surges with ice-flow velocities of ~120 m/day. Eyjabakkajökull covers about 110 km2, is constrained in a valley with a 2-3 km long margin, and advances 0.6-2.8 km during surges with ice-flow velocities of ~30 m/day (Björnsson et al., 2003). The glaciers are exposed to similar climate, have advanced into similar type of proglacial sediments, and the largest surge advances occurred during the same year (1890). It is, therefore, interesting to compare the end moraines produced by these two different glaciers because climatic forces and foreland properties are similar and can therefore be excluded as factors controlling the difference in architecture and structural evolution.

Despite recent research on surging-glacier end moraines, some uncertainties remain about their characteristics and the conditions under which they form. These include, (i) what characterizes their morphology and internal architecture?; (ii) what causes lateral variation in morphology and internal architecture?; (iii) how does thickness and composition of the foreland wedge affect the end-moraine architecture?; (iv) why do surging glaciers couple to their forelands to initiate end moraine formation?; and (v) what is the time frame for the end moraine formation? This study contributes to a better understanding of these uncertainties.

2 Study areas

Fieldwork was carried out in the forefield of two surge-type glaciers in Iceland; Brúarjökull and Eyjabakkajökull (Fig. 1), both of which are located at the northern margin of the Vatnajökull ice cap. The Brúarjökull study involves mainly one field season in 2005 although data from two previous field seasons are also included. Three additional field seasons were spent at Eyjabakkajökull in 2006-2008. The duration of each field season was 3-5 weeks.

2.1 Brúarjökull

Brúarjökull is a surge-type outlet glacier in the northern part of the Vatnajökull ice cap in Iceland (Fig. 1). It descends from about 1500 m a.s.l. to 600 m a.s.l. where it terminates with a 55-km long ice margin (Björnsson et al., 1998; Fig. 1). Known historical surges of Brúarjökull occurred in 1625, ~1730, ~1775(?), 1810, 1890, and 1963-64. This gives a surge cycle of 80-100 years, within which the duration of the advance of the active phase is only 2-3 months (Eythorsson 1963, 1964; Thorarinsson 1964, 1969; Björnsson et al. 2003). During the last two surges, the maximum advance of Brúarjökull in the central forefield was 10 and 9 km, respectively, with maximum ice-flow velocities of at least 100-120 m/day (Kjerúlf 1962; Thorarinsson 1964, 1969; Guðmundsson et al. 1996).

The forefield of Brúarjökull is glacially streamlined with an up to 6-7 m thick sediment

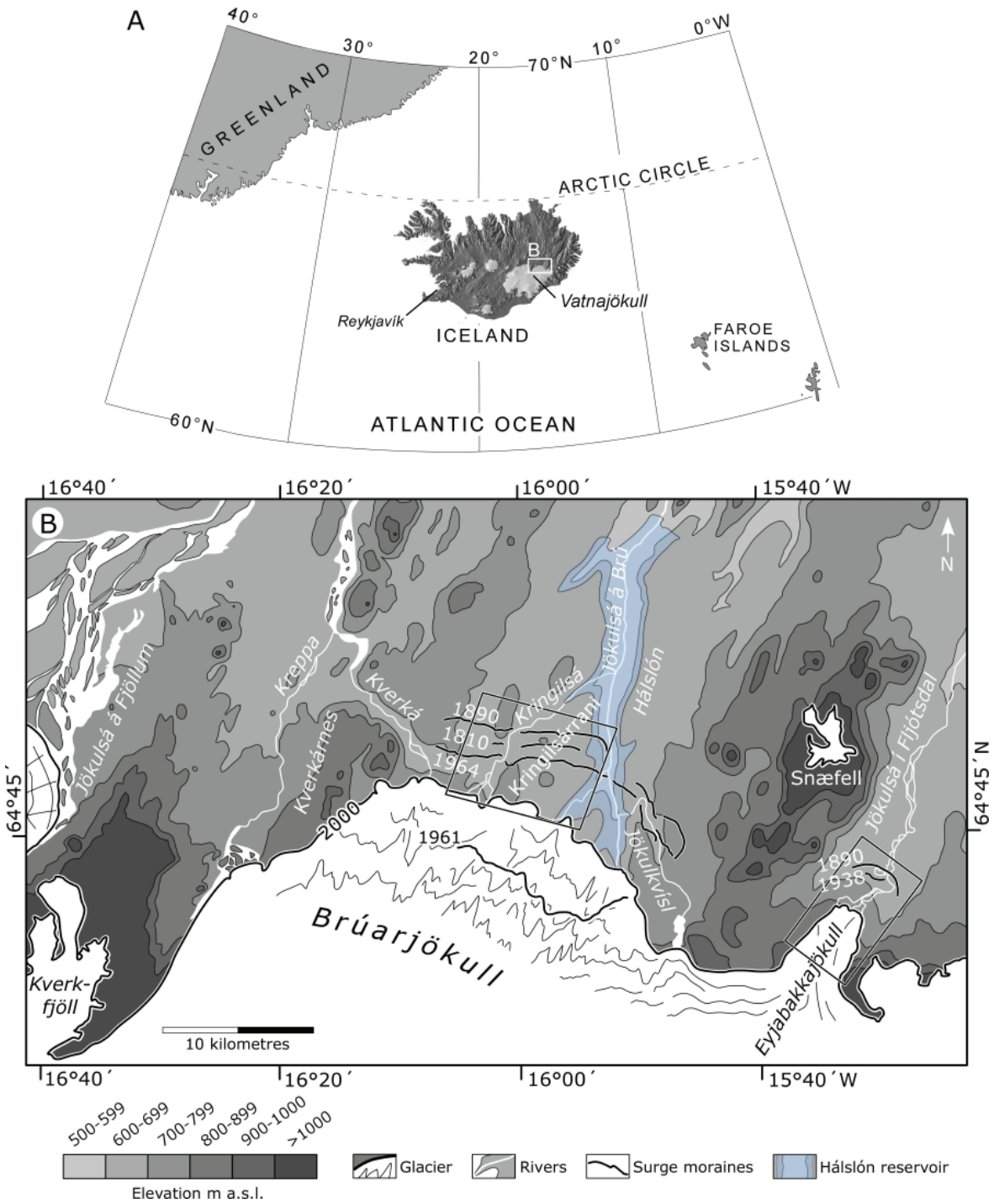

Figure 1. A) The study areas are located at the north-east margin of the Vatnajökull ice cap in Iceland. B) Location of Brúarjökull and Eyjabakkajökull. The squares indicate the main study areas shown on Figs. 2 and 3.

sequence in between widely spaced and elongated bedrock hills culminating at 700-750 m a.s.l. (Fig. 2). The most prominent features of the surging-glacier landsystem are end-moraine ridges, ice-cored and ice-free hummocky moraines, eskers, concertina eskers, flutes, drumlins, and crevasse-squeeze ridges (Evans & Rea 1999, 2003; Kjær et al. 2008; Schomacker et al. 2006; Bjarnadóttir 2007; Evans et al. 2007; Schomacker 2007; Schomacker & Kjær 2007; Papers I-III). At present, ice movement in the marginal 1-2 km of Brúarjökull is negligible; the snout is rapidly retreating and downwasting, and covered in places by a thin sediment

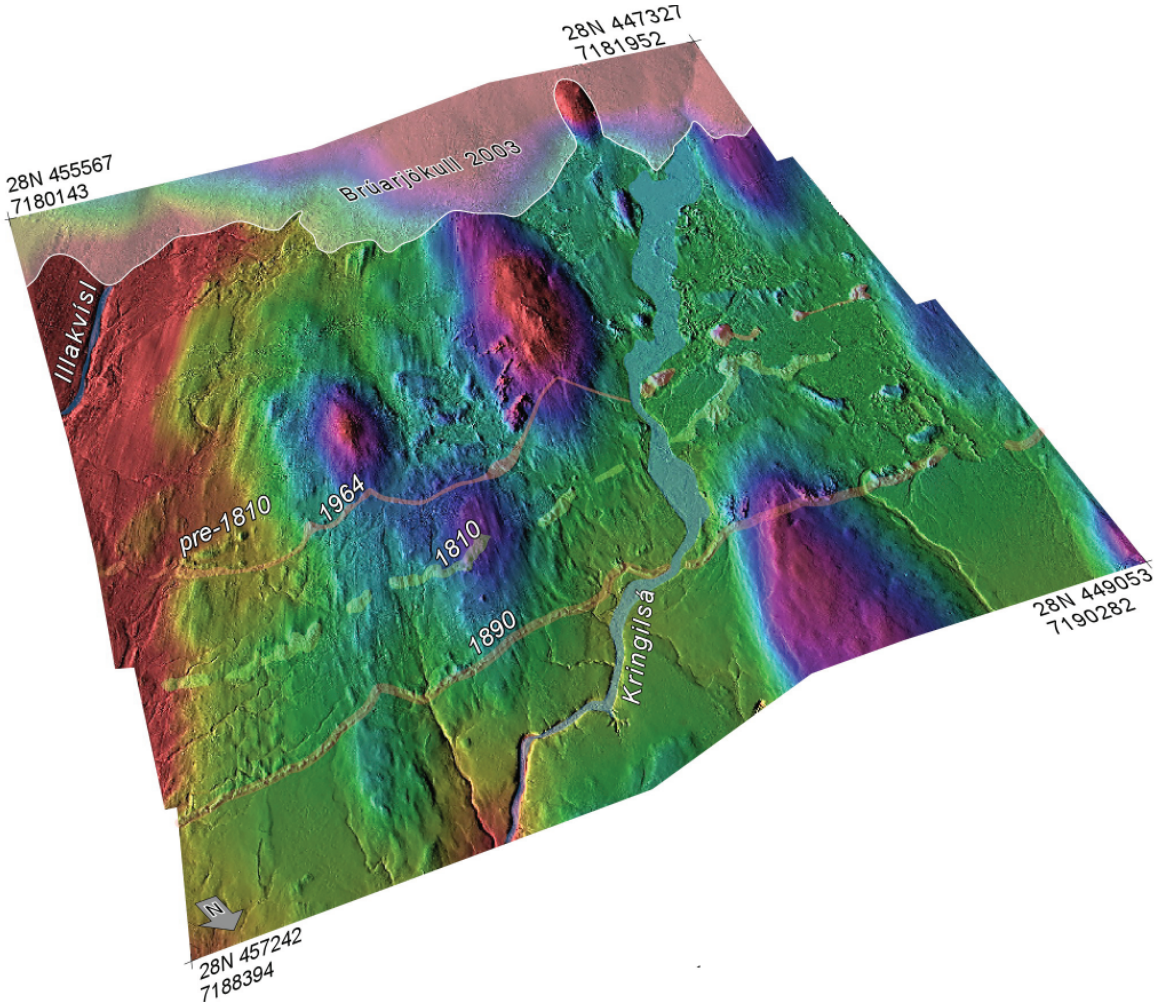

Figure 2. The forefield of the surge-type glacier Brúarjökull. Digital elevation model, generated from stereopairs of aerial photographs recorded in 2003, visualized as a Terrain Shade Relief model. The ice-marginal positions of the most recent surges are indicated. See Fig. 1 for location. Modified from Papers I-III.

layer from disintegrating crevasse-squeeze ridges and debris bands emerging from the ice (Evans & Rea 1999, 2003; Schomacker 2007; Schomacker & Kjær 2007; Papers I-III).

Circular depressions, ice-cored peat mounds and frost-crack polygons occur immediately outside the 1890 end moraine. The depressions are surrounded by rim-ridges, which are up to 0.8 m high and 10-15 m in diameter, and contain ponds or minor lakes. They have been interpreted as periglacial landforms and are thought to represent collapsed palsas, an indicator of deteriorating permafrost (Todtmann 1955, 1960; Friedman et al. 1971; French 1996; Ravn 2006; Kjær et al. 2008; Paper II). Sporadic permafrost has also been mapped in the area north of Brúarjökull (van Vliet-Lanoë et al., 1998; Etzelmüller et al., 2007). This is consistent with automated hourly measurements of air temperature between August 2003 and 2006, showing an annual mean of -0.9°C (Ravn 2006; Schomacker & Kjær 2007). Meteorological data have allowed the mean annual air temperature (MAAT) to be extrapolated back to 1830. The data show that the MAAT in the Brúarjökull forefield has ranged from -1 to -3°C since 1830 (Ravn 2006; Schomacker & Kjær 2007), indicating that permafrost existed to some extent during the time of the surges.

2.2 Eyjabakkajökull

Eyjabakkajökull is a surge-type outlet glacier draining the north-east part of the Vatnajökull ice cap in Iceland (Fig. 1). Eyjabakkajökull is composed of three distinct glacier outlets that

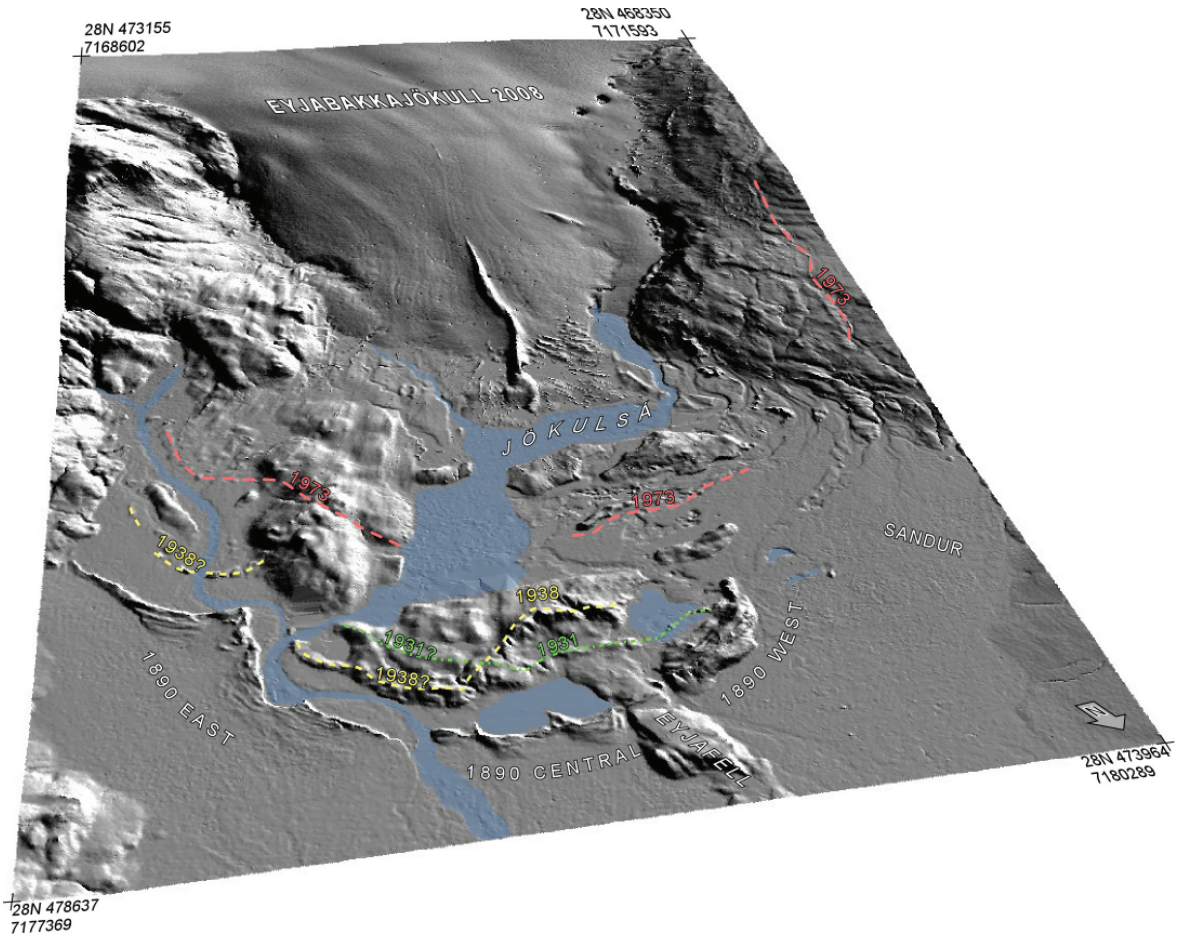

Figure 3. Eyjabakkajökull and its forefield visualized as a hillshade model. The 1890 end moraine is described in Paper IV. Ice-marginal positions from subsequent surges are indicated. See Fig. 1 for location. Modified from Paper IV.

descend from the main ice cap at 1200-1500 m a.s.l. and combine to form a ~10-km long and 4-km wide glacier tongue which terminates at around 700 m a.s.l. In the ablation zone, the outlets are separated by two prominent medial moraines that originate from nunataks further upglacier (Björnsson, 1982; Björnsson et al., 2003; Fig. 3).

The recent surge history of Eyjabakkajökull is well documented with advances recorded in 1890, 1931, 1938 and 1972-73 (Thoroddsen, 1914; Thorarinsson, 1938, 1943; Todtmann, 1953, 1960; Williams, 1976; Kaldal and Víkingsson, 2000; Björnsson et al., 2003). The largest advance (3-4 km) occurred in 1890 when the glacier terminated at the Eyjafell bedrock knob and formed the end moraines described in Paper IV (Fig. 3). The surges in 1931 and 1938 were probably smaller as they terminated 250 and 750 m upglacier from the 1890 moraines (Kaldal and Víkingsson, 2000). During the 1972-73 surge, the glacier advanced approximately 2 km between late August 1972 and September 1973 with maximum flow rates of up to 30 m/day (Williams, 1976; Björnsson, 1982; Sharp and Dugmore, 1985). At present, the snout of Eyjabakkajökull has a low profile and is retreating with crevasse-squeeze ridges and debris bands emerging from the ice.

The forefield of Eyjabakkajökull is characterized by sandur, end moraines, ice-cored and ice-free hummocky moraines, flutes, crevasse-squeeze ridges and concertina eskers (Fig. 3; Todtmann, 1953; Sharp 1985a, b; Croot 1987, 1988a; Evans and Rea, 1999, 2003; Evans et al., 1999; Kaldal and Víkingsson, 2000). Prior to the 1890 surge, the distal part of the proglacial sandur had developed a thick vegetated soil cover of loess, peat and tephra (LPT) (Croot 1987, 1988a). Known tephra horizons indicate

that the LPT sequence accumulated during sustained periods of low glacial activity, probably during the late Holocene and the Medieval Warm Period. End moraines resulting from the 1890, 1931 and 1938 surges are conspicuous in the proglacial area, whereas end moraines from the 1972-73 surge are indistinct. There is a small end moraine about 1 km upglacier of the 1973 terminal position in the eastern part of the area. The age of this moraine is not known but Kaldal and Víkingsson (2000) speculate that it could be the result of a minor surge around 1990. They also suggest the possibility that the three glacier outlets that confluence in Eyja-bakkajökull do not surge simultaneously.

Indicators of permafrost are rare in the forefield of Eyjabakkajökull. Indistinct frost-crack polygons were observed on the Eyjafell bedrock knob and circular ponds occur in places in front of the 1890 moraine and in clusters on the Eyjabakkar outwash plain to the north. Similar ponds observed in the forefield of the adjacent Brúarjökull have been interpreted as collapsed palsas, an indicator of deteriorating permafrost (Kjær et al., 2008; Schomacker and Kjær, 2007; Paper II). The mean annual air temperature on the Eyjabakkar outwash plain, approximately 10 km from the glacier, was 0.1°C between November 1997 and October 2008, indicating that the present climate is too warm for any substantial permafrost to be sustained. However, as temperatures in Iceland were 1.5-2°C lower during the Little Ice Age (LIA; Bergþórsson, 1969; Guðmundsson, 1997; Flowers et al., 2008), it is possible that thin and discontinuous permafrost existed in the forefield of Eyjabakkajökull at the time of the 1890 surge.

3 Methods

3.1 Geomorphological mapping

The end moraines and associated landforms at Brúarjökull and Eyjabakkajökull were originally identified and studied on a series of aerial photographs dating from 1945 to 1993 and from 1967 to 1998, respectively (Papers II-IV). New high-resolution aerial photographs taken at Brúarjökull in 2003 and at Eyjabakkajökull in 2008 allowed the production of Digital Elevation Models (DEM) of the study areas. The high-resolution aerial photographs and the DEMs facilitated accurate analysis and interpretation of the end moraine morphology and geometry, and spatial relationships between landforms, sediments, and structures (Fig. 4).

Detailed mapping of the area occupied by the marginal ice of the 1963-64 surge was carried out on a Digital Photogrammetric Workstation (DPW) on the basis of aerial photographs recorded before the surge (1945), during surge termination (1964), and after the surge (2003) (Fig. 5; Paper III). This was done in order to compare the position of the ice margin at surge termination to the present end moraine, and to distinguish between those parts of the end moraine that formed in either proglacial or submarginal settings. In addition to the end moraine, other associated features were mapped from the aerial photographs. Basins, with their included sediment, and pre-surge glaciotectonic ridges were mapped from the 1945 photographs. The position of the ice margin, the end moraine, and the location of meltwater outlets at the time of surge termination were mapped from the 1964 photographs. The end moraine and other ice-marginal landforms, as they appear at present, were mapped from the 2003 aerial photographs. Subsequently, the data were handled in a Geographical Information System (GIS) and finally in Canvas X cartography and drawing software. Cross-profiles of the area occupied by the marginal ice at surge termination were extracted from the 1964 and 2003 DEMs in order to compare the location of the ice margin with the end moraine. The profiles extend from the foreland up to the glacier surface and show whether or not an end moraine formed in front of the glacier (Paper III).

Horizontal (ice flow) and vertical (downwasting) displacement of the frontal 1-2 km of Brúarjökull was measured along three transects from a stable benchmark to fixed points on the ice surface with a TopCon precision levelling instrument with ±3 mm accuracy (Paper I). The precision levelling instrument was also used to survey terrain cross profiles across the end moraine ridges at Brúarjökull and Eyjabakkajökull,

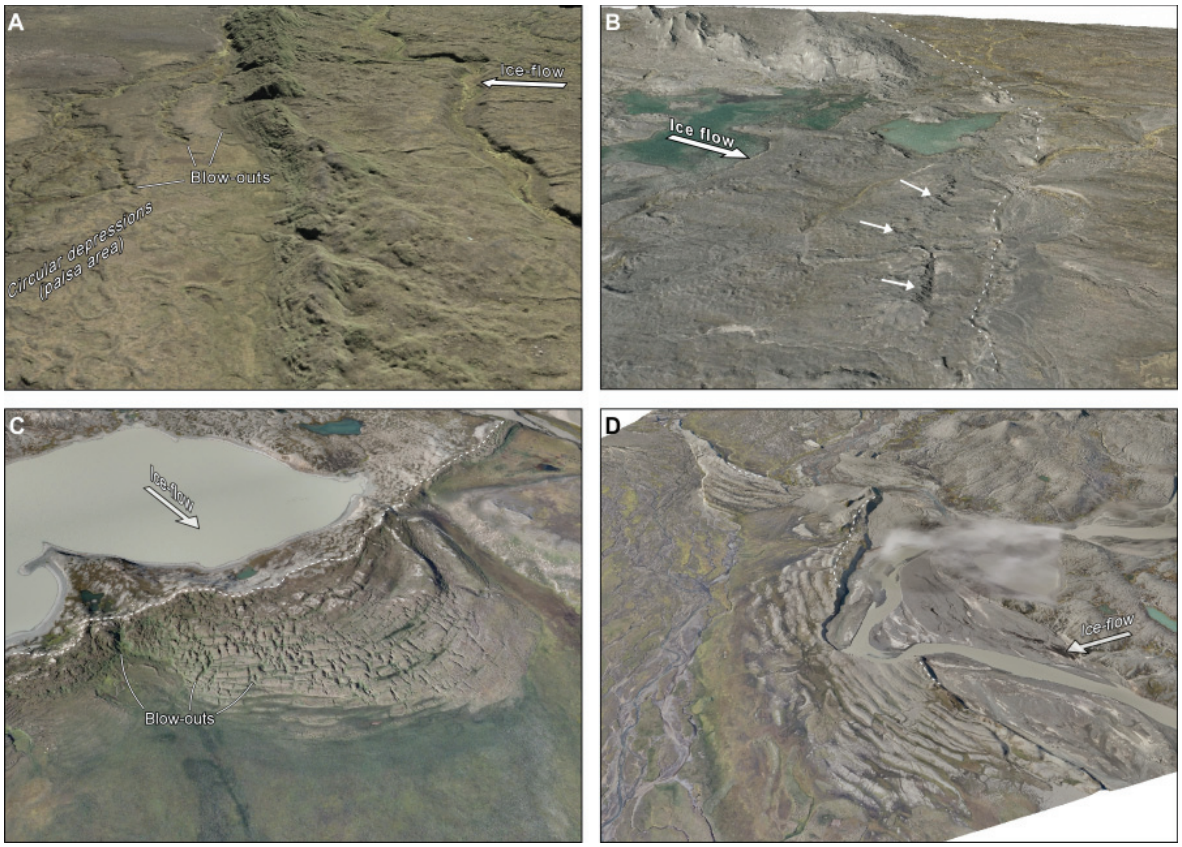

Figure 4. Examples of high resolution aerial photographs draped on digital elevation models. A: The 1890 end moraine at Brúarjökull and blow-out structures and circular depressions in front. Modified from Paper II. B: The 1964 submarginal end moraine (dashed line) and thrust ridges (arrowed) at Brúarjökull. Modified from Paper III. C: The central part of the 1890 end moraine at Eyjabakkajökull with blow-outs on the foreslope. Modified from Paper IV. D: The eastern part of the 1890 end moraine at Eyjabakkajökull. Dashed line indicates the position of the former ice margin. Modified from Paper IV.

in order to demonstrate their geomorphological and geometrical characteristics. The profiles were surveyed approximately perpendicular to the moraine strike (Papers II-IV).

3.2 Sedimentology

The sedimentology and stratigraphy in the forefield of Brúarjökull was studied in a number of pits and sections (Paper I). The sedimentology of the end moraines at Brúarjökull and Eyjabakkajökull was investigated in eight natural cross-sections that were extended and cleaned by hand (Papers II-IV). Sediment lithologies, structures and properties were documented using the Eyles et al. (1983) lithofacies classification and the data chart by Krüger and Kjær (1999). Section diagrams were produced in Canvas 9, X and 11 drawing software.

3.3 Structural geology and analysis of directional elements

The internal architecture of the end moraines was mapped from five cross-sections at Brúarjökull and three cross-sections and Eyjabakkajökull. All sections were manually cleaned and enlarged except section 3 at Eyjabakkajökull (Paper IV), the steepness of which prohibited any close-up mapping and cleaning. The section was therefore mapped, using binoculars, and photographed from *c.* 50 m distance. The glaciotectonic architecture was mapped at scales of 1:20, 1:100 and 1:200, depending on the size of the sections, accessibility, and the complexity of glaciotectonic deformation (Papers II-IV). The terminology used for describing deformation structures was adapted from Marshak and Mitra (1988), Twiss and Moores (1992) and Evans and Benn (2004). Measurements of

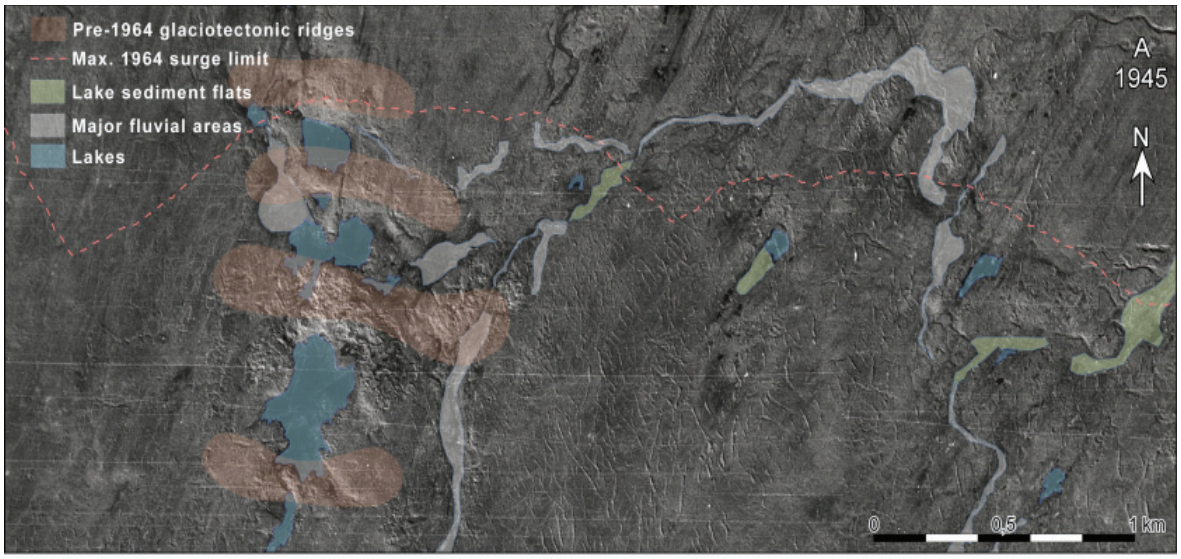
Pre-1964 glaciotectonic ridges
Max. 1964 surge limit
Lake sediment flats
Major fluvial areas
Lakes
A
1945
N
0
0,5
1 km

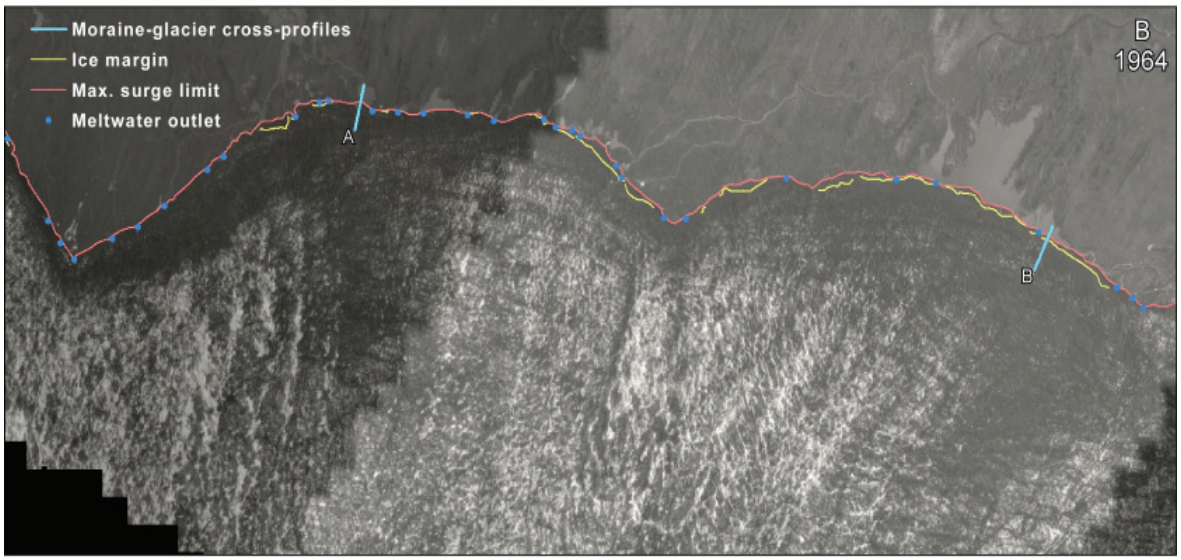
Moraine-glacier cross-profiles
Ice margin
Max. surge limit
Meltwater outlet
A
B
B
1964

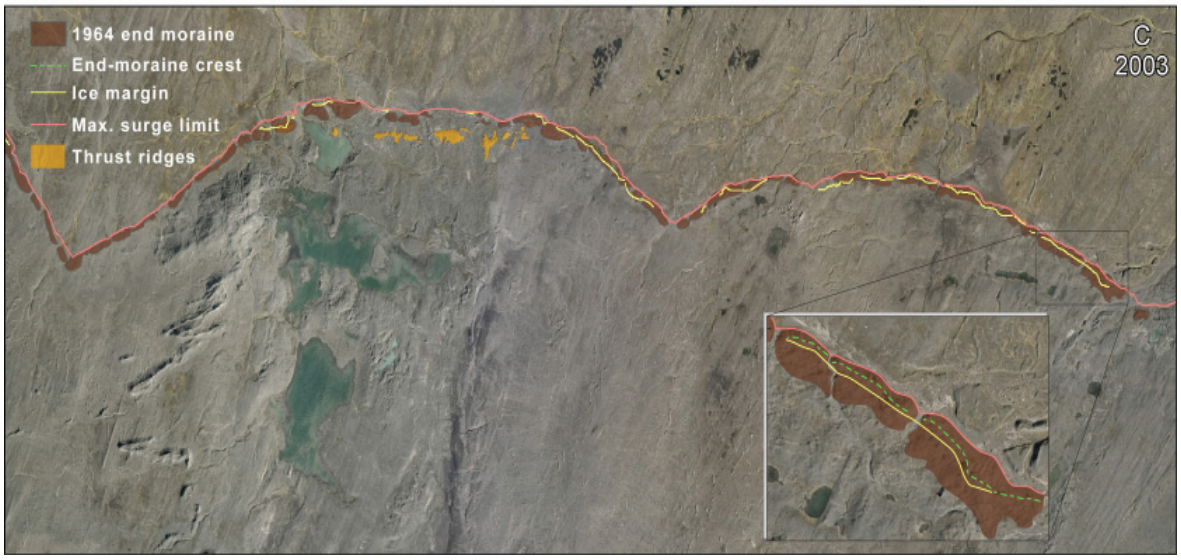
1964 end moraine
End-moraine crest
Ice margin
Max. surge limit
Thrust ridges
C
2003

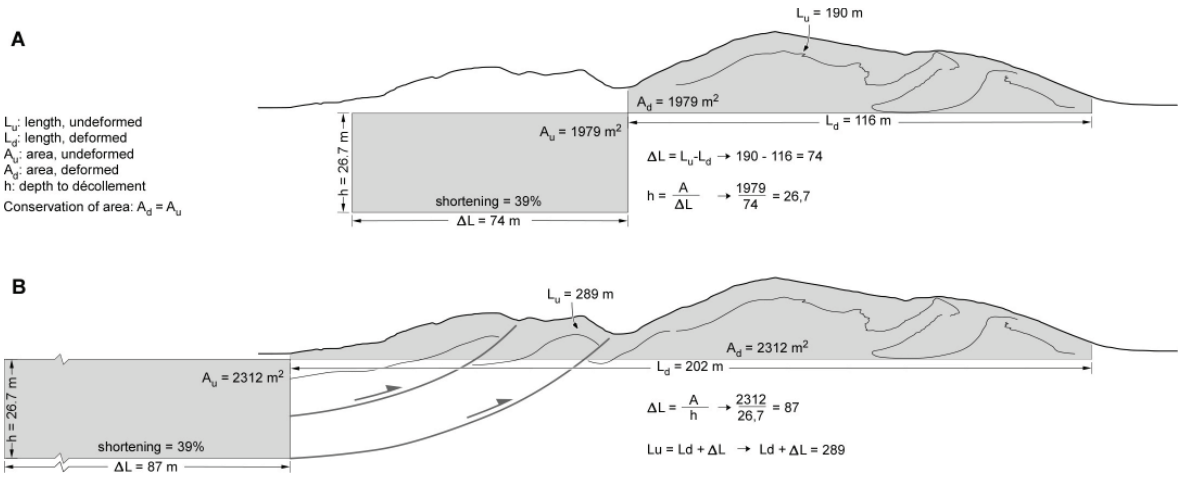

Figure 6. Balancing of the western part of the 1890 moraine at Eyjabakkajökull, with calculations of horizontal shortening of the original strata and depth to the décollement. A) Balancing of the exposed section 2. B) Balancing of the proximal part of the ridge on the basis of the décollement derived from balancing of section 2. Similar section-balancing was applied to section 3 and the three GPR profiles. From Paper IV.

structural elements included the strike and dip of fault planes and primary bedding, as well as plunge and direction of fold axes. The structural data were plotted and statistically analysed in a Schmidt equal-area stereonet with SpheriStat 2.2© for Windows software.

3.4 Clast fabric analysis

Following the method of Kjær and Krüger (1998), seventeen clast fabric analyses were carried out on a single flute that became exposed in the Brúarjökull forefield during 2003 (Paper I). By scraping and cleaning a 25×25 cm horizontal till surface, 25 clasts with a length of 0.6-6 cm and a width-to-length axis ratio of <0.67 were exposed, and their dip and dip direction recorded. The clast fabric data were plotted and analyzed, and eigenvectors, eigenvalues, and contours calculated in SpheriStat 2.2© software.

3.5 Cross-section balancing

Section balancing was carried out on the Eyjabakkajökull moraines (Fig. 6). The method was applied to geological cross-sections and ground penetrating radar (GPR) profiles following the methodology of Dahlström (1969), Marshak and Mitra (1988) and Pedersen (1996, 2005). Line balancing was applied to demonstrate the total horizontal shortening of the original strata and area balancing was used to calculate the depth to the décollement. The line balancing gives the difference (ΔL) between the length of a marker bed in the undeformed (Lu) and deformed (Ld) states, so that

$$\Delta L = Ld - Lu$$

where Lu is measured by tracing the marker between the proximal and distal ends of the section, and (Ld) is the horizontal (shortening) distance occupied by the deformed markers. The total shortening (s) can then be described as:

$$s = \frac{Ld - Lu}{Lu}$$

The area balancing assumes that the area of the body subjected to stress remained constant before (Au) and after (Ad) the deformation, meaning that Ad = Au, and that a décollement plane demarcates the lower boundary of the displaced sequence. By calculating the total area (A) of the deformed section, the depth to the

Figure 5. Mapping of the ice-marginal area of the 1963-64 surge of Brúarjökull was carried out in order to compare the position of the ice margin at surge termination to the position of the present end moraine, and to distinguish between those parts of the end moraine that formed in either proglacial or submarginal setting. A: The pre-surge (1945) glacier forefield. B: The area by the termination of the 1963-64 surge (1964). C: The situation after the surge (2003). From Paper III.

décollement surface (h) could be estimated by:

$$h = \frac{A}{\Delta L}$$

Despite its simplicity, the method has rarely been applied in glacial environments to quantify total shortening and depth of décollement surfaces, perhaps because of the general absence of continuous marker horizons that allow one to measure the shortening of the original strata, or because the glaciotectonic disturbances are too complex (e.g. Croot, 1987, 1988a; Pedersen, 1996, 2005; Boulton et al., 1999). Prominent and continuous marker beds exposed in the Eyjabakkajökull moraines allowed both line and area balancing of two excavated cross-sections and three ground penetrating radar (GPR) profiles (Paper IV).

In cases where sections could not be balanced, the aspect ratio of the foreland sediments, i.e. the thickness:width ratio of the foreland sediment wedge that is deformed to give the end moraine, was calculated to give an indication of the degree of glaciotectonic shortening involved (van der Wateren, 1995b; Bennett, 2001). This method was applied to the moraines at Brúarjökull as the glaciotectonic deformation was too complex and marker horizons were discontinuous or absent.

3.6 Ground Penetrating Radar

In order to map the internal architecture of the end moraines where exposures are absent, transverse ground penetrating radar (GPR) profiles were surveyed across the end moraines at Brúarjökull and Eyjabakkajökull with a Sensors & Software Inc. pulseEKKO PRO system with a pulsar voltage of 90 or 400 V (Fig. 7; Papers III and IV). A centre frequency of 100 MHz gave the best balance between penetration depth and resolution of the reflectors. During surveying, step size was 0.25 m and antennas were orientated perpendicular-broadside to the survey line with a separation of 1 m. Data processing included dewowing and Automatic Gain Control in order to equalize amplitude and compensate for rapid fall off in radar signals from greater depths. Common-Mid-Point (CMP) analyses gave velocities of c. 0.07 m/ns, which was used to convert the recorded two-way travel time to depth. The CMP velocity corresponds well to table values of 0.06-0.1 m/ns for saturated and damp sand (Jol & Bristow, 2003), and to velocities recorded in other glacial environments in Iceland (e.g. Cassidy et

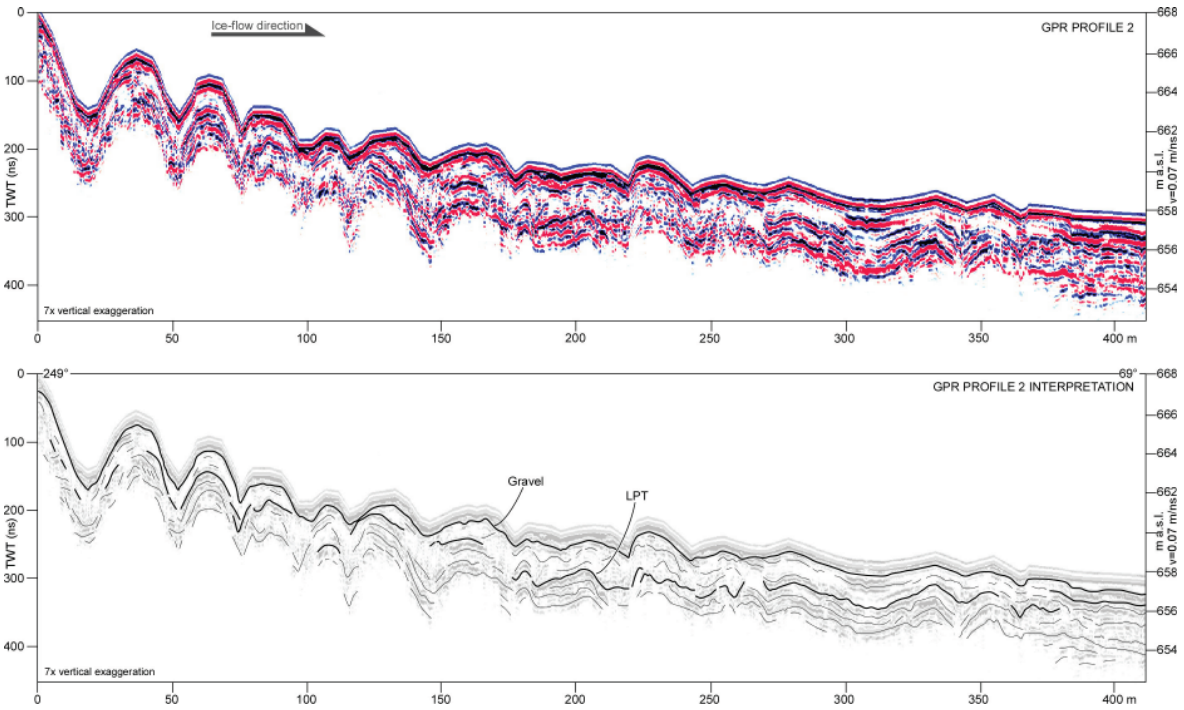

Figure 7. Example of a GPR profile and interpretation from Eyjabakkajökull showing the internal architecture of the end moraine. From Paper IV.

al., 2003; Kjær et al., 2004; Burke et al., 2008). Data were processed with the pulseEKKO 4.2 and EKKO_View Deluxe 1.3 software from Sensors & Software Inc. Topographic data from a TopCon precision levelling instrument and from a GPS directly linked to the GPR data logger were incorporated to the GPR profiles during data processing.

4 Results: Summary of papers

The main work for this thesis has been carried out by the present author. However, several researchers have contributed to this study. Those who have been involved in data collection, scientific discussions, data interpretation and preparation of publications appear as authors on Papers I-IV. Contributions are listed in Table 1.

4.1 Paper I

Kjær, K.H., Larsen, E., van der Meer, J.J.M., Ingólfsson, Ó., Krüger, J., Benediktsson, Í.Ö., Knudsen, C.G., Schomacker, A. 2006: Subglacial decoupling at the sediment/bedrock interface: a new mechanism for rapid flowing ice. Quaternary Science Reviews 25, 2704-2712.

The aim of Paper I was to describe the subglacial mechanism behind the rapid surge advances of Brúarjökull. Rapid ice flow has hitherto been explained by two modes of basal motion that is largely dependant on the nature of the ice/bed interplay. Decoupling of the glacier from its bed due to distributed

Table 1. Contributors to the research results presented in Papers I-IV.

Task	Paper I	Paper II	Paper III	Paper IV
Fieldwork planning and leading	K.H. Kjær E. Larsen	Í.Ö. Benediktsson Ó. Ingólfsson K.H. Kjær	Í.Ö. Benediktsson Ó. Ingólfsson	Í.Ö. Benediktsson Ó. Ingólfsson
Fieldwork	K.H. Kjær E. Larsen J.J.M. van der Meer Ó. Ingólfsson J. Krüger Í.Ö. Benediktsson C.G. Knudsen A. Schomacker	Í.Ö. Benediktsson P. Möller Ó. Ingólfsson J.J.M. van der Meer K.H. Kjær J. Krüger	Í.Ö. Benediktsson Ó. Ingólfsson A. Schomacker	Í.Ö. Benediktsson A. Schomacker H. Lokrantz Ó. Ingólfsson
Aerial photograph analysis and geomorphological mapping	-	Í.Ö. Benediktsson K.H. Kjær	Í.Ö. Benediktsson K.H. Kjær	Í.Ö. Benediktsson
Structural geological analysis and section balancing	-	Í.Ö. Benediktsson P. Möller	Í.Ö. Benediktsson	Í.Ö. Benediktsson
Ground Penetrating Radar	-	-	Í.Ö. Benediktsson A. Schomacker	Í.Ö. Benediktsson A. Schomacker
Data interpretation	K.H. Kjær E. Larsen J.J.M. van der Meer Ó. Ingólfsson J. Krüger Í.Ö. Benediktsson C.G. Knudsen A. Schomacker	Í.Ö. Benediktsson P. Möller Ó. Ingólfsson J.J.M. van der Meer K.H. Kjær	Í.Ö. Benediktsson Ó. Ingólfsson A. Schomacker K.H. Kjær	Í.Ö. Benediktsson A. Schomacker H. Lokrantz Ó. Ingólfsson
Preparation of text and figures	K.H. Kjær	Í.Ö. Benediktsson	Í.Ö. Benediktsson	Í.Ö. Benediktsson

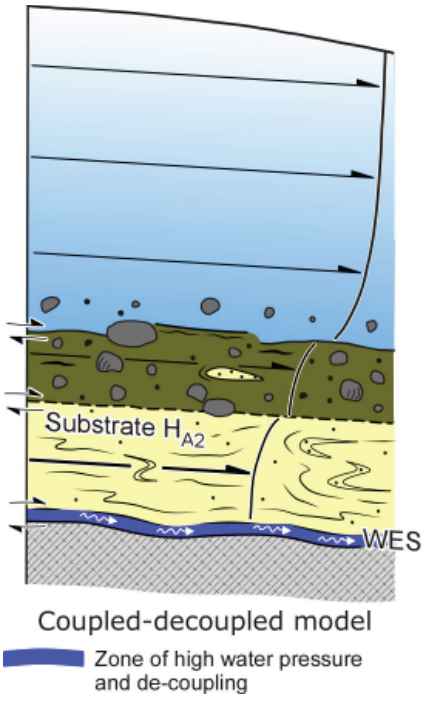

Figure 8. The basal motion model explaining the dominating mechanism behind the rapid ice flow of Brúarjökull during surges. From Paper I.

drainage with high water pressure enables fast ice flow through enhanced basal sliding across the bed, or very shallow subglacial deformation. Alternatively, fast ice flow can be sustained by deformation of water-saturated sediment that is strongly coupled to the ice. Both modes have inherent problems with respect to the landform-sediment association produced by fast flowing glaciers. Landforms and sediments related to rapid ice flow often display depositional and deformational features that suggest strong ice/bed coupling rather than enhanced basal sliding across the bed. It is, however, still debated whether fast ice flow can be sustained by spatially continuous subglacial deformation. Morphological and sedimentological data from the exposed bed of Brúarjökull show an extensively fluted till plain above a deformed sequence of loess, peat and tephra (LPT), and a shear zone between the two. Strong clast fabric in the flutes and the deformation of the entire LPT down to the bedrock indicate strong coupling at the ice/till and till/LPT interfaces. Waterlain laminated sediments between the LPT and the bedrock are widespread in the forefield of Brúarjökull. They unconformably truncate the base of the LPT sequence while they conformably superimpose the bedrock surface. These laminated sediments are interpreted as water escape structures (clastic dykes/hydrofractures) resulting from the movement of pressurized water between the bedrock and the moving LPT during surges. Circular depressions at the abrupt-head of channels outside the 1890 and 1964 end moraines are thought to indicate blow-out of overpressurized water from the subglacial sequence.

The evidence for strong coupling at the ice/till and till/LPT interfaces preclude enhanced basal sliding as the principal mechanism for the rapid ice flow during the surges of Brúarjökull. In contrast, the widespread water escape structures at the LPT/bedrock interface suggest that the overpressurized water carried the burden of both the ice and the sediment. Therefore, it is concluded that the fast ice flow during the Brúarjökull surges was sustained by overpressurized water in the subglacial sequence, and that the principal velocity component was located at the sediment/bedrock interface (Fig. 8).

4.2 Paper II

Benediktsson, Í.Ö., Möller, P., Ingólfsson, Ó., van der Meer, J.J.M., Kjær, K.H., Krüger, J. 2008: Instantaneous end moraine and sediment wedge formation during the 1890 glacier surge of Brúarjökull, Iceland. Quaternary Science Reviews 27, 209-234.

Paper II focuses on ice-marginal processes and end moraine formation during the 1890 surge of Brúarjökull. The morphology of the end moraine was studied and documented from aerial photographs draped on a DEM and from terrain profiles surveyed across the end moraine, and the sedimentology and internal architecture was investigated in four excavated cross-sections. Also, the sediment distribution in the area upglacier of the end moraine was examined. A profile survey of this terrain and the sediment thickness beneath it showed that the sediment thickness gradually increases towards the end moraine, and that the moraine is in fact a morphological expression of a marginal sediment wedge. A conceptual model shows that the wedge formed as a result of gradual thickening and compressive deformation of the

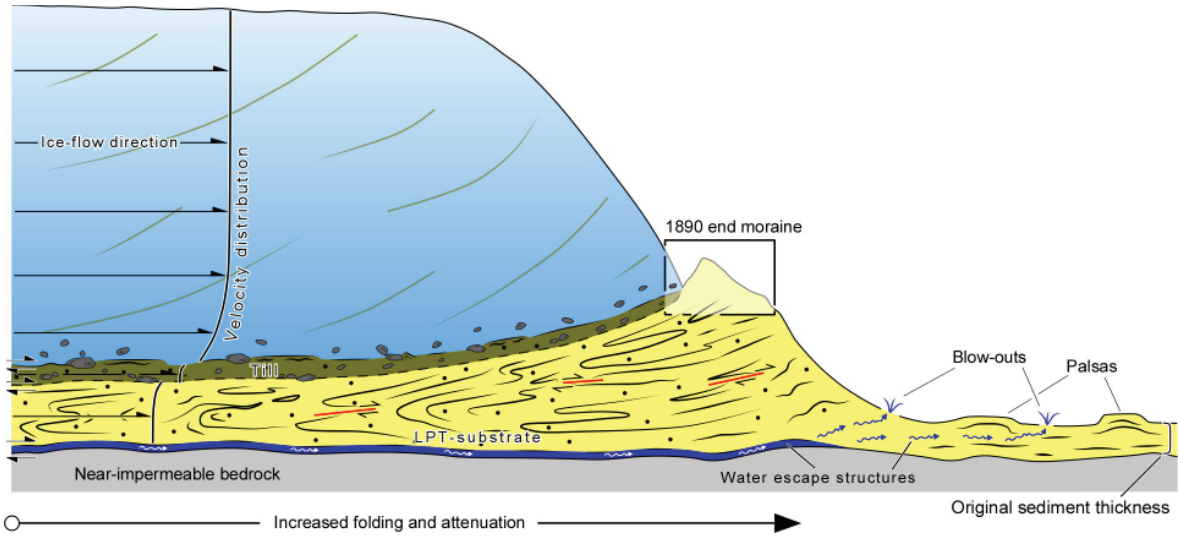

Figure 9. A conceptual model explaining the formation of the marginal sediment wedge. The wedge formed as a result of gradual thickening and compressive deformation of the subglacial sediment which was displaced across the bedrock surface due to sediment/bedrock decoupling. From Paper II.

subglacial sediment which was displaced across the bedrock surface due to sediment/bedrock decoupling (Fig. 9). The decoupling was caused by porewater overpressures in the subglacial sequence (Paper I).

A new model is presented to illustrate the formation of the marginal sediment wedge and the end moraine. During the surge phase, sediment/bedrock decoupling and associated subglacial sediment transport occurred where the subglacial sequence was fine-grained. This resulted in the build-up of a sediment wedge through ductile deformation in the marginal zone towards the end of the surge. At the very end of the surge, porewater pressures dropped and coupling was established at the sediment/bedrock interface leading to stress transfer up into the subglacial sequence. In response, brittle deformation dominated over ductile deformation and completed the moraine-ridge formation at the distal top of the wedge. The morphology and tectonic architecture are mainly controlled by the competence of the sediment, with ductile deformation dominating the fine-grained (LPT) parts and brittle deformation dominating the coarse-grained parts.

The sediment wedge and the end moraine represent a twofold marginal product of the 1890 surge. Considering ice velocities of 100-120 m/day during the Brúarjökull surges, the sediment wedge formed during the last ~5 days of the surge and the end moraine instantly during the last day or so of the surge.

4.3 Paper III

Benediktsson, Í.Ö., Ingólfsson, Ó., Schomacker, A., Kjær, K.H. 2009: Formation of submarginal and proglacial end moraines: implications of ice-flow mechanism during the 1963-64 surge of Brúarjökull, Iceland. Boreas 38, 440-457.

Paper III aims to explain the formation of proglacial and submarginal end moraines and their relation to the ice flow mechanism during the 1963-64 surge of Brúarjökull. Detailed mapping and production of DEMs on the basis of aerial photographs recorded before, during and after the 1963-64 surge, allowed the present position of the 1964 end moraine to be compared to the pre-surge forefield and the exact position of the ice margin during surge termination. The comparison showed that the end moraine formed in a proglacial position in areas where the sediment sequence was thick and fine-grained, but in a submarginal position where coarser grained sediment comprised a thinner subglacial bed. Mapping of meltwater outlets at surge termination implies that the formation of end moraines in either proglacial or submarginal setting is highly dependant on the subglacial drainage and the associated porewater pressure. Notably, the submarginal moraines occur in areas of efficient subglacial

drainage, as indicated by numerous meltwater outlets along the ice margin in those areas. In contrast, proglacial end moraines primarily occur where meltwater outlets are few along the ice margin and where blow-out depressions are apparent in front of the moraine, indicating inefficient drainage of overpressurized water through the subglacial bed. The morphology of the moraines reflects the depositional environment. Proglacial moraines are usually sharp crested and prominent, while the submarginal moraines bear signs of having been formed under ice and overridden. The internal architecture of the submarginal moraines is characterized by thrusting of gravel over a folded and faulted sequence of loess, peat and tephra. The thrusting is thought to dominate over folding because the sediment was relatively competent, owing to the efficient subglacial drainage and associated low porewater pressures in the area upglacier of these moraines.

Negligible deformation of the foreland during the 1963-64 surge indicates that the end moraines formed at the closing stage of the surge. The proglacial moraines formed as the distal expression of a marginal sediment wedge in areas where the ice flow mechanism was dominated by sediment/bedrock decoupling, with associated downglacier transport of subglacial sediment. The submarginal end moraines formed in well drained areas where the ice flow mechanism was dominated by basal sliding and shear deformation of the till. Gravel beneath the till had low strain rates and deformed through thrusting. Higher strain rates in the till than in the gravel allowed the glacier to override the thrust sheets that constitute the end moraine. At present, the submarginal end moraines are composed primarily of gravel thrust sheets that overlie and overprint pre-existing glaciotectonic landforms produced by previous surge advances.

4.4 Paper IV

Benediktsson, Í.Ö., Schomacker, A., Lokrantz, H., Ingólfsson, Ó. in press: The 1890 surge end moraines at Eyjabakkajökull, Iceland: a re-assessment of a classic glaciotectonic locality. Quaternary Science Reviews (2009), doi:10.1016/j.quascirev.2009.10.004.

The overall goal of Paper IV is to investigate the morphology, glaciotectonic architecture and sequential evolution of the end moraines formed by the 1890 surge of Eyjabakkajökull, and to re-assess a previous study of the end moraines. Analysis of new aerial photographs and resultant DEM, morphological field surveys, detailed mapping of excavated cross-sections, and ground penetrating radar surveys demonstrate that the morphology, sedimentology and glaciotectonic architecture of the end moraine vary along its length. Consequently, a previous model is only applicable for a certain part of the end moraines. The paper presents three different qualitative and conceptual models that explain the genesis of the entire Eyjabakkajökull moraine complex. Firstly, a narrow, single crested moraine ridge formed at the distal end of a marginal sediment wedge or ramp that developed in response to decoupling of subglacial sediment from the bedrock and associated downglacier sediment transport. Secondly, large lobate end-moraine ridges with multiple, closely spaced, narrow asymmetric crests formed by proglacial piggy-back thrusting. Thirdly, a new model shows that moraine ridges with different morphologies may reflect different members of an end-moraine continuum. This is true for the eastern and western parts of the Eyjabakkajökull moraines as they show similar morphological and structural styles that developed to different degrees. The former represents an intermediate member with décollement at 4-5 m depth and 27-33% shortening through multiple open anticlines that are reflected as moderately spaced symmetric crests on the surface. The latter represents an end member with décollement at about 27 m depth and 39% horizontal shortening through multiple high amplitude, overturned and overthrusted anticlines, appearing as broadly spaced symmetric crests. It is proposed that the opposite end member would be a moraine of multiple symmetric, wide open anticlinal crests of low amplitude. Our data suggest that the glacier coupled to the foreland to initiate the end-moraine formation when it had surged to within 70-190 m of its terminal position. This indicates a time frame of 2-6 days for the formation of the end moraines.

5 Discussion

5.1 Implications of ice-flow mechanism

Two models have hitherto been used to explain the mechanism behind rapid ice flow of surging glaciers and ice streams. Firstly, distributed subglacial drainage with high water pressures causes decoupling of a glacier from its bed and enhanced basal sliding or very shallow subglacial deformation (Björnsson, 1998; Engelhardt and Kamb, 1998). Secondly, subglacial deformation of water-saturated sediment that is strongly coupled to the glacier sustains fast ice flow (Boulton and Hindmarsh, 1987; Alley et al., 1989). These classic models are challenged by Paper I, in which the rapid ice flow of Brúarjökull during surges is explained by a decoupling between the bedrock and a sediment sequence that is strongly coupled to the ice (Fig. 8). This mechanism is dependant upon a range of factors: (i) the subglacial bed and the foreland must be comprised of low-permeable fine-grained sediments that can support very high porewater pressures, (ii) the rate of water input to the sediments from basal melting or upstream sources must be in excess of the permeability of the sediments in order to raise porewater pressures, and (iii) the presence of a weak horizon or stratigraphic discontinuity at depth is essential for the decoupling and associated hydrofracturing. The decoupling mechanism at the sediment/bedrock interface dominated in areas of the Brúarjökull forefield where these conditions occurred, leading to very fast ice flow (>5 m/hr) and extensive advance (9-10 km). In contrast, deformation of the bed in areas with relatively porous and permeable sediments contributed to relatively slower (but still rapid) movement of the glacier and a shorter advance (Nelson et al., 2005). This indicates that a mosaic of decoupling (mobile) and deforming spots exists under Brúarjökull during surges (Piotrowski et al., 2004, Stokes et al., 2007). This is, moreover, exemplified by the end moraines and associated ice-marginal landforms. Where the sediment/bedrock decoupling occurred, large quantities of subglacial sediment were transported downglacier, leading to ductile compression and gradual thickening of the substrate and the formation of marginal sediment wedges. A drop in porewater pressure at the end of the surge initiated the formation of the end moraine, with folds overprinted by faults, on the distal top of the wedge. By comparison, where porewater pressures were relatively low and the ice-flow mechanism was dominated by deformation of the bed, no marginal sediment wedge developed and the submarginal sediment deformed primarily in brittle manner because of higher shear strength, resulting in thrust-dominated moraines. The thrusting in the submarginal zone was probably associated with thrusting in the ice, as indicated by ice-cored thrust ridges upglacier from the end moraines in these areas.

Compared to Brúarjökull, little is known about the ice-flow mechanism operating during the surges of Eyjabakkajökull, owing to the extensive, post-surge glaciofluvial erosion of the former subglacial bed. However, one segment of the Eyjabakkajökull moraine complex contains morphology and sedimentary composition similar to the moraines at Brúarjökull, which developed in association with sediment/bedrock decoupling. Thus, by analogy, sediment/bedrock decoupling likely occurred beneath Eyjabakkajökull where the bedrock rises to the surface. In other parts of the forefield, deformation of the bed is thought to have been the principal mechanism of ice flow.

This new information on subglacial and submarginal processes of surge-type glaciers contributes to a better understanding of the mechanism behind other fast flowing ice masses, whether they are modern or ancient surge-type glaciers or ice streams. For example, sedimentary wedges have recently been discovered at the grounding lines of both modern and Pleistocene ice streams (Mosola and Anderson, 2006; Alley et al., 2007; Anandakrishnan et al., 2007; Andreassen et al., 2007) but their formation is poorly understood. The models proposed in Papers I and II may aid in understanding the formation of these grounding line wedges and therefore increase our knowledge of ice stream dynamics.

5.2 Glacial stress field

The speed of glacier advances should determine the thickness and gradient of end moraines, giving that the deformed sediments are of the same density and viscosity in different forelands (van der Wateren 1995a). Thus, theoretically, fast glacier advances should apply greater stresses to the foreland than slower advances, resulting in a greater scale of deformation and larger end moraines. In practice, this is complicated by the properties of the foreland and its susceptibility to deformation (Bennett, 2001). Consequently, it might be suspected that Brúarjökull would produce much larger end moraines than Eyjabakkajökull because of faster and more extensive surge advances. In fact, this is the opposite as the moraines at Eyjabakkajökull are generally larger than those at Brúarjökull (Papers II-IV). As fine-grained LPT sediments, of similar density and viscosity, are the controlling facies in the deformation of the foreland wedges at both glaciers, the foreland wedges should be equally susceptible to deformation; hence, differences in density and viscosity of the foreland sediments can be excluded as a factor influencing the size of the moraines. In contrast, there are large differences in the thickness of the foreland wedges that were deformed to create the end moraines; with a foreland wedge thickness of ~ 3 m at Brúarjökull but generally 10-30 m at Eyjabakkajökull.

It has been shown that large, multi-crested end moraines on Svalbard and in Arctic Canada form in areas of continuous permafrost, which transmits the stress away from the glacier and extends the zone of glaciotectonic formation (Kälin, 1971; Croot, 1988b; Boulton et al., 1999). Because of the width and the multi-crested morphology of the Eyjabakkajökull end moraines, the question therefore arises whether permafrost affected their structural evolution. But, as permafrost in the forefields of Brúarjökull and Eyjabakkajökull was most likely discontinuous and relatively thin during the LIA, the stress from the advancing ice could not be transmitted to extend the zone of glaciotectonic deformation. Thus, permafrost is not thought to have played a significant role in the glacial stress.

Once the glacier has coupled to the foreland, usually because of a drop in submarginal water pressure, the glacial stress is applied by a push-from-within where the glacier, the subglacial bed and the foreland wedge act as a single unit that is deformed by folds and thrusts rising from a décollement that underlies both the glacier and the foreland (Bennett, 2001; Fig. 10). This is obvious from Brúarjökull where proglacial end moraines are a morphological expression of a sediment wedge that developed under the glacier margin, and where transverse ice-cored ridges and submarginal end moraines signify deformation within and under the snout (Papers II and III). Likewise, asymmetric ridges on the proximal part of the Eyjabakkajökull end moraines are the result of thrusting in the ice margin, thus indicating coupling between the glacier and the bed (Paper IV). This mode of coupling (push-from-within) between the glacial stress field and the foreland is well known for polythermal glaciers where the marginal zone is frozen to the bed (Hambrey and Huddart, 1995; Huddart and Hambrey, 1996; Bennett et al., 1999) but has rarely been documented

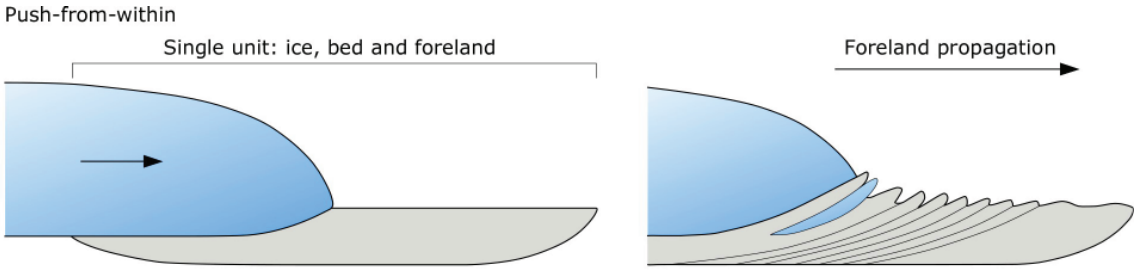

Figure 10. A model explaining a push-from-within as the principal way in which the glacial stress is applied to the foreland in association with the surges of Brúarjökull and Eyjabakkajökull. Once the glacier couples to the bed, the ice, bed and foreland act as a single unit that is deformed. Modified from Bennett (2001).

at temperate surge-type glaciers. Two other glaciotectonic models, gravity spreading or ice-pushing into an ice-contact fan or delta, have often been considered as the principal mechanisms responsible for end-moraine formation at surge-type glaciers (Boulton et al., 1996, 1999; Bennett et al., 2004b). However, the results from Brúarjökull and Eyjabakkajökull show that push-from-within is an integral part of the formation of end moraines by temperate surge-type glaciers.

5.3 Glaciotectonic shortening and timing of glacier-foreland coupling

The amount of shortening within end moraines of some surging glaciers has been taken to indicate the extent of their surge advances (e.g. Boulton et al., 1999). This is not true for the Brúarjökull and Eyjabakkajökull moraines as the shortening within them is at least an order of magnitude smaller than the extent of the advances, indicating that they formed at the very end of the surges. This agrees with actual descriptions of the surges (Eythorsson 1963, 1964, Williams, 1976). By calculating the horizontal shortening of the foreland strata that was deformed to give the end moraine, the position at which the glacier coupled to the foreland can be reconstructed. The shortening distance can then be compared to the ice-flow velocities to estimate the time it took for the end moraines to form. With this simple method it has been demonstrated that the time frame, within which the Brúarjökull and Eyjabakkajökull end moraines formed, was one to six days. Consequently, the coupling between the glaciers and their forelands occurred one to six days before surge termination. The glaciotectonic shortening within the end moraines varies along their lengths, sometimes so that adjacent locations show contrasting amounts of shortening. This is true for Eyjabakkajökull, in particular, where these variations probably reflect the timing of the glacier-foreland coupling before surge termination, with a large and small amount of shortening (large and small moraines) resulting from early and late coupling, respectively (Paper IV). Alternatively, if the coupling was synchronous along the entire ice margin, the variations in the glaciotectonic shortening indicate that different parts of the surging ice did not terminate simultaneously. At Brúarjökull, the coupling between the glacier and the foreland seems to have been synchronous along the most of the margin, as supported by small lateral variations in the morphology and aspect ratio of the moraine (Paper II and III).

The actual timing of the glacier-foreland coupling at temperate surge-type glaciers occurs towards the very end of the surge when submarginal water pressures decrease in association with minor flooding or blow-out of water that was stored behind the surge front (e.g. Christiansen et al., 1982; Kamb et al., 1985; Raymond et al., 1987; Humphrey and Raymond, 1994; Björnsson, 1998). This is very different from end moraines of non-surging glaciers (e.g. Humlum, 1985; Krüger, 1985, 1993, 1996; Matthews et al., 1995; Bennett et al., 1996; Winkler and Nesje, 1999; Motyka and Echelmeyer, 2003; Kuriger et al., 2006; Krüger et al., 2010; Winkler and Matthews, in press) and surging, generally polythermal, polar glaciers (e.g. Boulton et al., 1996, 1999; Bennett et al., 1999; Kristensen et al., 2009; Roberts et al., 2009) that usually form during longer periods resulting from more sustained glacier-foreland coupling. The results of this study may, therefore, help to understand the timing and duration of end-moraine and sediment-wedge formation at fast-flowing glaciers and to differentiate between surge and non-surge end moraines in palaeoglaciological reconstructions. The latter would require detailed analysis of the morphology and structures of the end moraines and coupling with proxies from e.g. glaciological investigations or modelling.

5.4 Morphology and internal architecture

The morphology and the internal architecture of the end moraines are strongly related to their sedimentary composition, the thickness of the foreland wedge, and the subglacial ice-flow mechanism (Fig. 11). The sedimentary composition and thickness of the foreland wedge control the style of deformation and the size of

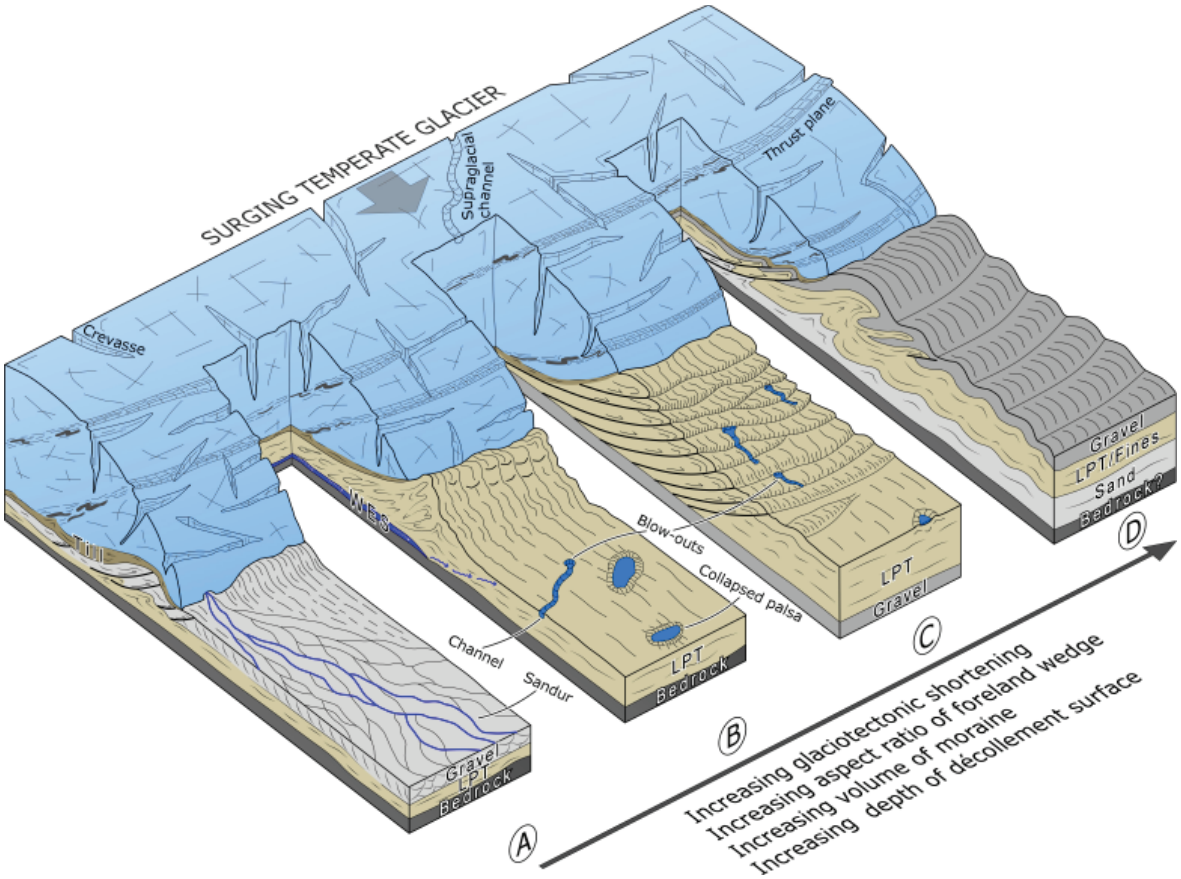

Figure 11. A conceptual model summarizing the end moraine formation at Brúarjökull and Eyjabakkajökull. A: Where the glacier advances across glaciofluvial sediments, wedges of gravel and sand are thrusted and stacked beneath and in front of the ice margin to form a single- but broad-crested end moraine. This occurs in association with deformation of the bed, which allows the glacier to partly or fully override the moraine because strain rates are higher in the upper part than the lower part. B: A single-crested moraine with multiple rooted folds in LPT forms on the distal end of a marginal sediment wedge. The formation of the marginal wedge occurs due to decoupling at the sediment/bedrock interface and the associated downglacier sediment transport. This occurs in areas of inefficient subglacial drainage and very high porewater pressures. C: A wide moraine ridge with multiple asymmetric crests on the foreslope. Each crest represents a thrust sheet within which open and inclined folds signify the initial style of deformation. The most distal ridges stem from open folding or potentially blind thrusts. D: A wide, multi-crested moraine with symmetric crests in the central and distal zones but asymmetric crests in the proximal zone that was located under the ice margin. The architecture is dominated by large-scale folding, although brittle deformation commenced when the folding could not accommodate for the shortening anymore.

the moraines, which together determine their morphology. Single- but broad-crested end moraines composed of imbricate thrust sheets formed where the subglacial bed consisted of till and glaciofluvial sediments with relatively high shear strength, and the ice-flow mechanism was dominated by deformation of the bed. Low friction at the décollement surface (bedrock), favoured by water that percolated through the bed, induced dislocation and stacking of the thrust sheets (Fig. 11A), a structural style previously recognized in surge-moraines at Hagafellsjökull-Eystri, Iceland (Bennett et al., 2004b) and Kongsvegen, Svalbard (Bennett et al., 1999). Single- and narrow-crested end moraines, usually 5-15 m high and 20-80 m wide, are composed of fine-grained LPT and comprise rooted folds because of high friction along the décollement, which usually coincides with the bedrock surface. They occur where the foreland wedge is relatively thin on top of bedrock, which corresponds to the areas where

sediment/bedrock decoupling was the dominating ice-flow mechanism (Fig. 11B). This type of end moraine is common at Brúarjökull but is also found at Eyjabakkajökull where similar ice-marginal conditions occur. The large moraines at Eyjabakkajökull (up to 40 m high and 450 m wide), result from the deformation of a thick foreland wedge. Their internal architecture determines their morphology but is largely controlled by the properties of the sediments deformed. For example, asymmetric crests on the foreslope of the moraine imply that imbricate thrusting was the principal deformation style in end moraines consisting solely of LPT overlying gravel (Fig. 11C), whereas moraine-ridges with broad symmetric crests represent large-scale folding of fines, sands and gravels (Fig. 11D). The width of the Eyjabakkajökull moraines results from the transmission of glacial stress far into the foreland. For this to occur, the foreland wedge must have had relatively high shear strength. Continuous and thick permafrost has often been regarded as the most important factor in raising sediment shear strength for transmitting glacial stress away from an advancing glacier, and thereby extending and deepening the zone of glaciotectonic deformation (Kälin, 1971; Croot, 1988b; Boulton et al., 1999). Any permafrost that might have existed in the forefield of Eyjabakkajökull at the time of the 1890 surge (at the peak of the LIA) was most likely discontinuous and too thin to extend the zone of deformation down to 10-30 m depth. Similarly, seasonal frost would be too thin to facilitate deformation below a few metres depth. Other factors may therefore have controlled the foreland shear strength and the stress transmission into the foreland. It is hypothesized that relatively low porewater pressures favoured high shear strength of the foreland sediments, which were, therefore, capable of transmitting the applied glacial stress up to 500 m into the foreland.

The morphology and architecture of the end moraines provide important information on the properties of the foreland wedge and the glacier dynamics. With detailed morphological analysis of end moraines and other ice marginal landforms, valuable information on glacier dynamics, ice-flow mechanism and ice-marginal processes may therefore be obtained. This is important when studying inaccessible ice margins, for example in tidewater glaciers and ice streams, or where geological sections in terrestrial end moraines are absent.

6 Implications for future research

Recent studies of end moraines have focused mainly on the structural evolution of the moraines while the link to the glacier dynamics has received less attention. This study emphasizes the importance of integrated research where end moraines, other ice marginal features, and the subglacial bed are investigated to provide a holistic understanding of the relation between glacier dynamics and landform-sediment associations.

An obvious improvement in the studies of end moraines would be to monitor the process of their formation. Numerous studies have advanced the understanding of the formation of end moraines of non-surging glaciers through actual observations (e.g. Kälin, 1971; Humlum, 1985; Krüger, 1985, 1993, 1996; Matthews et al., 1995; Winkler and Nesje, 1999; Krüger et al., 2002; Motyka and Echelmeyer, 2003; Kuriger et al., 2006; Winkler and Matthews, in press) but, to the author's knowledge, the actual formation of surge end moraines has rarely been documented. Many glaciers in Svalbard have recently surged while others are currently in different stages of a surge phase with expected termination within a few years (Sund et al., 2009). These surges, in particular those of Comfortlessbreen and Nathorstbreen (M. Sund, personal communication, 2009), provide an ideal opportunity to observe and monitor processes at their margins, including potential end moraine formations. However, as glaciers on Svalbard occur in permafrost environment, and often have cold-based margins, they may not provide usable analogues to temperate surge-type glaciers. Few temperate and terrestrially terminating glaciers have surged in recent years (e.g. in Iceland and Alaska). Nevertheless, some Icelandic glaciers are expected to surge within the next decade as they have

passed their regular quiescent phase duration (Björnsson et al., 2003), although overall negative mass balance for the past 10-15 years may delay future surges (Björnsson and Pálsson, 2008). Therefore, an opportunity lies ahead to observe and monitor end moraine formation at terrestrially terminating temperate surge-type glaciers. This study implies that when studying glaciotectonic end moraines, the subglacial bed should also be investigated in order to relate the ice-flow mechanism to the formation of the end moraines. This can be done with traditional sedimentological methods, but recently invented wireless subglacial probe sensors that measure tilt, water pressure, temperature, strain, and resistance (Hart et al., 2006, 2009), could be applied to record in situ processes beneath the ice margin that could subsequently be linked to the formation of end moraines. Knowing the aforementioned parameters, together with ice-flow velocity, geometry of the ice margin (e.g. thickness, gradient) and the properties of the foreland wedge, would provide an ideal opportunity for numerical modelling of the formation of end moraines, and thereby to identify the most important parameters. This is important for studies of Pleistocene glaciotectonic end moraines and associated palaeoglaciological reconstructions.

There has been a trend in the glacial geological literature to explain ice-marginal processes and end-moraine formation with a single model for each glacier. Lateral variability in the morphology and architecture of the Brúarjökull and Eyjabakkajökull moraines suggests that different processes operated along different parts of ice margins, thus implying that moraine ridges along the margin of a glacier may be of different geneses. Thus, future research on the formation of glaciotectonic end moraines should embrace a range of study sites and methods applied on morphologically different ridges along the ice margin.

The subglacial environment and the end moraines at Brúarjökull are well documented in Papers I-III. However, uncertainties remain about the ice-flow mechanism in the western part of the Brúarjökull forefield where the surge advances were shorter, and its relation to the imbricate thrust moraines. Future research at Brúarjökull might therefore be directed towards an investigation of the subglacial bed between the Kringilsá and Kverká rivers.

At Eyjabakkajökull, technical problems prevented radar surveys of the central part of the end moraine complex, the architecture of which remains poorly understood therefore (Paper IV). An obvious research task at Eyjabakkajökull would be to survey this part of the moraine complex with a GPR to map the internal glaciotectonic structures and to detect a potential décollement surface. This would also allow one to estimate the horizontal shortening and volume involved, and to compare that with the width and size of the water-filled depression on the proximal side of the moraine.

7 Conclusions

Two mechanisms can explain the rapid ice flow of Brúarjökull during surges. Firstly, decoupling at the sediment/bedrock interface, resulting from very high porewater pressures in a fine-grained and low-permeable sediment sequence that was coupled to the ice, was the dominating ice-flow mechanism. Secondly, deformation of the bed (without substrate/bedrock decoupling) also contributed to rapid ice flow in areas with more permeable sediments and lower water pressures. Due to the sediment/bedrock decoupling, the glacier substrate was dislocated across the bedrock resulting in the formation of marginal sediment wedges at the end of the surges. In contrast, no such wedges were formed where the ice flow was dominated by deformation of the bed only.

At Brúarjökull, the end moraines formed instantaneously at the last day of the surges. Single-crested end moraines formed proglacially on the distal end of the marginal sediment wedges in areas where the ice-flow mechanism was dominated by the sediment/bedrock decoupling. They are dominated by rooted folds that are overprinted by brittle deformation from the last phase of the end-moraine formation. In contrast, submarginal end moraines are dominated by imbricate thrust sheets that were mainly stacked under the glacier snout. These moraines formed in areas where deformation

of the bed was the dominating ice-flow mechanism.

The time frame within which the end moraines at Eyjabakkajökull formed was 2-6 days, derived from calculations on the horizontal shortening and comparison with the ice-flow velocity. The moraines are characterized by lateral variation in morphology and internal architecture. Large moraines with multiple broad symmetric crests are dominated by overturned and overthrusted anticlines while moraines with multiple narrow asymmetric crests indicate imbricate thrust sheets. Both type of moraines formed where the foreland wedge was thick and the subglacial ice-flow mechanism was most likely dominated by deformation of the bed. In contrast, small, single-crested moraines formed in relation to thin foreland wedge and sediment/bedrock decoupling under the ice.

This study demonstrates an integral relationship between the subglacial ice-flow mechanism and the ice-marginal moraines. Therefore, it implies that studies of end moraine ridges, whether they are modern or ancient, should not only concentrate on their internal architecture and structural evolution, but also on their relation to the glacier dynamics, and thus include investigations of the subglacial bed. Actual observations, instrumental monitoring and numerical modelling of the formation of surge end moraines would provide information on the role of the different parameters involved and their effect on the glacier dynamics and structural evolution. This would contribute to increased understanding of dynamics and marginal formations of modern and ancient fast flowing ice masses.

References

Aber, J., Croot, D.G., Fenton, M.M., 1989. *Glaciotectonic Landforms and Structures*. Kluwer, Dordrecht. 200 p.

Aber, J.S., Ber, A., 2007. Glaciotectonism. Elsevier, Amsterdam. *Developments in Quaternary Science 6*, 1-246.

Alley, R.B., Blankenship, D.D., Rooney, S.T., Bentley, C.R., 1989. Water-pressure coupling of sliding and bed deformation: III. Application to ice stream B, Antarctica. *Journal of Glaciology 35*, 130–139.

Alley, R.B., Anandakrishnan, S., Dupont, T.K., Parizek, B.R., Pollard, D., 2007. Effect of sedimentation on ice-sheet grounding-line stability. *Science 315*, 1838–1841.

Anandakrishnan, S., Catania, G.A., Alley, R.B., Horgan, H.J., 2007. Discovery of till deposition at the grounding line of Whillans Ice Stream. *Science 315*, 1835–1838.

Andreassen, K., Laberg, J.S., Vorren, T.O., 2007. Seafloor geomorphology of the SW Barents Sea and its glaci-dynamic implications. *Geomorphology 97*, 157-177.

Benn, D.I., Evans, D.J.A., 1998. *Glaciers and glaciation*. Arnold, London. 734 p.

Bennett, M.R., 2001. The morphology, structural evolution and significance of push moraines. *Earth-Science Reviews 53*, 197-236.

Bennett, M.R., 2003. Ice streams as the arteries of an ice sheet: their mechanics, stability and significance. *Earth Science Reviews 61*, 309-339.

Bennett, M.R., Huddart, D., Hambrey, M.J., Ghienne, J.F., 1996. Moraine development at the High-Arctic valley glacier Pedersenbreen, Svalbard. *Geografiska Annaler 78A*, 209-222.

Bennett, M.R., Hambrey, M.J., Huddart, D., Glasser, N.F., Crawford, K., 1999. The landform and sediment assemblage produced by a tidewater glacier surge in Kongsfjorden, Svalbard. *Quaternary Science Reviews 18*, 1213-1246.

Bennett, M.R., Huddart, D., Waller, R.I., Midgley, N.G., Gonzalez, S., Tomio, A., 2004a. Styles of ice-marginal deformation at Hagafellsjökull-Eystri, Iceland, during the

1998/99 winter-spring surge. *Boreas 33*, 97-107.

Bennett, M.R., Huddart, D., Waller, R.I., Cassidy, N., Tomio, A., Zukowskyj, P., Midgley, N.G., Cook, S.J., Gonzalez, S., Glasser, N.F., 2004b. Sedimentary and tectonic architecture of a large push moraine: a case study from Hagafellsjökull-Eystri, Iceland. *Sedimentary Geology 172*, 269-292.

Bergthórsson, P., 1969. An estimate of drift ice and temperature in Iceland in 1000 years. *Jökull 19*, 94-101.

Bjarnadóttir, L.R. 2007. *Ice-marginal environments of a surge-type glacier: Distribution, formation and morphological evolution of flutes and crevasse cast ridges at Brúarjökull, Iceland*. Unpublished M.Sc. Thesis, University of Iceland, 119 pp.

Björnsson, H., 1982. Drainage basins on Vatnajökull mapped by radio echo soundings. *Nordic Hydrology, 1982*, 213-232.

Björnsson, H., 1998. Hydrological characteristics of the drainage system beneath a surging glacier. *Nature 395*, 771-774.

Björnsson, H., Pálsson, F., Guðmundsson, M.T., Haraldsson, H.H., 1998. Mass balance of western and northern Vatnajökull, Iceland, 1991-1995. *Jökull 45*, 35-38.

Björnsson, H., Pálsson, F. & Sigurðsson, O. 2003. Surges of glaciers in Iceland: *Annals of Glaciology 36*, 82-90.

Björnsson, H., Pálsson, F., 2008. Icelandic glaciers. *Jökull 58*, 365-386.

Boulton, G.S., 1986. Push-moraines and glacier-contact fans in marine and terrestrial environments. *Sedimentology 33*, 677-698.

Boulton, G.S., Hindmarsh, C.A., 1987. Sediment deformation beneath glaciers: Rheology and geological consequences. *Journal of Geophysical Research 92*, 9059-9082.

Boulton, G.S., van der Meer, J.J.M., Hart, J., Beets, D.J., Ruegg, G.H.J., van der Wateren, F.M., Jarvis, J., 1996. Till and moraine emplacement in a deforming bed surge – an example from a marine environment. *Quaternary Science Reviews 15*, 961-987.

Boulton, G.S., van der Meer, J.J.M., Beets, D.J., Hart, J., Ruegg, G.H.J., 1999. The sedimentary and structural evolution of a recent push moraine complex: Holmstrømbreen, Spitsbergen. *Quaternary Science Reviews 18*, 339-371.

Burke, M.J., Woodward, J., Russell, A.J., Fleisher, P.J., Bailey, P.K., 2008. Controls on the sedimentary architecture of a single event englacial esker: Skeiðarárjökull, Iceland. *Quaternary Science Reviews 27*, 1829–1847.

Cassidy, N.J., Russell, A.J., Marren, P.M., Fay, H., Knudsen, Ó., Rushmer, E.L., van Dijk, T.A.G.P., 2003. GPR derived architecture of November 1996 jökulhlaup deposits, Skeiðarársandur, Iceland. In: Bristow, C.S., Jol, H.M. (Eds.), *Ground Penetrating Radar in Sediments*, vol. 211. Geological Society, London, pp. 153–166. Special Publications.

Christiansen, E.A., Gendzwill, D.J., Meneley, W.A., 1982. Howe Lake: a hydrodynamic blowout structure. *Canadian Journal of Earth Sciences 19*, 1122-1139.

Croot, D.G., 1987. Glacio-tectonic structures: a mesoscale model of thin-skinned thrust sheets? *Journal of Structural Geology 9*, 797-808.

Croot, D.G., 1988a. Morphological, structural and mechanical analysis of neoglacial ice-pushed ridges in Iceland. In: Croot, D.G. (Ed.), *Glaciotectonics: Forms and Processes*. Balkema, Rotterdam, pp. 33-47.

Croot, D.G., 1988b. Glaciotectonics and surging glaciers: a correlation based on Vestspitsbergen, Svalbard, Norway. In: Croot, D.G. (Ed.), *Glaciotectonics: Forms and Processes*. Balkema, Rotterdam, pp. 49-61.

Dahlström, C.D.A., 1969. Balanced cross sections. *Canadian Journal of Earth Sciences 6*, 743–757.

Dowdeswell, J.A., Ó Cofaigh, C., Pudsey, C.J., 2004. Thickness and extent of the subglacial till layer beneath an Antarctic palaeo-ice stream. *Geology 32*, 13-16.

Engelhardt, H., Kamb, B., 1998. Basal sliding of ice stream B, West Antarctica. *Journal of Glaciology 44*, 223-230.

Etzelmüller, B., Farbrot, H., Guðmundsson, Á., Humlum, O., Tveito, O.E., Björnsson, H., 2007. The regional distribution of mountain permafrost in Iceland. *Permafrost and*

Periglacial Processes 18, 185-199.

Evans, D.J.A., Rea, B.R., 1999. Geomorphology and sedimentology of surging glaciers: a landsystem approach. *Annals of Glaciology 28*, 75-82.

Evans, D.J.A., Lemmen, D.S., Rea, B.R., 1999. Glacial landsystems of the southwest Laurentide Ice Sheet: modern Icelandic analogues. *Journal of Quaternary Science 14*, 673-691.

Evans, D.J.A., Rea, B.R., 2003. Surging glacier landsystem. In: Evans, D. J. A. (Ed.): *Glacial landsystems*. Arnold, London, pp. 259-288.

Evans, D.J.A., Benn, D.I., 2004. *A Practical Guide to the Study of Glacial Sediments*. Arnold, London. 266 p.

Evans, D.J.A., Twigg, D.R., Rea, B.R., Shand, M., 2007. Surficial geology and geomorphology of the Brúarjökull surging glacier landsystem. *Journal of Maps 2007*, 349-367.

Evans, D.J.A., Clark, C.D., Rea, B.R., 2008. Landform and sediment imprints of fast glacier flow in the southwest Laurentide Ice Sheet. *Journal of Quaternary Science 23*, 249-272.

Eyles, N., Eyles, C.H., Miall, A.D., 1983. Lithofacies types and vertical profile models: an alternative approach to the description and environmental interpretation of glacial diamict and diamictite sequences. *Sedimentology 30*, 393–410.

Eythorsson, J., 1963: Brúarjökull hlaupinn (A sudden advance of Brúarjökull). *Jökull 13*, 19-21.

Eythorsson, J., 1964. Brúarjökulsleiðangur 1964 (An expedition to Brúarjökull 1964). *Jökull 14*, 104-107.

French, H.M., 1996. *The periglacial environment*. Longman, Harlow. 341 p.

Friedman, J.D., Johanson, C.E., Óskarsson, N., Svenson, H., Thorarinsson, S., Williams, R.S. jr., 1971. Observations on Icelandic polygon surfaces and palsa areas. Photo interpretations and field studies. *Geografiska Annaler 53A*, 115-145.

Flowers, G.E., Björnsson, H., Geirsdóttir, Á., Miller, G.H., Black, J.L., Clarke, G.K.C., 2008. Holocene climate conditions and glacier variation in central Iceland from physical modelling and empirical evidence. *Quaternary Science Reviews 27*, 797-813.

Guðmundsson, H., 1997. A review of the Holocene environmental history of Iceland. *Quaternary Science Reviews 16*, 81-92.

Guðmundsson, M.T., Högnadóttir, Þ., Björnsson, H., 1996. Brúarjökull: Framhlaupið 1963-1964 og áhrif þess á rennsli Jökulsár á Brú. *Raunvísindastofnun Háskólans, RH-11-96*. 33 p.

Gripp, K., 1929. Glaciological and geological results of the Hamburg Spitsbergen-expedition of 1927. In: van der Meer, J.J.M. (Ed.), Spitsbergen Push Moraines. Elsevier, Amsterdam. *Developments in Quaternary Science 4*, 3-98.

Hambrey, M.J., Huddart, D., 1995. Englacial and proglacial glaciotectonic processes at the snout of a thermally complex glacier in Svalbard. *Journal of Quaternary Science 10*, 313-326.

Hart, J.K., Watts, R., 1997. Comparison of the styles of deformation associated with two recent push moraines, south Van Keulenfjorden, Svalbard. *Boreas 25*, 277-243.

Hart, J.K., Martinez, K., Ong, R., Riddoch, A., Rose, K.C., Padhy, T., 2006. An autonomous multi-sensor subglacial probes: Design and preliminary results from Briksdalsbreen, Norway. *Journal of Glaciology 52*, 389-397.

Hart, J.K., Rose, K.C., Martinez, K., Ong, R., 2009. Subglacial clast behaviour and its implications for till fabric development: new results derived from wireless subglacial probe experiments. *Quaternary Science Reviews 28*, 597-607.

Houmark-Nielsen, M., Kjær, K.H., 2003. Southwest Scandinavia, 40-15 kyr BP: palaeogeography and environmental change. *Journal of Quaternary Science 18*, 769-786.

Huddart, D., Hambrey, M.J., 1996. Sedimentary and tectonic development of a high-Arctic thrust-moraine complex: Comfortlessbreen, Svalbard. *Boreas 25*, 227-243.

Humlum, O., 1985. Genesis of an imbricated push moraine, Höfðabrekkujökull, Iceland. *Journal of Geology 93*, 185-195.

Humphrey, N.F., Raymond, C.F., 1994.

Hydrology, erosion and sediment production in a surging glacier: Variegated Glacier, Alaska, 1982-83. *Journal of Glaciology 40*, 539-552.

Jennings, C.E., 2006. Terrestrial ice streams; a view from the lobe. *Geomorphology 75*, 100-124.

Jol, H.M., Bristow, C.S., 2003. GPR in sediments: advice on data collection, basic processing and interpretation, a good practice guide. In: Bristow, C.S., Jol, H.M. (Eds.), *Ground Penetrating Radar in Sediments*, vol. 211. Geological Society, London, pp. 9–27. Special Publications.

Kaldal, I., Víkingsson, S., 2000. Jarðgrunnskort af Eyjabökkum. *Orkustofnun, OS-2000/068*, 10 p.

Kamb, B. Raymond, C.F., Harrison, W.D., Engelhardt, H., Echelmeyer, K.A., Humphrey, N., Brugman, M.M., Pfeffer, T., 1985. Glacier surge mechanism: 1982–1983 surge of Variegated glacier, Alaska. *Science, 227(4686)*, 469–479.

Kjær, K.H., Krüger, J., 1998. Does clast size influence fabric strength? Journal of *Sedimentary Research 68*, 746–749.

Kjær, K.H., Sultan, L., Krüger, J., Schomacker, A., 2004. Architecture and sedimentation of fan-shaped outwash in front of the Mýrdalsjökull ice cap. Iceland. *Sedimentary Geology 172*, 139–163.

Kjær, K.H., Korsgaard, N.J., Schomacker, A., 2008. Impact of multiple glacier surges – a geomorphological map from Brúarjökull, East Iceland. *Journal of Maps 2008*, 5-20.

Kjerúlf, Þ., 1962. Vatnajökull hlaupinn (Brúarjökull 1890). *Jökull 12*, 47-48.

Kristensen, L., Benn, D.I., Hormes, A., Ottesen, D., 2009. Mud aprons in front of Svalbard surge moraines: Evidence of subglacial deforming layers or proglacial tectonics? *Geomorphology 111*, 206-221.

Krüger, J., 1985. Formation of a push moraine at the margin of Höfðabrekkujökull, South Iceland. *Geografiska Annaler 67A*, 199-212.

Krüger, J., 1993. Moraine-ridge formation along a stationary ice front in Iceland. *Boreas 22*, 101-109.

Krüger, J., 1994. Glacial processes, sediments, landforms and stratigraphy in the terminus region of Mýrdalsjökull, Iceland. *Folia Geographica Danica 21*, 1-233.

Krüger, J., 1996. Moraine ridges formed by subglacial frozen-on sediment slabs and their differentiation from push moraines. *Boreas 25*, 57-63.

Krüger, J., Kjær, K.H., 1999. A data chart for field description and genetic interpretation of glacial diamicts and associated sediments – with examples from Greenland, Iceland, and Denmark. *Boreas 28*, 386–402.

Krüger, J., Kjær, K.H., van der Meer, J.J.M., 2002. From push moraine to single-crested dump moraine during a sustained glacier advance. *Norsk Geografisk Tidsskrift 56*, 87-95.

Krüger, J., Schomacker, A., Benediktsson, Í.Ö., 2010. Ice marginal environments: Geomorphic and structural genesis of marginal moraines at Mýrdalsjökull. In: Schomacker, A., Krüger, J., Kjær, K.H. (Eds): The Mýrdalsjökull Ice Cap, Iceland. Glacial processes, sediments and landforms on an active volcano. *Developments of Quaternary Science 13*, 79-104.

Kuriger, E.M., Truffer, M., Motyka, R.J., Bucki, A.K., 2006. Episodic reactivation of large-scale push moraines in front of the advancing Taku Glacier, Alaska. *Journal of Geophysical Research 111*, F01009, doi:10.1029/2005JF000385.

Kälin, M., 1971. *The active push moraine of the Thompson Glacier, Axel Heiberg Island, Canadian Arctic Archipelago*. Axel Heiberg Island Research Reports, Glaciology No. 4, McGill University, Montreal. PhD thesis, ETH Zurich.

Lønne, I., Lauritsen, T., 1996. The architecture of a modern push-moraine at Svalbard as inferred from ground-penetrating radar measurements. *Arctic, Antarctic and Alpine Research 28*, 488-495.

Lyså, A., Lønne, I., 2001. Moraine development at a small high-Arctic valley glacier: Rieperbreen, Svalbard. J*ournal of Quaternary Science 16*, 519-529.

Marshak, S., Mitra, G., 1988. *Basic Methods of Structural Geology*. Prentice-Hall, Englewood Cliffs, NJ. 446 p.

Matthews, J.A., McCarrol, D., Shakesby, R.A., 1995. Contemporary terminal-moraine ridge formation at a temperate glacier, Styggedalsbreen, Jotunheimen, southern Norway. *Boreas 24*, 129-139.

McCarrol, D., Rijsdijk, K.F., 2003. Deformation styles as a key for interpreting glacial depositional environments. *Journal of Quaternary Science 9*, 209-233.

Mosola, A.B., Anderson, J.B., 2006. Expansion and rapid retreat of the West-Antarctic Ice Sheet in eastern Ross Sea: possible consequence of over-extended ice streams? *Quaternary Science Reviews 25*, 2177–2196.

Motyka, R.J., Echelmeyer, K.Á., 2003. Taku Glacier (Alaska, U.S.A.) on the move again: active deformation of proglacial sediments. *Journal of Glaciology 49*, 50-58.

Möller, P., 1995. Subrecent moraine ridge formation on Cuff Cape, Victoria Land, Antarctica. *Geografiska Annaler 77A*, 83-94.

Nelson, A.E., Willis, I.C., O'Cofaigh, C., 2005. Till genesis and glacier motion inferred from sedimentological evidence associated with the surge-type glacier, Brúarjökull, Iceland. *Annals of Glaciology 42,* 14-22.

Pedersen, S.A.S., 1996. Progressive glaciotectonic deformation in Weichselian and Palaeogene deposits at Feggeklit, northern Denmark. *Bulletin of the Geological Society of Denmark 42*, 153–174.

Pedersen, S.A.S., 2005. Structural analysis of the Rubjerg Knude Glaciotectonic Complex, Vendsyssel, northern Denmark. *Geological Survey of Denmark and Greenland Bulletin 8*, 1-192.

Phillips, E., Lee., J.R., Burke, H., 2008. Progressive proglacial to subglacial deformation and syntectonic sedimentation at the margins of Mid-Pleistocene British Ice Sheet: evidence from north Norfolk, UK. *Quaternary Science Reviews 27*, 1848-1871.

Piotrowski, J., Larsen, N.K., Junge, F.W., 2004. Reflections on soft subglacial beds as a mosaic of deforming and stables spots. *Quaternary Science Reviews 23*, 993-1000.

Ravn, L. 2006. *Interaktionen mellem klima og landskab-sediment-jordsystemet i et periglacialt miljø foran Brúarjökull, Island*. Cand. scient. (MSc) thesis, University of Copenhagen, 57 p.

Raymond, C.F., Johannesson, T., Pfeffer, T., 1987. Propagation of a glacier surge into stagnant ice. *Journal of Geophysical Research 92 (B9)*, 9037-9049.

Rignot, E., Kanagaratnam, P., 2006. Changes in the velocity structure of the Greenland ice sheet. *Science 311*, 986-990.

Roberts, D.H., Yde, J.C., Knudsen, N.T., Long, A.J., Lloyd, J.M., 2009. Ice marginal dynamics during surge activity, Kuannersuit Glacier, Disko Island, West Greenland. *Quaternary Science Reviews 28*, 209-222.

Schomacker, A. 2007. Dead-ice under different climate conditions: processes, landforms, sediments and melt rates in Iceland and Svalbard. *LUNDQUA Thesis 59*, 25 p. + 4 app.

Schomacker A., Krüger, J. & Kjær, K. H. 2006. Ice-cored drumlins at the surge-type glacier Brúarjökull, Iceland: a transitional-state landform. *Journal of Quaternary Science 21*, 85-93.

Schomacker, A., Kjær, K.H., 2007. Origin and de-icing of multiple generations of ice-cored moraines at Brúarjökull, Iceland. *Boreas 36*, 411-425.

Shakesby, R.A., 1989. Variability in Neoglacial moraine morphology and compositions, Storbreen, Jotunheimen, Norway: within-moraine patterns and their implications. *Geografiska Annaler 71A*, 17-29.

Sharp, M., 1985a. Sedimentation and stratigraphy at Eyjabakkajökull – an Icelandic surging glacier. *Quaternary Research 24*, 268-284.

Sharp, M., 1985b. "Creveasse-fill" ridges – a landform type characteristic of surging glaciers? *Geografiska Annaler 67A*, 213-220.

Sharp, M., Dugmore, A., 1985. Holocene glacier fluctuations in Eastern Iceland. *Zeitschrift für Gletcherkunde und Glazialgeologie 21*, 341-349.

Stokes, C.R., Clark, C.D., 2001. Palaeo-ice streams. *Quaternary Science Reviews 20*, 1437-1457.

Stokes, C.R., Clark, C.D., Lian, O.B., Tulaczyk, S., 2007. Ice stream sticky spots: a review of

their identification and influence beneath contemporary and palaeo-ice streams. *Earth-Science Reviews 81*, 217-249.

Sund, M., Eiken, T., Hagen, J.O., Kääb, A., 2009. Svalbard surge dynamics derived from geometric changes. *Annals of Glaciology 50*, 50-60.

Thorarinsson, S., 1938. Über anomale Gletcherswankungen mit besonderer Berücksichtigung des Vatnajökullgebietes. *Geologiska föreningen i Stockholms förhandlingar 60*, 3. Maj-oktober, 490-506.

Thorarinsson, S., 1943. Oscillations of the Icelandic glaciers in the last 250 years. *Geografiska Annaler 25*, 1-54.

Thorarinsson, S., 1964. On the age of the terminal moraines of Brúarjökull and Hálsajökull. *Jökull 14*, 67-75.

Thorarinsson, S., 1969. Glacier surges in Iceland, with special reference to the surges of Brúarjökull. *Canadian Journal of Earth Sciences 6*, 875-882.

Thoroddsen, Th., 1914. *Ferdabók. Skýrslur um rannsóknir á Íslandi 1882- 1898*. Þriðja bindi. Kaupmannahöfn, Hið íslenzka fræðafélag, 1914. 1-360.

Todtmann, E.M., 1953. Am Rand des Eyjabakkagletchers, Sommer 1953. *Jökull 3*, 34-36.

Todtmann, E.M., 1955. Übersicht über die Eisrandlagen in Kringilsárrani von 1890-1955. *Jökull 5*, 8-10.

Todtmann, E.M., 1960. Gletcherforschungen auf Island (Vatnajökull). *Universität Hamburg. Abhandlungen aus dem Gebiet der Auslandskunde 65C*, 1-95.

Twiss, R.J., Moores, E.M., 1992. *Structural Geology*. W.H. Freeman, New York, 532pp.

van Vliet-Lanoë, B., Bourgeois, O. & Dauteuil, O. 1998. Thufur formation in Northern Iceland and its relation to Holocene climate change. *Permafrost and Periglacial Processes 9*, 347-365.

van der Wateren, F.M., 1995a. Structural geology and sedimentology of push moraines: processes of soft sediment deformation in a glacial environment and the distribution of glaciotectonic styles. *Mededelingen Rijks Geologische Dienst, 54*.

van der Wateren, F.M., 1995b. Processes of glaciotectonism. In: Menzies, J. (Ed.), *Modern glacial environments: Processes, dynamics and sediments. Glacial Environments, vol. 1*. Butterworth-Heineman, London, pp. 309-335.

van der Wateren, F.M., 2003. Ice-marginal terrestrial landsystems: southern Scandinavian ice sheet margin. In: Evans, D.J.A.: *Glacial landsystems*. Arnold, London; 166-203.

Williams, R.S. jr., 1976. Vatnajökull ice cap, Iceland. *USGS Prof. Paper 929*, 188-193.

Winkler, S., Nesje, A., 1999. Moraine formation at an advancing temperate glacier: Brigdalsbreen, western Norway. *Geografiska Annaler 81A*, 17-30.

Winkler, S., Matthews, J.A., in press. Observations on terminal moraine-ridge formation during recent advances of southern Norwegian glaciers. *Geomorphology (2009)*, doi:10.1016/j.geomorph.2009.10.011.

APPENDIX I

Quaternary Science Reviews 25 (2006) 2704–2712

Subglacial decoupling at the sediment/bedrock interface: a new mechanism for rapid flowing ice

Kurt H. Kjær[a,*], Eiliv Larsen[b], Jaap van der Meer[c], Ólafur Ingólfsson[d], Johannes Krüger[e], Ívar Örn Benediktsson[d], Carita G. Knudsen[f], Anders Schomacker[g]

[a]*Natural History Museum of Denmark, Geological Museum, University of Copenhagen, Øster Voldgade 5-7, DK-1350 Copenhagen K, Denmark*
[b]*Geological Survey of Norway, N-7491 Trondheim, Norway*
[c]*Department of Geography, University of London, Queen Mary, Mile End Road, London E1 4NS, UK*
[d]*Department of Geology and Geography, University of Iceland, Askja, IS-101 Reykjavík, Iceland*
[e]*Geocenter Copenhagen, Institute of Geography, University of Copenhagen, Øster Voldgade 10, DK-1350 Copenhagen K, Denmark*
[f]*Department of Earth Science, University of Bergen, Allegaten 41, N-5007 Bergen, Norway*
[g]*GeoBiosphere Science Centre, Department of Geology, Quaternary Sciences, Lund University, Sölvegatan 12, S-223 62 Lund, Sweden*

Received 28 February 2006; accepted 17 June 2006

Abstract

On millennial or even centennial time scales, the activity of rapid flowing ice can affect climate variability and global sea level through release of meltwater into the ocean and positive feedback loops to the climate system. At the surge-type glacier Brúarjökull, an outlet of the Vatnajökull ice cap, eastern Iceland, extremely rapid ice flow was sustained by overpressurized water causing decoupling beneath a thick sediment sequence that was coupled to the glacier. This newly discovered mechanism has far reaching consequences for our understanding of fast-flowing ice and its integration with sediment discharge and meltwater release.

1. Introduction

Interest in fast ice flow behaviour is stimulated by recent events along the periphery of contemporary ice sheets, where interior collapse subsequent to ice shelf disintegration is suddenly a realistic possibility (De Angelis and Skvarca, 2003). In the present state of rapid global environmental changes there is a growing wish to understand the causal mechanisms behind ice sheet instability and its contribution to global sea level rise (Alley and Bindschadler, 2001; Clark et al., 2002; Domack et al., 2005). Fast flowing ice streams and surging glaciers exert a strong control on the discharge of the Antarctic and Greenland ice sheets acting as regulators on their configuration and stability (Dowdeswell et al., 2004; Rignot and Kanagaratnam, 2006). Consensus in the literature dictates that mechanisms behind ice flow variability and distribution of meltwater are linked to subglacial processes influencing basal motion and not to ice-mechanical processes (Boulton and Hindmarsh, 1987; Fischer and Clarke, 2001). An important issue is, however, to identify and quantify the different hydro-mechanical processes beneath the ice and in particular the significance of deep-seated sediment deformation as it is directly linked to predictions of ice sheet stability (Clarke, 2005). Surge-type glaciers provide an opportunity to probe this problem as they experience major fluctuations in velocity between phases of active surging and quiescence. Between surge events as the glacier ice retreats—a landform association and sediment succession re-emerges imprinted with vital information on subglacial driving processes.

2. Setting

Brúarjökull, a northern outlet of the Vatnajökull ice cap in eastern Iceland, has experienced major velocity fluctuations switching between active winter surging of some 3 months duration and quiescent phases lasting from 70 to 90 years (Todtmann, 1960; Thorarinsson, 1969; Raymond,

*Corresponding author. Tel.: +45 3532 2374; fax: +45 3523 2325.
E-mail address: kurtk@snm.ku.dk (K.H. Kjær).

0277-3791/$ - see front matter © 2006 Elsevier Ltd. All rights reserved.
doi:10.1016/j.quascirev.2006.06.010

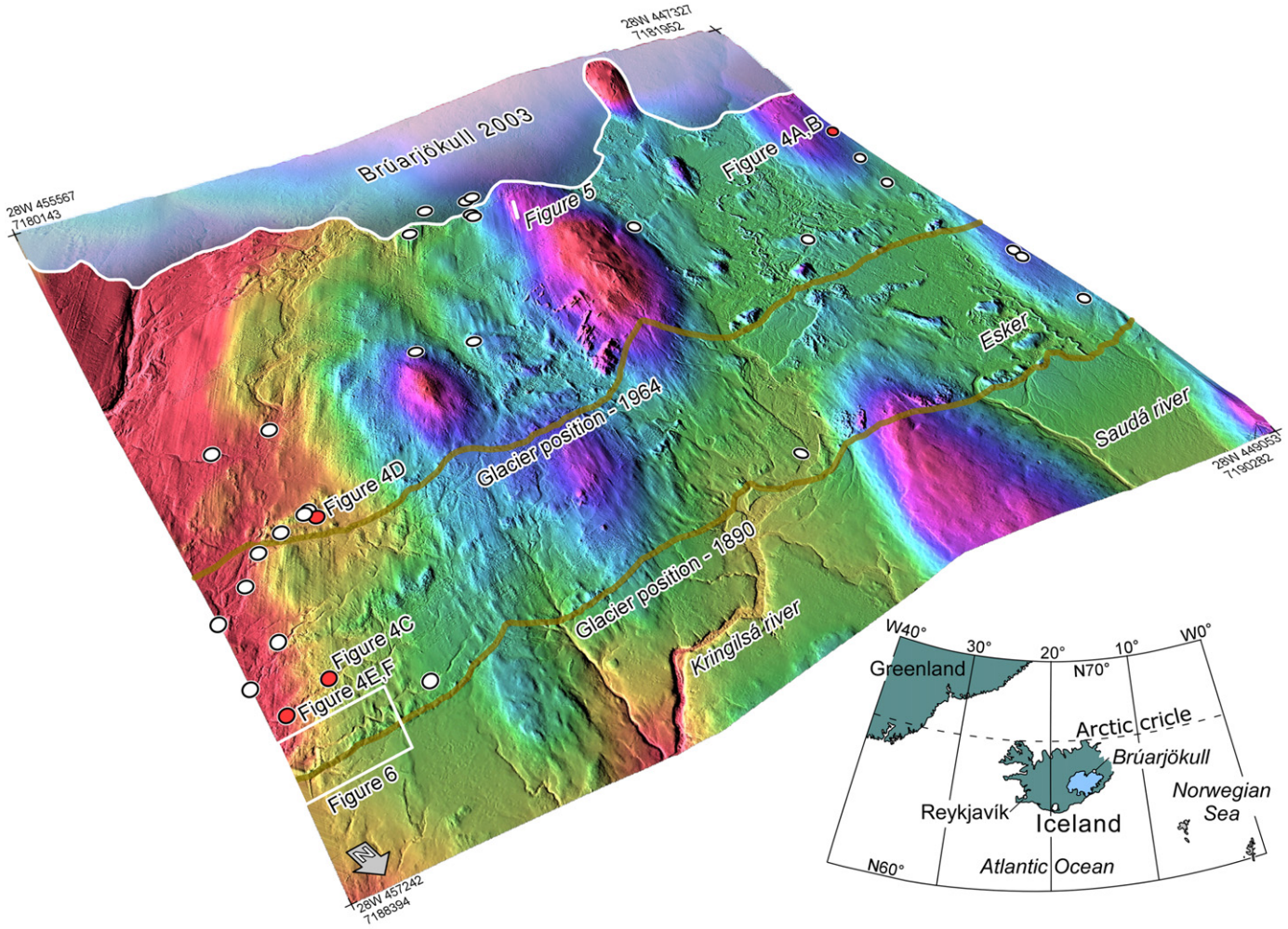

Fig. 1. The forefield of the surge-type glacier Brúarjökull, eastern Iceland. Terrain-Shaded Relief (TSR) draped over a digital elevation model based on a 3 m grid generated from ortho-rectified 1:15,000 aerial photographs recorded in 2003. Dots mark localities used for detailed sedimentological and stratigraphical studies.

1987). During the most recent surges initiated in 1890 and 1963 the glacier advanced respectively, 10 and 8 km affecting an area of roughly 1400 km^2 (Fig. 1). Recent surges in 1890 and 1963 were documented in the field and the meltwater discharge was described prior and subsequent to surges (Thoroddsen, 1914; Thorarinsson, 1969). The peak velocity was at least 125 m/day over a period of almost three months (Thorarinsson, 1969), which exceeds even the fastest ice streams in Antarctica and Greenland (Echelmeyer and Harrison, 1990; Joughin et al., 2002). Basaltic rocks overlain by $\leqslant$6 m unlithified sediments comprise the subglacial lithologies around the fringe of Brúarjökull.

Oblique 1964 aerial photographs of the surging Brúarjökull testify that it was heavily crevassed and disintegrated as internal ice deformation was unable to compensate sufficiently for extreme lateral extension during the active phase. In the succeeding quiescent phase, the glacier retreated passively as seen from consecutive aerial photographs and satellite imagery recorded in 1964, 1988, 1993, 2002 and 2003. Measurements of ice displacement between 2003 and 2005 show negligible glacier movement, while the glacier front retreated up to 250 m/year and the surface lowered 6–7 m/year (Fig. 2). Therefore, the glacier experiences no forward movement during the quiescent phase and except for stagnation features all processes related to depositional landforms and subglacial deformation are restricted to the surge phase. Effectively, the glacier in the present quiescence state behaves like a dead-ice body.

3. Earlier models for fast ice flow

Rapid ice flow velocities reached either by ice streams or surging glaciers, have hitherto been explained by two modes of basal motion largely dependent on ice/bed coupling (Fischer and Clarke, 2001). Decoupling of a glacier from its bed enables fast ice flow through enhanced basal sliding across the ice/bed interface or very shallow subglacial deformation, i.e. the basal sliding model in Fig. 3A (Engelhardt and Kamb, 1998). Alternatively, fast ice flow is sustained by deformation of water-saturated subglacial sediment that is strongly coupled to the glacier,

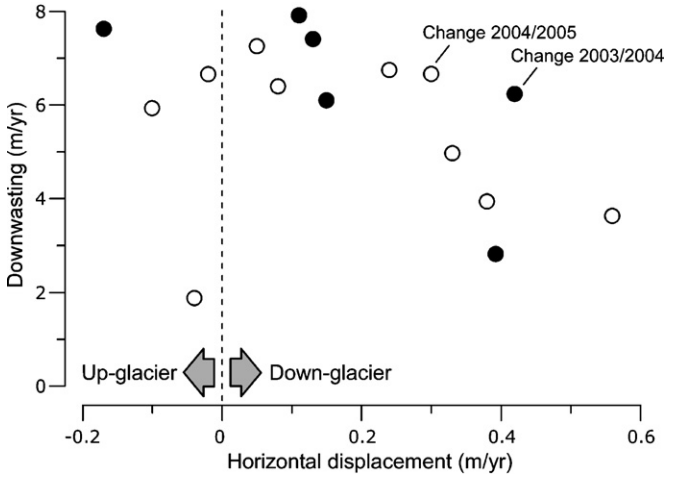

Fig. 2. Ice velocity—horizontal displacement of the frontal 1–2 km of Brúarjökull, as a function of downwasting in the period 2003–05. Measurements were carried-out along three transects from a stable benchmark to fix points on the ice surface using a precision levelling instrument with an accuracy of ±5 mm. As no bulge or other compressional features were observed beyond 2 km, the area of limited ice velocity must extend for an unknown distance upstream of the marginal zone.

i.e. the deformable bed model in Fig. 3B (Alley et al., 1989). Irrespective of the flow mechanism, the driving process is associated with disruption and reorganization of the hydrological drainage system along the ice/bed interface (Harrison and Post, 2003). It has been suggested that a discrete canalized drainage system with low basal water pressure across the bed favours a strong ice/bed coupling, while an inefficient, distributed drainage system with high basal water pressures sustains decoupling (Boulton et al., 2001). Also, it has been proposed that switching from efficient to inefficient subglacial drainage might trigger surge activity (e.g. Kamb, 1987; Björnsson, 1998). Both the basal sliding and deformable bed models for fast ice flow have inherent problems (Fig. 3A and B). In model (A), because landforms and sub-surface sediments related to rapid ice flow often display depositional and deformational features that suggest strong ice/bed coupling and little evidence for enhanced basal sliding across the ice/bed interface. Regarding model (B) it is still debated whether spatial continuity of subglacial deformation is able to support fast ice flow or whether it is linked to steady slower flowing ice (van der Meer et al., 2003; Piotrowski et al.,

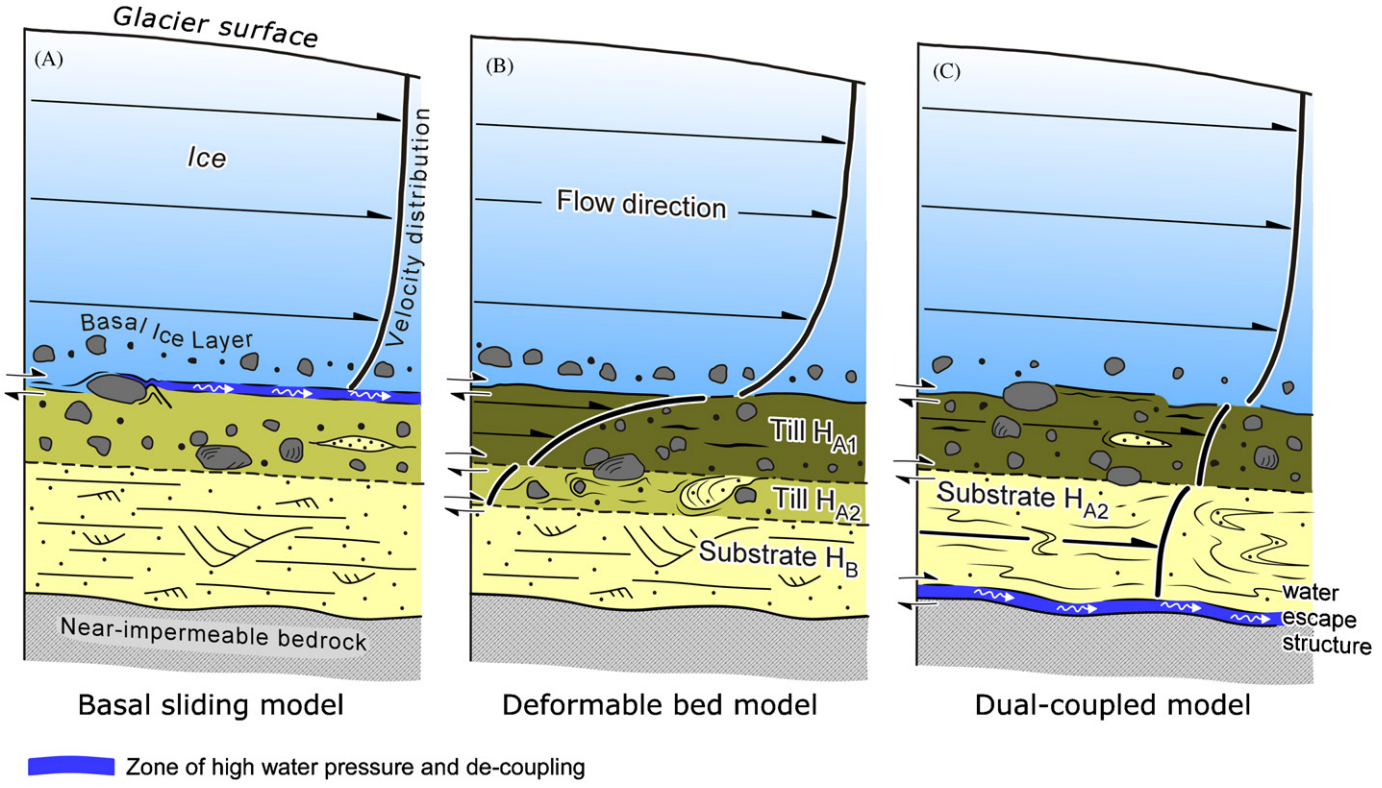

Fig. 3. Basal motion models associated with ice streams and surging glaciers. (A) Decoupling is sustained by enhanced basal sliding across the glacier–till interface with limited or no subglacial deformation (Engelhardt and Kamb, 1998). Flutes may develop by boulders ploughing through the bed or generated by downstream extension of grooves in the basal ice (Tulaczyk, 1999). (B) The glacier is coupled to its bed and fast ice flow is sustained through subglacial deformation of water-saturated sediment with a low effective pressure (Alley et al., 1989). A horizon with fast deforming sediment and high strain rates (H_{A1}) overlies a horizon with more slowly deforming sediment and low strain rates (H_{A2}) that is superimposed on stable horizon without deformation (H_B) (Boulton and Hindmarsh, 1987). (C) In the dual-coupled model from Brúarjökull developed, herein, the glacier is coupled to its bed as expressed in slow subglacial deformation, while the substrate is decoupled from the bedrock leading to fast ice flow and a substantial dislocation of sediments. Water escape structures indicate that water and sediment were forced along a near-impermeable bedrock surface leading to substrate separation due to overpressurized water.

2004). Arguments for a thinner and discontinuous deformable bed are provided from observations at modern glaciers and laboratory experiments that fail to simulate any significant thickness of deformable beds (Piotrowski et al., 2004).

4. Glaciodynamic interfaces

The continued recession of Brúarjökull by frontal retreat reveals a streamlined till plain superimposed on larger bedrock features and subglacial landforms developed across the ice/till interfaces (Schomacker et al., 2006) during the 1890 and 1964 surges (Fig. 1). Narrow, regularly spaced flutes are traced across the entire area from the present-day ice margin to the end moraines that mark former surge terminations (Fig. 1). Some flutes continue for more than 1.5 km with an elongation ratio >500, many of them initiated by a proximal boulder (Fig. 4A). Minor, less than 10 m long, incipient flutes and sediment prows also occur upon the till plain (Fig. 4B). A case study was carried out in a 70 m long and up to 1 m wide flute released from the glacier during 2003 (Figs. 1 and 5). The principal eigenvectors (V_1) of all clast fabrics ($n = 16$) deviate on average 11° from the ice-flow direction as indicated by the flute orientation (209°–029°). This variation in orientation is related to the flow pattern associated with stoss-side divergence and lee-side convergence of flow trajectories around high-lying bedrock or boulders. Differences in fabric strength, on the other hand, as indicated by the eigenvalues show a higher degree of clustering in fabric measurements from the central part of the flute ridge (average S_1: 0.80 ± 0.04) than on the flanks (average S_1: 0.65 ± 0.08) with a total average S_1 of 0.68 ± 0.09.

Beneath the till plain, the 6 m of glacial sediments were accumulated during multiple surge advances and retreats as indicated by superimposed till beds interbedded by sorted sediments and the signature left by several generations of deformation. The simplest sediment architecture is recognized below the 1890 surge surface; comprising a till and a loess-peat-tephra (LPT) sequence overlying bedrock. The till is dark grey-brownish, shear banded, silty-sandy, matrix-supported, firm and less than 1 m thick. The till/substrate interface is transitional including a 5–10 cm thick shear zone, often truncating the upper flank of drag folds or shear-rotational structures. Similar shear structures and overturned folds are identified in the underlying LPT-sequence, which overprints reverse and normal fractures (Fig. 4C and D). Without exception these ductile-brittle deformations extends down to the bedrock surface reflecting a 4–6 m thick deformable bed.

At the substrate-bedrock interface a set of waterlain interlaminated sediments are hosted between the LPT-sequence and near-impermeable basaltic bedrock (Fig. 4E and F). This laminated unit sharply truncates the base of the LPT-sequence unconformably, while it conformably superimposes even the smallest irregularities of the bedrock surface (Fig. 4E). A range of lithofacies is recognized, such as interlaminated clay and silt, massive or down- and upward-directed gradation of fine sand, and stringers of fine gravel together with occasional angular blocks of laminated stiff silt and clay. Within the surge field of Brúarjökull, these bedrock-contact interlaminated sediments are widespread and their bedding is always parallel with the bedrock surface. In the proximal part of the forefield i.e. inside the 1964 surge moraine, these interlaminated sediments are predominately disturbed probably associated with repeated ice advances. Outside the maximum surge limit interlaminated sediments have not been observed below the LPT-sequence. We interpret the interlaminated sediments as an indication of pressurized water movement and the associated structures as water escape structures (clastic dykes/hydrofractures) related to hydrofracturing between near-impermeable bedrock and a soft-bedded sediment succession as a result of increased subglacial porewater pressure during active surge (Boulton and Caban, 1995; van der Meer et al., 1999). Lateral intrusion and the expansion of hydrofractures probably occurred repeatedly during the surge phase as subglacial porewater pressure fluctuated and a symmetric pattern of lamina developed on across the centre of the intrusion (Fig. 4F). Furthermore, immediately outside the 1890 and 1964 end moraines several circular dry depressions form the abrupt head of proglacial channels. Excavations in one of these depressions revealed the presence of an open tunnel extending upglacier (Fig. 6). We interpret these features as blow-outs in front of the end moraine caused by overpressurized water linked to piping of subsurface running water in a discrete network of interconnected tunnels (Jones, 1977).

5. The dual-coupled model and its wider implications

The sediment succession and its properties at Brúarjökull provide evidence as to where decoupling and displacement leading to fast ice flow must occur: at the ice/till interface, within the LPT-sequence, or at the interface between the bedrock and the LPT-sequence. Rapid displacement along the interface between the till and LPT-sequence is excluded as it precludes the flute formation that demonstrably took place during the entire surge phase. Weak clast orientation

Fig. 4. Sediment interfaces identified in the stratigraphical succession at Brúarjökull. Ice/bed interface: (A) Long flute ridges, up to 1.5 km, mirroring ice-flow trajectories. (B) Sediment prows in front of boulders and minor incipient flutes developed subsequent to long flute ridges. Till/substrate interface: (C) Tills are dark grey-brownish, shear banded, silty-sandy, matrix-supported, firm and less than 1 m thick. Deformed 4–5 metre thick Loess-Peat-Tephra (LPT) sequence beneath subglacial till. Each ruler is 2 m long. Discordant basal contact at the till/substrate interface associated with a minor shear zone: (D). Substrate-bedrock interface: (E) Water escape structures discordantly breaking through the lower part of the LPT-sequence. (F) Close-up of water escape structures showing internal details within the feature. Ice flow direction from right to left.

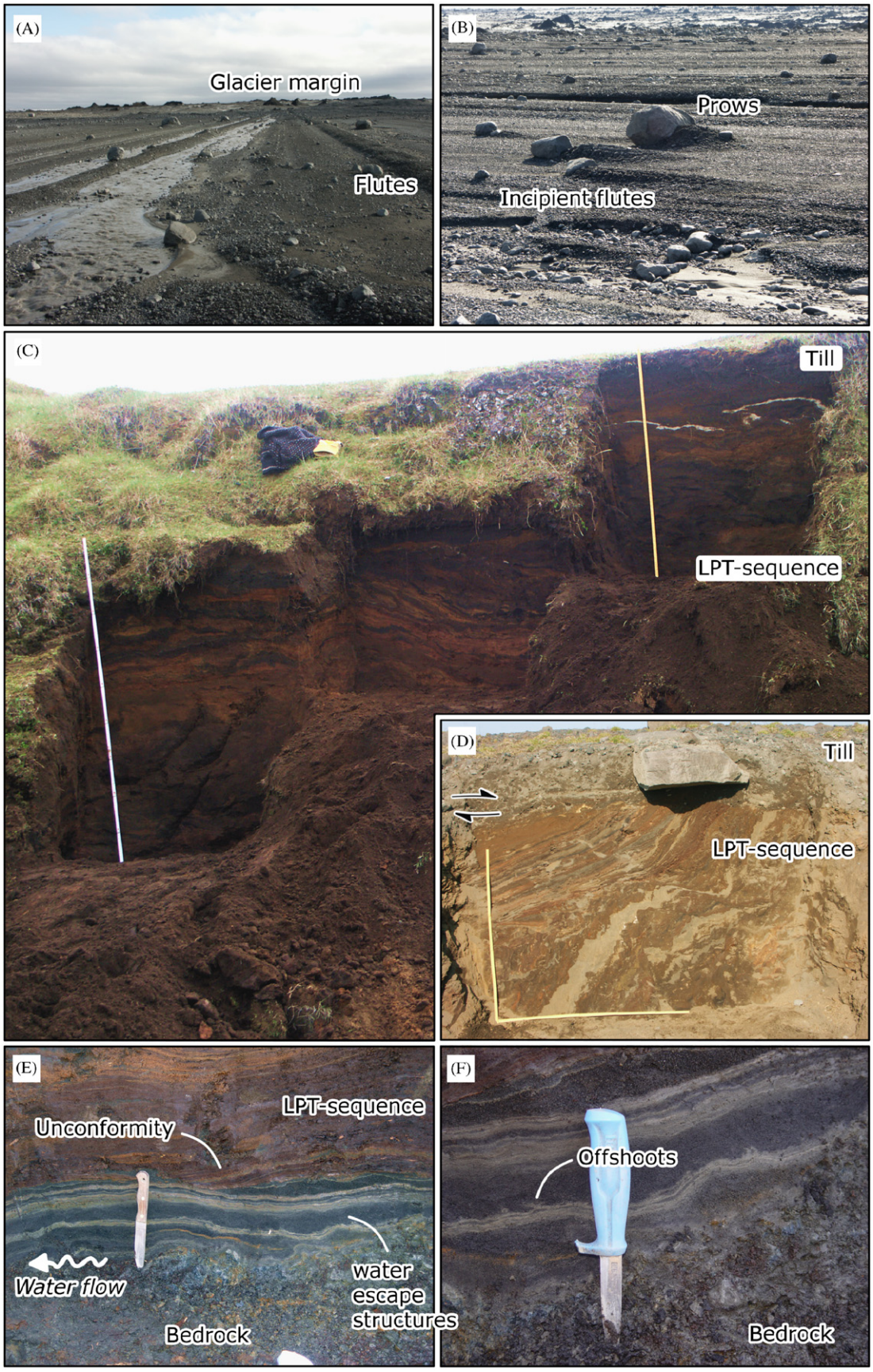
(A)
Glacier margin
Flutes
(B)
Prows
Incipient flutes
(C)
Till
LPT-sequence
(D)
Till
LPT-sequence
(E)
LPT-sequence
Unconformity
Water flow
water escape structures
Bedrock
(F)
Offshoots
Bedrock

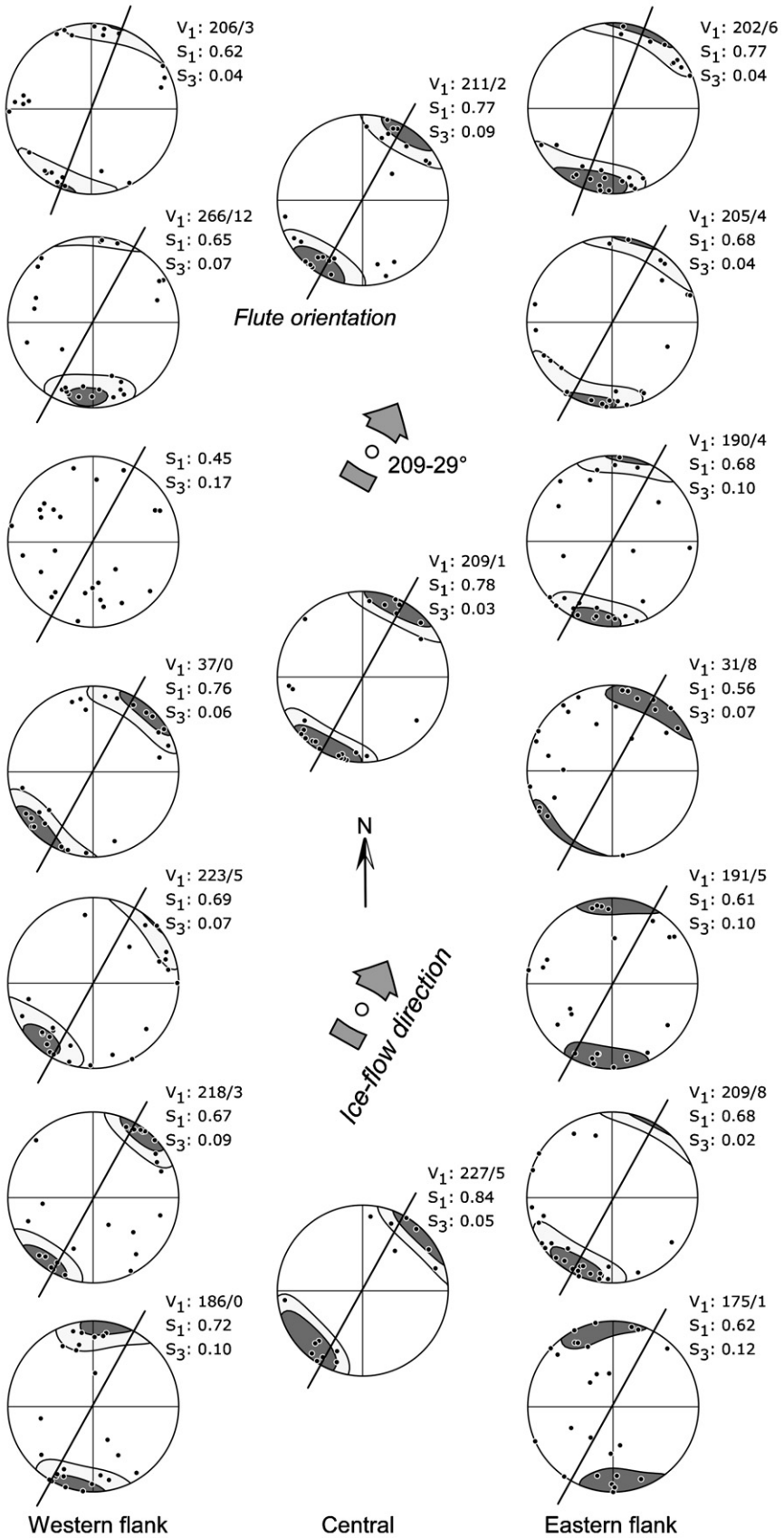

Fig. 5. Clast fabrics on both flanks and central part of a 100 metres long flute ridge exposed in 2004. All clast fabrics were acquired from small sub-horizontal volumes ($25 \times 25 \times 10$ cm) using clasts with an *a:b*-axis ratio $\geqslant 1.5$ and an axis length between 0.6 and 6 cm. Each clast fabric consists of 25 observations evaluated through the (Mark, 1973) eigenvector method using the program SpheriStat for actual calculations. Clast fabric interpretation is validated and supported by contoured diagrams after Kamb (1959) using three and six times the standard deviation to identify non-random distribution.

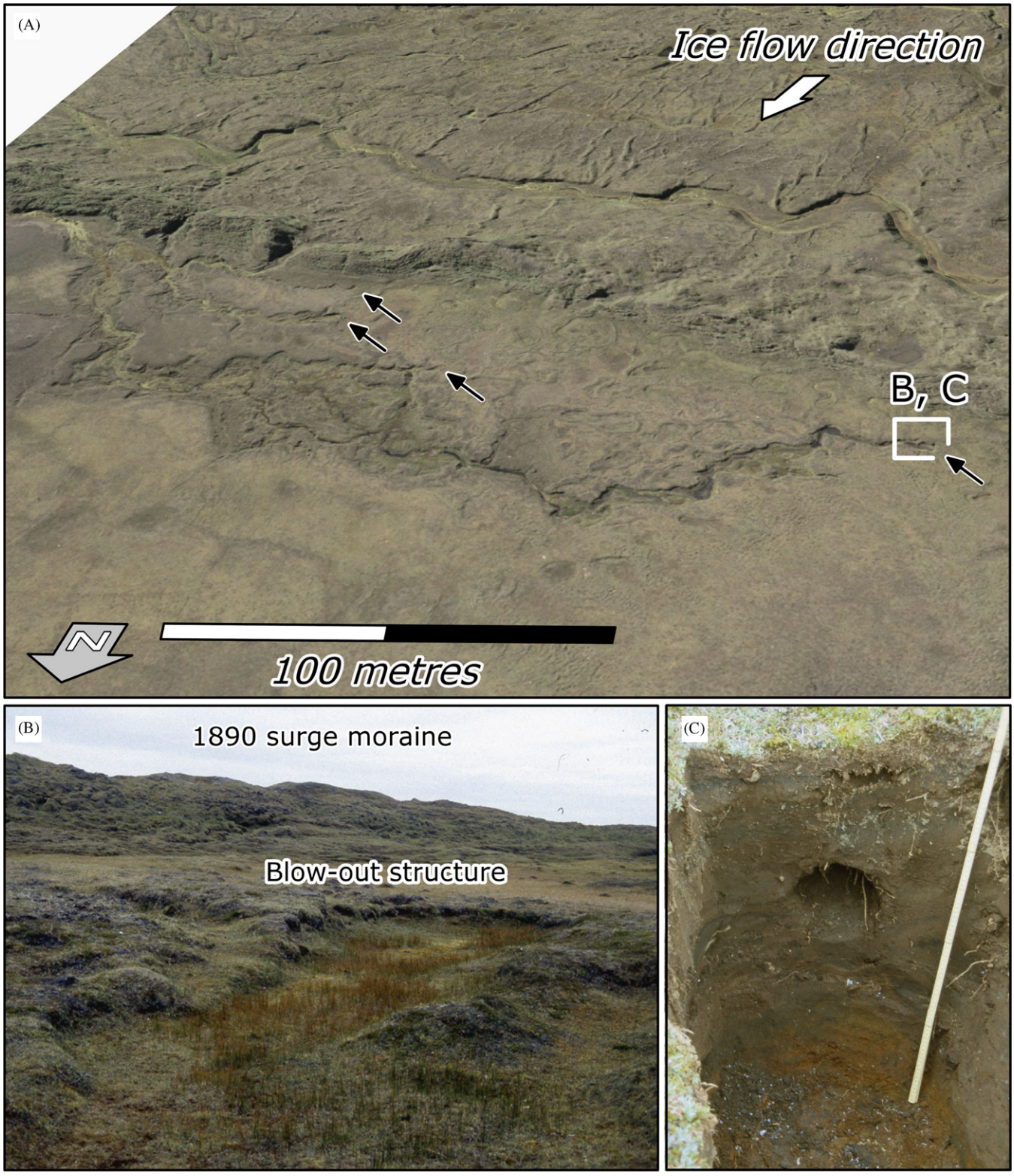

Fig. 6. Blow-out structures distally to the 1890 surge termination indicating the emergence of overpressurized water beyond the hydraulic head of the glacier. (A) Ortho-photographs draped over a digital elevation model based on a 3 m grid. Arrows mark abruptly appearing channels initiated by a circular structure. (B) Upstream part of blow-out structure. (C) Section through the initiating channel showing an open tunnel indicating piping of water. The ruler is 1 m long.

in flutes has previously been taken to indicate limited coupling between the glacier and its bed (Evans and Rea, 2003). However the case study of clast fabrics in our work does not confirm this conclusion and we find no evidence for a decoupling at the ice/till interface as clast fabrics in the flute have a preferred orientation and many flute

initiates with an obstruction boulder (Rose, 1989) (Fig. 5). Subglacial deformation within the LPT-sequence that sustained the displacement necessary for the fast ice flow reported during the Brúarjökull surges is likewise considered unlikely as structures only reflects moderate strain rates. On the other hand, the widespread occurrence of hydrofractures within the Brúarjökull forefield implies evacuation of large quantities of meltwater along the substrate/bedrock interface, which suggests that overpressurized water carried both the sediment burden and the weight of the glacier. Therefore, the decoupling or principal velocity component driving the surges of Brúarjökull was located across the bedrock (Fig. 3C) and not at the ice/till interface as commonly assumed for surge-type glaciers (Evans and Rea, 2003). This implies that during surges copious water is supplied from upstream sources other than basal melting as the relative thick succession of sediments would insulate the ice from frictional heating generated by fast sliding or deformation near the ice-bed interface.

Thus the data from Brúarjökull provides us with a new concept to explain glacier motion for surge-type glaciers. This concept may offer explanations to results obtained at localities where emplaced geophysical instruments demonstrate an absence of enhanced basal sliding or ploughing. It is as such complementary to the results from Black Rapids Glacier where deep-seated displacement was sought to explain basal motion (Truffer et al., 2000), and therefore provides important information to the ongoing discussion on the significance of deep deformation (Clarke, 2005). Our results would also suggest that the target for quantitative modelling of basal motion should be redirected from the ice/sediment interface to the sediment/bedrock interface. A further qualitative prediction that might be drawn from the vertical velocity model at Brúarjökull is that well drained areas may have acted as zones of compression or 'sticky spots' due to the possibilities for subglacial water to evacuate. A sudden decrease in porewater pressure at the substrate/bedrock interface should transfer shear stress into the succession of dislocated sediments leading to internal compression, overthrusting of sediment and formation of glaciotectonic ridges orientated perpendicular to the ice flow direction. The end moraine ridges that mark the surge termination in 1890 and 1964 may have formed where subglacial drainage permitted overpressurized water to escape, which led to compressional build-up of submarginal sediments.

Acknowledgement

Financial support for this study was received from the Swedish National Research Council (Kurt H. Kjær, contract no. 621-2002-4753), The Royal Physiographic Society in Lund, Crafoord Foundation, Landsvirkjun, the University of Iceland Research Fund, Icelandic Research Council (Rannís) and the Danish Natural Research Council.

The National Museum of Iceland is thanked for providing permission and access to the photo archive of Sigurður Thorarinsson, and his son, Sven Sigurðsson, is acknowledged for retrieving the photographic material from Brúarjökull. Also we extent our gratitude to all the members of the 2003–2005 field campaigns at Brúarjökull. Niels S. Christensen and Niels J. Korsgaard provided invaluable assistance with 3D presentations and orthorectification of aerial photographs. Constructive comments and suggestions for improvements of the manuscript by John Menzies and Richard C. A. Hindmarsh are much appreciated. T. Murray and J. Rose supplied excellent and highly useful reviews.

References

Alley, R.B., Bindschadler, R.A. (Eds.), 2001. The West Antarctic Ice Sheet. American Geophysical Union, Washington, DC, (296pp).

Alley, R.B., Blankenship, D.D., Rooney, S.T., Bentley, C.R., 1989. Water-pressure coupling of sliding and bed deformation: III. Apllication to ice stream B, Antarctica. Journal of Glaciology 35, 130–139.

Björnsson, H., 1998. Hydrological characteristics of the drainage system beneath a surging glacier. Nature 395, 771–774.

Boulton, G.S., Caban, P., 1995. Groundwater flow beneath ice sheets: part II—its impact on glacier tectonic structures and moraine formation. Quaternary Science Reviews 14, 563–587.

Boulton, G.S., Hindmarsh, R.C.A., 1987. Sediment deformation beneath glaciers: rheology and geological consequences. Journal of Geophysical Research 92, 9059–9082.

Boulton, G.S., Dobbie, K.E., Zatsepin, S., 2001. Sediment deformation beneath glaciers and its coupling to the subglacial hydraulic system. Quaternary International 86, 3–28.

Clark, P.U., Mitrovica, J.X., Milne, G.A., Tamisiea, M.E., 2002. Sea-level fingerprinting as a direct test for the source of global meltwater pulse IA. Science 295, 2438–2441.

Clarke, G.K.C., 2005. Subglacial processes. Annual Review of Earth and Planetary Science 33, 247–276.

De Angelis, H., Skvarca, P., 2003. Glacier surge after ice shelf collapse. Science 299, 1560–1562.

Domack, E., Duran, D., Leventer, A., Ishman, S., Doane, S., McCallum, S., Amblas, D., Ring, J., Gilbert, R., Prentice, M., 2005. Stability of the Larsen B ice shelf on the Antarctic Peninsula during the Holocene epoch. Nature 436, 681–685.

Dowdeswell, J.A., Ó Cofaigh, C., Pudsey, C.J., 2004. Thickness and extent of the subglacial till layer beneath an Antarctic paleo-ice stream. Geology 32, 13–16.

Echelmeyer, K., Harrison, W.D., 1990. Jakobshavn Isbræ, west Greenland: seasonal variations in velocity—or the lack thereof. Journal of Glaciology 36, 82–88.

Engelhardt, H., Kamb, B., 1998. Basal sliding of ice stream B, West Antarctica. Journal of Glaciology 44, 223–230.

Evans, D.J.A., Rea, B.R., 2003. Surging glacier landsystem. In: Evans, D.J.A. (Ed.), Glacial Landsystems. Arnold, London, pp. 259–288.

Fischer, U.H., Clarke, G.K.C., 2001. Review of subglacial hydro-mechanical coupling: Trapridge glacier, Yukon Territory, Canada. Quaternary International 86, 29–43.

Harrison, W., Post, A., 2003. How much do we really know about glacier surging? Annals of Glaciology 36, 1–6.

Jones, J.A.A., 1977. Global Hydrology. Longman, Harlow (pp. 1–399).

Joughin, I., Tulaczyk, S., Bindschadler, R.A., Price, S.J., 2002. Changes in West Antarctica ice stream velocities: observations and analysis. Journal of Geophysical Research 107, 2289.

Kamb, B., 1987. Glacier surging mechanism based on linked cavity system configuration of the basal water conduit system. Journal of Geophysical Research 92, 9083–9100.

Kamb, W.B., 1959. Ice petrofabric observations from Blue Glacier, Washington, in relation to theory and experiment. Journal of Geophysical Research 64, 1891–1909.

Mark, D.M., 1973. Analysis of axial orientation data, including till fabrics. Geological Society of America, Bulletin 84, 1369–1374.

Piotrowski, J., Larsen, N.K., Junge, F.W., 2004. Reflections on soft subglacial beds as a mosaic of deforming and stable spots. Quaternary Science Review 23, 993–1000.

Raymond, C.F.J., 1987. How do glaciers surge? A review. Journal of Geophysical Research 92, 9121–9134.

Rignot, E., Kanagaratnam, P., 2006. Changes in the velocity structure of the Greenland ice sheet. Science 311, 986–990.

Rose, J., 1989. Glacier stress patterns and sediment transfer associated with the formation of superimposed flutes. Sedimentary Geology 62, 151–176.

Schomacker, A., Krüger, J., Kjær, K.H., 2006. Ice-cored drumlins at the surge-type glacier Brúarjökull, Iceland: a transitional-state landform. Journal of Quaternary Science 21, 85–93.

Todtmann, E.M., 1960. Gletscherforschungen auf Island (Vatnajökull). Abhandlungen aus dem Gebiet der Auslandskunde 65, 95.

Thorarinsson, S., 1969. Glacier surges in Iceland, with special reference to the surges of Brúarjökull. Canadian Journal of Earth Sciences 6, 875–882.

Thoroddsen, TH., 1914. Ferðabók. Skýrslur um rannsóknir á Íslandi 1882–1898. 3. bindi. Hið íslenzka fræðafélag, Kaupmannahöfn, pp. 1–360.

Truffer, M., Harrison, W.D., Echelmeyer, K.A., 2000. Glacier motion dominated by processes deep in underlying till. Journal of Glaciology 46, 213–221.

Tulaczyk, S., 1999. Ice sliding over weak, fine-grained tills: dependence of the ice–till interactions on till granulometry. In: Mickelson, D.M., Attig, J.W. (Eds.), Glacial Processes: Past and Present. Geological Society of America Special Papers 337, pp. 159–177.

van der Meer, J.J.M., Kjær, K.H., Krüger, J., 1999. Subglacial water escape structures and till structures, Sléttjökull, Iceland. Journal of Quaternary Science 14, 191–205.

van der Meer, J.J.M., Menzies, J., Rose, J., 2003. Subglacial till: the deforming glacier bed. Quaternary Science Reviews 22, 1659–1685.

APPENDIX II

ELSEVIER

Quaternary Science Reviews 27 (2008) 209–234

QSR

Instantaneous end moraine and sediment wedge formation during the 1890 glacier surge of Brúarjökull, Iceland

Ívar Örn Benediktsson[a,*], Per Möller[b], Ólafur Ingólfsson[a], Jaap J.M. van der Meer[c], Kurt H. Kjær[d], Johannes Krüger[e]

[a]*Institute of Earth Sciences, University of Iceland, Askja, Sturlugata 7, IS-101 Reykjavík, Iceland*
[b]*GeoBiosphere Science Centre, Department of Geology/Quaternary Sciences, Lund University, Sölvegatan 12, SE-22362 Lund, Sweden*
[c]*Department of Geography, Queen Mary University of London, Mile End Road, London E1 4NS, UK*
[d]*Natural History Museum of Denmark, Geological Museum, University of Copenhagen, Øster Voldgade 5-7, DK-1350 Copenhagen K, Denmark*
[e]*Department of Geography and Geology, University of Copenhagen, Øster Voldgade 10, DK-1350 Copenhagen K, Denmark*

Received 31 May 2007; received in revised form 19 September 2007; accepted 8 October 2007

Abstract

Contemporary understanding of the behaviour of surging glaciers and ice streams is hampered by the lack of data on landsystem evolution and sedimentary environments. This study concerns the ice-marginal environment of the surge-type Brúarjökull in Iceland. The sediment distribution in the glacier forefield as well as the morphology, sedimentology and tectonic architecture of the 1890 end moraine is investigated for highlighting the interaction between very dynamic ice and sediment/landform associations.

As a result of substrate/bedrock decoupling during the 1890 surge, subglacial sediment was dislocated across the bedrock surface and deformed compressively, leading to gradual substrate thickening and the formation of a sediment wedge in the marginal zone. A drop in subglacial porewater pressure at the very end of the surge led to substrate/bedrock coupling and a stress transfer up into the sediment sequence causing brittle deformation of the substrate. Simultaneously, the glacier toe ploughed into the topmost part of the marginal sediment wedge initiating the moraine-ridge construction. Fine-grained and incompetent sediment deformed in ductile manner, resulting in a narrow moraine dominated by rooted folds, while coarse-grained and competent sediment deformed in brittle fashion, resulting in a wider moraine dominated by thrust blocks.

A new sequential model of subglacial and ice-marginal processes operating during a glacier surge is proposed, illustrating the stepwise formation of a marginal sediment wedge and an end moraine—a twofold, inseparable marginal end-product that formed during the last days of the 1890 surge.

1. Introduction

Ridge-shaped end moraines are among the most prominent and important landforms of glacial landsystems; they parallel the glacier margin and are produced during glacier advances or still-stands. As end moraines outline the configuration of past and present glaciers, they are very important when interpreting modern glacial landsystems or reconstructing ancient glacial environments. End moraines display wide variety of morphologies, sediments and tectonic architectures, and are reliable indicators of sedimentary and glaciotectonic processes, whether these are of a subglacial, ice-marginal or proglacial nature. End moraines also reflect both varying dynamics of glaciers and different sedimentary and topographic conditions of the forelands across which glaciers advance (van der Wateren, 1995b; Benn and Evans, 1998; Bennett, 2001; Bennett et al., 2004a).

End moraines at contemporary glacier margins have increasingly been investigated to serve as analogues to Pleistocene end moraines. Most of this research has concentrated on end moraines of non-surging glaciers (e.g. Kälin, 1971; Humlum, 1985; Krüger, 1985, 1993, 1994, 1996; Boulton, 1986; Shakesby, 1989; Hambrey and Huddart, 1995; Matthews et al., 1995; Möller, 1995;

*Corresponding author. Tel.: +354 525 4305.
E-mail address: iob2@hi.is (Í.Ö. Benediktsson).

0277-3791/$ - see front matter © 2007 Elsevier Ltd. All rights reserved.
doi:10.1016/j.quascirev.2007.10.007

Bennett et al., 1996; Huddart and Hambrey, 1996; Lønne and Lauritsen, 1996; Winkler and Nesje, 1999; Lyså and Lønne, 2001; Krüger et al., 2002), while end moraines of surging glaciers have attracted less attention (e.g. Croot, 1987, 1988a; Boulton et al., 1996, 1999; Hart and Watts, 1997; Bennett et al., 2004a, b). It is, however, increasingly important to understand the link between the dynamics of surging glaciers and their formation of end moraines because surging glaciers are thought to be the best analogue to the fast-flowing ice streams that controlled the discharge and regulated the stability and configuration of Pleistocene ice sheets (Gripp, 1929; Bennett, 2001; Stokes and Clark, 2001; Dowdeswell et al., 2004; Kjær et al., 2006; Rignot and Kanagaratnam, 2006).

Surging glaciers deposit and deform proglacial and ice-marginal sediments significantly during their fast advances creating a variety of morphologies and tectonic architectures (Sharp, 1985; Drozdowski, 1987; Croot, 1988a, b; Boulton et al., 1996, 1999; Hart and Watts, 1997; Bennett et al., 1999, 2004a, b; Evans and Rea, 1999, 2003; Andrzejewski, 2002). Croot (1988a), Hart and Watts (1997), Boulton et al. (1999) and Bennett et al. (2004b) have demonstrated that the formation of large end-moraine ridges by surging glaciers in Svalbard and Iceland chiefly originates from thrusting and glaciotectonism, primarily as a result of ice pushing into a pre-existing foreland wedge and of gravity spreading (van der Wateren, 1985, 1995a; Aber et al., 1989; Bennett, 2001). Both brittle and ductile deformation styles have been observed, but commonly in different structural zones (Croot, 1988a; Hart and Watts, 1997; Boulton et al., 1999; Bennett et al., 2004a, b). It is, however, neither fully understood what controls the morphological and structural characteristics of surging-glacier end moraines, nor how their properties are related to the glacier dynamics.

The aim of this paper is threefold: (i) to investigate and describe the morphology, sedimentology and tectonic architecture of an end-moraine ridge produced by a major glacier surge in 1890; (ii) to study the sediment distribution in the glacier forefield and its association with the end moraine and subglacial processes and (iii) to establish a sequential model that summarizes the results and illustrates the stepwise formation of a surging-glacier end moraine. The study field is the forefield of the surge-type glacier Brúarjökull in eastern Iceland (Fig. 1).

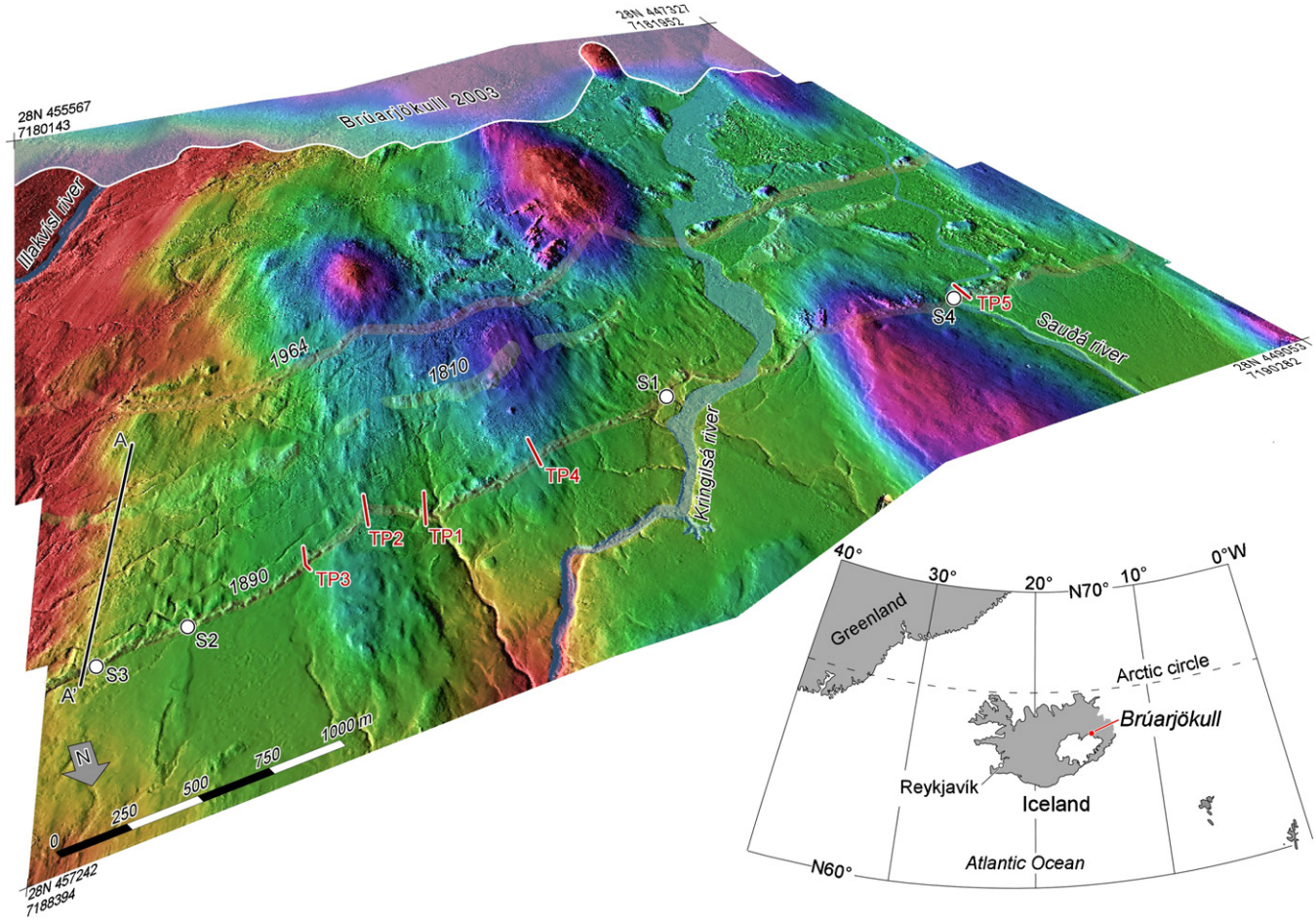

Fig. 1. The forefield of the surge-type glacier Brúarjökull, eastern Iceland. Digital elevation model, generated from stereopairs of aerial photographs recorded in 2003, visualized as a Terrain Shade Relief model. Red lines marked TP1–TP5 indicate terrain cross-profiles (Fig. 2), black line A–A′ represents sediment distribution profile (Fig. 12) and dots S1–S4 mark excavated cross-sections (Figs. 4, 6, 8 and 10).

2. Setting

Brúarjökull is the largest outlet glacier of the Vatnajökull ice cap in eastern Iceland (Fig. 1). It descends from about 1500 m a.s.l and terminates with a 55 km long glacier margin at roughly 600 m a.s.l (Björnsson et al., 1998; Fig. 1). Its surge cycle is characterized by active surging of about 3 months and a subsequent quiescent phase of 70–90 years duration. The known historical surges of Brúarjökull occurred in 1625, ~1730, ~1775?, 1810, 1890 and 1963–1964 (Thorarinsson, 1964, 1969; Björnsson et al., 2003). During the last two surges the glacier advanced 10 and 8 km, respectively, with maximum ice-flow velocities of at least 120 m/day (Thorarinsson, 1969). Currently, the Brúarjökull glacier is in its quiescent phase with a quickly retreating and downwasting ice margin covered by a thin layer of sediment from emerging and disintegrating crevasse-squeeze ridges and debris bands in the ice (Kjær et al., 2006; Bjarnadóttir, 2007; Schomacker and Kjær, 2007).

As a result of repeated glacier advances, the forefield of Brúarjökull consists of a 6–7 m thick sediment sequence overlying basaltic bedrock. The forefield is glacially streamlined with the most prominent features—such as end-moraine ridges, ice-cored landforms and ice-free hummocky moraines, crevasse-squeeze ridges, eskers and flutings—located in valleys between widely spaced elongated bedrock hills (Kjær et al., 2006; Schomacker et al., 2006). Three distinct end moraines, originating from the three last surges, are present in the glacier forefield (Fig. 1).

At present, several indicators of permafrost are found in the glacier forefield, such as rounded lakes and circular rim ridges (indicators of deteriorating palsas), ice-cored mounds and frost-crack polygons (Todtmann, 1960; French, 1996; Benediktsson, 2005; Ravn, 2006). Sporadic permafrost has also been mapped in the area north of Brúarjökull (van Vliet-Lanoë et al., 1998; Etzelmüller et al., 2007). At the end of the Little Ice Age (around 1890), the extent of permafrost was most likely larger than today since air temperatures at that time were 1–2 °C lower than that at present (Bergthorsson, 1969; Guðmundsson, 1997; Ravn, 2006; Schomacker and Kjær, 2007).

Between August 2003 and August 2005, the mean annual air temperature (MAAT) in the forefield of Brúarjökull was −0.3 °C. Official meteorological data have allowed the MAATs to be extrapolated back to 1830. These data show that MAATs in the glacier forefield have been well below 0 °C since 1830 (Ravn, 2006; Schomacker and Kjær, 2007), indicating that permafrost existed to some extent during the time of surges.

3. Methods

Identification of the 1890 end moraine and associated landforms was carried out on the basis of aerial photographs (scale 1:15 000, recorded in 2003). Geomorphological analysis was carried out by combining the aerial photographs with a digital elevation model, generated from the ortho-rectified 2003 aerial photographs (Fig. 1). More detailed geomorphological mapping was undertaken by measuring transverse terrain profiles with TopCon GTS-226 precision levelling instrument at five different sites which were deemed to reflect the characteristics of the end-moraine morphology and geometry (Figs. 1 and 2).

Investigations of internal sedimentology and glaciotectonics in the 1890 moraine were carried out in four natural cross-sections that were cleaned up and extended by hand both laterally and vertically in various degrees. Sediment lithologies and structures were documented on the basis of the Eyles et al. (1983) lithofacies classification and the

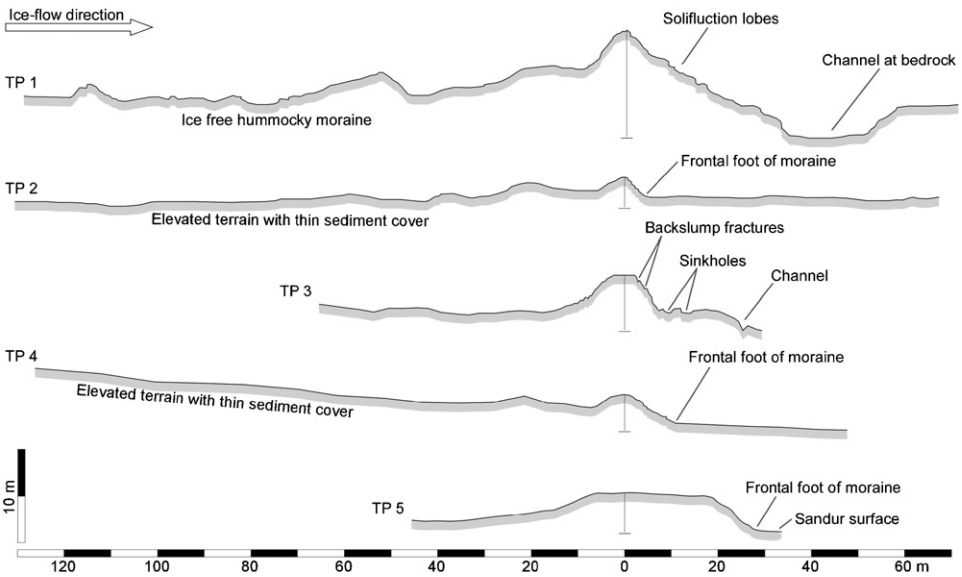

Fig. 2. Terrain profiles (TP) 1–5, measured across the 1890 end moraine. Vertical lines indicate the height from the crest of the end moraine to the bottom of the profile. See Fig. 1 for locations of the profiles.

Krüger and Kjær (1999) data chart. Sediment facies architecture was mapped at a scale of 1:20, except in subsections 4A and 4B where the scale was 1:100. The terminology used for describing deformation structures was adapted from Marshak and Mitra (1988), Twiss and Moores (1992) and Evans and Benn (2004). Measurements of structural elements included strike and dip of shear planes and primary bedding, and plunge and direction of fold axes. The structural measurements were plotted and statistically evaluated in a Schmidt equal-area net with *SpheriStat* 2.2© Windows software that facilitates the subsequent analysis of the structural elements.

Data for reconstruction of sediment thickness below the 1890 surge surface were obtained through a digital photogrammetry grid, based on the 2003 aerial photographs. Detailed vertical measurements (±34 cm) on bedrock exposed at the bottom of channels (point h1) and the terrain surface above the channels (point h2) allowed the thickness of the sediment sequence resting on the bedrock to be measured by point h1−point h2 = sediment thickness. The sedimentary thickness profile A–A′ (Figs. 1 and 12) has been extracted from the resultant grid.

4. Geomorphology of the 1890 end moraine

The Terrain Shaded Relief (TSR; Fig. 1) demonstrates that the 1890 moraine is most prominent in valley-like low-lying areas between streamlined bedrock hills slightly draped by sediment. In these areas, the end moraine is 5–20 m high and 40–80 m wide with a steep frontal slope. As shown by Benediktsson (2005), Schomacker and Kjær (2007) and Kjær et al. (in press), dead-ice and ice-free hummocky moraine is located in wide belts in the backslope area. Here, backslumping resulting from active downwasting (Kjær and Krüger, 2001) is commonly associated with highly permeable sediment such as gravels and sands, whereas active downwasting of buried ice is rare where the moraine consists of fine-grained sediments, such as loess, peat and tephra (LPT). Occasionally, sinkholes are present on the foreslope of the moraine as a result of downwasting of buried ice or snow. These morphological characteristics are well demonstrated by terrain profiles 1 and 3 where the moraine is high and wide with a hummocky backslope and consisting mainly of fine-grained sediment (Fig. 2). Terrain profile 3 shows the only site at which active downwasting was observed in fine-grained parts of the end moraine (Figs. 2 and 3A). The 1890 end moraine displays the morphological characteristics described above solely in low-lying areas where the bedrock is at considerable depths and the sediment cover is thick (Fig. 1). Terrain profile 5 is situated in the easternmost part of a depression west of Sauðá (Fig. 1). The depression is occupied by sandur surfaces both proximal and distal to the end moraine, which is about 10 m high and 80–200 m wide (Fig. 2). As the terrain rises towards the east over a bedrock hill, the moraine loses height and turns into a narrow bouldery ridge often associated with isolated

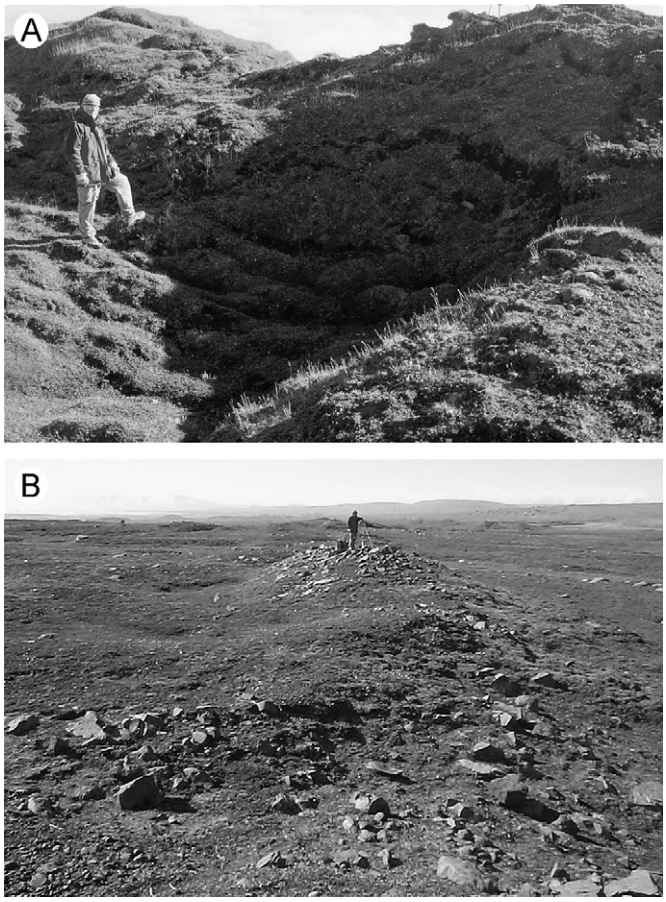

Fig. 3. (A) Active downwasting observed on the frontal slope of the 1890 end moraine at TP3. Excavation exposed small crystal-sized ice, probably derived from snow incorporated during moraine formation. (B) Typical view of the low and narrow dump moraines, consisting of coarse sediments and large boulders. Ice flow was from left to right.

islands of ice-cored and ice-free hummocky moraine (Schomacker and Kjær, 2007; Fig. 1). This is typical for the 1890 end moraine where it is situated on, or is in association with, bedrock heights on which the sediment cover is thin (Fig. 1). As a result, the low and narrow ridges are primarily composed of large boulders and very coarse sediments (Fig. 3B). Terrain profile 2 is situated at the convergence of two former surge lobes at the downglacier side of a bedrock height and terrain profile 4 is located in the centre of a former surge lobe (Fig. 1). Both profiles show a low and narrow ridge upglacier of which there is a bedrock height with negligible sediment cover (Fig. 2).

The terrain profiles described above clearly demonstrate differences in morphological and geometrical characteristics that can be related to specific conditions in the glacier forefield. The 1890 end moraine is high and wide and most prominent in low-lying areas where the glacier body must have been thick and the supply of sediment probably high. In contrast, the end moraine is low and narrow in elevated areas with bedrock at shallow depths and thus a thinner sediment cover. Here, the glacier also must have been thinner than in between the bedrock hills. These relations

are supported by multi-temporal aerial orthophotographs that allow comparison between the elevation of the glacier surface during the surge in 1963–1964 and the elevation of the present ice-free terrain at the same locations. This comparison shows that the glacier was considerably thicker in the low-lying areas than up on the bedrock hills during the 1963–1964 surge. Presumably, the same applied to the surge in 1890.

5. Identified sediment facies and their genetic interpretation

The sediments of the 1890 end moraine were investigated in four excavated cross-sections (1–4; Fig. 1) in which seven sediment facies were distinguished. These are (1) diamict, (2) gravel, (3) interbedded sand and silt, (4) sandy glaciotectonite, (5) deformed LPT, (6) sand and gravel with peat clasts and (7) tephra. As these sediment facies are the same throughout, they are described here and interpreted for all sections.

Facies 1, *diamict*—Facies 1 was only observed in sections 1 and 4 (Figs. 1, 4 and 10). It is a matrix-supported, usually massive, silty–sandy to sandy diamict, rich in clasts. In section 4 the diamict is very hard while in section 1 it is friable and easy to excavate. In section 1, the diamict is discontinuously present in the lower part with a sharp, possibly erosional boundary to the underlying gravels of facies 2 (Fig. 4). At places, the diamict interfingers with, or carries, inclusions of LPT and lenses of sand and gravel, showing small-scale stretch-out deformation structures. The clasts—with rare and non-preferred striae orientation—have a random or at places upwards-decreasing distribution and have the same sizes (up to 10 cm) and shapes as the clasts of the underlying gravel.

Diamict occurs as both an upper and a lower unit in section 4 (Fig. 10). The lower diamict is poorly exposed at the base of the section, but is involved in a complex post-depositional thrust/fold sequence together with facies 3 sand and silt, with the diamict forming wedge-shaped bodies tapering in the thrust direction (north; Fig. 10). The diamict in section 4 carries angular, cobble- to boulder-sized clasts (10–25 cm), and the tapering ends continue in cobble and boulder pavements along steeply inclined thrust planes into deformed silt and sand. The upper diamict occurs on the backslope of the end moraine, being 2 m thick in the proximal part of section 4 and gradually thinning and disappearing distally (Fig. 11A). The diamict has a sharp contact with underlying facies 3 silts and sands, at places with drag structures but also fold and plough structures in connection with large boulders (up to 70 cm) at the lower contact (Figs. 10 and 11B).

Facies 1, *interpretation*—The diamict in the lower part of section 1 probably predates the 1890 surge event. This is supported by the fact that it stratigraphically is on top of the underlying gravel, but beneath a thick package of deformed sediment constituting the main part of the end moraine. It is, however, not thought to relate to the surges known to have occurred in the 17th and 18th century as no surge signature is found outside the 1890 end moraine. The diamict thins and disappears in distal direction probably due to fluvial erosion followed by deposition of the thick gravel body forming the terraces in front of the moraine (Fig. 4). Due to its properties, the diamict in section 1 is interpreted as till (Eyles et al., 1983; Menzies, 1995; Benn and Evans, 1998) deposited at the interface between a glacier and the pre-existing sandur deposits of facies 2, from which rounded clasts were incorporated in a deforming-bed zone. As the diamict has clearly been deformed, its genetic origin is not specified more fully.

The lower diamict in section 4 is also interpreted as a pre-surge diamict of unknown age, incorporated in the lower part of the 1890 end moraine and also being a source for the boulders along thrust planes in higher strata. The upper diamict can be tied to the 1890 surge event forming the end moraine. This diamict carries clasts much larger and a matrix more fine-grained than underlying sediments of facies 3. It must therefore be concluded that the bulk of the diamict was transported within and derived from the melting base of the surging glacier and was thus not formed due to subglacial penetrative deformation of sub-sole sediment, but rather formed as a subglacial traction till (Evans et al., 2006).

Facies 2, *gravel*—Facies association 2 occurs both as a pre-surge sediment in front of and beneath the frontal part of the end moraine at section 4, as well as a post-surge sediment in sandur terraces on the backslope of the same moraine (Fig. 10). Here, and in front of the moraine, facies 2 sediment forms the ground surface and reveals series of braided channel networks. At section 1, facies 2 occurs as a pre-surge sediment beneath the end moraine where it forms the lowermost unit, with a sharp boundary to overlying diamict and a shallow slope in a downglacier direction. Facies 2 also constitutes a post-surge braided sandur in front of section 1 (Fig. 4). Facies 2 gravel is predominantly massive and clast supported, with maximum clast size of 3–8 cm, though outsized clasts of 15–20 cm in diameter occur. The clasts are sub-rounded to well rounded, elongated in shape and often imbricated. Minor facies constituents are interbedded planar parallel-laminated gravelly sand, thin beds (3–5 cm) of laminated fine sand and silt, and the occasional infilled scour troughs.

Facies 2, *interpretation*—Facies 2 is interpreted as sandur deposits associated with high meltwater discharge (Maizels, 1993; Benn and Evans, 1998). The coarse gravel units were deposited due to vertical accretion from migrating longitudinal bars with the interbedded silt and fine sand representing late-stage deposition during successive waning flows.

The genesis of facies 2 is evident from its surface morphology at both sections 1 and 4 (Figs. 4A and 10E). At section 4, the gravel in front of and beneath the frontal part of the moraine is interpreted as pre-surge sandur deposits, while the gravel on the backslope postdates the 1890 surge. At section 1, the sandur terraces dominating the surroundings are at different levels and of different

ages. The gravel along the base of the section is within a low-lying terrace, formed during down-cutting of the Kringilsá River in sandur sediment deposited prior to the 1890 surge. The sediments in which the upper terraces are formed are thought to be deposited during or soon after the 1890 surge.

Facies 3, *interbedded sand and silt*—Facies association 3 constitutes the bulk sediment in the middle parts of sections 2 and 4, occurring, respectively, as a heavily sheared unit and as dislocated high-angle thrust blocks (Figs. 6D, 7A and 10C, F, G). In section 2, facies 3 consists of interbedded fine to coarse sand, often interbedded with thin (1–10 mm) silty layers of facies 5 LPT, in which rusty organic matter gives this unit a slightly yellowish hue in places, particularly in and around folded beds (Figs. 6D and 7A). The unit exhibits a faint stratification, appearing as alternating dark-brown, dark grey and light-brown layers, which is thought to represent the original bedding prior to deformation. The unit has contacts with facies 5, an erosive one at its proximal side and one defined by two high-angle normal faults at the distal side (Fig. 6D).

In section 4 (Fig. 10), primary bedding is usually preserved, but folding and penetrative deformation occur along thrust surfaces. In situ facies 3 sediments occur in front of the end moraine, but are reversely faulted at increasing angles and frequency in the proximal direction (e.g. Fig. 11D, K). The colour of the sand is usually black or dark grey, whereas the silt is brownish. The dominating facies is coarse silt with thin intrabeds of massive fine sand and occasional ripple form-sets. The silt is interbedded with thick units of diffusely planar parallel-laminated medium sand, intrabedded with thin (1–3 cm) beds of silt, coarse sand, gravelly sand and gravel stringers, with the maximum particle size being 4–5 cm (Fig. 11D). Minor facies constituents are rhythmically laminated beds of clay/silt and silt/fine sand with 0.5–4 cm thick lamina, cosets of climbing ripple cross-laminated fine sand, often with silt drapings, shallow erosional trough infills of sand to gravelly sand and cosets of trough cross-laminated sand (Fig. 11L, M). In section 4, random tephra beds (facies 7) occur as intrabeds within facies 3, and inclusions of organic detritus are also observed, especially in association with the silt beds.

In the other sections, facies association 3 is not the main constituent, and does not show the same facies diversity. There, facies 3 often appears as small single patches or lenses within facies 5 (LPT), or as a minor constituent in a mixture of sediment in the core of the sections as a result of external deformation. In such cases, the colour of facies 3 may turn to brown or black-brownish as a result of mixing with the organic matter from facies 5 (LPT).

Facies 3, *interpretation*—In section 4 the sediments of facies association 3 resemble those found in distal reaches of contemporary proglacial outwash, similar to those found in the surroundings of sections 1 and 4 (Figs. 1, 4 and 10). These are characterized by low bars and shallow braiding to meandering channels, between and within which depressions and ponds are common (Maizels, 1993, 2002; Marren, 2005). The horizontally laminated beds of sand, gravelly sand and gravel stringers are thus interpreted to represent vertical accretion of bar sediments, whereas the small- to large-scale cross-laminated units and interbedded thin silt beds represent deposition at variable flow regimes within channels. Thicker silt beds, some rhythmically laminated, were deposited from suspension in shallow ponds. In section 4, facies association 3 is assumed to have been deposited over a proglacial braidplain prior or simultaneous to the 1890 surge.

In section 2, the facies 3 sediments are inferred as shallow ponds or stream sediments, similar to those observed in channels and in circular lakes behind and in front of the section. In both cases, organic matter is abundant, explaining the appearance of facies 5 within or in association with facies 3.

Facies 4, *sandy glaciotectonite*—This facies was observed in section 4 (Fig. 10), where it occurs in distinctly different positions. In the lowermost part of section 4, but above the lower diamict unit, there is a subhorizontal sequence of sand and gravelly sand showing a pronounced shear lamination (38–41 m; Figs. 10 and 11C). Coarse sand intraclasts in fine-sand beds reveal three-dimensional pinch and swell, suggesting both extension and compression of these more rigid sediment clasts. Shear-laminated gravelly silty sand also forms an ~40 cm thick, highly imbricated unit between less deformed sand and silt thrust wedges in the middle part of section 4 (47–50 m; Figs. 10 and 11H, I). The lower contact is a thrust surface with well-developed drag folds in the footwall and from the upper contact—also a thrust surface—sand is injected along water escape structures into overlying sediments. Facies 4 also occurs in a topmost position in the central part of section 4. In distal direction from the pinch-out of the upper diamict, a 40–50 cm thick zone of shear-laminated sand can be seen to cut the steeply imbricated thrust wedges of facies 3, and lying on top of a pronounced décollement (Figs. 10 and 11D, E). A lodged boulder has ploughed up a silt wedge on its lee-side showing buckled lamination, whereas the shear lamination in the sand on the stoss-side and above the boulder is conformable to the boulder. The basal décollement is associated with overturned bedding or fully developed drag folds in underlying sediments.

Facies 4, *interpretation*—Facies 4 sand units are interpreted as glaciotectonite (Benn and Evans, 1996; Evans et al., 2006) as they have been deformed by shearing induced by the 1890 surging glacier, but retain some original structural characteristics. The primary sediment is thought to be facies 3 silt and sand, i.e. sandur braidplain sediments that have been incorporated into deformation zones dominated by ductile simple shear. Discontinuously lined-up intraclasts (boudinage) and more isolated sand intraclasts (tectonic inclusions), associated with drawn-out tectonic lamination from these, indicate finite extension in the direction of shearing (e.g. Hart and Roberts, 1994). The deformation zones seem to have developed both between

subglacial packages of sediments, and beneath the sole of the glacier thrusting the sediments into the end moraine (uppermost deformation zone).

Facies 5, *deformed LPT sequence*—Distal to all sections in the 1890 end moraine (Fig. 1), undisturbed facies 5 sediment occurs in thicknesses of 1–3 m, lying in depressions on fossil sandur surfaces (section 4; Fig. 10) or as sediment sequences resting on bedrock (sections 1–3; Figs. 4, 6 and 8). Within sections 1–3, deformed facies 5 LPT is a dominating facies, whereas dislocated coherent blocks of facies 5 occur uniquely in the frontal slope of section 4, sometimes as large, non-deformed rafts but also as isoclinally folded peat beds (Fig. 11G).

Facies 5 usually consists of 0.1–2 cm thick clay, silt and fine-sand laminae of yellowish to orange and red-brown peat and light-brown to dark-brown minerogenic loess, interbedded with tephra. The laminae vary considerably in strength, some being soft and easy to excavate while others are firm and more difficult to work on. The sediment often exhibits traces of roots and is dry and fractured, making determination of deformation structures difficult. As a result of external deformation, the LPT is totally mixed at some places, making differentiation of the LPT impossible. At other places facies 5 cannot be distinguished from facies 3 and 7, i.e. sand and tephra, but, where this is possible, the contact is usually quite sharp. Likewise, the contacts between different LPT beds and laminae are often sharp but may also be gradational.

Facies 5, *interpretation*—The loess is suggested to have been deposited on a terrain dominated by moss, grasses and shrubberies, which subsequently got buried and transformed into peat during the loess aggradation. The vertical accretion of the loess and peat was frequently interrupted by deposition of tephra, resulting in complexly interbedded facies 5 sequences of LPT, thus representing multiple palaeosols, as typified by colour, organic matter and root traces (Brady and Weil, 1999). The LPT sequences were obviously originally formed on the pre-1890 surge surface and then partly overridden during the 1890 surge. Consequently, facies 5 is the main constituent in a 4–6 m thick deformable bed beneath the 1890 surge surface in large parts of the glacier forefield (Kjær et al., 2006). At some places, like at section 4, blankets of facies 5 were bulldozed, sometimes folded, and deposited in the frontal part of the terminal zone. The incorporation of facies 5 in the end moraine is demonstrated by a tectonic overprinting indicated by e.g. folds and faults, inclusions and mixing with other facies. As a result of the external deformation, some of the thinnest facies 5 laminae observed in sections 1–3 may represent tectonic foliation resulting from high finite strains (van der Wateren, 1995b).

Facies 6, *sand and gravel with peat clasts*—This facies was only observed in section 4 (Fig. 10). Here, in the topmost, frontal part of the end moraine (Fig. 10) the sediment is composed of angular to folded peat clasts, 10–20 cm thick and up to half a metre long, all lying in a loose, massive matrix of cobbles, sand and gravel, and with large boulders on the surface. Peat clasts are also lying in sandy silt with outsized cobbles and small boulders (Fig. 11J). Facies 6 sediments are situated on top of an erosional unconformity to facies 3 sand.

Facies 6, *interpretation*—The loose character, the chaotic composition and the morphological position of facies 6 suggest redeposition of sediments of various facies, primarily delivered at the maximum surge position, followed by gravitational movement down the frontal slope of the end moraine.

Facies 7, *tephra*—This facies is observed in all four sections, mostly as very well-sorted black basaltic glass but occasionally as white rhyolithic tephra. The thickness of the tephra layers varies somewhat, especially those that have been subject to post-depositional deformation. They are usually 0.5–3 cm thick but can be found as thick as 10 cm often in association with folds. Thus, the thickness of tephra layers as they appear in the sections does not necessarily represent their original thickness. Individual tephra grains are usually very angular in shape and predominantly less than 2 mm in diameter, thus falling within the ash range. Tephra beds have been identified as interbeds in facies 3 sands and silts and facies 5 LPT. When deformed, the tephra beds are discontinuous or occur as patches or lenses of various thicknesses depending on the degree of external deformation.

Facies 7, *interpretation*—It can sometimes be difficult to distinguish tephra beds from facies 3 sand and silt and facies 5 LPT, especially where the tephra has been mixed to some degree with these sediments. However, if examined carefully, the tephra is usually better sorted, it contains no organic matter, the grains show different morphology and crystals are scarce. The tephra originates from various Icelandic volcanoes from which it has been transported by wind and deposited in the Brúarjökull forefield. Thus, we consider as tephra only those units that appear to be primary air-falls and not the redeposited material in loess.

6. Section 1

Section 1 is situated along a fossil stream channel associated with one of the major meltwater outlets of the 1890 surge. At present, the Kringilsá River cuts the end moraine just west of the section (Figs. 1 and 4). At section 1, the moraine ridge is symmetric in shape, approximately 20–25 m wide and rises about 1.5–2.5 m above the surrounding terrain (Fig. 4). The surface is well vegetated and no fractures indicating active wasting of buried ice can be identified. However, sinkholes do occur a few metres east of the section, indicating earlier wastage of buried ice in the moraine. Proximal to the end moraine, the nearest terrain is slightly undulating and forms a small system of abandoned meandering channels. Thus, the terrain is draped by medium to coarse sands and fine gravel.

6.1. Facies architecture of section 1

Four of the identified sediment facies were recognized in section 1: facies 1 diamict, facies 2 gravel, facies 4 LPT and facies 7 tephra. The facies architecture within section 1 can be divided into three parts due to different styles and magnitude of deformation: (i) the proximal part (0–3 m), (ii) the core (3–15 m) and (iii) the distal part (15–22 m).

Proximal part, 0–3 *m*—This part of the section is dominated by the deformed diamict overlying gravel (Fig. 4). The upper boundary of the diamict interfingers with other sediment, particularly LPT, which also includes several small inclusions of sand. Although occasional bedding can be identified, the LPT is relatively poor of sedimentary and deformational structures due to destruction by roots, particularly at the uppermost levels. The proximal part of section 1 is characterized by deformation of the pre-1890 diamict.

The core, 3–15 *m*—The core of the section exhibits the most severe deformation and the most pronounced deformation structures. At 3–5 m in the lower part, there are two prominent folds—a relatively tight overturned one and a recumbent one (Figs. 4 and 5A). Their axes dip to north and south, respectively, but both verge towards west and south-west, indicating stresses applied from easterly directions.

The upper part of the moraine core is characterized by a north-facing asymmetric anticline–syncline pair overlying the heavily deformed sediment (Fig. 4). The anticline is wide while the syncline is much tighter. The distal limb of the syncline is truncated close to the surface, indicating some post-tectonic erosion. Strikes and dips were not measured on the limb of the anticline due to poor accessibility. However, its layers are seemingly tilted towards the observer when facing the section, and could therefore indicate the plunge and orientation of the fold axis. On the other hand, measurements on the syncline show that the proximal limb plunges at 26–40° to the north-west while the distal limb plunges at 44–53° to west and south. A direct measurement on a small fold at the base of the syncline gave a fold axis plunging at 32° towards south-west, corresponding to the measurements of the syncline and indicating stress applied from southerly or south-easterly directions.

The lower limit of the anticline–syncline pair is marked by a shear zone, indicated by non-periodic asymmetric box folds (Fig. 5B) that terminate in north–south attenuated sheath folds, both typical of shear zones (Cobbold and Quinquis, 1980; van der Wateren, 1995a, b, 1999; Alsop and Holdsworth, 1999). The vergence of the asymmetric box folds is to the north while the vergence of the sheath folds is to the west, indicated by the sheath-fold structure at 12 m (Figs. 4 and 5C) and fold axes plunging at 2–3° to the south. Together the asymmetric folds and sheath folds represent a gradual downwards increase in deformation to the structure-poor and homogeneous mixture of facies 3, 5 and 7.

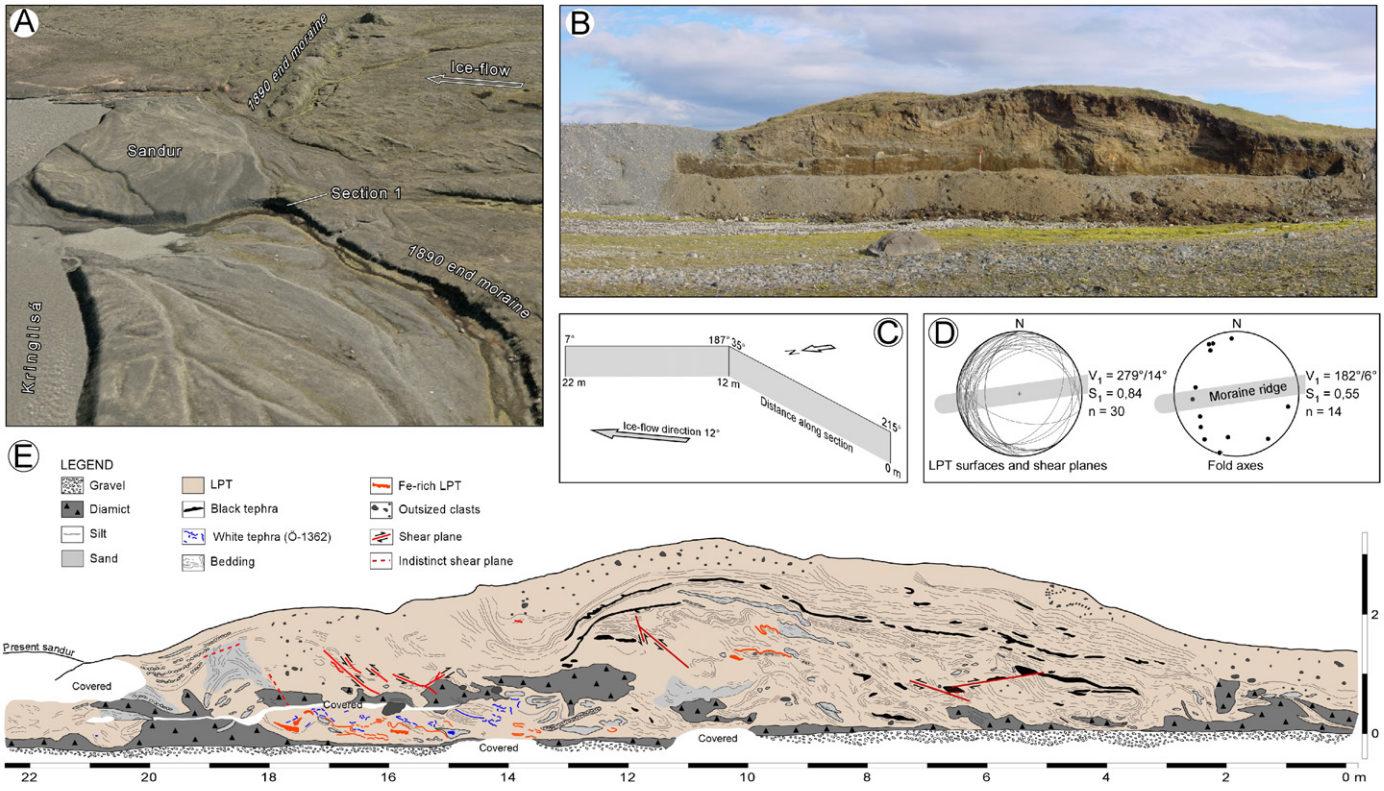

Fig. 4. Section 1. (A) Overview of the section's surroundings. Aerial orthophotograph draped over a DEM with 1.5 × vertical exaggeration. (B) Overview of section 1. (C) Outline of section orientation. (D) Structural data. (E) Diagram of the section, no vertical exaggeration.

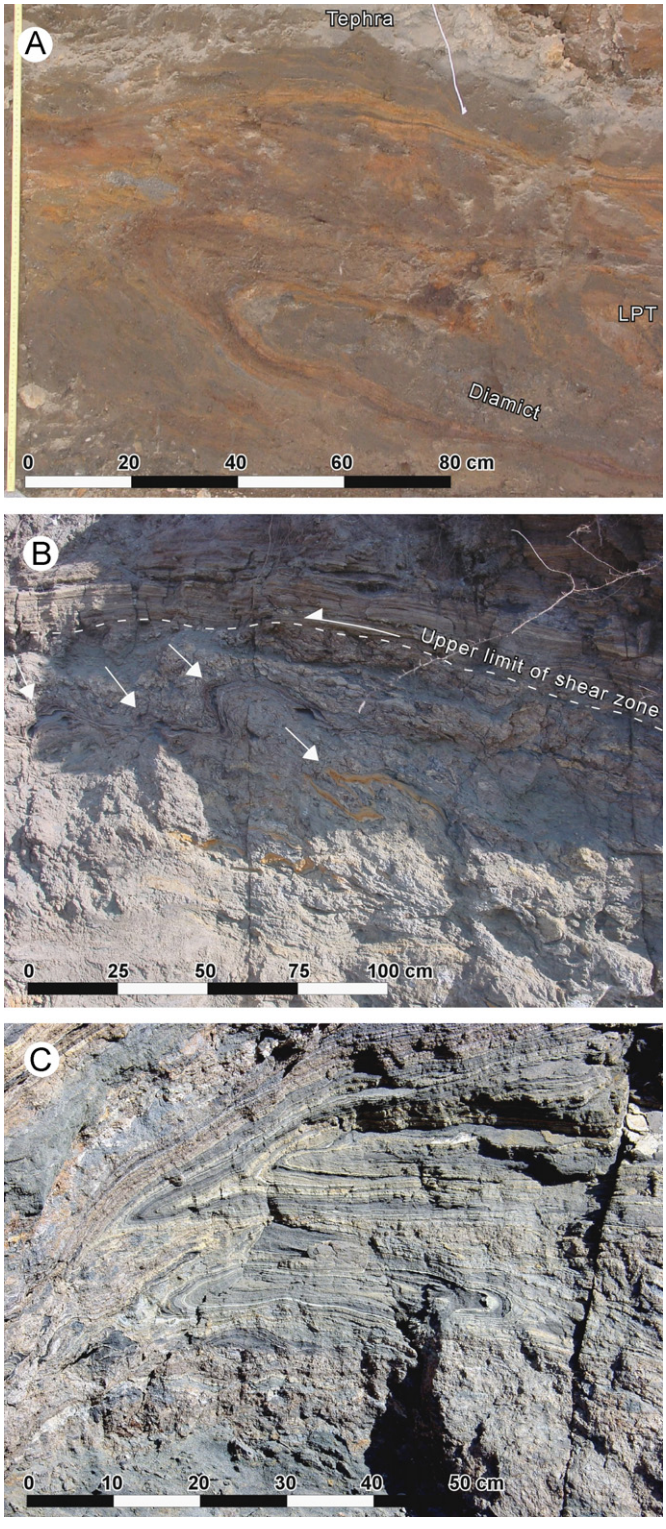

Fig. 5. Tectonic structures in section 1. Tectonic stress from right to left in all photos. (A) Recumbent fold in LPT (facies 5) with diamict (facies 1) in the core. (B) Shear zone at the boundary of the anticline, indicated by north-verging asymmetric box folds (arrowed) in LPT. (C) Sheath fold in the shear zone below the anticline.

The very core is otherwise dominated by shear planes and small-scale open, recumbent, inclined and overturned folds (Fig. 4).

Distal part, 15–22 *m*—Facies 1 diamict dominates the lower distal part, whereas facies 3, 5 and 7 are dominant in the upper part (Fig. 4). The diamict is up to 1 m thick but attenuates from 20 m towards the sandur terrace in front of the section. Thrust faults were found in facies 3 at 16–17 m, showing dips of 16–24° in easterly, southerly and westerly directions. In the lower part of the distal extremity, minor folding of gravel and LPT seems to die out and merge imperceptibly with the undeformed sandur terrace in the foreland (Fig. 4).

6.2. Genetic interpretation of glaciotectonics

The deformation is presumed to have started with the compression of the foreland sediment strata, resulting in the formation of an open fold that subsequently developed into an asymmetric anticline–syncline pair (Fig. 4). Simultaneously, the anticline–syncline sheared over the underlying sediments, as indicated by the asymmetric box folds and sheath folds (Fig. 5B, C). Both the anticline–syncline pair and the box folds are north-verging with approximately east–west orientated fold axes as a result of pressure application from the south. However, the axes of the asymmetric and sheath-fold system gradually rotate, respectively, from north-west to south. Thus, the sheath fold has vergence to the west and fold axes lying approximately north–south, indicating a shear from the east. This can be explained by the fact that fold axes initiating at high angles to the bulk direction of shearing tend to rotate towards an orientation parallel to the main shear direction (van der Wateren, 1995a). The paucity of structures in the core of the moraine may be explained by a continuous deformation which often produces completely homogenized tectonite in the central part of shear zones (van der Wateren, 1995b).

The rooted anticline–syncline pair, dominating the architecture of section 1, indicates a high internal and basal friction and explains the relatively narrow deformation zone of the end moraine (Boulton and Caban, 1995; Bennett, 2001). The high basal friction was caused by facies 2 gravel, which acted as a décollement due to low porewater pressures and high shear strength, giving rise to the detachment of the overlying fine-grained sediments (Croot, 1988a; van der Wateren, 1995b). The thickness of the pre-1890 sediment sequence, as indicated north of the section, is estimated to have been up to 3 m giving an aspect ratio of the pre-1890 sequence of ~1:7, indicating little shortening of the pre-1890 foreland wedge.

The structural data show a trend of fold axes, primary bedding and shear surfaces towards westerly directions, possibly indicating stress application from easterly directions (Fig. 4D). Primary bedding and shear surfaces indicate that the dominant anticline–syncline pair is upright but with a hinge plunging moderately in westerly directions. Similar trends can be seen for axes measured directly on smaller folds in the section (Fig. 4D), although an interpretation of their principal vector is statistically

irrelevant due to some dispersion. The west-plunging nature of the primary bedding indicates bulk stress application from easterly or south-easterly directions, approximately perpendicular to the moraine ridge. The structural data are interpreted to indicate a localized marginal ice-flow direction from south to south-east, from which the surging glacier pushed the foreland sediments to construct the end moraine. This is supported by crevasse-fill ridges to the south-east of the section that are thought to represent transverse crevasses developed at surge termination. This assumption suggests that the ice-flow direction in the terminal zone may not necessarily coincide with the main ice-flow direction farther upglacier.

7. Section 2

Section 2 is situated in the 1890 end moraine, approximately in the centre of the former surge lobe in the eastern Brúarjökull forefield (Fig. 1). Here, the moraine is ~50 m wide and up to 10 m high. Wind erosion has exposed a nearly 4 m high section extending from the backslope towards the foreslope, but without the most proximal and distal extremities of the moraine being visible (Fig. 6A).

The terrain to the south of section 2 is undulating, with a depression in the large-scale topography (Fig. 1). The terrain to the north of the section is flat and comprises a deteriorating palsa area represented by rounded lakes and circular rim ridges, an indicator of local permafrost conditions (Fig. 6A; French, 1996). The stratigraphy of this terrain is similar to that of section 2, i.e. dominated by interbedded LPT and tephra.

7.1. Facies architecture of section 2

Three of our identified sediment facies were recognized in section 2: facies 3 sand, facies 5 LPT and facies 7 tephra. The facies architecture within section 2 can be divided into three parts due to different styles and magnitude of deformation: (i) the proximal core (0–11 m), (ii) the central core (11–16 m) and (iii) the distal core (16–23 m).

The proximal core, 0–11 *m*—Here, the upper part reveals far less deformation than the lower part. The boundary between the upper and lower parts is clearly marked by

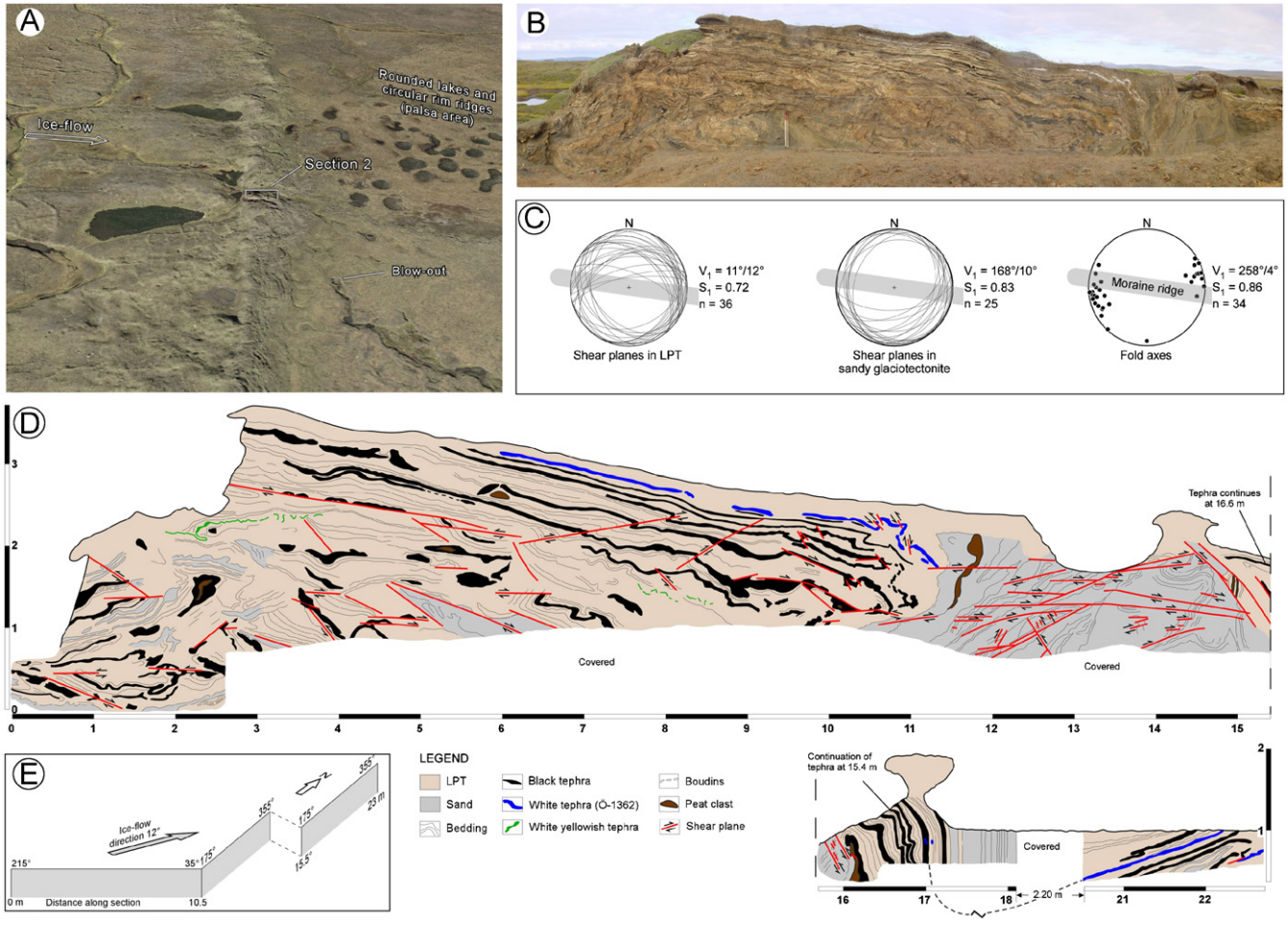

Fig. 6. Section 2. (A) Overview of the section's surroundings. Aerial orthophotograph draped over a DEM with 1.5 × vertical exaggeration. (B) Overview of section 2. (C) Structural data. (D) Diagram of the section. (E) Outline of section orientation.

a low-angle normal fault from 2.6 to 5.7 m dipping at 20° towards north-east (Fig. 6). The structures of the hanging wall are characterized by lightly disturbed alternating layers of facies 5 LPT and facies 7 tephra. Below the normal fault, the deformation is characterized by compressive structures such as small-scale open, inclined and recumbent folds (Fig. 6D). The lower part also reveals a number of shear planes forming both normal faults and thrust faults, of which some are backthrusts.

Between 6 and 9 m, two prominent thrust faults were observed, dipping at 27–35° towards westerly directions, cutting a number of facies 5 and 7 beds (Fig. 6D). To accommodate the deformation, fault-propagation folds have formed in less competent layers, primarily facies 5 (LPT), while ductile thrusts have formed in more competent layers, such as tephra. Distal of these thrusts, brittle deformation increases somewhat as demonstrated by small shear planes cutting, e.g. the Öræfajökull (1362 AD) tephra marker in the upper part (Fig. 7B).

The central core, 11–16 *m*—The central core is dominated by intensely sheared facies 3 sand (Figs. 6D and 7A). Most proximal, from 10.5 to 12 m, there are two prominent subhorizontal thrust faults dipping towards south-east and south-west. Distal of these, layers of facies 3 exhibit imbrication and are frequently sheared, revealing low-angle thrust faults that preferably dip in westerly and southerly directions. Nearly all thrust faults in the central core show a hanging wall displacement in a downglacier direction, indicating a compression from the rear, although the opposite may be observed as shown by a set of conjugate faults in the lower part (Fig. 6D).

Between 13 and 16 m, the style of deformation in the central core changes slightly as folds become more pronounced (Fig. 6D). Most prominent is an inclined fold with vergence to the north and a frequently sheared lower limb. The upper limb reveals a north-verging recumbent fold that has been sheared by a thrust fault dipping 24° towards west.

The distal core, 16–23 *m*—The distal core is characterized by steeply dipping alternating layers of facies 3, 5 and 7 (Fig. 7C), exposed at 16–18 and 20–23 m, and interpreted as the proximal and distal limbs of a partly buried north-facing syncline (Fig. 6D). This conclusion is strongly supported by the white Öræfajökull (1362 AD) tephra marker that is found on both limbs, and by the appearance of an anticline–syncline pair on the surface (Fig. 7D). Between 16 and 17 m, three fold axes in tephra layers (facies 7) plunge 10–27° towards west (Fig. 6D). This is compatible with the previously described fold in the distal part of the central core and with a stress application from the south.

7.2. Genetic interpretation of glaciotectonics

The deformation style of section 2 changes considerably from the proximal to the distal part of the moraine. The most severe deformation occurred in the proximal and central cores, dominated by intense shearing but also folding of facies 3 sediment. In contrast, the distal part is characterized by ductile deformation (Fig. 6D). The upper layers of the proximal core are suggested to represent the limb of an upwards facing anticline, similar to the one observed in section 1. The hinge zone and the proximal part of the limb must have been removed by wind erosion. As in section 1, the anticline in section 2 has sheared on top of the underlying core sediments, as demonstrated by the normal fault at 2.6–5.7 m (Fig. 6D). Occasionally, the three sediment facies within the section have developed into a structureless mixture as a result of continuous deformation (van der Wateren, 1995b). The sand (facies 3) at 11–13 m behaved more competently during their incorporation and deformation in the sediment wedge forming the moraine, as indicated by the dominating brittle deformation in this part of the section.

As the deformation of the foreland sediment progressed, an upright syncline developed in front of the sandy central core (Fig. 6D). During further propagation of the deformation, the distal limb of the anticline is assumed to have become broken by fault-propagation folds, while the syncline became simultaneously deeper and narrower.

The structural data from section 2 vary in consistency. Shear planes observed and measured in facies 5 LPT show hardly any consistency but are, however, dispersed close to the fringe of the equal-area stereonet, indicating that most of them are low-angle shears (Fig. 6C). Normal faults have dominantly a gentle dip towards the north or north-east, possibly as a result of syn-tectonic slope failure on the evolving foreslope during the moraine formation. Fold axes measured in section 2 show good consistency with a reconstructed principal vector plunging towards west (Fig. 6C), representing the axes of north-verging folds and suggesting a stress application from a southerly direction.

The style of deformation in section 2 corresponds with that of section 1; however, the approximate aspect ratio of the foreland sediments is smaller, or ~1:17. Because shearing is more common and the syncline seems tighter, this section is thought to represent a more developed stage in the pushing process thought to form the 1890 end moraine.

8. Section 3

Section 3 is situated just east of section 2 (Fig. 1) along a small abandoned stream channel (Fig. 8B, C). Here, the moraine ridge is 30–50 m wide and rises approximately 5–15 m above the surrounding terrain but becomes considerably higher and broader to the east but slightly lower and narrower to the west (Figs. 1 and 8C). The ridge rises relatively steeply towards the crest but slopes more gently at the distal side (Fig. 8B, C). No sign of active downwasting of dead-ice was observed at the moraine surface but inactive sinkholes occur frequently on the hummocky backslope, indicating either the former existence of dead-ice or no current melting of buried ice.

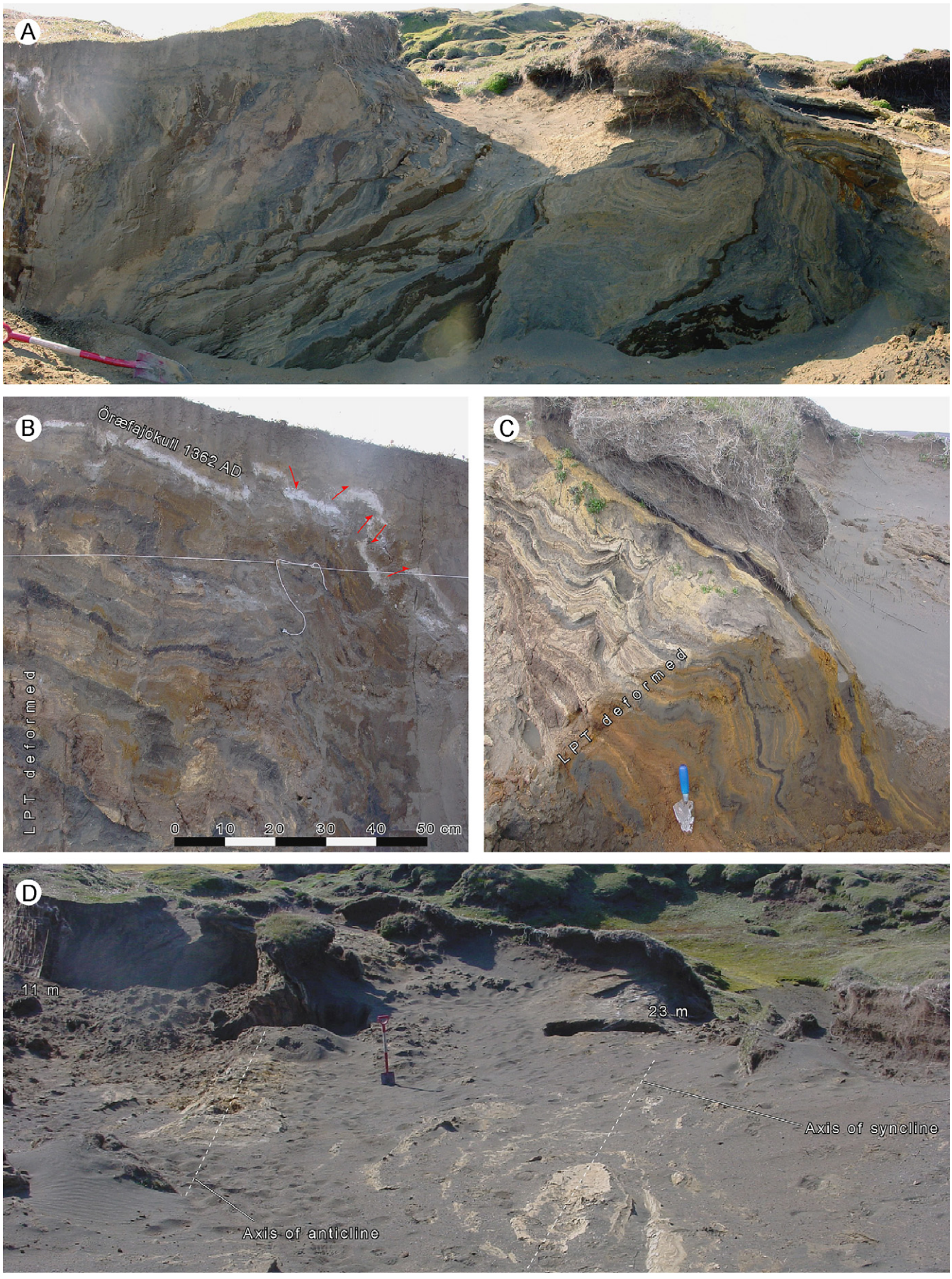
A
B
Öræfajökull 1362 AD
LPT deformed
0 10 20 30 40 50 cm
C
LPT deformed
D
11 m
23 m
Axis of syncline
Axis of anticline

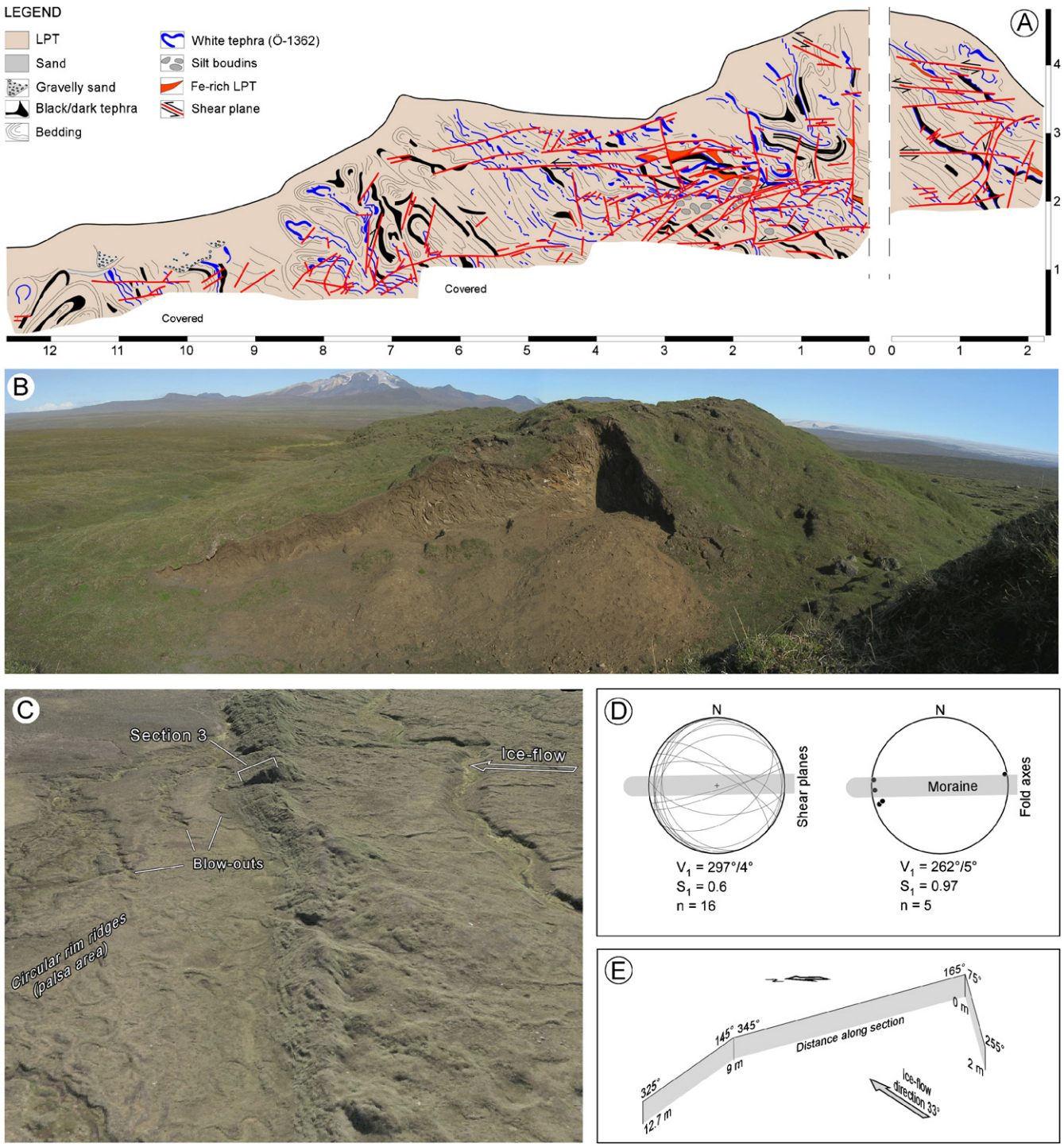

Fig. 8. Section 3. (A) Diagram of the section. (B) Overview of the section on the frontal slope of the end moraine. (C) Overview of the section's surroundings. Aerial orthophotograph draped over a DEM with 1.5 × vertical exaggeration. (D) Structural data. (E) Outline of section orientation.

In proximal direction the terrain abounds with crevasse-fill ridges and flutes, the latter indicating the 1890 ice-flow direction towards 33°. In front of the end moraine, three abruptly emerging channels (Figs. 8C and 9D) represent blow-outs of overpressurized water escaping away from the 1890 surging glacier in a discrete network of interconnected tunnels (Christiansen et al., 1982; Kjær et al., 2006).

Fig. 7. Tectonic structures in section 2. Tectonic stress from left to right in all photos. (A) Heavily sheared and folded sand (facies 3) in the central core. Spade for scale. (B) Deformed LPT sequence at 10–11 m in the proximal core, with ductile thrusts below sheared white tephra. (C) Near-vertical LPT layers representing the proximal limb of a syncline in the distal core. Trowel for scale. (D) Anticline–syncline pair exposed at the surface in the distal part of the section.

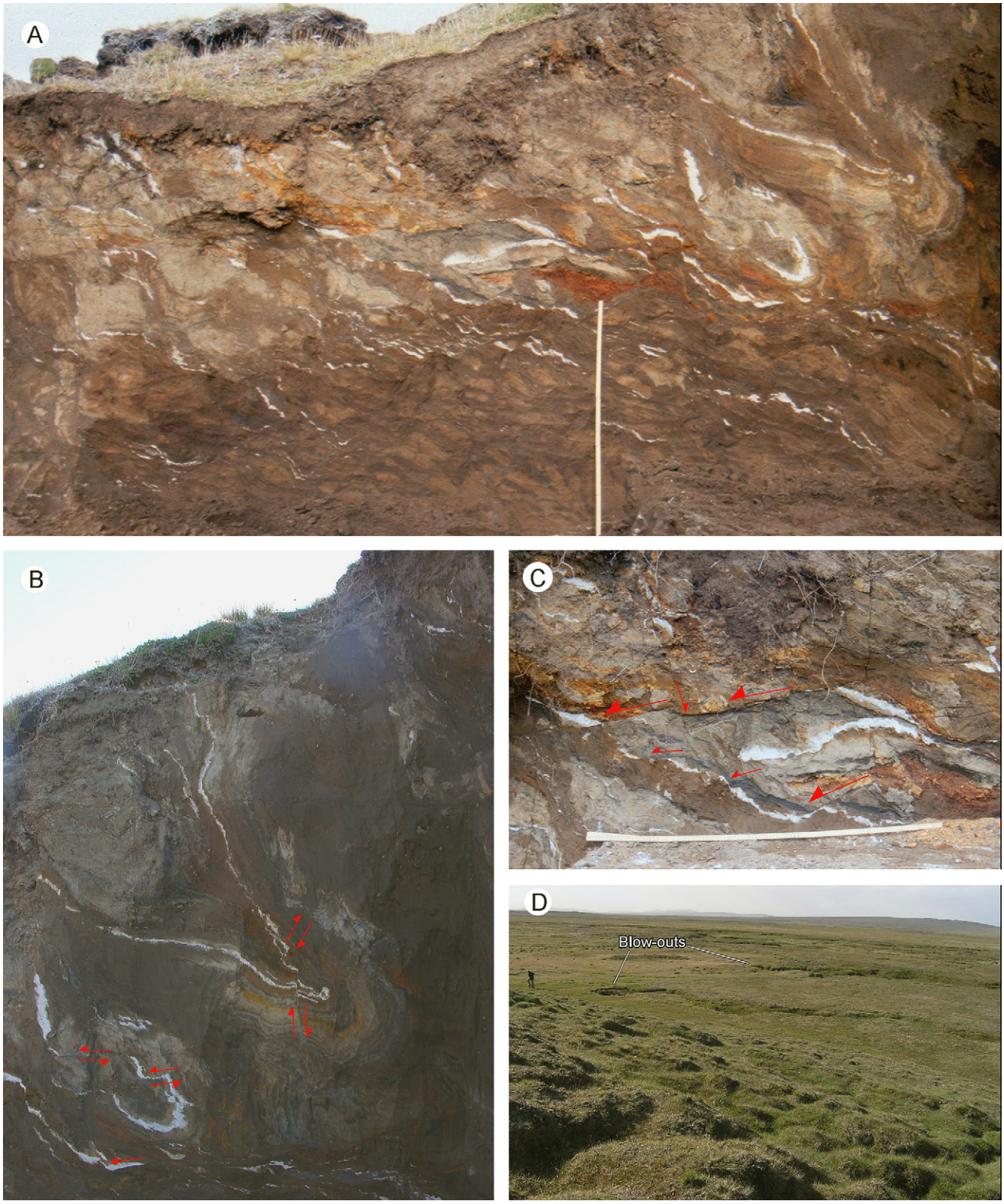

Fig. 9. Tectonic structures in section 3. Tectonic stress from right to left in (A)–(C). (A) Multiple folding and shearing of facies 5 (LPT) and 7 (tephra) in the core. (B) North-verging polyclinal folds in the core. (C) Examples of shears in the core section. (D) View of circular blow-out structures at the abrupt head of channels in front of the end moraine at section 3. Person for scale to the left.

Section 3 covers the distal slope of the end moraine, approximately between the crest and the distal extremity (Fig. 8B, C). The section is composed of two parts, a 2 m long and nearly 3 m high proximal section oriented sub-parallel to the ridge and a main section that runs perpendicular to the moraine and the former ice margin (Fig. 8E).

8.1. Facies architecture of section 3

Three sediment facies were identified in section 3: facies 3 sand and silt, facies 5 LPT and facies 7 tephra. The section reveals different styles of deformation but is characterized by multiple folding and shearing. Based on the facies architecture the section can be divided into three parts: (i) the proximal section sub-parallel to the moraine ridge, (ii) the core area between 0 and 9 m and (iii) the distal part between 9 and 12.7 m.

Proximal section, 0–2 *m*, *sub-parallel to the moraine ridge*—This section is characterized by frequently sheared layers of facies 5 LPT and facies 7 tephra. The layers dip mainly towards the stream channel at the foot of the section but are typically cut by both low- to high-angle shear planes (Fig. 8A). Two of these are normal faults probably representing syn-tectonic slope failure at a progressing frontal slope during the moraine formation. A high-angle thrust fault measured in the upper part of the proximal section gave a 46° dip towards south-east, and likely correlates with a thrust in the upper proximal part of the core section (Fig. 8A).

The core section, 0–9 *m*—This part of the section reveals the most severe deformation, characterized by prevalent shearing and multiple folding (Fig. 9A). The intense shearing appears as both normal and thrust faults. Examples of these are a few high-angle normal faults at 1–3 m, dipping 80–85° in southerly directions, and a high-angle backthrust at ~7 m, dipping 75° towards north-east (Fig. 8A).

One of the most prominent structures in the core section is a large polyclinal overturned fold at ~0–2 m, with a vergence to the north and axial surfaces dipping upglacier (Figs. 8A and 9B). The fold axis, plunging 8° towards west, is well outlined by the white Öræfajökull (1362 AD) tephra marker as well as by several distinct layers of LPT and other tephras. The fold has been subject to shearing, in part along the above-mentioned near-vertical normal faults at 0–2 m (Fig. 8A). Thrust faults cutting the upper part of the fold are thought to correspond to the thrusts previously described from the upper part of the proximal section. Another prominent fold nose was observed at ~1 m, marked by relatively thick layers of the white tephra. However, the fold limbs have not been well preserved because of a subsequent intense shearing along normal faults (Fig. 8A).

The zone of the most intense shearing extends approximately between 0 and 4 m (Fig. 9A, C), and from 4 m to roughly 6 m the facies architecture is characterized by repeated upglacier-inclined beds of LPT and white tephra beds. Shearing remains an important factor and is mainly represented by normal faults in the upper part. At 6–9 m the style of deformation changes slightly as ductile deformation becomes more significant. This zone is mainly characterized by inclined north-verging folds with axes plunging 3–5° towards west. These folds are well outlined by the white tephra marker and bedding in facies 5 LPT (Fig. 8A).

The distal part, 9–12.7 *m*—The deformation in the distal part is predominantly ductile, though shear planes do occur, primarily cutting upglacier-inclined sediment beds of facies 3, 5 and 7. The most prominent structures of this zone are thus inclined folds with vergence to the south and fold axes plunging 4° towards east (Fig. 8A). Fold axis orientations and the inclination of the axial surfaces indicate stress from a northerly direction, which suggests the possibility of an obstacle in front of the moraine during its formation, causing a counter-pressure from the north.

8.2. Genetic interpretation of glaciotectonics

Section 3 reveals both ductile and brittle deformation styles that are, however, dominant in different zones of the section. The proximal section contains structures similar to those in the core, which exhibits multiple folding and shearing that distinguishes section 3 from sections 1 and 2. Folds, most of which are considered rooted, are north-verging with their axial planes dipping upglacier and shearing appears both in the form of normal and thrust faults. The style of deformation changes at around 9 m where ductile deformation becomes dominating with upglacier-verging folds (Fig. 8A).

Compared to sections 1 and 2, section 3 shows the most severe deformation. This is suggested to reflect the latest and most developed stage in the moraine formation where fine-grained sediments are the main constituent. However, the approximate aspect ratio of the foreland sediments is similar to that of section 2, or ~1:17, indicating a significant shortening of the pre-1890 sediment sequence. As described from sections 1 and 2, the end-moraine construction is presumed to have started with the formation of anticline–syncline pairs, where the distal limb of the anticline became sheared and the syncline became deeper and tighter as the deformation progressed. In section 3 we interpret the prominent north-verging polyclinal folds in the proximal part and the core as due to subsequent re-folding of the original anticline–syncline pair (Fig. 8A). During the last phase of the deformation the folds became subject to frequent shearing along both normal and thrust faults.

During the latest stage of the moraine formation the forward movement of the deformed sediment is thought to have been prevented by an obstacle in front of the end moraine. Consequently, this obstacle created a counter-stress applied towards the foreslope of the moraine from a northerly direction. This is proposed to explain the occurrence of the south-verging folds in the distal extremity and the north-dipping faults at the base of the section, indicating that the moraine was ploughing into the foreland rather than overriding it (Fig. 8A). The obstacle might have been a pile of frozen sediment, of which the consequent shear strength was too large for the applied glacial stress to overcome. The proposed frozen condition of the foreland is supported

by the existence of an area of deteriorating palsas in front of the end moraine (Fig. 8C).

Fold axes measured in section 3 are predominantly east–west orientated, which corresponds to stress application from southerly directions (Fig. 8D). They are therefore considered to be the most reliable structural indicator of the direction of the stress applied during the most developed stage of the end-moraine formation. In contrast to the fold axes, shear surfaces show little consistency. However, steeply dipping thrusts and normal faults are more common in section 3 than in sections 1 and 2 (Fig. 8D). This may be explained by a strong compression in a relatively narrow zone with high basal friction, as indicated by domination of rooted folds (Boulton and Caban, 1995; Bennett, 2001). This causes the material to be displaced in the direction of smallest resistance, i.e. upwards, explaining the high number of steeply dipping thrust faults and axial planes of folds. Due to compression in a narrow zone, the end moraine became high and steep, giving rise to slope failure on the evolving foreslope and resulting in the formation of both high- and low-angle normal faults.

As in sections 1 and 2, we interpret the structural elements of section 3 as indicators of push-from-the-rear induced by the glacier during the very last phase of the surge.

9. Section 4

Section 4 is located in the western part of the Brúarjökull forefield, roughly 3 km west of section 1 (Fig. 1). The 1890 end moraine is located on a ~2 km wide sandur area, lying between bedrock heights to the east and west. The moraine is up to ~10 m high and in total 150–200 m wide over the sandur area but shrinks considerably over the adjoining high areas. On the backslope, post-depositional erosion has left a series of fossil terraces and two break-through channels, just one of which is operating today as the outlet for the Sauðá River (Fig. 10E). The moraine has an asymmetric cross-profile with a more gently sloping, but at places hummocky backslope, whereas the front is steep and well vegetated, partly as a function of thick translocated units of peat that drape the distal crest and frontal slope. The section, cut by the Sauðá River, is barely 80 m long, and the moraine crest is ~9 m above the riverbed and ~6 m above the frontal sandur plain (Fig. 10D). The whole section was not continuously documented along its full length, but was recorded in four parts: sub-section 4A covering 0–5 m, 4B covering 22–38 m, 4C covering 38–50 m and 4D covering 63–77 m including the frontal and pro-front area of the moraine (Fig. 10D). Section 4 sub-parallels the former ice flow towards 20°N (Fig. 10B).

9.1. Facies architecture of section 4

Compared to sections 1–3, the facies composition and architecture in the Sauðá section is somewhat different. The LPT (facies 5), dominant in the other sections, is hardly present. The Sauðá moraine is instead dominated by silt, sand and gravel (facies 2 and 3) and the architecture is characterized by brittle deformation and with ductile folding as a minor constituent.

4A, the proximal part, 0–5 *m*—The section shows a basal unit of shear-laminated silt and sand (facies 4 sandy glaciotectonite) overlain by a nearly 2 m thick diamict (facies 1) forming the uppermost constructional part of the moraine (Fig. 10A). The upper surface of the diamict is erosional, marked by a fluvial lag consisting of clast-supported gravel with dispersed cobbles. The lag is overlain by interbedded sand and silt (facies 3), forming a fossil sandur terrace from an early post-surge fluvial break-through of the end moraine.

4B, the proximal part, 22–38 *m*—This sub-section also shows a basal unit of facies 4 sandy glaciotectonite, with subhorizontally shear-laminated sand and well-developed boudinage intraclasts consisting of coarser sand (Fig. 10C). This basal unit disappears in the central part of the section and is substituted with a very hard, silty and clast-rich diamict (facies 1). The diamict is dragged into tapering-off wedges in the general deformation direction, with synclinal folded facies 3 sand and silt in between. Cobble- and boulder-sized clasts are lined up along thrust surfaces as continuations of the diamict wedges, both of which are inclined ~32° towards the south (Fig. 10C), thus indicating stress from that direction. The deformed facies 1 and 3 have a sharp contact with an overlying upper diamict, carrying large clasts up to boulder size, while a few inclusions of sorted sediment beds reveal folding in association with the larger boulders.

4C, the core, 38–50 *m*—On top of subhorizontally shear-laminated sandy glaciotectonite (facies 4) there is a 5 m thick stacked unit of facies 3 interbedded sand and silt (Fig. 10F). All primary bedding is steeply inclined towards the south, at ~30–35° in the lower part increasing to 50–60° in the upper part (Fig. 10F). The primary bedding is cut by numerous thrust planes, at some places paralleling the bedding surfaces and thus making them hard to differentiate, but at other places revealing the tectonic stacking pattern by lower inclination (Fig. 11D, H). Measured thrust planes and fold surfaces parallel the direction and dip of tectonically imbricated sediment bedding (Fig. 10F). Some thrust planes have developed into a few to 40 cm thick thrust zones, with internal shear lamination paralleling the bounding thrust surfaces. Sediments in the footwall of thrust planes and thrust zones often reveal deformation, ranging from small-scale drag folds up to larger-scale isoclinal to polyclinal folding of the sediments (e.g. Fig. 11I). Boulders, with diameters of 20–70 cm, were also encountered along thrust planes and thrust zones, not belonging to the primary sediments. These boulders, as indicated from sub-section B (Fig. 10C), are suggested to be retrieved from the lower diamict further down and dragged up during the deformational construction of the moraine.

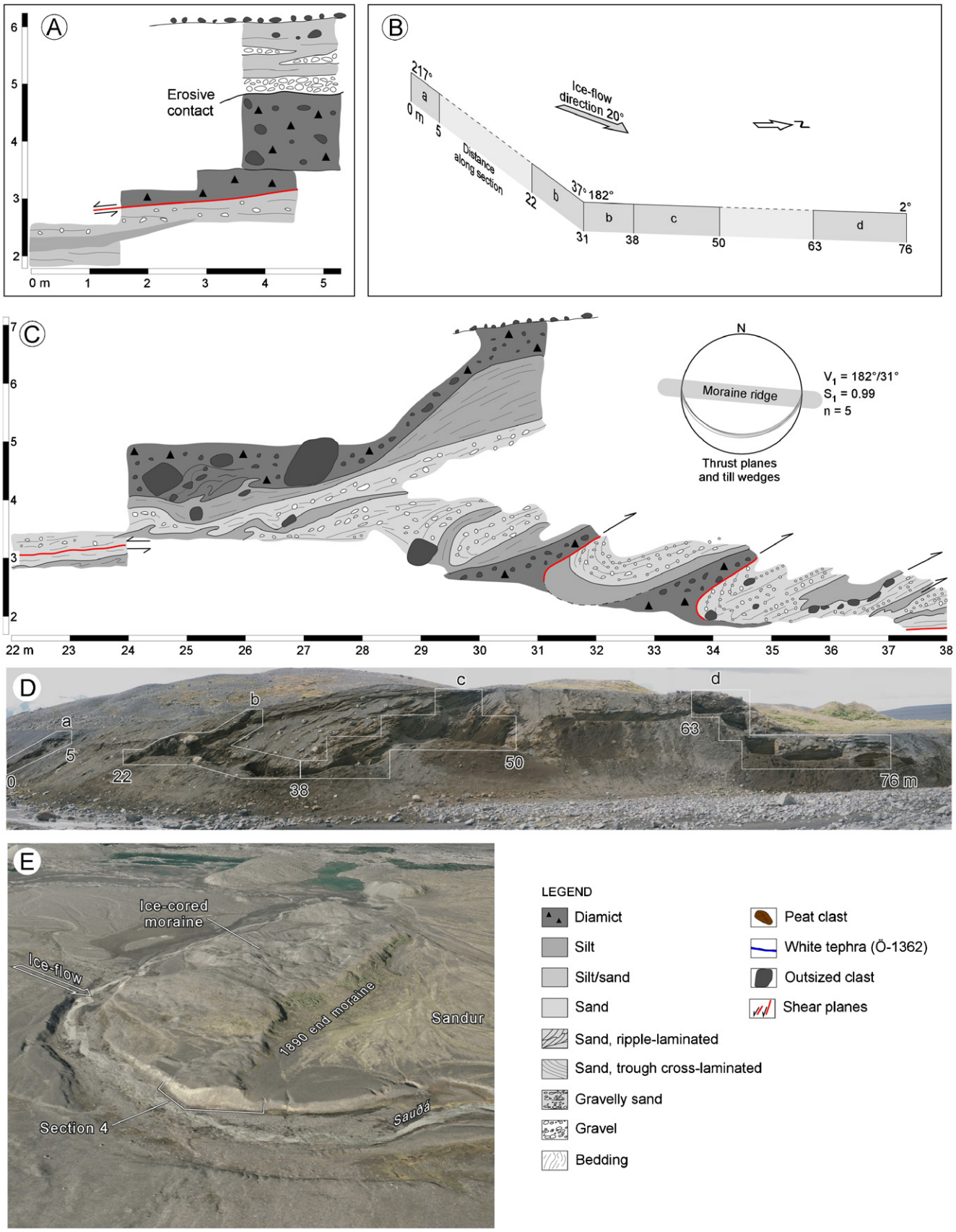

Fig. 10. Section 4. (A) Sub-section 4A, 0–5 m. (B) Outline of section orientation. (C) Sub-section 4B, 22–38 m. (D) Photograph of section 4, with sub-sections marked. (E) Overview of the section and its surroundings. Aerial orthophotograph draped over a DEM with 1.5 × vertical exaggeration. (F) Sub-section 4C, 38–50 m. (G) Sub-section 4D, 63–76 m. Note slight differences in scale between sub-sections.

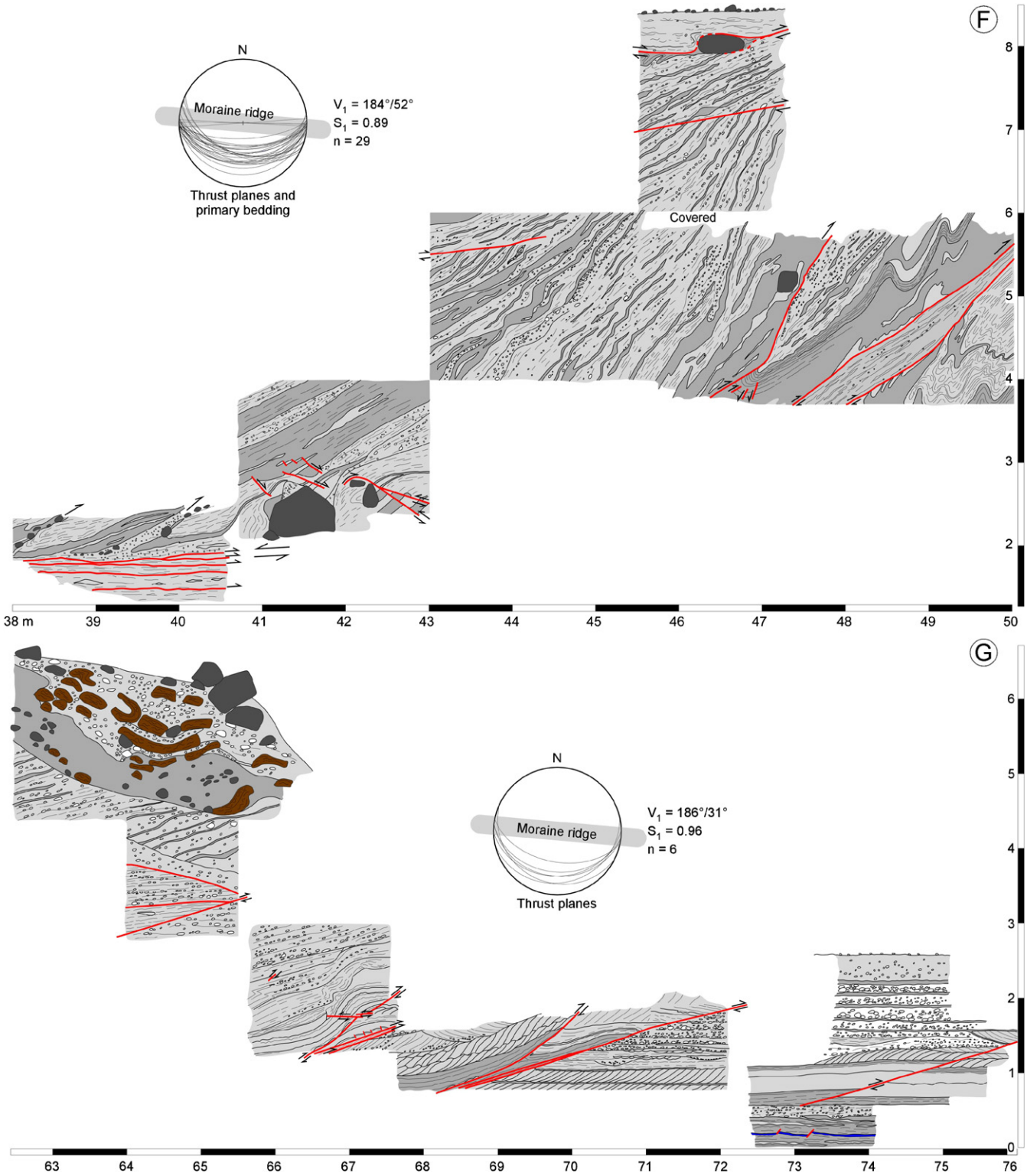

Fig. 10. (*Continued*)

The top of the section is marked by a subhorizontal décollement cutting the high-angle facies 3 sands and silts, overlain by a ~40 cm thick unit of shear-laminated sandy glaciotectonite (facies 4; Fig. 11D). The décollement plane is also marked by a number of boulders, ploughing into underlying sediments and with nearby shear lamination conforming to the shape of the boulders (e.g. Fig. 11E).

4D, the distal slope and moraine foreland, 63–77 *m*—The moraine foreland is sedimentologically characterized by an ~2.5 m thick, inversely graded sequence of facies 3 to facies 2 sandur sediments (Fig. 10G). In the lowermost distal

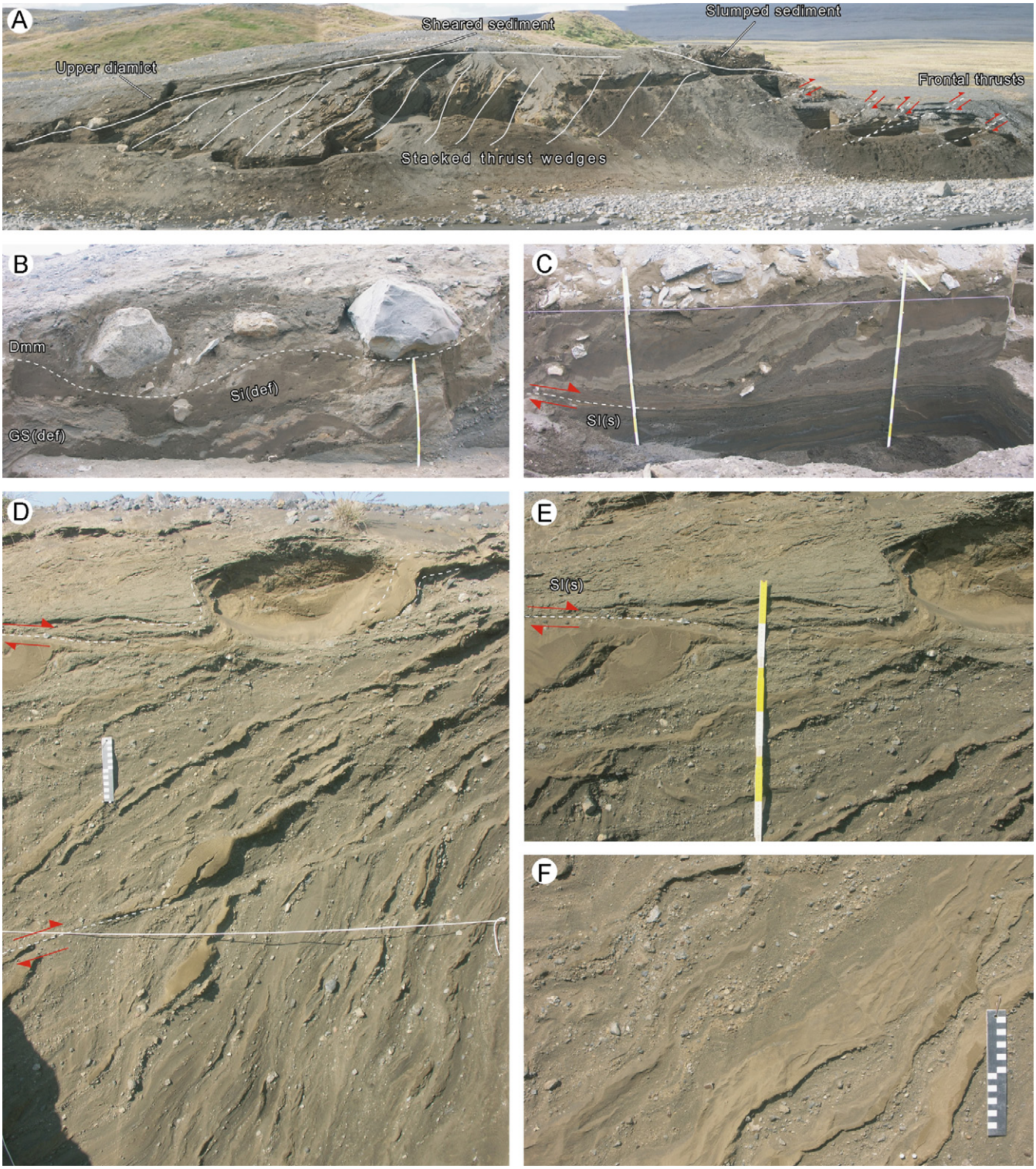

Fig. 11. Tectonic structures in and around section 4. Tectonic stress from left to right in all photos. (A) Overview of the section with main thrusts marked. (B) The upper diamict (facies 1) with drag structures, folds and ploughs, overlying facies 3. (C) Subhorizontal sequence of sand and gravelly sand showing shear lamination. (D) Glaciotectonite (facies 4) above the topmost décollement overlying facies 3. (E) A 40–50 cm thick zone of shear-laminated sand above pronounced décollement cutting steeply imbricated thrust wedges of facies 3. (F) Close-up of imbricated and interbedded facies 3 sediments. (G) Isoclinally folded layers of LPT west of the section. Height of the wall is approximately 3 m. (H) Shear-laminated gravelly silty sand forms a ~40 cm thick and imbricated unit between less deformed sand and silt thrust wedges. (I) Ductile deformation in gravelly silty sand. (J) Chaotically bedded peat clasts in a matrix of fluvial sands and gravels. (K) Thrust plane with drag folds and buckled sediments, associated with another thrust, in the hanging wall. (L) Normal grading in gravel overlying trough cross-laminated sand at the footwall of a thrust in the distal part. (M). Thrust planes in facies 3, with small vertical and lateral off-sets, in the distal part of the moraine. Dmm: diamicton, matrix supported; GS(def): gravel, sandy, deformed; Sl: sand, laminated; Stc: sand, trough cross-laminated; Spp: sand, planar parallel laminated; Sr; sand, ripple laminated; Si: silt; Si/S(s): silt, sandy, stratified. Lithofacies codes modified from Eyles et al. (1983).

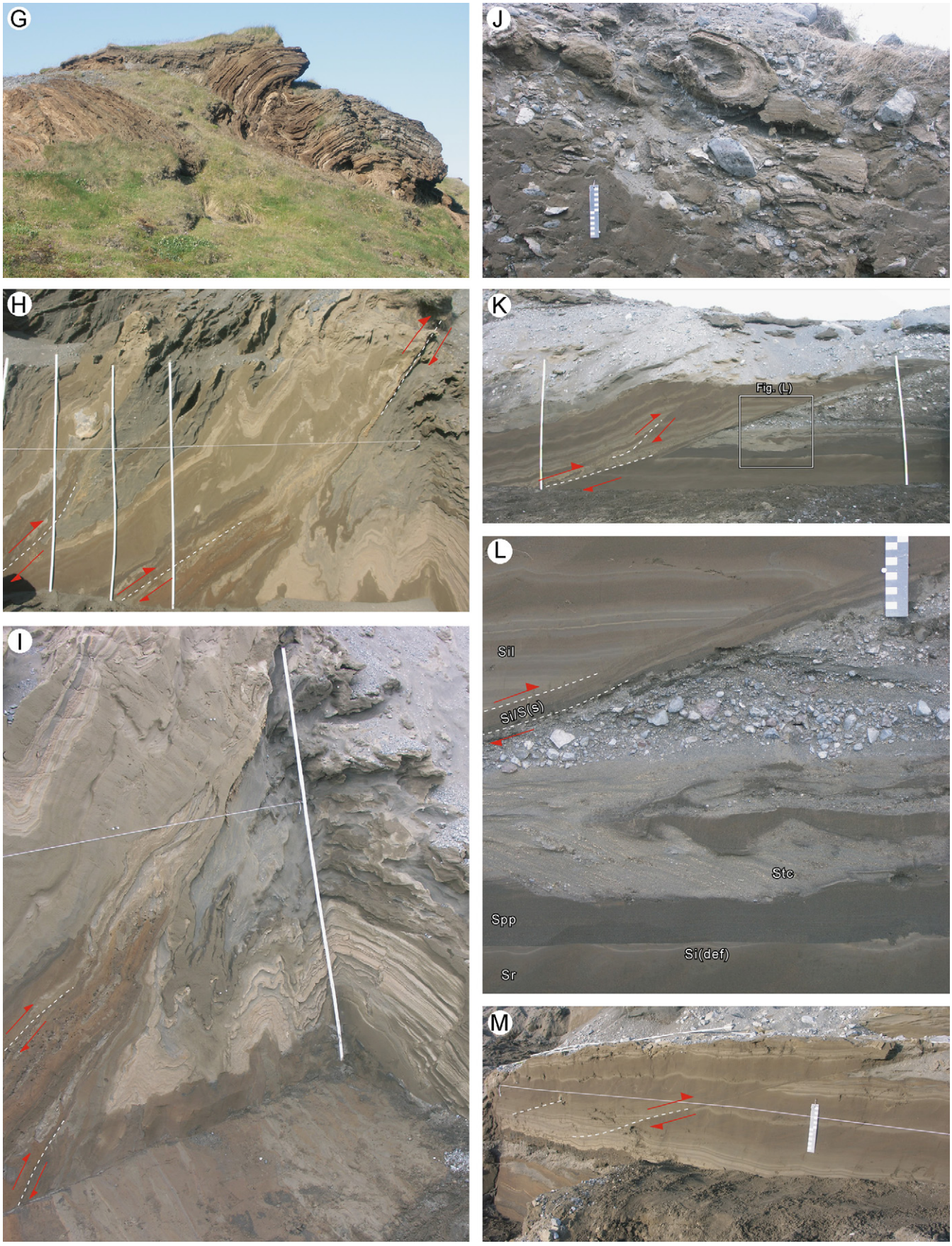

Fig. 11. (*Continued*)

part, a 5 mm thick layer of the white to yellowish Öræfajökull (1362 AD) tephra marker was found.

The sequence is cut by a number of thrust planes in distal direction from the moraine ridge (Figs. 10G and 11A). The thrust planes are planar to listric (concave) in their geometry, with small lateral and vertical off-sets in the distal part of the section (Fig. 11M), but increase in angles and vertical/lateral off-sets in proximal direction. Here, the fault planes are also characterized by drag folds in the footwall and compressive buckling of the sediments in the hanging wall (Fig. 11K). Some of the thrust planes have—or develop in distal direction—thin thrust zones with shear lamination. When traced backwards the thrust planes are seen to emanate from subhorizontal, in situ-positioned clay beds in the lower part of the succession. The thrust planes follow these beds for some distance before setting off with upwards increasing angles, usually as a listric fault plane. Measurements on fault planes indicate a deformational stress and displacement from more or less due south (Fig. 10G).

Beneath the frontal slope of the moraine there is an increased angle of block-thrusted sand and silt (facies 3), terminated by an erosional unconformity. Above this surface the frontal part of the moraine consists of facies 6, i.e. chaotically bedded peat clasts in a matrix of predominantly fluvial sands and gravels (Fig. 11J). It is suggested that these sediments were gravitationally deposited in front of the glacier margin at its maximum position during the 1890 surge. Close to this site the upper frontal part of the moraine consists of isoclinal folded LPT (facies 5; Fig. 11G).

9.2. Genetic interpretation of glaciotectonics

As the constructional part of the 1890 end moraine at Sauðá is totally dominated by imbricated thrust wedges, the moraine can here be classified as a thrust-dominated moraine, resulting from very friction-low or -free sliding along a basal décollement (Boulton and Caban, 1995; Bennett, 2001), which at this site is assumed to be the bedrock surface. The deformational architecture at Sauðá is thus very different from the other sites along the 1890 end moraine, being fold-dominated with higher basal friction.

The pre-existing, deformable sediments had a thickness of ~3 m, as indicated from the surface altitude of the foreland sandur down to the basal till surface, exposed in the present Sauðá River channel. As the ridge composed of imbricated thrust slices has a width of ~50 m, this gives an aspect ratio of the foreland sediments of ~1:17, indicating a substantial compressive shortening of the pre-existing sediment wedge.

The basal, subhorizontal unit of shear-laminated sand (facies 4 glaciotectonite) is suggested to have functioned as a ductile zone along which décollement occurred. A high porewater pressure at this level, decreasing the yield strength of the sediments, was enhanced by the underlying diamict with low hydraulic conductivity preventing downwards porewater escape. It is most probable that the thrusts slabs, riding on the basal décollement, were gradually emplaced and stacked from distal to proximal direction. This assumption is based on the general architecture of the imbricated sediment slabs, the fact that thrust surfaces cut the basal décollement zone and incorporate the underlying diamict into the glaciotectonic displacement, and that low-angle thrusts cut more highly imbricated thrust slabs.

During late-stage ridge formation the ice margin advanced over most part of the frontally thrusted sediment slab, eroding and smoothing the proximal slope and depositing the upper diamict on the lower part of the slope. However, the glacier advanced further than as indicated by the distribution of the upper diamict (Fig. 11A). As shown by the continuation of the topmost glaciotectonite above the shallow-lying décollement over the crestline of the moraine (Fig. 11D), the ice front advanced very close to the frontal slope.

10. The sediment distribution below the 1890 surge surface

Profile A′–A (Fig. 12) shows a sediment distribution typical of low-lying areas where the sediment sequence is thick and end-moraine ridges are prominent (Fig. 1). The profile extends across the 1810 and 1890 moraine ridges, and a fluted and hummocky ground moraine incised by post-surge channels. Upglacier of the 1810 moraine, there is a thin cover of sediment resting on a bedrock knob. But just proximal to the moraine the sediment thickness increases and reaches a maximum of 5 m at the centre of the moraine but decreases down to about 3 m in front of it. Thus, the 1810 moraine apparently consists of a thick sediment sequence that was overridden and drumlinized during the 1890 surge; hence it has a broad appearance (Fig. 12). The sediment thickness increases dramatically towards the high and single-crested 1890 end moraine and culminates in roughly 7 m at the crest (Fig. 12). By comparing the sediment thickness to the 1890 surface morphology it is obvious that upglacier-tapering sediment wedges occur at the proximal side of both the 1810 and 1890 end moraines (Fig. 12). This can be explained by a conceptual sediment distribution model (Fig. 13) based on the basal motion model from Brúarjökull by Kjær et al. (2006). They deduced that there was a strong coupling at the ice/bed interface during the 1890 surge, indicated by preferred orientation of clast fabric in flutes, but a decoupling at the substrate/bedrock interface due to lowered effective pressures caused by overpressurized subglacial porewater, indicated by a set of waterlain interlaminated sediments between the substrate and the bedrock, as discussed in detail by Kjær et al. (2006). As a result of the substrate/bedrock decoupling, subglacial sediment was dislocated across the bedrock surface, though at a lower velocity than that of the ice, resulting in a high sediment influx from upglacier sources to the marginal

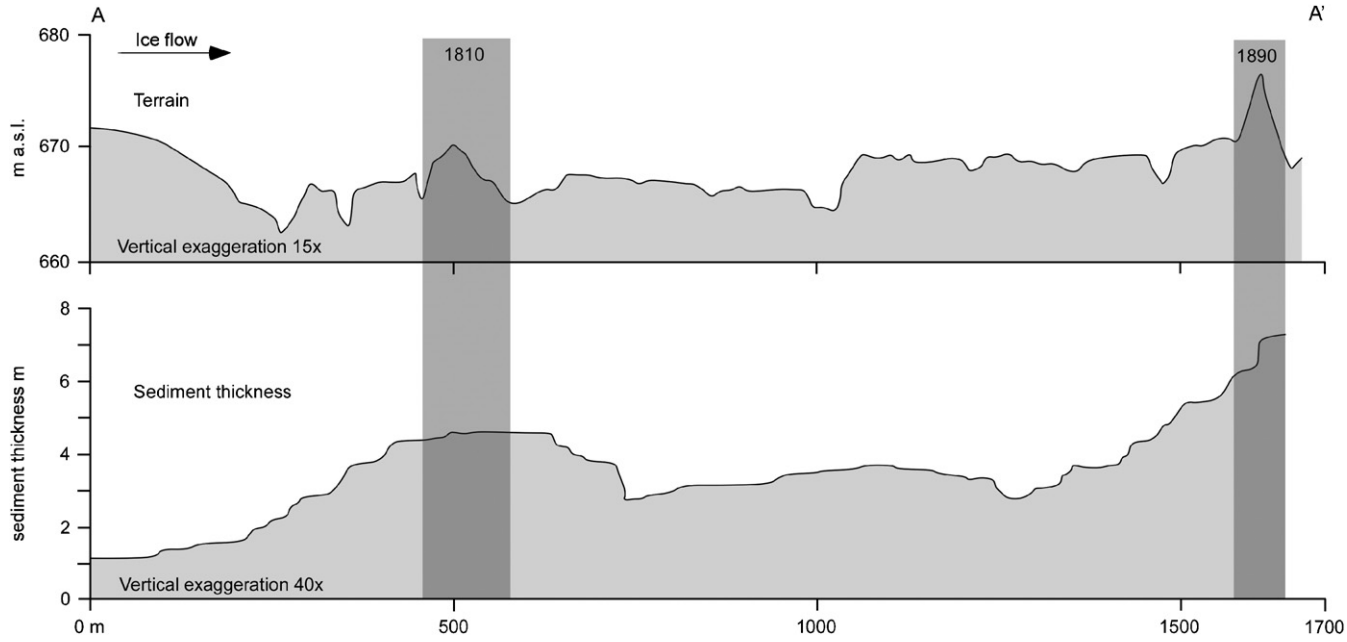

Fig. 12. Profile A–A′ in the eastern part of the study area (see Fig. 1 for location). Above is a terrain profile and below is a profile showing thickness of sediments above bedrock. Two sediment wedges are clearly visible on the proximal sides of the overridden 1810 moraine and the 1890 end moraine.

zone. To accommodate the high sediment influx and the difference in velocity at which the ice and the substrate moved, the latter deformed compressively through multiple folding and fold attenuation. This is demonstrated by repeated occurrence of the white Öræfajökull 1362 AD tephra marker in the stratigraphy below the 1890 surge surface, and by original sedimentary structures recognizable in the deformed sequence (Fig. 13; Kjær et al., 2006). The sediment influx and compressive deformation resulted in a downglacier gradual thickening of the subglacial sediment succession and the formation of a reverse sloping sediment wedge in the marginal zone (Figs. 12 and 13).

11. Sequential model for the formation of the 1890 end moraine

Based on our observations and those by Kjær et al. (2006), an interpretative sequential model is proposed, illustrating both the sub-marginal processes operating during the last phase of the surge and the late formation of the end moraine (Fig. 14). The model includes five stages ranging from the quiescent-phase situation before the surge, throughout the 1890 surge phase. The stages of the model are as follows:

1. In the quiescent phase, the glacier was inactive and downwasting. Sediments from disintegrating crevasse-fill ridges and debris bands partly covered the snout and glaciolacustrine sediments accumulated in topographic depressions at the margin.
2. During the surge, compressive flow in the surge-wave caused thrusts and associated debris entrainment in the ice, and the release of debris to the glacier surface. Where the substrate was fine-grained, porewater overpressure occurred because water from upstream sources could not be dissipated at the same rate as it was supplied. Drainage occurred along the bedrock surface, probably in pulses, as demonstrated by waterlain interlaminated sediment at the substrate/bedrock interface (see van der Meer et al., 1999; Kjær et al., 2006). The porewater overpressure caused reduction of effective normal stress and a decoupling of the substrate from the bedrock. Thus, the substrate sediment was displaced across the bedrock surface and thus initiating a sediment flux towards the marginal zone.
3. Where and when the surge-wave had passed, the glacier thinned, extended flow set in and the crevasse network opened up. Overpressurized subglacial porewater found its way along thrust planes and debris bands up into surface crevasses, leading to supraglacial drainage. The marginal sediment wedge had developed and a reverse slope had formed below the ice margin. Overpressurized subglacial porewater blew out in front of the ice margin, as demonstrated by circular blow-out structures at the abrupt head of channels outside the 1890 end moraine (Christiansen et al., 1982; Boulton and Caban, 1995; Kjær et al., 2006; Figs. 4A, 8C and 9D). Probably the water blew out through gaps in the discontinuous permafrost.
4. At the last days of the surge, the volume of ice available for the advance became exhausted and the upstream meltwater reservoir was more or less emptied. Less water was thus added to the subglacial sediments, causing porewater pressure to drop, leading to stiffening of the fine-grained substrate and strengthened coupling at the ice/bed interface. Consequently, the slip at the ice/

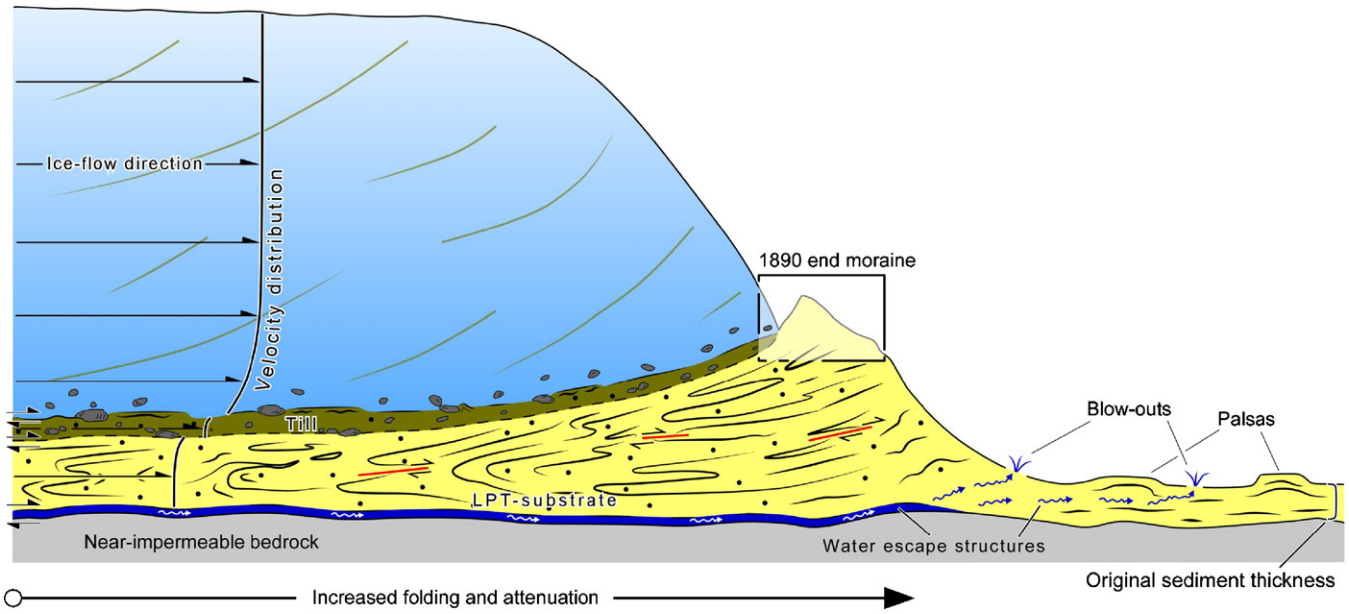

Fig. 13. Conceptual model illustrating the formation of a sedimentary wedge in the marginal zone of the 1890 Brúarjökull surge. See text for an explanation.

bed interface ceased, explaining the termination of flutes 100–200 m upglacier of the 1890 moraine. Due to the drop in subglacial porewater pressure and a consequent rise in effective normal stress, the substrate also became coupled to the bedrock, leading to increased friction and stress transfer up into the substrate, causing it to deform in brittle manner (Boulton et al., 2001; Clarke, 2005). This explains the overprinting of brittle structures on the overall ductile deformed subglacial sediment in the marginal wedge. The strengthened ice/bed coupling allowed the glacier toe to plough into the reverse slope of the marginal sediment wedge. This further deformed the topmost part of the wedge and initiated the moraine-ridge formation. The degree to which the deformation developed within the end moraine is different from one part to another, as demonstrated by the increased intensity of the deformation from sections 1 and 2 to sections 3 and 4. However, the entire end-moraine ridge is thought to have formed within this stage of the model, i.e. when the sediment wedge had mostly or fully developed at the very end of the surge. At some places, the moraine ridge acted as an obstacle against which the glacier pushed, causing thrusting in the ice margin and associated upward sediment transport along thrust planes. This sediment subsequently covered the underlying ice, later resulting in differential ablation during the quiescent phase. This is supported by wide belts of hummocky moraine on the backslope of the 1890 end moraine (Benediktsson, 2005; Schomacker and Kjær, 2007; Kjær et al., in press).

5. The morphology and tectonic architecture of the 1890 end-moraine ridge were mainly controlled by the competence of the sediment that was deformed to give the moraine, and by how far the deformation developed during the moraine-ridge construction. (A) Fine-grained sediment with high porewater pressures during the surge phase behaved incompetent and thus predominantly deformed in ductile manner, resulting in a fold-dominated moraine. All glaciotectonic stress was absorbed within a relatively narrow zone (50–100 m). This is demonstrated by sections 1–3 where proximal–distal widths of the moraine are not particularly great and folds are usually rooted, indicating high internal and basal friction (Boulton and Caban, 1995; Bennett, 2001). (B) Where the sediments were overall coarse-grained and competent, the tectonic stress was translocated in distal direction and the sediment succession deformed in brittle fashion, resulting in imbricated sediment slabs with low-angle thrusts in the distal zone, as revealed by section 4. Here, the width of the moraine is greater (100–200 m), probably due to very low friction along the basal décollement.

The deformation observed in the moraine ridge can be regarded, to a large extent, as a part of the marginal sediment-wedge formation. The drainage that set in during the last 1–2 days of the surge contributed to brittle deformation and continued folding, leading to the construction of the moraine ridge at the top of the marginal sediment wedge. In effect, no actual basal décollement developed in the end moraine as it is a part of the wedge, the décollement of which lies across the bedrock surface. As a result, the sediment wedge and the end moraine represent a twofold, inseparable marginal end-product of the 1890 surge. Considering ice velocities of 100–120 m/day during the Brúarjökull surges, the ~500 m marginal sediment wedge most likely formed during the last ~5 days and the end-moraine ridge in the last ~1 day of the 1890 surge. The late

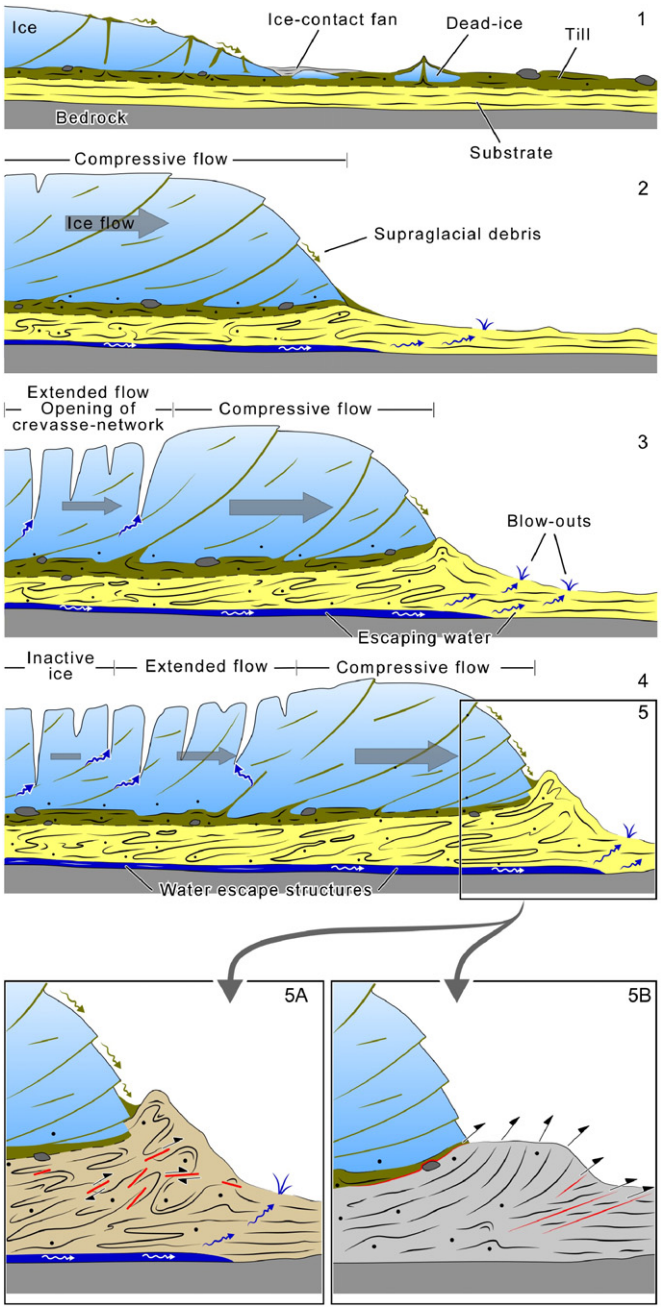

Fig. 14. Sequential model of the 1890 sediment-wedge and end-moraine formation. See text for an explanation.

development of the moraine is supported by actual observations and descriptions of the 1963–1964 Brúarjökull surge, during which no marginal moraines were observed and the glacier did not seem to plough the ground (Eyþórsson, 1963). However, prominent moraines from that surge are found in the forefield of Brúarjökull at present (Thorarinsson, 1969; Benediktsson, 2005).

12. Conclusion

The 1890 end moraine exhibits two kinds of morphology. Firstly, low and narrow ridges consisting of cobbles and boulders are associated with elevated areas in the glacier forefield where bedrock is at shallow depths and sediment cover is thin. These moraines are thought to have been formed by dumping of englacial and supraglacial debris at the margin (e.g. Evans and Twigg, 2002; Krüger et al., 2002; Benediktsson, 2005). Secondly, there are high, wide and single-crested ridges, at many places composed of soft sediments such as interbedded LPT, but at other places consisting of coarse sediments such as gravels and sands. These ridges occur in low-lying areas where the sediment supply available for deformation was abundant.

It is argued that the morphology and tectonic architecture of the 1890 end-moraine ridge are mainly controlled by the competence of the sediment. Fine-grained sediment predominantly deformed in ductile manner, resulting in a narrow moraine dominated by rooted folds, while coarse-grained sediment deformed in brittle fashion, leading to the formation of a wide imbricated moraine.

As a conclusion, the ice-marginal position of the 1890 surge is marked by a twofold end-product: a sedimentary wedge in the marginal ~500 m and the end-moraine ridge as a surface expression of this wedge. As ice-flow velocities are usually around 100–120 m/day during a Brúarjökull surge (Thorarinsson, 1969), the sedimentary wedge is thought to have formed within approximately 5 days and the moraine ridge in about 1 day.

This study provides us with new information about subglacial and sub-marginal processes of fast-flowing glaciers and may help to understand the mechanism behind the formation of sediment wedges at the grounding line of ice streams, such as those recently discovered at the margin of the Whillans Ice Stream in the west Antarctic (Alley et al., 2007; Anandakrishnan et al., 2007) and at the margins of palaeo-ice streams in the eastern Ross Sea (Mosola and Andersen, 2006) and in the Bjørnøyrenna Trough, Barents Sea (Andreassen et al., 2007). The two models proposed may be applicable in areas where fast-flowing ice overrides subglacial sequences that favour porewater overpressures and subsequent decoupling at the interface between the substrate and a weak stratum below. The decoupling leads to enhanced ice-flow velocities and a high influx of sediment to the marginal zone, resulting in the formation of marginal sediment wedges with end-moraine ridges on top.

Acknowledgements

Financial support for the Brúarjökull project was provided by the Swedish National Research Council, the Royal Physiographic Society in Lund, the Crafoord Foundation, the Icelandic Research Council, the University of Iceland Research Fund, Landsvirkjun and the Danish National Research Council. The National Museum of Iceland and Sven Sigurðsson kindly provided access to and retrieved photographic material from the photo archive of Sigurður Þórarinsson. We express our sincere thanks to Anders Schomacker, Carita G. Knudsen, Svante

Björck, Eiliv Larsen, Louise Ravn, Lilja Rún Bjarnadóttir, Jón Björn Ólafsson, Ida H.E.O. Jönsson and Silvana Correa Kjær for their companionship and collaboration during the 2003–2005 fieldwork at Brúarjökull. Í.Ö.B. acknowledges scholarships from Landsvirkjun, the Icelandic Research Fund for Graduate Students and the University of Iceland Research Fund. Thanks are due to one anonymous reviewer and Jim Rose for constructive and useful comments on the paper.

References

Aber, J., Croot, D.G., Fenton, M.M., 1989. Glaciotectonic Landforms and Structures. Kluwer, Dordrecht.

Alley, R.B., Anandakrishnan, S., Dupont, T.K., Parizek, B.R., Pollard, D., 2007. Effect of sedimentation on ice-sheet grounding-line stability. Science 315, 1838–1841.

Alsop, G.I., Holdsworth, R.E., 1999. Vergence and facing patterns in large-scale sheath folds. Journal of Structural Geology 21, 1335–1339.

Anandakrishnan, S., Catania, G.A., Alley, R.B., Horgan, H.J., 2007. Discovery of till deposition at the grounding line of Whillans Ice Stream. Science 315, 1835–1838.

Andreassen, K., Laberg, J.S., Vorren, T.O., 2007. Seafloor geomorphology of the SW Barents Sea and its glaci-dynamic implications. Geomorphology, in press, doi:10.1016/j.geomorph.2007.02.050.

Andrzejewski, L., 2002. The impact of surges on the ice-marginal landsystem of Tungnaárjökull, Iceland. Sedimentary Geology 149, 59–72.

Benediktsson, Í.Ö., 2005. The 1890 and 1964 push moraines at Brúarjökull, a surge-type glacier in Iceland: morphology, sediments and structural geology. M.Sc. Thesis, Institute of Geography, University of Copenhagen, Denmark.

Benn, D.I., Evans, D.J.A., 1996. The interpretation and classification of subglacially-deformed materials. Quaternary Science Reviews 15, 23–52.

Benn, D.I., Evans, D.J.A., 1998. Glaciers and Glaciation. Arnold, London.

Bennett, M.R., 2001. The morphology, structural evolution and significance of push moraines. Earth-Science Reviews 53, 197–236.

Bennett, M.R., Huddart, D., Hambrey, M.J., Ghienne, J.F., 1996. Moraine development at the high-Arctic valley glacier Pedersenbreen, Svalbard. Geografiska Annaler 78A, 209–222.

Bennett, M.R., Hambrey, M.J., Huddart, D., Glasser, N.F., Crawford, K., 1999. The landform and sediment assemblage produced by a tidewater glacier surge in Kongsfjorden, Svalbard. Quaternary Science Reviews 18, 1213–1246.

Bennett, M.R., Huddart, D., Waller, R.I., Midgley, N.G., Gonzalez, S., Tomio, A., 2004a. Styles of ice-marginal deformation at Hagafellsjökull-Eystri, Iceland, during the 1998/99 winter–spring surge. Boreas 33, 97–107.

Bennett, M.R., Huddart, D., Waller, R.I., Cassidy, N., Tomio, A., Zukowskyj, P., Midgley, N.G., Cook, S.J., Gonzalez, S., Glasser, N.F., 2004b. Sedimentary and tectonic architecture of a large push moraine: a case study from Hagafellsjökull-Eystri, Iceland. Sedimentary Geology 172, 269–292.

Bergthorsson, P., 1969. An estimate of drift ice and temperatures in Iceland in 1000 years. Jökull 19, 94–101.

Bjarnadóttir, L.R., 2007. Ice-marginal environment of a surge-type glacier: distribution, formation and morphological evolution of flutes and crevasse cast ridges at Brúarjökull, Iceland. M.Sc. Thesis, Department of Geology and Geography, University of Iceland, Reykjavík, Iceland.

Björnsson, H., Pálsson, F., Guðmundsson, M.T., Haraldsson, H.H., 1998. Mass balance of western and northern Vatnajökull, Iceland, 1991–1995. Jökull 45, 35–38.

Björnsson, H., Pálsson, F., Sigurðsson, O., 2003. Surges of glaciers in Iceland. Annals of Glaciology 36, 82–90.

Boulton, G.S., 1986. Push-moraines and glacier-contact fans in marine and terrestrial environments. Sedimentology 33, 677–698.

Boulton, G.S., Caban, P., 1995. Groundwater flow beneath ice sheets: part II—its impact on glacier tectonic structures and moraine formation. Quaternary Science Reviews 14, 563–587.

Boulton, G.S., van der Meer, J.J.M., Hart, J., Beets, D., Ruegg, G.H.J., van der Wateren, F.M., Jarvis, J., 1996. Till and moraine emplacement in a deforming bed surge—an example from a marine environment. Quaternary Science Reviews 15, 961–987.

Boulton, G.S., van der Meer, J.J.M., Beets, D.J., Hart, J., Ruegg, G.H.J., 1999. The sedimentary and structural evolution of a recent push moraine complex: Holmstrømbreen, Spitsbergen. Quaternary Science Reviews 18, 339–371.

Boulton, G.S., Dobbie, K.E., Zatsepin, S., 2001. Sediment deformation beneath glaciers and its coupling to the subglacial hydraulic system. Quaternary International 86, 3–28.

Brady, N.C., Weil, R.R., 1999. The Nature and Properties of Soils, 12th ed. Prentice-Hall, Englewood Cliffs, NJ.

Christiansen, E.A., Gendzwill, D.J., Meneley, W.A., 1982. Howe Lake: a hydrodynamic blowout structure. Canadian Journal of Earth Sciences 19, 1122–1139.

Clarke, G.C.K., 2005. Subglacial processes. Annual Review of Earth and Planetary Sciences 33, 247–276.

Cobbold, P.R., Quinquis, H., 1980. Development of sheath folds in shear regimes. Journal of Structural Geology 2, 119–126.

Croot, D.G., 1987. Glacio-tectonic structures: a mesoscale model of thin-skinned thrust sheets? Journal of Structural Geology 9, 797–808.

Croot, D.G., 1988a. Morphological, structural and mechanical analysis of neoglacial ice-pushed ridges in Iceland. In: Croot, D.G. (Ed.), Glaciotectonics: Forms and Processes. Balkema, Rotterdam, pp. 33–47.

Croot, D.G., 1988b. Glaciotectonics and surging glaciers: a correlation based on Vestspitsbergen, Svalbard, Norway. In: Croot, D.G. (Ed.), Glaciotectonics: Forms and Processes. Balkema, Rotterdam, pp. 49–61.

Dowdeswell, J.A., Ó Cofaigh, C., Pudsey, C.J., 2004. Thickness and extent of the subglacial till layer beneath an Antarctic paleo-ice stream. Geology 32, 13–16.

Drozdowski, E., 1987. Surge moraines. International Geomorphology, Part II 675–691.

Etzelmüller, B., Farbrot, H., Guðmundsson, Á., Humlum, O., Tveito, O.E., Björnsson, H., 2007. The regional distribution of mountain permafrost in Iceland. Permafrost and Periglacial Processes 18, 185–199.

Evans, D.J.A., Benn, D.I., 2004. A Practical Guide to the Study of Glacial Sediments. Arnold, London.

Evans, D.J.A., Rea, B.R., 1999. Geomorphology and sedimentology of surging glaciers: a land-system approach. Annals of Glaciology 28, 75–82.

Evans, D.J.A., Rea, B.R., 2003. Surging glacier landsystem. In: Evans, D.J.A. (Ed.), Glacial Landsystems. Arnold, London.

Evans, D.J.A., Twigg, D.R., 2002. The active temperate glacial landsystem: a model based on Breiðamerkurjökull and Fjallsjökull, Iceland. Quaternary Science Reviews 21, 2143–2177.

Evans, D.J.A., Philipps, E.R., Hiemstra, J.F., Auton, C.A., 2006. Subglacial till: formation, sedimentary characteristics and classification. Earth-Science Reviews 78, 115–176.

Eyles, N., Eyles, C.H., Miall, A.D., 1983. Lithofacies types and vertical profile models: an alternative approach to the description and environmental interpretation of glacial diamict and diamictite sequences. Sedimentology 30, 393–410.

Eyþórsson, J., 1963. Brúarjökull hlaupinn (with summary). Jökull 13, 19–21.

French, H.M., 1996. The Periglacial Environment. Longman, Harlow, London.

Gripp, K., 1929. Glaciological and geological results of the Hamburg Spitsbergen-expedition of 1927. In: van der Meer, J.J.M. (Ed.),

Spitsbergen Push Moraines. Elsevier, Amsterdam. Developments in Quaternary Science 4, 3–98.
Guðmundsson, H., 1997. A review of the Holocene environmental history of Iceland. Quaternary Science Reviews 16, 81–92.
Hambrey, M.J., Huddart, D., 1995. Englacial and proglacial glaciotectonic processes at the snout of a thermally complex glacier in Svalbard. Journal of Quaternary Science 10, 313–326.
Hart, J.K., Roberts, D.H., 1994. Criteria to distinguish between subglacial glaciotectonic and glaciomarine sedimentation. I. Deformation styles and sedimentology. Sedimentary Geology 91, 191–213.
Hart, J.K., Watts, R., 1997. Comparison of the styles of deformation associated with two recent push moraines, south Van Keulenfjorden, Svalbard. Earth Surface Processes and Landforms 22, 1089–1107.
Huddart, D., Hambrey, M.J., 1996. Sedimentary and tectonic development of a high-Arctic, thrust-moraine complex: Comfortlessbreen, Svalbard. Boreas 25, 227–243.
Humlum, O., 1985. Genesis of an imbricated push moraine, Höfðabrekkujökull, Iceland. Journal of Geology 93, 185–195.
Kälin, M., 1971. The active push moraine of the Thompson Glacier, Axel Heiberg Island, Canadian Artic Archipelago. Axel Heiberg Island Research Reports, Glaciology No. 4, McGill University, Montreal. Ph.D. Thesis, ETH Zürich.
Kjær, K.H., Krüger, J., 2001. The final phase of dead-ice moraine development: processes and sediment architecture, Kötlujökull, Iceland. Sedimentology 48, 935–952.
Kjær, K.H., Larsen, E., van der Meer, J., Ingólfsson, Ó., Krüger, J., Benediktsson, Í.Ö., Schomacker, A., Knudsen, C.G., 2006. Subglacial decoupling at the sediment/bedrock interface: a new mechanism for rapid flowing ice. Quaternary Science Reviews 25, 2704–2712.
Kjær, K.H., Larsen, N.J., Schomacker, A. (in press). Impact of multiple glacier surges – a geomorphological map from Brúarjökull, East Iceland. Journal of Maps.
Krüger, J., 1985. Formation of a push moraine at the margin of Höfðabrekkujökull, South Iceland. Geografiska Annaler 67A, 199–212.
Krüger, J., 1993. Moraine-ridge formation along a stationary ice front in Iceland. Boreas 22, 101–109.
Krüger, J., 1994. Glacial processes, sediments, landforms, and stratigraphy in the terminus region of Mýradalsjökull, Iceland. Folia Geographica Danica 21, 1–233.
Krüger, J., 1996. Moraine ridges formed by subglacial frozen-on sediment slabs and their differentiation from push moraines. Boreas 25, 57–63.
Krüger, J., Kjær, K.H., 1999. A data chart for field description and genetic interpretation of glacial diamicts and associated sediments—with examples from Greenland, Iceland, and Denmark. Boreas 28, 386–402.
Krüger, J., Kurt, K.H., van der Meer, J.J.M., 2002. From push moraine to single-crested dump moraine during a sustained glacier advance. Norsk Geografisk Tidsskrift 56, 87–95.
Lønne, I., Lauritsen, T., 1996. The architecture of a modern push-moraine at Svalbard as inferred from ground-penetrating radar measurements. Arctic, Antarctic and Alpine Research 28, 488–495.
Lyså, A., Lønne, I., 2001. Moraine development at a small high-Arctic valley glacier: Rieperbreen, Svalbard. Journal of Quaternary Science 16, 519–529.
Maizels, J., 1993. Lithofacies variations within sandur deposits: the role of runoff regime, flow dynamics and sediment supply characteristics. Sedimentary Geology 85, 299–325.
Maizels, J., 2002. Sediments and landforms of modern proglacial terrestrial environments. In: Menzies, J. (Ed.), Modern and Past Glacial Environments, revised student ed. Butterworth-Heinemann, Oxford, pp. 279–316.
Marren, P.M., 2005. Magnitude and frequency in proglacial rivers: a geomorphological and sedimentological perspective. Earth-Science Reviews 70, 203–251.
Marshak, S., Mitra, G., 1988. Basic Methods of Structural Geology. Prentice-Hall, Englewood Cliffs, NJ.
Matthews, J.A., McCarrol, D., Shakesby, R.A., 1995. Contemporary terminal-moraine ridge formation at a temperate glacier, Styggedalsbreen, Jotunheimen, southern Norway. Boreas 24, 129–139.
Menzies, J. (Ed.), 1995. Modern Glacial Environments: Processes, Dynamics and Sediments. Butterworth-Heinemann, Oxford.
Möller, P., 1995. Subrecent moraine ridge formation on Cuff Cape, Victoria Land, Antarctica. Geografiska Annaler 77A, 83–94.
Mosola, A.B., Andersen, J.B., 2006. Expansion and rapid retreat of the West-Antarctic Ice Sheet in eastern Ross Sea: possible consequence of over-extended ice streams? Quaternary Science Reviews 25, 2177–2196.
Ravn, L., 2006. Interaktionen mellem klima og landskab-sediment-jordsystemet i et periglacialt miljø foran Brúarjökull, Island. Cand. scient. (M.Sc.) Thesis, University of Copenhagen (in Danish).
Rignot, E., Kanagaratnam, P., 2006. Changes in the velocity structure of the Greenland ice sheet. Science 311, 986–990.
Schomacker, A., Kjær, K.H., 2007. Origin and de-icing of multiple generations of ice-cored moraines at Brúarjökull, Iceland. Boreas 36, in press, doi:10.1080/03009480701213554.
Schomacker, A., Krüger, J., Kjær, K.H., 2006. Ice-cored drumlins at the surge-type Brúarjökull, Iceland: a transitional state landform. Journal of Quaternary Science 21, 85–93.
Shakesby, R.A., 1989. Variability in Neoglacial moraine morphology and composition, Storbreen, Jotunheimen, Norway: within-moraine patterns and their implications. Geografiska Annaler 71A, 17–29.
Sharp, M., 1985. Sedimentation and stratigraphy at Eyjabakkajökull—an Icelandic surging glacier. Quaternary Research 24, 268–284.
Stokes, C.R., Clark, C.D., 2001. Palaeo-ice streams. Quaternary Science Reviews 20, 1437–1457.
Thorarinsson, S., 1964. On the age of the terminal moraines of Brúarjökull and Hálsajökull. Jökull 14, 67–75.
Thorarinsson, S., 1969. Glacier surges in Iceland, with special reference to the surges of Brúarjökull. Canadian Journal of Earth Sciences 6, 875–882.
Todtmann, E.M., 1960. Gletcherforschungen auf Island (Vatnajökull). Universität Hamburg. Abhandlungen aus dem Gebiet der Auslandskunde 65C, 1–95.
Twiss, R.J., Moores, E.M., 1992. Structural Geology. W.H. Freeman, New York, 532pp.
van der Meer, J.J.M., Kjær, K.H., Krüger, J., 1999. Subglacial water escape structures and till structure, Sléttjökull, Iceland. Journal of Quaternary Science 14, 191–205.
van der Wateren, D.F.M., 1985. A model of glaciotectonics, applied to the ice-pushed ridges in the Central Netherlands. Bulletin of Geological Society of Denmark 34, 55–74.
van der Wateren, D.F.M., 1995a. Structural geology and sedimentology of push moraines: processes of soft sediment deformation in a glacial environment and the distribution of glaciotectonic styles. Mededelingen Rijks Geologische Dienst 54.
van der Wateren, D.F.M., 1995b. Processes of Glaciotectonism. In: Menzies, J. (Ed.), Modern Glacial Environments: Processes, Dynamics and Sediments. Glacial Environments, vol. 1. Butterworth-Heinemann, London, pp. 309–335.
van der Wateren, D.F.M., 1999. Structural geology and sedimentology of the Heiligenhafen till section, Northern Germany. Quaternary Science Reviews 18, 1625–1639.
van Vliet-Lanoë, B., Bourgeois, O., Dauteuil, O., 1998. Thufur formation in Northern Iceland and its relation to Holocene climate change. Permafrost and Periglacial Processes 9, 347–365.
Winkler, S., Nesje, A., 1999. Moraine formation at an advancing temperate glacier: Brigdalsbreen, western Norway. Geografiska Annaler 81A, 17–30.

APPENDIX III

BOREAS An international journal of Quaternary research

Formation of submarginal and proglacial end moraines: implications of ice-flow mechanism during the 1963–64 surge of Brúarjökull, Iceland

ÍVAR ÖRN BENEDIKTSSON, ÓLAFUR INGÓLFSSON, ANDERS SCHOMACKER AND KURT H. KJÆR

BOREAS

Benediktsson, Í. Ö., Ingólfsson, Ó., Schomacker, A. & Kjær, K. H. 2009 (August): Formation of submarginal and proglacial end moraines: implications of ice-flow mechanism during the 1963–64 surge of Brúarjökull, Iceland. *Boreas*, Vol. 38, pp. 440–457. 10.1111/j.1502-3885.2008.00077.x. ISSN 0300-9483.

The morphology, sedimentology and architecture of an end moraine formed by a ~9 km surge of Brúarjökull in 1963–64 are described and related to ice-marginal conditions at surge termination. Field observations and accurate mapping using digital elevation models and high-resolution aerial photographs recorded at surge termination and after the surge show that commonly the surge end moraine was positioned underneath the glacier snout by the termination of the surge. Ground-penetrating radar profiles and sedimentological data reveal 4–5 m thick deformed sediments consisting of a top layer of till overlying gravel and fine-grained sediments, and structural geological investigations show that the end moraine is dominated by thrust sheets. A sequential model explaining the formation of submarginal end moraines is proposed. The hydraulic conductivity of the bed had a major influence on the subglacial drainage efficiency and associated porewater pressure at the end of the surge, thereby affecting the rates of subglacial deformation. High porewater pressure in the till decreased its shear strength and raised its strain rate, while low porewater pressure in the underlying gravel had the opposite effect, such that the gravel deformed more slowly than the till. The principal velocity component was therefore located within the till, allowing the glacier to override the gravel thrust sheets that constitute the end moraine. The model suggests that the processes responsible for the formation of submarginal end moraines are different from those operating during the formation of proglacial end moraines.

Ívar Örn Benediktsson (e-mail: iob2@hi.is), Ólafur Ingólfsson and Anders Schomacker, Institute of Earth Sciences, University of Iceland, Askja, Sturlugata 7, IS-101 Reykjavík, Iceland; Kurt H. Kjær, Natural History Museum of Denmark, University of Copenhagen, Øster Voldgade 5-7, DK-1350 Copenhagen K, Denmark; *received 31st July 2008, accepted 8th November 2008.*

End moraines are among the most prominent landforms of glacial landsystems and often the most obvious evidence of glaciotectonism occurring below, at or in front of ice margins (Aber *et al.* 1989; Benn & Evans 1998; Aber & Ber 2007). They vary greatly in morphological, sedimentary and architectural composition and provide important information about glacier dynamics and mechanics, physical conditions of the glacier substratum and foreland properties at the time of moraine formation (Aber *et al.* 1989; Benn & Evans 1998; Bennett *et al.* 1999, 2004a, b; Bennett 2001; Aber & Ber 2007). Consequently, end moraines record glacier activity and serve as modern analogues in palaeoglaciological reconstructions (e.g. Gripp 1929; Kälin 1971; Boulton 1972, 1986; Krüger 1994; van der Wateren 1995a, b; Benn & Evans 1998; Boulton *et al.* 1999; Bennett 2001; Menzies 2002; Evans 2003).

End moraines of surging glaciers have attracted attention in recent years as means of gaining information on the behaviour and mechanics of fast-flowing ice (Sharp 1985a; Croot 1988; Boulton *et al.* 1996, 1999; Hart & Watts 1997; Bennett *et al.* 1999, 2004a, b; Benediktsson *et al.* 2008). Much of this research has focused on the structural properties of end moraines and on the evolution of deformation within them, which primarily is caused by large-scale thrusting and folding as a result of ice pushing (bulldozing) and/or gravity spreading. The link between the dynamics of surging glaciers and the morphological and structural properties of their end moraines, however, is not well understood. Kjær *et al.* (2006) and Benediktsson *et al.* (2008) proposed new models of subglacial and ice-marginal processes operating during the 1890 surge of Brúarjökull, Iceland. Their models explain a decoupling between the substrate and the underlying bedrock caused by porewater overpressures in the substrate and the formation of a dual marginal end-product of the surge, i.e. a ~500 m long sediment wedge with an end-moraine ridge on the distal top. The wedge formed as a consequence of a down-glacier dislocation and associated compressive deformation of the substrate with gradual thickening in the marginal zone, whereas the end-moraine ridge formed on top of the wedge due to a drop in subglacial porewater pressure at the very end of the surge (cf. Benediktsson *et al.* 2008). In the present article, we investigate the morphology and architecture of an end moraine related to the most recent surge of Brúarjökull in 1963–64, with the main focus on the parts of the end moraine that formed submarginally.

Setting

Brúarjökull is a surge-type northern outlet of the Vatnajökull ice cap in Iceland. It descends from about 1500 to 600 m a.s.l., where it terminates with a 55 km long

DOI 10.1111/j.1502-3885.2008.00077.x

glacier margin. The glacier is drained by the large glacial rivers Kverká, Kringilsá and Jökulsá á Brú (Björnsson *et al.* 1998) (Fig. 1). The historical surge record of Brúarjökull extends back to the 17th century, with the first known surge taking place in 1625 and subsequent surges in ~1730, ~1775?, 1810, 1890 and 1963–64. This gives a surge cycle of 80–100 years within which the active phase duration is only 2–3 months (Eythorsson 1963, 1964; Thorarinsson 1964, 1969; Björnsson *et al.* 2003). During the last two surges, the maximum advances of Brúarjökull in the central forefield in Kringilsárrani were 10 and 9 km, respectively, with maximum ice-flow velocities of at least 100–120 m/day (Kjerúlf 1962; Thorarinsson 1964, 1969; Guðmundsson *et al.* 1996).

The forefield of Brúarjökull is glacially streamlined with an up to 6–7 m thick sediment sequence overlying basaltic bedrock. The most prominent landforms of the surging glacier landsystem are end-moraine ridges, ice-cored landforms and ice-free hummocky moraines, eskers, flutes and drumlins, mainly located in valleys between elongated bedrock hills culminating at 700–750 m a.s.l. and crevasse-fill ridges that primarily cluster around the topographic highs, and usually drape the flutes where these two interact (Evans & Rea 1999, 2003; Benediktsson 2005; Kjær *et al.* 2006, 2008; Schomacker *et al.* 2006; Bjarnadóttir 2007; Evans *et al.* 2007; Schomacker 2007; Schomacker & Kjær 2007; Benediktsson *et al.* 2008) (Fig. 1). At present, ice movement in the marginal 1–2 km of Brúarjökull is negligible; the snout is rapidly retreating and downwasting and is covered by a thin sediment layer originating from emerging and disintegrating crevasse-squeeze ridges and debris bands in the ice (Evans & Rea 1999, 2003; Kjær *et al.* 2006; Schomacker 2007; Schomacker & Kjær 2007; Benediktsson *et al.* 2008).

Circular rim-ridges, ice-cored peat mounds and frost-crack polygons occur immediately outside the 1890 end moraine. Many of the rim-ridges, which are up to 0.8 m

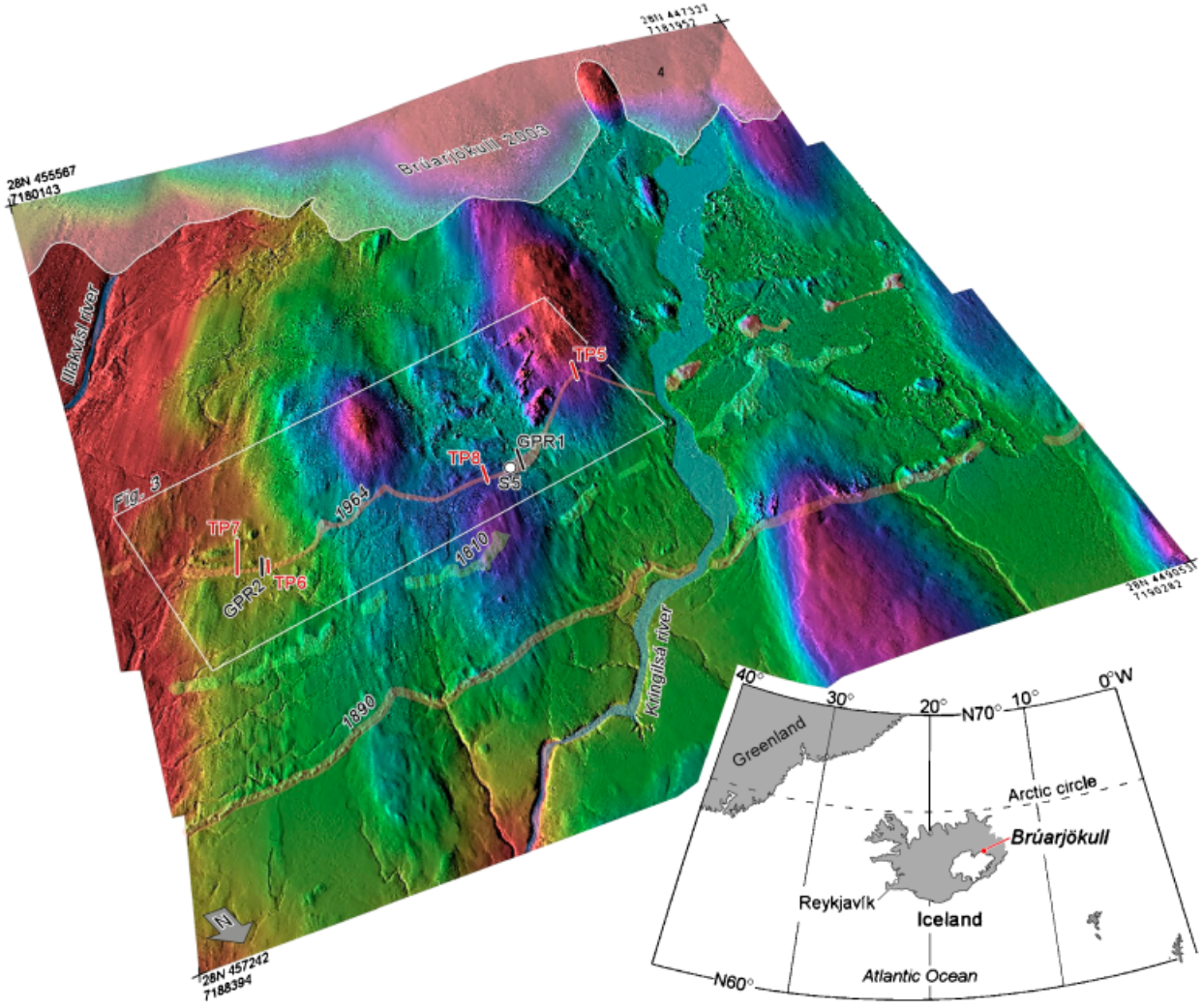

Fig. 1. The forefield of the surge-type Brúarjökull, eastern Iceland. Digital elevation model, generated from stereopairs of aerial photographs recorded in 2003, visualized as a Terrain Shaded Relief model. Red lines marked TP1-TP4 indicate terrain profiles surveyed across the 1964 end moraine (Fig. 5); dot S5 represents the excavated cross-section (Fig. 8); and the box indicates area of Fig. 3. UTM coordinates are in metres.

high and 10–15 m in diameter, surround ponds or minor lakes. They have been interpreted as periglacial landforms and are thought to represent collapsed palsas (Todtmann 1955, 1960; Friedman *et al.* 1971; French 1996; Ravn 2006; Benediktsson *et al.* 2008; Kjær *et al.* 2008). Evans *et al.* (2007) map these features as being of paraglacial origin, though without providing data to substantiate that interpretation. Periglacial origin for the circular rim-ridges is supported by the observation of discontinuous permafrost in the area by van Vliet-Lanoë *et al.* (1998) and Etzelmüller *et al.* (2007). The mean annual air temperature of −0.9 °C, recorded in hourly measurements between August 2003 and August 2006, indicates a possibility for sporadic permafrost in the area (Ravn 2006; Schomacker & Kjær 2007).

Methodology

Aerial photograph interpretation and geomorphological mapping

The 1964 end moraine was identified on aerial photographs recorded in 2003 (Table 1). Geomorphological analysis was carried out using a Digital Elevation Model generated from stereopairs of the 2003 aerial photographs (Fig. 1). Four terrain cross profiles were measured across the end moraine with a TopCon GTS-226 levelling instrument for detailed geomorphological mapping at different sites reflecting the morphology and geometry of the end moraine.

Accurate mapping of the ice-marginal area of the 1963–64 surge was carried out on a Digital Photogrammetric Workstation (DPW) in which pairs of vertical aerial photographs could be viewed in stereo (Table 1). Selected features of the area occupied by the 1964 ice margin were mapped on the DPW from aerial photographs recorded before the surge (1945), at the time of surge termination (1964) and after the surge (2003), before being handled further in a Geographical Information System (GIS) (Table 1). The distribution of large pre-surge basins and sediment bodies was mapped in order to locate potential sediment supplies for the end moraine formed by the surge in 1963–64. Also, pre-1964 glaciotectonic ridges previously mapped by Todtmann (1955, 1960) were geocoded on the basis of her map and added to the GIS. The ice-marginal situation at surge maximum was mapped from aerial photographs recorded in mid-June 1964, a few months after surge termination, when no forward momentum occurred in the ice front (Eythorsson 1964; Kjær *et al.* 2006). Meltwater outlets at the ice margin were mapped to gain insight into the subglacial drainage system. The boundary between the foreland and the outermost signature of the surge, whether being the ice margin or the end moraine in front of it, was mapped as one feature named 'maximum surge limit'. In some places along the ice margin, no end moraines occurred in front of it; hence, the maximum surge limit was marked by the ice front. In other places, the ice margin was clearly separated from an end moraine in front of it, and was therefore mapped as a separated feature named 'ice margin'. These two features were subsequently compared to the 1964 end moraine as mapped from the 2003 ortho-rectified aerial photographs (Kjær *et al.* 2008).

The morphology of the ice margin and the end moraine at surge termination was also examined by extracting moraine-glacier cross profiles from a Digital Elevation Model (DEM) generated from stereopairs of the June 1964 aerial photographs. These profiles extend from the forefield up to the glacier surface and show whether or not an end moraine formed in front of the glacier.

Sedimentology and structural geology

Sedimentological and structural geological investigations of the 1964 end moraine were undertaken in a natural cross-section that was cleaned up and enlarged by hand. Documentation of sediment lithologies and structures was done on the basis of the data chart by Krüger & Kjær (1999). Sediment facies architecture was mapped at a scale of 1:20 and structural elements were described according to the terminology of Twiss & Moores (1992) and Evans & Benn (2004).

Ground-penetrating radar

Two transverse ground-penetrating radar (GPR) profiles were surveyed across the 1964 end moraine with a

Table 1. Properties of aerial photographs and derived DEMs, with classification of mapped features.

Year	Photographic scale	DEM grid size (m)	DEM mean error (m)	Classes	Mapped features
1945	1:45 000	5	2.4	Sediment basins and bodies	Lakes Lake sediment flats Major fluvial areas Glaciotectonic ridges
1964	1:40 000	5	1.9	Marginal situation. Boundary between foreland and max. position of surge	Ice margin Max. surge limit
2003	1:15 000	3	0.3	End moraines and ice-marginal landforms	End moraine Thrust ridges

Sensors and Software pulseEKKO IV system (Fig. 1). The best combination of resolution and penetration was obtained by 100 MHz antennae with a separation of 1 m. Common-mid-point (CMP) measurements were used for depth conversion of the recorded two-way travel time. The CMP survey gave a velocity of 0.085 m/ns, which corresponds well with the table value of 0.06–0.1 m/ns for saturated and damp sand (Jol & Bristow 2003) and to velocities recorded in other glacial environments in Iceland (e.g. Cassidy *et al*. 2003; Kjær *et al*. 2004). Data were processed with the pulseEKKO software, version 4.2, from Sensors and Software Inc. Topographic data were collected with a TopCon GTS-226 precision levelling instrument and incorporated within the GPR lines during data processing.

The 1963–64 surge

Before the 1963–64 surge, the ice front of Brúarjökull had long been flat, debris-covered and little crevassed, and had retreated 10–11 km from the end moraines formed by the 1890 surge (Eythorsson 1963; Benediktsson *et al*. 2008). In late August 1963, a great bulge on the glacier was observed on oblique aerial photographs, but no advance had occurred (Thorarinsson 1969). In the autumn, the glacier was heavily crevassed, the Jökulsá á Brú glacial river was unusually debris-laden and the discharge was greater than normal. On 14 October, a local farmer visited the glacier, which was very rough but not yet advancing. In mid-November, the glacier had advanced 2–3 km east of Jökulsá á Brú and perhaps even further in the central forefield in Kringilsárrani. The entire glacier was heavily crevassed and the front was 20–50 m high and very steep (Eythorsson 1963). In early January 1964, an expedition to Brúarjökull experienced a rhythmic ice advance of at least 1 m/h accompanied by ground shivering. Neither ploughing of the ground in front of the glacier nor moraine-ridge formation was observed at that time. However, ridges of snow were being pushed forward by the glacier in some places (Eythorsson 1963; Thorarinsson 1969). During expeditions to the Brúarjökull forefield west of Kringilsá in July and August 1964, measurements revealed that the glacier had advanced only 200–300 m since early January (Eythorsson 1964). The glacier had stagnated and was much crevassed; the ice front was about 30 m high and precipitous and no end moraines were observed in the western part of the forefield, whereas prominent end moraines were observed from a reconnaissance flight over the eastern part (Fig. 2) (Eythorsson 1964; M. Hallgrímsson pers. comm. 2007).

Glaciological studies show that Brúarjökull advanced 4–5 km west of Kringilsá, but 9–9.5 km in the eastern part of Kringilsárrani, with a maximum advance rate of at least 100–120 m/day (Guðmundsson *et al*. 1996; Magnússon *et al*. 2004). During the surge, the area of Brúarjökull increased by about 160 km^2 when 62 km^3 of ice was transported from the accumulation area to the ablation area. The maximum thickening in the ablation area was 260 m and the average lowering of the accumulation area was 60 m (Guðmundsson *et al*. 1996; Magnússon *et al*. 2004). Since the surge in 1963–64, the average mass build-up

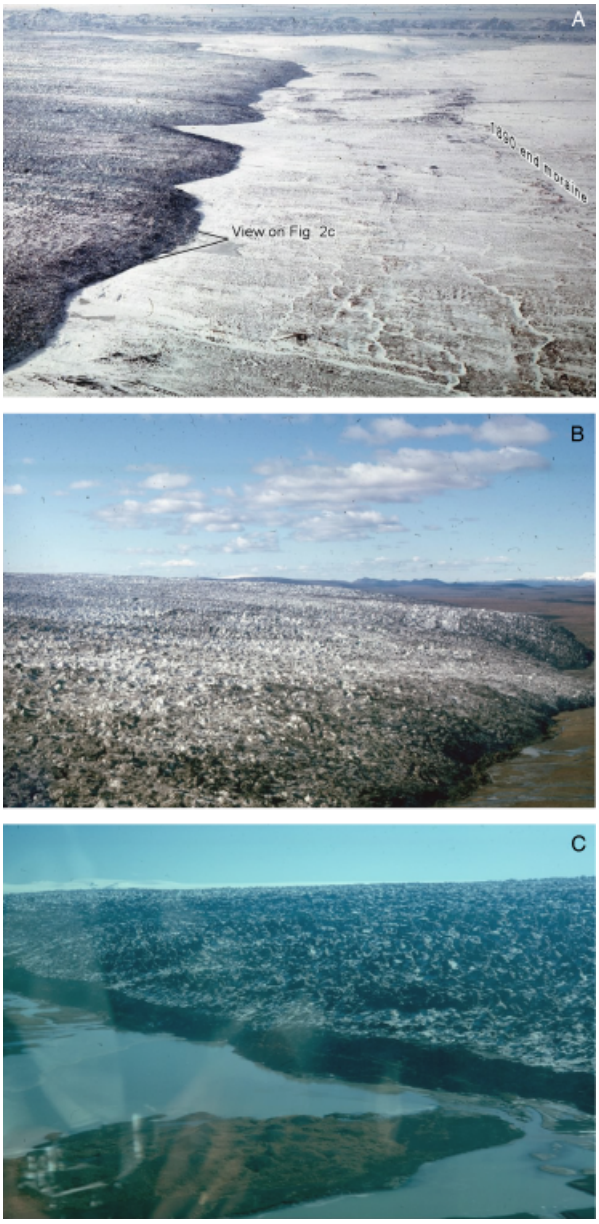

Fig. 2. Photographs of Brúarjökull during and after the 1963–64 surge. A. Brúarjökull at surge termination. Note the numerous lobes of the ice margin. The main study area is associated with the two lobes most adjacent to the viewer. View towards west. B. View towards west along the eastern part of the ice margin, early summer 1964. Note the end moraines at the ice margin. C. The ice margin adjacent to the area viewed in (B) and proximal to the proglacial lake seen in (A), as seen a few months after surge termination. Despite the reflection on the aeroplane window, end-moraine ridges are clearly visible at the margin. Photographs A and B by Sigurður Thorarinsson, C by Magnús Jóhannsson.

in the accumulation area of Brúarjökull has been ~0.8 km^3/yr (Magnússon *et al.* 2004). By comparison, the mean mass balance of the accumulation zone since 1993 equals 1.3 km^3 of ice per year, which means that only 0.5 km^3 of ice is transported to the ablation zone each year. This demonstrates that most of the ice transport in Brúarjökull occurs during surges (Magnússon *et al.* 2004). This has been verified by velocity measurements between 2003 and 2005 showing dead ice in the frontal 1–2 km of Brúarjökull (Kjær *et al.* 2006).

The 1964 end moraine

Surge termination situation and geomorphology of the end moraine

Accurate mapping and production of DEMs on the basis of the 1945, 1964 and 2003 aerial photographs allowed the present position of the 1964 end moraine to be compared to the pre-surge forefield and the exact position of the ice margin at the end of the surge (Figs 3, 4). Comparison shows that in the eastern part of the area, where the sediment sequence is 4–6 m thick, the end moraine formed mostly in a proglacial position (see inset in Fig. 3C), but in a submarginal position along a large part of the ice margin, mainly in the western part of the study area (Fig. 3B, C). Terrain profiles extracted from the 1964 and 2003 DEMs along the same transect support this observation and demonstrate that in many places the ice margin advanced 10–40 m further than indicated by the end moraine (Fig. 4A). This is typical for areas of efficient drainage, indicated by a number of meltwater outlets, or where the glacier advanced upon or across a reverse sloping foreland (Figs 1, 3). In the lower-lying eastern part of the study area, where the sediment sequence is thicker, the proximal slope of the end moraine was partly covered by the ice margin, while the crest and the foreslope remained in front of the glacier (Figs 3C, 4B). This implies a different glacier-foreland interaction leading to the formation of the end-moraine ridge mainly in a proglacial position.

Mapping of meltwater outlets at surge termination implies that formation of end moraines in both proglacial and submarginal settings is highly dependent on subglacial drainage. Proglacial end-moraine ridges primarily occur where meltwater outlets are few along the ice margin and where hydrodynamic blow-out depressions are apparent in front of the moraine (Figs 3B, 6D; Christiansen *et al.* 1982), indicating drainage of overpressurized water in a discrete network of interconnected subsurface tunnels (Kjær *et al.* 2006). Out of 32 meltwater outlets identified, only 9 occur where proglacial end moraines were formed. In contrast, 23 closely spaced meltwater outlets were observed along the margin where submarginal end moraines occur, indicating a distributed network of small meltwater tunnels at the ice/bed interface (Björnsson 1998). This suggests that the nature of the subglacial drainage at the end of the surge is an important factor in the formation of submarginal and proglacial end moraines.

The geomorphology of the 1964 end moraine varies along its length. Where the foreland sediment sequence is thin, typically on bedrock hills, the end moraine is low with a steep backslope and a gentle foreslope, and consists typically of coarse, clast-rich diamict and large boulders (Fig. 6B). This is clearly demonstrated by terrain profile 5, which occurs at the lee side of a streamlined bedrock hill (Figs 1, 5). In the low-lying eastern part of the forefield (Fig. 1), the end moraine is 30–60 m wide and 6–10 m high, with a steep frontal slope. Commonly, the backslope contains dead-ice and ice-free hummocky moraine (Fig. 6A, C) (Benediktsson 2005; Schomacker & Kjær 2007). Occasionally, the backslope rises steeply up from a plain of post-surge fluvial and glaciolacustrine sediments and the foreslope displays sinkholes and fractures because of downwasting of buried ice or snow. These morphological characteristics are clearly demonstrated in terrain profiles 6 and 7 (Fig. 5). Terrain profile 8 displays more complicated morphology of the ice-marginal zone (Fig. 5). There, the end moraine is composed of fluvial sediment and is of a very low amplitude and poorly defined, located at the proximal side of a small outwash fan. The end moraine is situated at the stoss side of a bedrock hill, favouring thrusting in the marginal zone and the entrainment of subglacial sediment up in the ice (Hambrey *et al.* 1996; Swift *et al.* 2006) (Fig. 1). Subsequent melting of the underlying ice was prevented, resulting in the development of a 3 m high, transverse ice-cored ridge located about 60 m up-glacier from the end moraine (Figs 5, 6C). The shape of the ridge is typical of ice-cored thrust ridges, with a steep distal slope showing

Fig. 3. Aerial orthophotographs of the 1964 ice-marginal area. A. The pre-surge (1945) glacier forefield with major sediment bodies and glaciotectonic ridges mapped. Note the fluted 1890 ground moraine with abundant crevasse-squeeze ridges. The maximum surge limit of the 1963–64 surge is indicated (dashed line). B. The ice-marginal area of Brúarjökull at surge termination. The 'maximum surge limit' is defined by the distal foot of the end moraine, or, in the absence of proglacial end moraines, by the ice front. In the presence of proglacial end moraines, the 'ice margin' was mapped separately where it was clearly located proximal to the end-moraine crest. Thus, in places where the yellow lines representing the 'ice margin' are absent, the surge limit is marked by the ice front only, not the end moraine. Blue dots indicate meltwater outlets. Note the frequency of outlets at the margin where proglacial end moraines are absent. Light-blue lines A and B indicate the moraine-glacier cross profiles shown in Fig. 4. C. The situation after the surge (2003) with the 1964 end moraine and thrust ridges mapped together with the 'maximum surge limit' and the 'ice margin'. Note that in many places the end moraine was located beneath the ice margin (indicated by a red line where a yellow line is absent). In the eastern part of the area, the end moraine formed primarily in proglacial position, as indicated by the 'ice margin' (yellow line) up-glacier of the end moraine crest (green line; see inset figure).

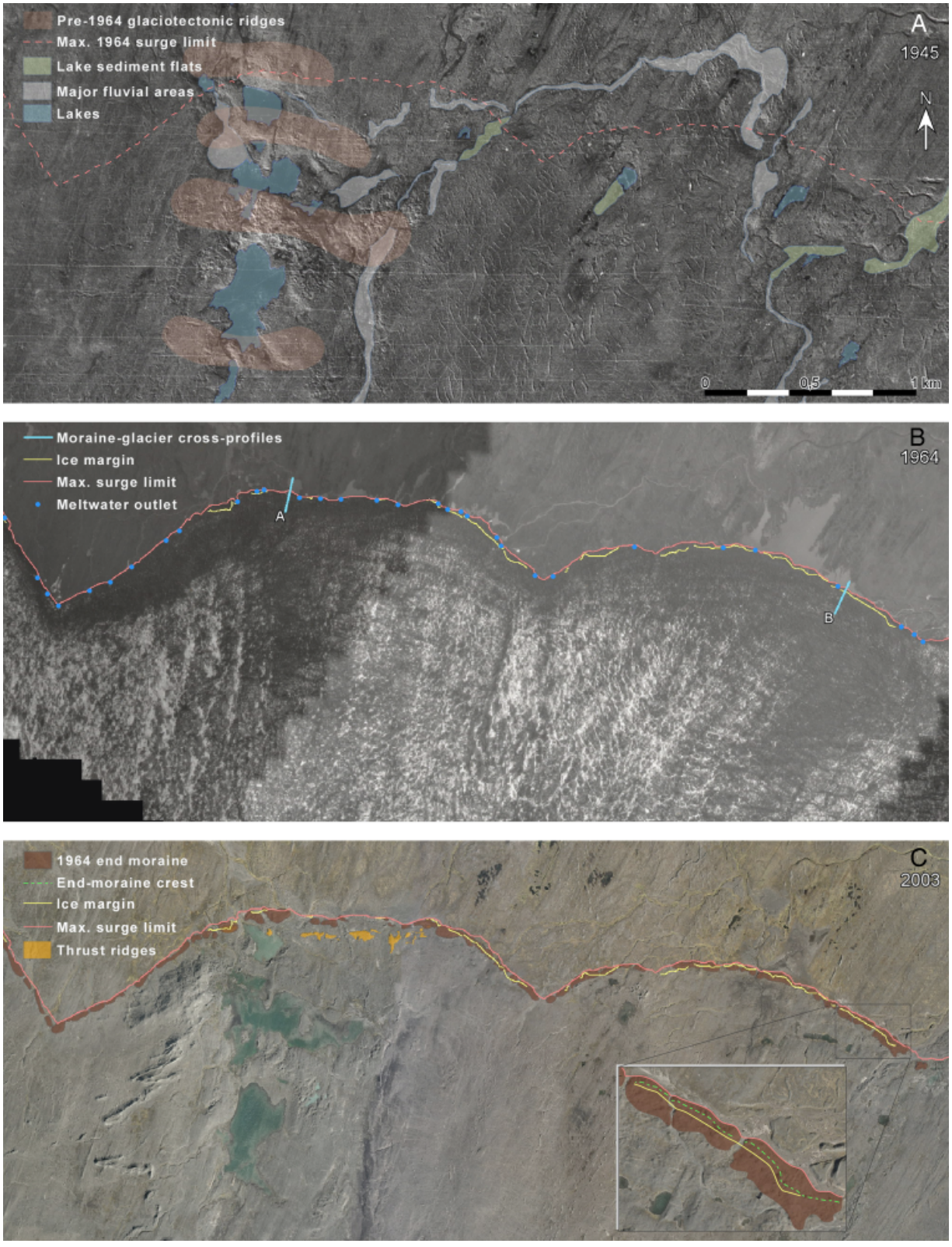
Pre-1964 glaciotectonic ridges
Max. 1964 surge limit
Lake sediment flats
Major fluvial areas
Lakes
A
1945
N
0
0,5
1 km
Moraine-glacier cross-profiles
Ice margin
Max. surge limit
Meltwater outlet
B
1964
A
B
1964 end moraine
End-moraine crest
Ice margin
Max. surge limit
Thrust ridges
C
2003

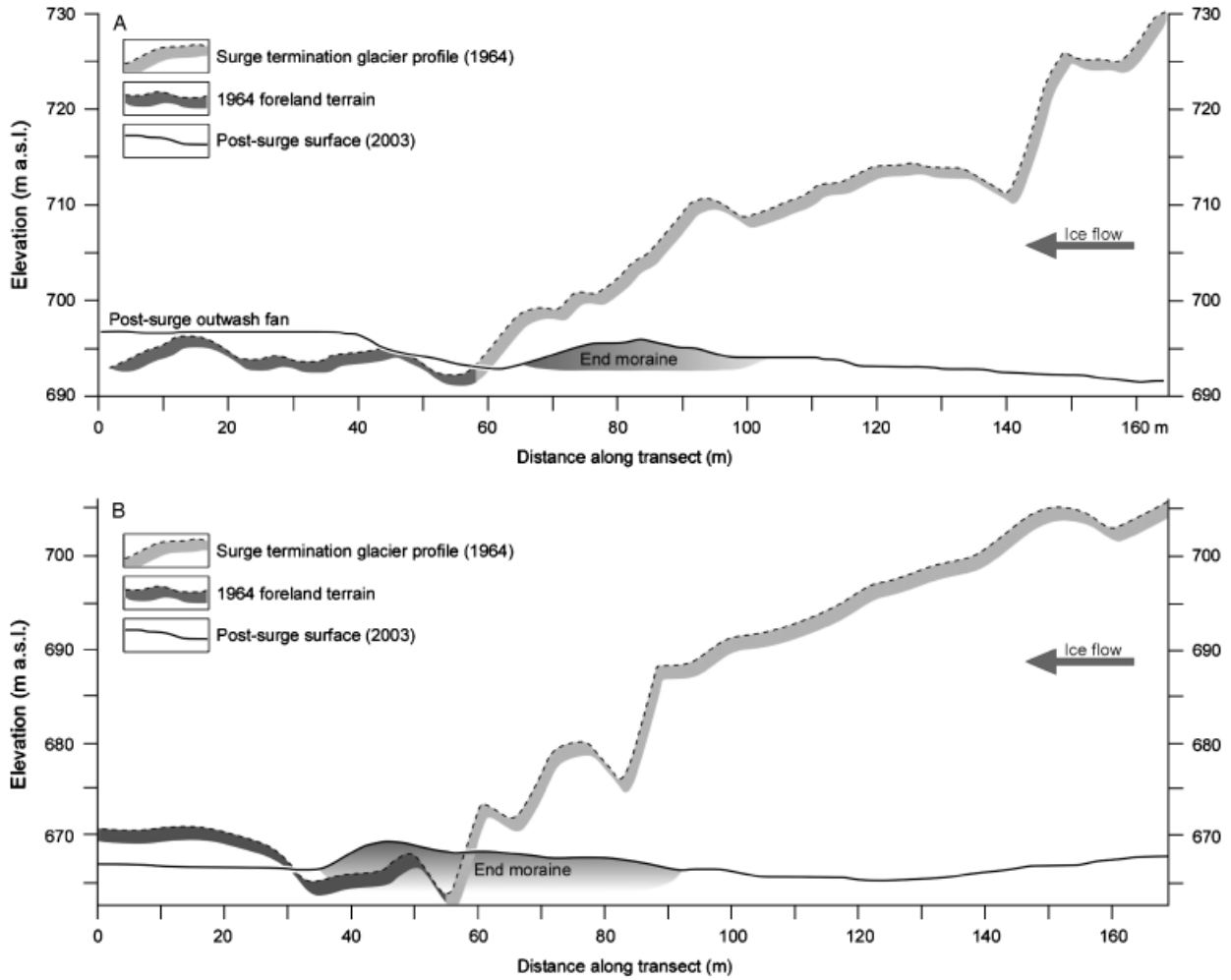

Fig. 4. Moraine-glacier terrain cross-profiles at surge termination (1964) compared with terrain profiles from 2003. The profiles have been extracted from the 1964 and 2003 DEMs (Table 1; see Fig. 3 for location of the profiles). A. Profile 1 shows the occurrence of the end moraine beneath the ice margin at the end of the surge. Note the outwash fan formed during or after the surge, indicating efficient drainage at this particular site. B. Profile 2 shows the end moraine in front of the ice margin, but with the proximal slope partly beneath the margin. A slight inaccuracy in the vertical resolution of the 1964 DEM causes the occurrence of the pre-surge foreland below the post-surge surface.

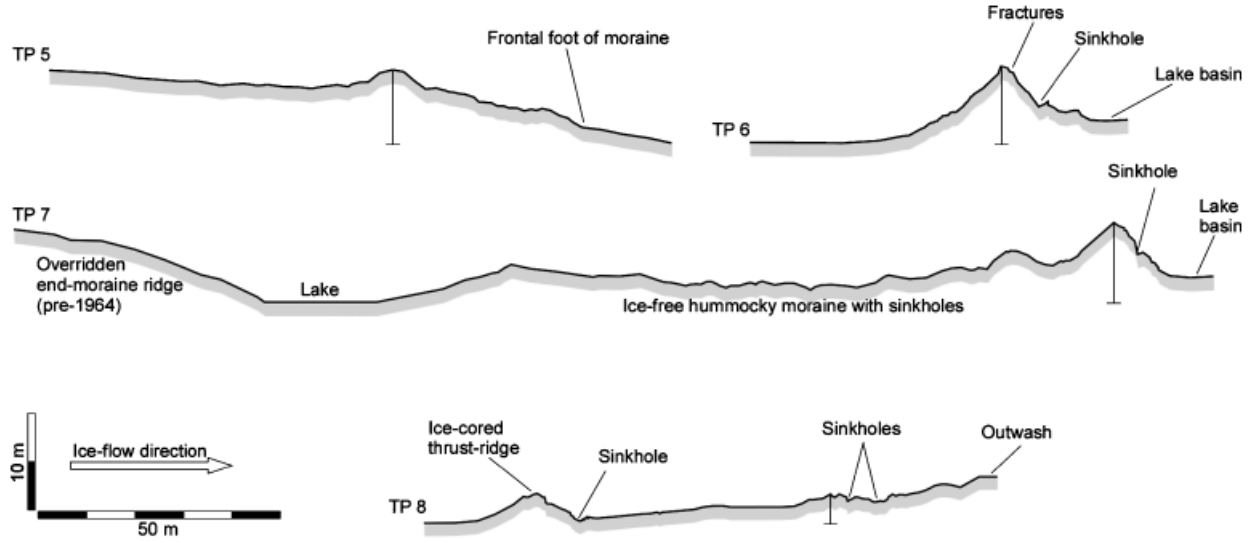

Fig. 5. Terrain profiles (TP) 1–4, surveyed across the 1964 end moraine. See Fig. 1 for locations of the profiles. Vertical lines indicate the crest of the moraine ridge.

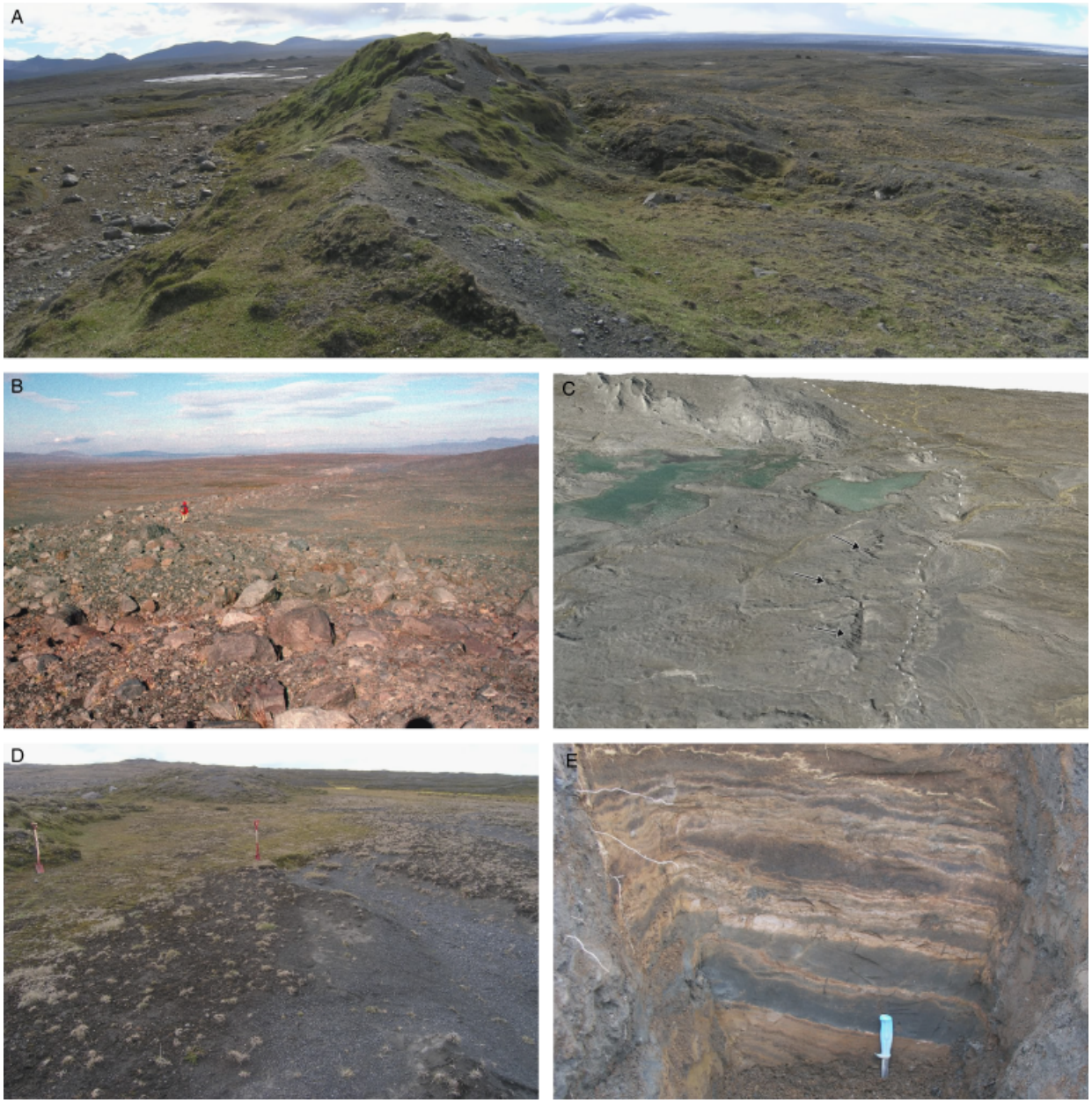

Fig. 6. Photographs of the 1964 end moraine. A. A view of the high and single-crested end moraine as it typically occurs in the eastern part of the study area. Ice flow was from right to left. B. Typical view of the 1964 dump moraine in the western part of the study area. Ice flow was from right to left. C. Aerial orthophotograph from 2003 draped over a DEM with 1.5× vertical exaggeration. A view of thrust ridges (arrowed) formed just up-glacier of the end moraine (dotted). Concertina ridges are visible in the background. Ice flow was from left to right. D. A semi-circular blow-out depression at the abrupt head of a channel in front of the 1964 end moraine in the eastern part of the area (just west of terrain profile 6) (Fig. 1). Spades for scale, the one to the left stands by the end moraine. Ice flow was from left to right. E. The LPT-sequence just outside the end-moraine ridge in (A) indicating the sedimentary composition of the end moraine in the eastern part of the area. Ice flow from left to right.

extension fractures and sinkholes due to a melting ice core and a gentle proximal slope with thicker till cover (e.g. Hambrey & Huddart 1995; Hambrey *et al.* 1996; Huddart & Hambrey 1996; Bennett *et al.* 1999; Bennett 2001). The morphology of the ice-cored ridge shows no signs of having been overridden. At Brúarjökull, pre-surge dead ice that is overridden by a new surge tends to be shaped into ice-cored drumlins (Schomacker *et al.* 2006). Thus, transverse ice-cored ridges showing the morphological characteristics described above can be regarded as a product of thrusting in the snout of Brúarjökull at the closing stage of the 1963–64 surge.

The terrain cross-profiles, interpretation of aerial photographs and field observations show that the 1964 end moraine comprises mainly two morphologies that are related to specific conditions in the glacier and the

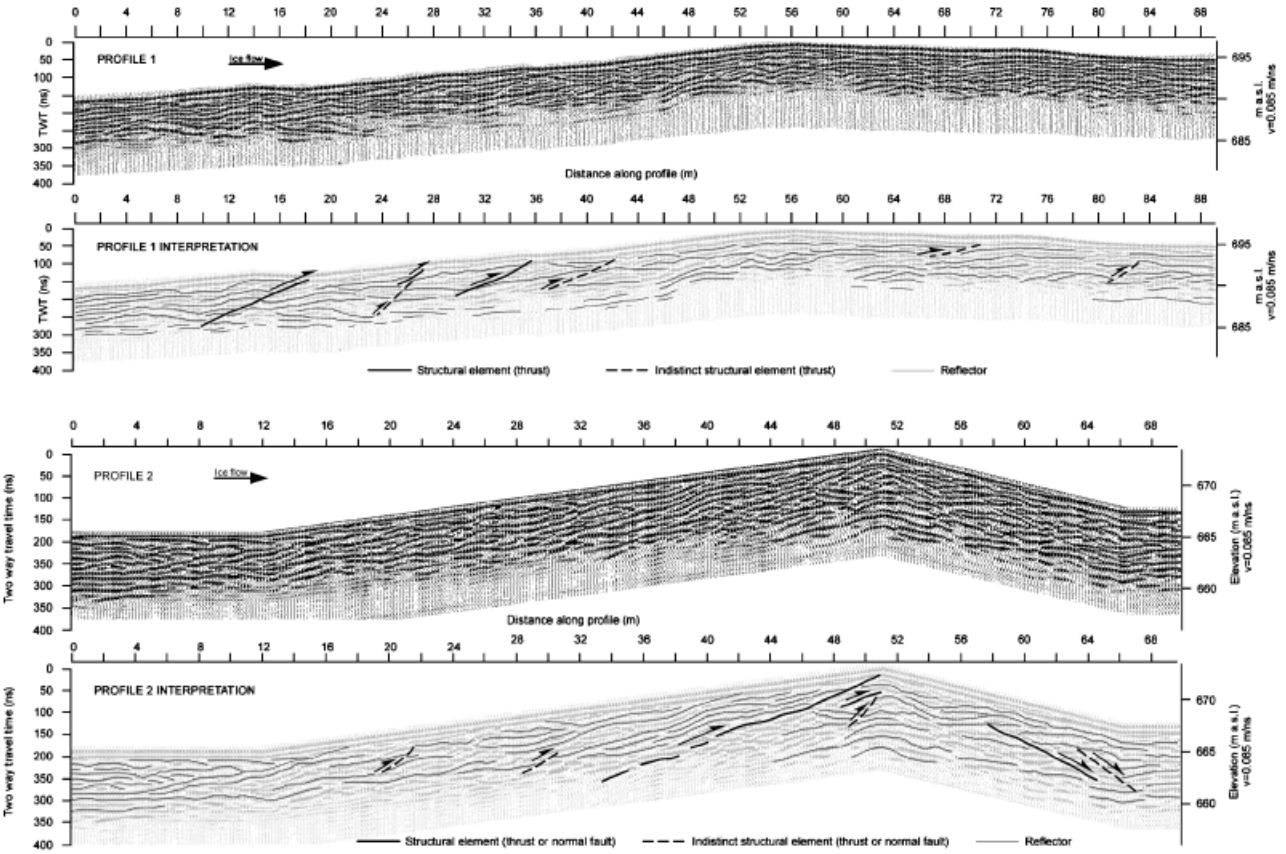

Fig. 7. 100 MHz GPR profiles and structural interpretation. See Fig. 1 for locations of the profiles.

forefield, specifically ice thickness, foreland topography and sediment supply. With only a few exceptions, the end moraine is low or even absent in areas of overall coarse-grained and highly permeable sediment succession (e.g. west of Kringilsá and just east of section 5) (Fig. 1) (Schomacker & Kjær 2007; Kjær *et al.* 2008). Furthermore, the end moraine is low and blocky on elevated areas where the bedrock was at shallow depths and the sediment supply was low. In contrast, the moraine is high and usually sharply crested in valleys and low-lying areas where the sediment succession was overall fine-grained and thick, and the glacier applied greater stress to the foreland. This is supported by the elevation difference between the present ice-free terrain and the surface of the 1963–64 surging glacier measured from post-surge and surge termination DEMs, respectively. The morphological investigation suggests that, in areas where the glacier flow was uphill, thrusting occurred in the ice margin developing transverse ice-cored ridges proximal to the former glacier margin.

Two-dimensional architecture

The two-dimensional architecture of the end moraine was surveyed with GPR at two transects perpendicular to the moraine strike (Fig. 1).

GPR profile 1 runs along an 89 m long transect approximately 50 m west of section 5 (Fig. 1). There, the end moraine is fairly low, with a poorly defined proximal foot and moderately defined distal foot. The profile displays undulating and equally strong reflectors, but with weaker reflectors in the lower proximal and distal parts (Fig. 7). Some reflectors can be traced several metres, but are difficult to follow for long distances due to irregularity and a strong reflection pattern in the profile. The weak near-horizontal reflectors in the lower proximal and distal parts do not completely parallel the overlying reflectors and seem to represent an undisturbed surface below, most likely the bedrock, as indicated by its appearance at the base of the adjacent section 5. As a result, the thickness of the overlying sediment succession is 5–6 m, and probably greater in the core of the moraine ridge (Fig. 7). The composition of the sediment succession is poorly known; however, the nearby section 5 indicates that the succession is composed of till, gravels and fine-grained sediments.

In the proximal extremity of profile 1, there are several subhorizontal reflectors that can, in part, be traced into a fault-propagation fold. Horizontal shortening of the reflectors is enhanced through a ~2 m displacement along a prominent low-angle thrust extending from the lower part of the succession towards the surface (12–18 m; Fig. 7). In the upper part, at around 26 m, minor offsets

occur around a low-angle thrust observed above an indistinct and steeper thrust. A displacement of 3–4 m occurs along a large low-angle thrust at 30–36 m in the profile. An indistinct thrust is observed at 38–42 m, indicated by a minor offset of the reflectors. The central part of the profile (*c.* 44–60 m) is characterized by irregular reflectors within which no faults could be observed. However, convex reflectors occur, possibly representing open anticlinal folding of the sediment layers. A slight change occurs in the styles of reflections around 60 m as reflectors become more horizontal and continuous, probably indicating decreased intensity of the deformation towards the foreland.

Profile 2 was surveyed across a 6–7 m high ridge in the eastern part of the study area (Fig. 1). The profile is approximately 68 m long, extending from a plain of fluvial sediments on the proximal side of the ridge towards a basin with fluvial and lacustrine sediments on the distal side. The fluvial sediments on the proximal side of the end moraine are clearly visible on the profile as subhorizontal reflectors lapping on a strong and continuous reflector that is inclined up-glacier (Fig. 7). The backslope of the profile is characterized by undulating reflectors that are frequently broken by small shear planes (Fig. 7), two of which are detectable as indistinct thrusts. A set of continuous reflectors occurs at ~32–48 m in the profile, representing the proximal limb of an up-glacier-inclined fault-propagation fold, the thrust of which extends from the bottom of the profile towards the surface at the top of the moraine ridge (Fig. 7). The reflectors of the foot wall are often convex upwards, indicating the hinge and distal limb of the fold. Subhorizontal reflectors in the distal part indicate undisturbed basin and fluvial sediments in front of the end moraine.

Sedimentology and internal structure

The sediments and the internal structure of the end moraine were studied in section 5 (Figs 1, 8), where the moraine is 4–5 m high and 25–35 m wide with a faint proximal foot but a moderately well-defined distal foot. Section 5 covers the backslope and the core of the moraine and can be divided into three parts due to a difference in sediment lithology and style of deformation (Fig. 8); (i) the backslope (~0–4 m), (ii) the lower core (2–8 m) and (iii) the upper core (4–8 m).

The backslope, ~0–4 m. – The base of the backslope is characterized by fine to coarse, poorly sorted clast-supported gravel that is interpreted as pre-surge outwash deposits (Maizels 1993). Above is a massive, matrix-supported, coarse-grained, clast-moderate and friable diamict that can be traced across the entire ridge and a further 10–40 m beyond it (Figs 8B, C, 9A). This diamict is interpreted as a subglacial traction till (Evans *et al.* 2006). On the backslope, the diamict becomes gradually looser upwards, where it includes stratified sand and gravel indicative of sedimentation at low flow regime associated with dead-ice melting (Maizels 1993) (Figs 8A, 9A). The upper part of the diamict is not therefore related to subglacial traction deposition by an active glacier, but rather to melt-out from the stagnant ice front after the 1963–64 surge (Paul & Eyles 1990) (Fig. 8). The gravel occurs in two parts separated by a loess-peat-tephra (LPT) and diamict at 2–3 m. At the base, the gravel is subhorizontal, while in the centre of the section it rises at an angle of 28° (dipping SE), indicating thrusting from a southerly direction (Figs 8A, 9A).

The lower core, 2–8 m, below ~2 m height. – The section below ~2 m is characterized by dark-brown loess, yellow to red-brown peat and black to white tephra. Together, these lithofacies types form a coherent and in places compacted LPT sequence that lies unconformably on top of gravel (Fig. 8A). The LPT layers are often folded and sheared, or even totally mixed as a result of pervasive deformation (van der Wateren 1995b). Immediately above the gravel at the base, the LPT layers are inclined up-glacier and slightly folded in places (Figs 8, 9). Further above, the white Öræfajökull AD 1362 tephra and a black tephra denote an inclined fold, the proximal limb of which rises at a high angle parallel with the gravel thrust wedge (Figs 8A, 9A, C). Between 4.5 and 8 m the section is characterized by up-glacier inclined LPT and tephra layers and low-angle faults, the footwalls of which include series of subhorizontal shear planes with down-glacier movement of the hanging wall (Figs 8A, 9B, E).

The upper core, 4–8 m, above ~2 m height. – The upper core is characterized by gravel and fissile LPT with occasional pebbles in the matrix. The fissile LPT is interpreted as glaciotectonite deposited prior to the 1963–64 surge as a result of shearing in a subglacial environment (Dreimanis 1989; Benn & Evans 1996; Krüger & Kjær 1999; Evans *et al.* 2006; Kilfeather & van der Meer 2008). Most likely, the glaciotectonite was deposited by the 1890 surge that terminated ~2 km beyond the 1964 end moraine. The glaciotectonite underlies gravel and is separated from the LPT sequence below by subhorizontal shear planes (Figs 8, 9B, D). The orientation of the fissile partings is usually parallel with the lower and upper boundaries of the glaciotectonite. This is exemplified by a downward convex pattern at 4–5 m that is interpreted as a weakly developed synclinal fold in the glaciotectonite. The fold is cut by two prominent thrusts with a displacement of < 1 m, suggesting an overprinting of ductile structures by brittle deformation, a deformation pattern typically observed in the 1890 Brúarjökull surge field (Kjær *et al.* 2006; Benediktsson *et al.* 2008). In the upper part, the fissile partings parallel the subhorizontal contact between the glaciotectonite and the

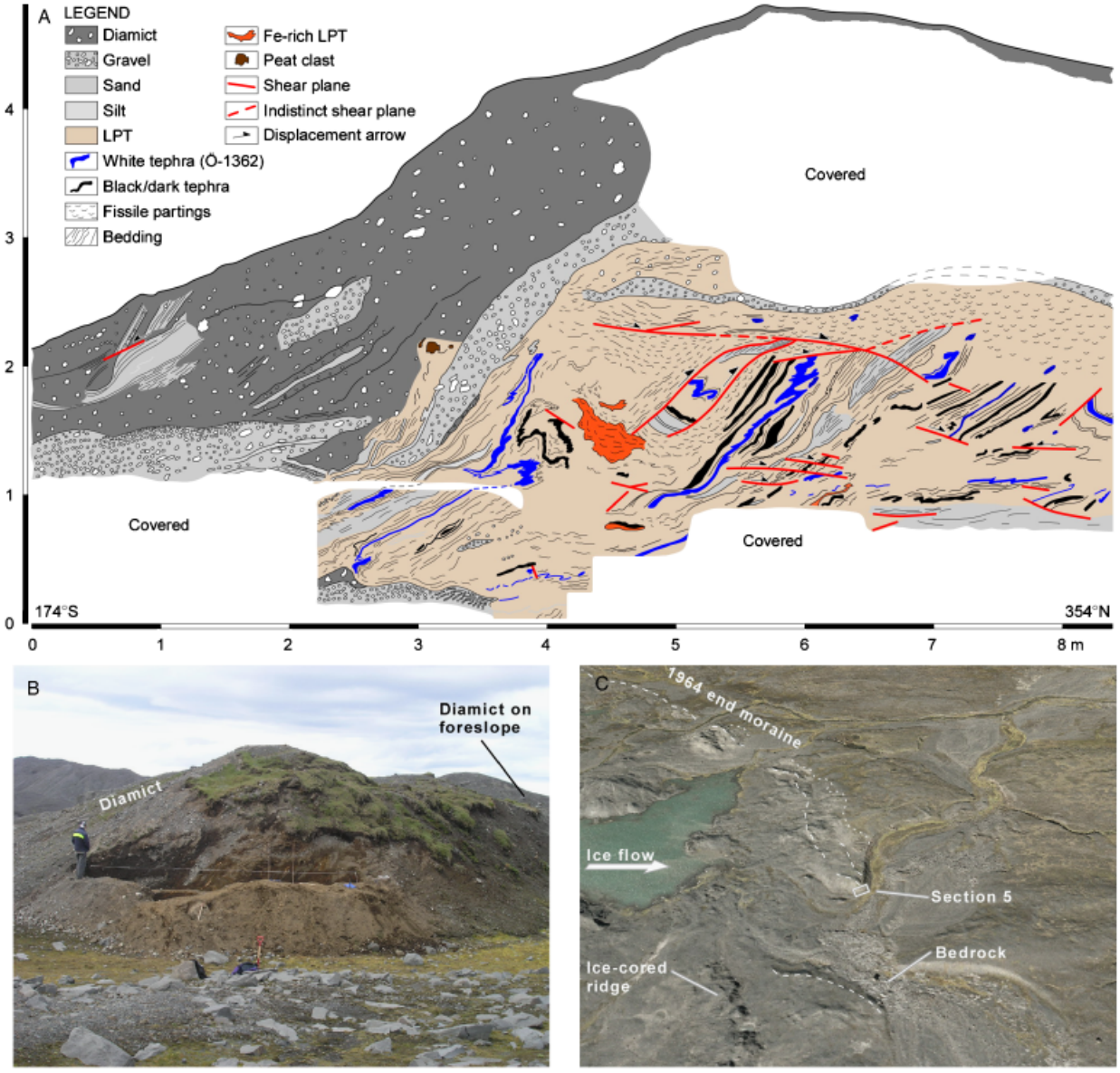

Fig 8. Section 5. A. Diagram of the section; no vertical exaggeration. B. Photograph of the section; person for scale. C. Overview of the surroundings of the section. Aerial orthophotograph from 2003 draped over a DEM with 1.5× vertical exaggeration. The dashed line indicates the crest of the moraine ridge, and the dotted line the extent of the diamict that is found on the backslope of section 5 (Fig. 8A).

overlying gravel. In the distal part of the section, the gravel is slightly convex upwards, indicating a wide open fold.

Structural interpretation

The two GPR profiles reveal the large-scale architecture of the end moraine. Both profiles show minor open folds in the core but thrust planes in different parts of the moraine ridge. In profile 1, frequent thrust planes in the backslope correspond with the up-glacier-inclined gravel and LPT layers in section 5, signifying that thrusting has played a major role in the deformation of the foreland as the primary style of deformation (Fig. 8). In contrast, profile 2 shows open folds and a fault-propagation fold in the core of the end moraine, and normal faults in the foreslope. Tightly inclined and overturned folds with near vertical limbs or hinge zones probably occur in the profile but are not readily detected with GPR. Because the brittle structures overprint the ductile structures, the moraine construction probably began with a folding of the foreland before faulting set in with significant displacement along fault planes. This is compatible with the deformation style of the 1890 end moraine in the eastern part of the study area (Benediktsson *et al*. 2008) (Fig. 1).

Section 5 shows frequent shearing and folding of LPT below fissile glaciotectonite and large-scale thrusting of gravel as two distinct styles of deformation. The fissile glaciotectonite indicates high cumulative

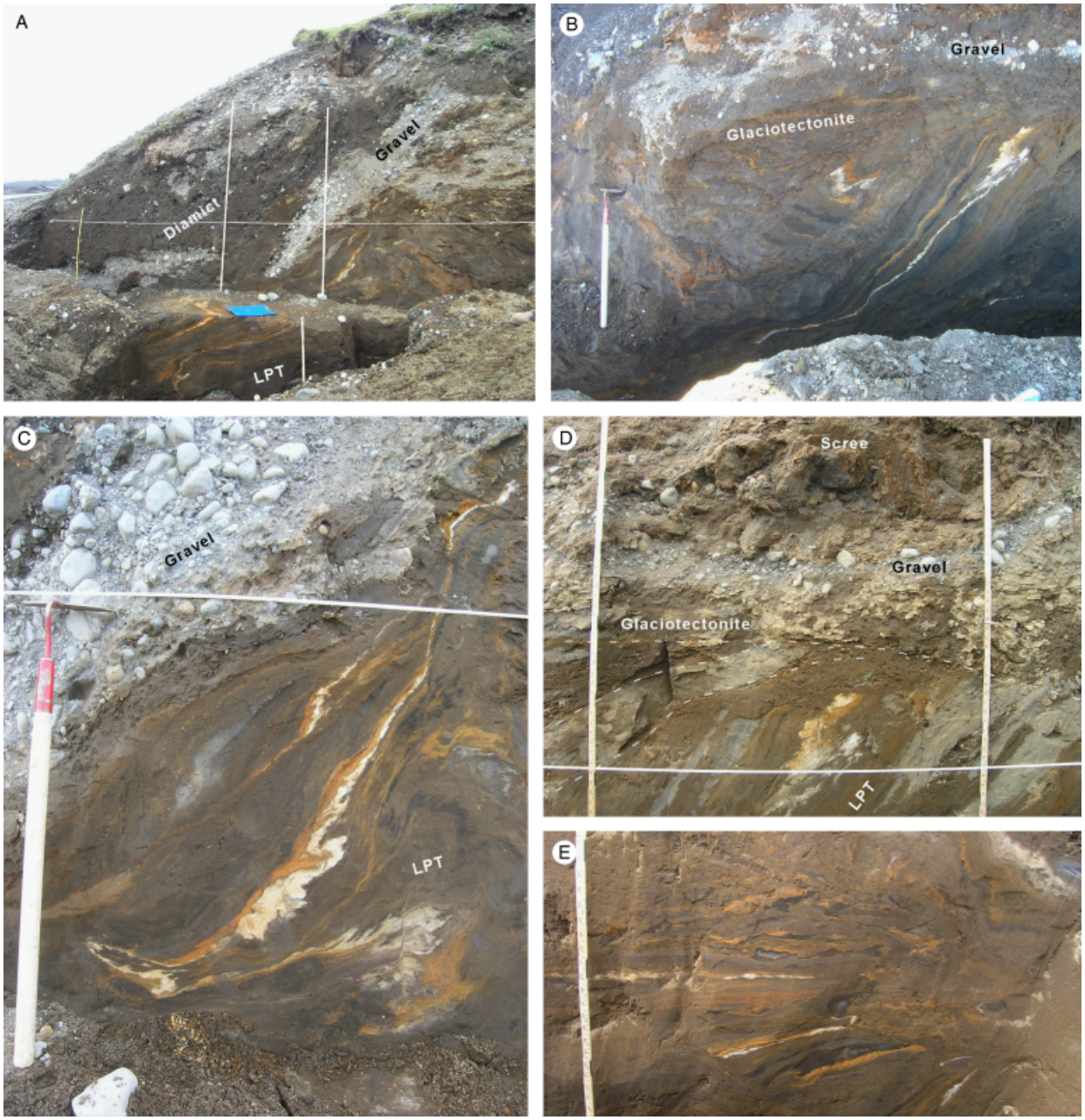

Fig. 9. Glaciotectonic structures and sediments in Section 5. Stress (and ice-flow direction) from left to right in all photographs. A. The proximal part of the section showing LPT underlain by up-thrusted gravel and diamict. B. Glaciotectonics of the lower core showing unconformity between the folded and thrusted LPT below glaciotectonite and gravel. C. Inclined flame-structured fold in LPT and tephra. The scraper is 50 cm long. D. The glaciotectonite above the LPT but below the gravel. Thrust planes in the LPT are indicated. The part of the ruler visible to the right is roughly 80 cm long. E. Deformed LPT in distal part of the section; a 40 cm long part of a ruler for scale.

strain typical of subglacial shear zones, and marks a shear zone that separates the upper part of the section from the deformed LPT below. The location of the glaciotectonite above the LPT is compatible with the glaciotectonics beneath the 1890 surge surface. There, the substrate (LPT), which is dominated by low-angle thrusting, folding and fold attenuation, is separated from a thin top layer of till by a minor shear zone (Kjær *et al*. 2006; Benediktsson *et al*. 2008). Using the glaciotectonics below the 1890 surge surface as an analogue to section 5 in the 1964 end moraine, we interpret the glaciotectonite and the deformation in the lower core as primarily related to the 1890 surge, and possibly to older advances, as the section overlaps with the pre-1964 glaciotectonic thrust ridges (Todtmann 1955) (Fig. 8). Furthermore, the depth at which the fissile glaciotectonite occurs within section 5 is probably too great to be related to the 1963–64 surge, as the overburden pressure and the amount of time required for a glaciotectonite to be created are unlikely

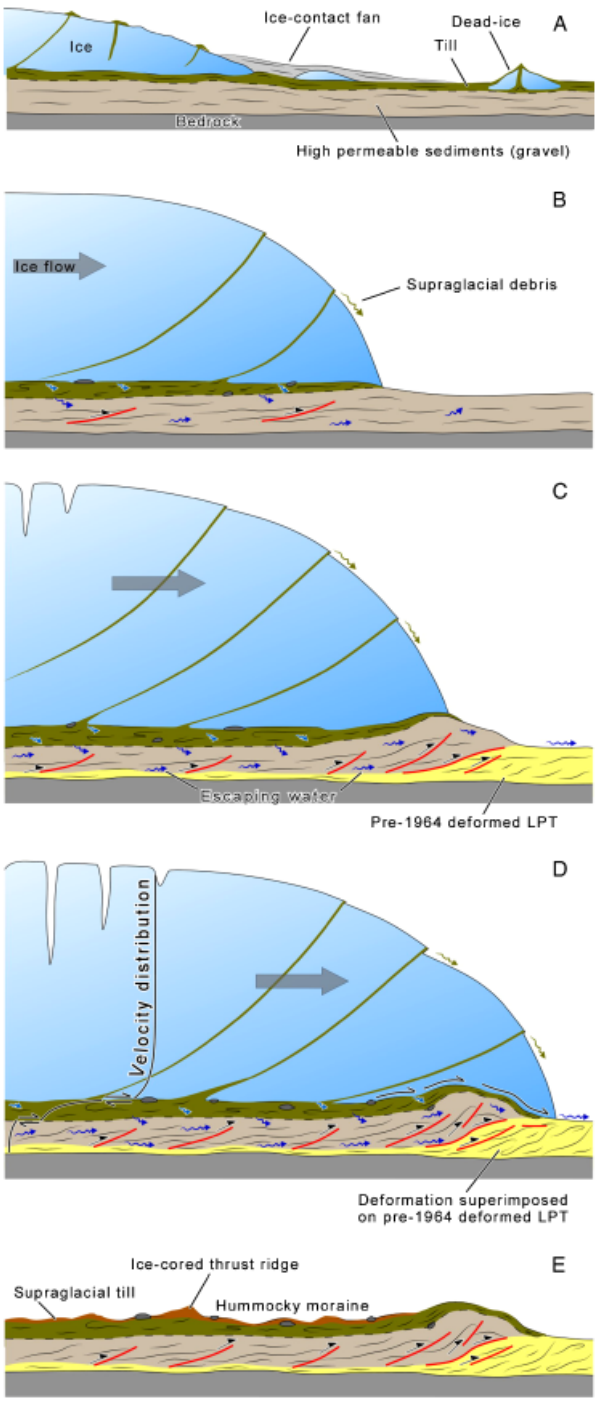

Fig. 10. Sequential model explaining the formation of the 1964 submarginal end moraines. See text for further explanation.

to have been reached below the snout at the end of the surge.

The gravel above the glaciotectonite was thrust up below the ice margin at the end of the surge (Fig. 10). The proximal part of the lower core shows signs of deformation associated with the thrusting of the gravel, namely LPT and tephra layers that subparallel the lower contact of the gravel. The fissile partings in the proximal lower core are lined up in a synclinal structure that is interpreted as a weakly developed synclinal fold that formed in the footwall of the gravel thrust wedge, but was subsequently cut by thrusts. This corresponds with the overturned fold displayed by the white and black tephras below.

The diamict in the proximal part is stratigraphically on top of the other sediment facies. Owing to its properties and position in the section, it is interpreted as a melt-out till associated with downwasting of the stagnant glacier snout after the 1963–64 surge (Fig. 10).

Formation of the submarginal 1964 end moraine: a model

According to field observations in January 1964, only negligible deformation of the foreland, e.g. by ploughing, occurred during the 1963–64 surge advance (Eythorsson 1963, 1964; M. Hallgrímsson, pers. comm. 2007). This indicates that the interaction between the glacier and its foreland, determined by the ice-flow mechanism and the physical properties of the foreland, did not cause any ridge formation in front of the ice margin during the surge. Consequently, the formation of end moraines probably occurred at surge termination and required changes in either the ice-flow mechanism or the foreland properties, or both, resulting in different glacier/foreland coupling. The morphology and internal architecture of the 1964 end moraine vary along its length, suggesting different glaciological or foreland conditions along the ice margin. In the eastern part of the study area, the 1964 moraine resembles the 1890 moraine in geometry, morphology and sedimentary composition (Figs 3–6) (Benediktsson *et al.* 2008). Thus, the model by Benediktsson *et al.* (2008) of a marginal sediment wedge, forming as a result of substrate/bedrock decoupling and associated sediment influx to the marginal zone, and an end moraine forming on top of the wedge in response to a sudden drop in subglacial porewater pressure at the very end of the surge, is applicable for the eastern part of the 1964 end moraine. The western part of the end moraine contrasts the eastern part in terms of morphology, sedimentary composition and position relative to the ice margin (Figs 3–6), thus requiring a different genetic explanation. The model proposed here explains the formation of end moraines beneath the ice margin, and includes the ice-flow mechanism operating during the last days of the surge (Fig. 10). The model assumes that the hydraulic conductivity of the bed had a major influence on the subglacial porewater pressure during the surge (Fig. 3), thereby affecting the rates of subglacial deformation and the velocity distribution. Characteristic signatures left by hydraulic conductivity processes in the geological and geomorphological record are rare, and thus their identification is difficult (Piotrowski *et al.*

2004). Our estimates of hydraulic conductivity are therefore based on the properties of the sediment. Where the sediment was relatively coarse-grained and permeable, the subglacial drainage was efficient enough to prevent build-up of porewater overpressures in the substrate. In contrast, inefficient drainage occurred in fine-grained and low permeable sediments, which favoured overpressurized porewater.

During the quiescent phase, the glacier was inactive and downwasting, with a shallow gradient. The snout was covered with sediment due to melt-out of crevasse fills and debris bands in the ice, and glaciolacustrine sediments accumulated in topographic depressions along the margin (Fig. 10A). We hypothesize that the subglacial ice-flow mechanism, operating in well-drained areas during the course of the surge, was dominated by sliding at the ice/bed interface and shear deformation of the till. This is evident by flutes with strong clast fabric in the area up-glacier of the end moraine (Kjær *et al.* 2006). Folding and thrusting probably occurred in the substrate (below the till); however, both were dependent on the shear strength of the sediments and thus dominated in different zones of the forefield. Thrusting and shearing were probably the principal style of deformation in zones of efficient subglacial drainage and relatively low porewater pressure (Fig. 10B), while folding and fold attenuation were predominant in poorly drained areas that were subjected to higher porewater pressure (Kjær *et al.* 2006; Benediktsson *et al.* 2008). At the closing stage of the surge, high porewater pressure in the till raised its strain rates, which facilitated the advance of the glacier through shear deformation in the uppermost part of the bed (Boulton & Hindmarsh 1987). The underlying gravel had relatively low porewater pressure, increasing the coupling at the till/gravel interface. Movement at this interface induced high friction and stress transfer into the gravel, which consequently deformed through thrusting with the décollement located at the boundary to the fine-grained LPT sediments below (Fig. 10C). Because of higher strain rates in the till than in the gravel, the principal velocity component was located within the till, allowing the glacier to override the thrust sheets that constitute the end moraine (Fig. 10D). At present, the end moraine has a smooth morphology with a hummocky backslope resulting from dead-ice melting. The end moraine ridge is composed primarily of gravel thrust sheets that partly overlie and overprint pre-existing glaciotectonic landforms produced by previous surge advances (Fig. 10E).

Discussion

Ice-flow mechanism and end-moraine formation

Kjær *et al.* (2006) argued that strong clast fabrics in flutes demonstrate a tight coupling between the ice and its bed during the Brúarjökull surges, and that this allowed the glacier to deform the subglacial succession significantly. Furthermore, they concluded that the rapid ice flow during the 1890 surge of Brúarjökull could be explained by a decoupling at the substrate/bedrock interface, favoured by inefficient drainage and associated porewater overpressures in a fine-grained LPT substrate. Benediktsson *et al.* (2008) supported this conclusion by showing that the substrate/bedrock decoupling led to high sediment influx into the marginal zone, resulting in the formation of a ~500 m long sediment wedge, on top of which an end moraine formed during the last day of the surge. The end-moraine formation was initiated by a sudden drop in porewater pressure and associated brittle deformation in the substrate. The sediment wedge and the end moraine represent a dual marginal product of the surge that reflects a certain mechanism of ice flow operating during the 1890 surge. Because the eastern part of the 1964 end moraine shows the same characteristics as the 1890 end moraine in terms of geometry, morphology and sedimentary composition, this mechanism may also be applicable to the eastern part of the 1963–64 surge field (Figs 1, 3). Excess porewater pressures likely caused substrate/bedrock decoupling and associated formation of a marginal sediment wedge. Although we have little evidence for substrate/bedrock decoupling or for a sediment wedge in the marginal zone of the 1963–64 surge, we have no reason to presume that the ice-flow mechanism was different from that of the 1890 surge in this part of the forefield, judged by the major similarity between the two surges in terms of end-moraine morphology and architecture, glaciological conditions and the properties of the subglacial sediment succession and the foreland.

The contrast in the end-moraine morphology and architecture between the central/western and eastern parts of the forefield (Figs 1, 7, 8) indicates a spatial variability in the glacier/foreland interaction and the ice-flow mechanism (Fig. 3). However, such a contrast can also arise from variations in, for example, sediment properties and thermal regime of the foreland (Bennett 2001). There are no indications, such as permafrost features, of significant variations in the thermal regime along the 1963–64 ice margin, and thus the thermal properties of the foreland are unlikely to have affected the moraine morphology. On the other hand, sediment properties vary in the glacier forefield, not just affecting the ice-flow mechanism during the surge but also the nature of the glacier/foreland coupling and the deformation style beneath and in front of the ice margin. The observation that the glacier overrode its own end moraine in the western part of the forefield points to an ice-flow mechanism that allowed the glacier to advance considerably faster than the foreland wedge deformed beneath and in front of the margin.

Owing to efficient subglacial drainage in the central/western forefield, porewater overpressures did not

occur in the substrate. Consequently, a process other than substrate/bedrock decoupling must account for the forward glacier motion in this area. It has been shown that subglacial bed deformation may account for most of the forward motion of temperate outlet glaciers and ice streams (e.g. Alley *et al.* 1987; Boulton & Hindmarsh 1987), and that deformation may concentrate where water pressures are highest in the bed (Boulton & Caban 1995; Alley 2000; Boulton *et al.* 2001). We propose that shear deformation of till was the main process of ice flow where efficient drainage inhibited porewater overpressures in the substrate, which otherwise would have decoupled from the bedrock. Towards the end of the surge, when the supply of water decreased, porewater pressure remained high in the low permeable till, while water pressure fell more rapidly in the high permeable gravel below. This weakened the till relative to the gravel, causing deformation to focus in the till as a deformable bed (van der Meer *et al.* 2003) and explaining why and how the glacier overrode the up-thrusted sediments that constitute the end moraine.

Some researchers have proposed subglacial gravity spreading, resulting from glacial load that is translated into lateral pressure gradient, as the principal process responsible for ice-marginal glaciotectonic deformation in both Pleistocene and contemporary glacial environments (Aber *et al.* 1989; van der Wateren 1995a, b; Bennett *et al.* 2004b; Pedersen 2005; Aber & Ber 2007). It has been argued that gravity spreading may set in at or immediately after surge termination when the glacier sinks to its bed and sediments are extruded from beneath the ice margin to create an end moraine in front of it. The observation that Brúarjökull overrode some parts of its end moraine at the closing stage of the 1963–64 surge indicates that the glacier was still dynamically active when the end moraine had been or was being created; hence the glacier had not sunk to the bed to cause gravity spreading. Moreover, it has been argued that basal till can be squeezed up into open crevasses to form crevasse-squeeze ridges when a glacier sinks to its bed after a surge (Sharp 1985a, b; Evans & Rea 2003; Evans *et al.* 2007). If this is true, crevasse-squeeze ridges should rise up through flutes that are created during the active surging. This is advocated by previous researchers at Brúarjökull, although without providing any sedimentological data that conclusively support this (Evans & Rea 1999, 2003; Evans *et al.* 1999, 2007). Sharp (1985b) showed that the crevasse-squeeze ridges may intersect with flutes in three different ways, i.e. '. . . strike/slip displacement of the flute along the line of the [crevasse-squeeze] ridge, undisturbed passage of the flute through the [crevasse-squeeze] ridge, and a rise in the crestline of the flute to intersect the [crevasse-squeeze] ridge'. The second scenario is in harmony with observations from Svalbard (Christoffersen *et al.* 2005) and detailed geomorphological mapping of the Brúarjökull forefield where 8806 crevasse-squeeze ridges almost exclusively drape flutes (Kjær *et al.* 2008). This is further supported by Bjarnadóttir (2007), who studied the morphology and sedimentology of crevasse-squeeze ridges at Brúarjökull and their interaction with flutes. The superposition of crevasse-squeeze ridges on top of flutes indicates that they are not squeezed up through the flutes but rather deposited onto them. According to Bjarnadóttir (2007), subglacial till is squeezed up into open basal crevasses due to reduction in effective pressure when the crevasse pattern opens up behind the surge bulge. During a short phase of extended glacier flow, the crevasse-squeeze ridges are cut off the bed and transported a short distance down-glacier before the ice behind the bulge stagnates and the ridges are lowered to the bed. As a result, the crevasse-squeeze ridges cannot be considered as an indicator of the glacier sinking to its bed at or immediately after surge termination. Therefore, there are no indications so far of gravity spreading at the end of the surge; hence, the formation of the 1964 end moraine in response to gravity spreading is excluded.

Glaciological studies have shown that Brúarjökull advanced by 9–9.5 km in the eastern part of the study area, which is dominated by a ~6 m thick sequence of loess, peat, tephra and till with low hydraulic conductivity. In contrast, the glacier advanced only 4–5 km west of Kringilsá (Fig. 1), where coarse and highly permeable fluvial sediments dominate (Guðmundsson *et al.* 1996; Schomacker & Kjær 2007; Kjær *et al.* 2008). While this difference in advance may, to some extent, be caused by a difference in ice volume within different parts of the glacier, the role of the subglacial bed cannot be excluded. Where substrate/bedrock decoupling occurred, it most probably added an extra component to the ice flow that both accelerated and extended the surge advance, as evident in the eastern part (Kjær *et al.* 2006), while coupling at the substrate/bedrock interface and low strain rate of the bed restricted the advance and limited the construction of end moraines in the western part.

Sediment re-distribution and end-moraine formation

There is a weak correlation between major pre-surge sediment bodies and the 1964 end moraine (Fig. 3). Neither the lithology nor the volume of sediment within the end moraine seems dependent upon pre-surge sediment bodies up-glacier of the moraine, implying that the source of the sediment within the moraine is local. This again indicates that the end moraines formed at the closing stage of the surge when the glacier had essentially reached its final marginal position. Furthermore, it shows that re-distribution of sediment through erosion and deposition by the surging glacier did not affect the end moraine directly but was related to the ice-flow mechanism. The marginal sediment wedge described by Benediktsson *et al.* (2008) from the 1890

surge occurs in the same part of the study area as the proglacial 1964 end moraines, supporting our conclusion that those are related to the subglacial mechanism of substrate/bedrock decoupling. In contrast, the absence of a marginal sediment wedge up-glacier of submarginal end moraines indicates no substrate/bedrock decoupling and negligible sediment re-distribution during the surge. Therefore, a different subglacial ice-flow mechanism must operate in the areas up-glacier of submarginal end moraines. This links the subglacial ice-flow mechanism, the re-distribution of sediments and the formation of end moraines. Moreover, it confirms that the largest and most prominent end moraines form in areas of substrate/bedrock decoupling and significant re-distribution of sediments.

Conclusions

From our observations on the morphology and internal architecture of the 1964 end moraine, and the comparative mapping of the forefield before, during and after the surge, we draw the following conclusions:

- Different mechanisms operated along different parts of the glacier margin during the 1963–64 surge, resulting in the formation of either proglacial or submarginal end moraines. This implies a spatial variability of deformation and sliding (at the substrate/bedrock interface) beneath Brúarjökull during surges, and that end moraines are important indicators of ice-flow mechanisms operating during glacier surges.
- The subglacial ice-flow mechanism was largely dependent on the hydraulic conductivity of the bed and the substrate. This conductivity influenced the subglacial porewater pressure, thereby affecting the rates of subglacial deformation and the velocity distribution.
- Where low hydraulic conductivity and porewater overpressure occurred, the substrate decoupled from the bedrock and dislocated down-glacier, resulting in the formation of a dual marginal product consisting of a submarginal sediment wedge and a proglacial end moraine.
- Submarginal end moraines formed in areas of a relatively high hydraulic conductivity where subglacial traction till overlies glaciofluvial gravel. High strain rate in the till, favoured by high porewater pressure, facilitated the glacier advance through shear deformation. In contrast to the till, porewater pressure was low in the underlying gravel, resulting in higher shear strength and lower strain rates. Thus, the principal velocity component was located within the till, allowing the glacier to override the gravel thrust sheets that constitute the end moraine.
- Submarginal end moraines formed as a consequence of changes in the subglacial hydrology and ice-flow mechanism at the very end of the surge. Thus, the advance was unlikely to extend far beyond the end moraines, and the moraine ridges can be assumed to indicate the maximum extent of the advance.
- The end moraines formed at the closing stage of the 1963–64 surge. This is supported by the local origin of the sediment within the end moraine, the high ice-flow velocities (100–120 m/day) of the surge and that no end-moraine formation was observed in the field a few weeks before surge termination. We suggest that submarginal end moraines only occur in the marginal zones of rapidly flowing glaciers.

Acknowledgements. - The Brúarjökull project was financed by the Swedish National Research Council, Kungliga Fysiografiska Sällskapet i Lund, Crafoordska Stiftelsen, the Icelandic Research Council, the University of Iceland Research Fund, Landsvirkjun and the Danish National Research Council. The National Museum of Iceland, Sven Sigurðsson and Gylfi Garðarsson kindly allowed us to study Sigurður Þórarinsson's and Magnús Jóhannsson's photographic collections. Furthermore, our thanks are extended to Johannes Krüger, Jaap van der Meer, Per Möller, Carita Grindvik Knudsen, Svante Björck, Eiliv Larsen, Lilja Rún Bjarnadóttir, Louise Ravn, Jón Björn Ólafsson, Ida H. E. O. Jönsson and Silvana Correa Kjær for invaluable companionship and collaboration during the 2003–05 fieldwork at Brúarjökull. Scholarships to Í.Ö.B. from Landsvirkjun, the Iceland Research Fund for Graduate Students and the University of Iceland Research Fund are gratefully acknowledged. Comments from David Huddart, Jan A. Piotrowski and an anonymous reviewer significantly improved the article.

References

Aber, J. & Ber, A. 2007: *Glaciotectonism. Developments in Quaternary Science 6*. 246 pp. Elsevier, Amsterdam.

Aber, J., Croot, D. G. & Fenton, M. M. 1989: *Glaciotectonic Landforms and Structures*. 200 pp. Kluwer, Dordrecht.

Alley, R. B. 2000: Continuity comes first: Recent progress in understanding subglacial deformation. *In* Maltman, A. J., Hubbard, B. & Hambrey, M. J. (eds.): *Deformation of Glacial Materials*, 171–179 *Geological Society of London, Special Publication 176*.

Alley, R. B., Blankenship, D. D., Bentley, C. R. & Rooney, S. T. 1987: Till beneath ice stream B. Till deformation: Evidence and implications. *Journal of Geophysical Research 92*, 8921–8929.

Benediktsson, Í. Ö. 2005: *The 1890 and 1964 push moraines at Brúarjökull, a surge-type glacier in Iceland: Morphology, sediments and structural geology*. M.Sc. thesis, University of Copenhagen, 103 pp.

Benediktsson, Í. Ö., Möller, P., Ingólfsson, Ó., van der Meer, J. J. M., Kjær, K. H. & Krüger, J. 2008: Instantaneous end moraine and sediment wedge formation during the 1890 glacier surge of Brúarjökull, Iceland. *Quaternary Science Reviews 27*, 209–234.

Benn, D. I. & Evans, D. J. A. 1996: The interpretation and classification of subglacially-deformed materials. *Quaternary Science Reviews 15*, 23–52.

Benn, D. I. & Evans, D. J. A. 1998: *Glaciers and Glaciation*. 734 pp. Arnold, London.

Bennett, M. R. 2001: The morphology, structural evolution and significance of push moraines. *Earth-Science Reviews 53*, 197–236.

Bennett, M. R., Hambrey, M. J., Huddart, D., Glasser, N. F. & Crawford, K. R. 1999: The landform and sediment assemblage

produced by a tidewater glacier surge in Kongsfjorden, Svalbard. *Quaternary Science Reviews 18*, 1213–1246.
Bennett, M. R., Huddart, D., Waller, R. I., Midgley, N. G., Gonzalez, S. & Tomio, A. 2004a: Styles of ice-marginal deformation at Hagafellsjökull-Eystri, Iceland during the 1998/99 winter–spring surge. *Boreas 33*, 97–107.
Bennett, M. R., Huddart, D., Waller, R. I., Cassidy, N., Tomio, A., Zukowskyj, P., Midgley, N. G., Cook, S. J., Gonzalez, S. & Glasser, N. F. 2004b: Sedimentary and tectonic architecture of a large push moraine: A case study from Hagafellsjökull-Eystri, Iceland. *Sedimentary Geology 172*, 269–292.
Bjarnadóttir, L. R. 2007: *Ice-marginal environments of a surge-type glacier: Distribution, formation and morphological evolution of flutes and crevasse cast ridges at Brúarjökull, Iceland.* M.Sc. thesis, University of Iceland, 119 pp.
Björnsson, H. 1998: Hydrological characteristics of the drainage system beneath a surging glacier. *Nature 395*, 771–774.
Björnsson, H., Pálsson, F., Guðmundsson, M. T. & Haraldsson, H. H. 1998: Mass balance of western and northern Vatnajökull, Iceland, 1991–1995. *Jökull 45*, 35–38.
Björnsson, H., Pálsson, F. & Sigurðsson, O. 2003: Surges of glaciers in Iceland. *Annals of Glaciology 36*, 82–90.
Boulton, G. S. 1972: Modern arctic glaciers as depositional models for former ice sheets. *Journal of the Geological Society of London 128*, 361–393.
Boulton, G. S. 1986: Push-moraines and glacier-contact fans in marine and terrestrial environments. *Sedimentology 33*, 677–698.
Boulton, G. S. & Caban, P. 1995: Groundwater flow beneath ice-sheets. Part II: Its impact on glacier tectonic structures and moraine formation. *Quaternary Science Reviews 14*, 563–587.
Boulton, G. S. & Hindmarsh, C. A. 1987: Sediment deformation beneath glaciers: Rheology and geological consequences. *Journal of Geophysical Research 92*, 9059–9082.
Boulton, G. S., Dobbie, K. E. & Zatsepin, S. 2001: Sediment deformation beneath glaciers and its coupling to the subglacial hydraulic system. *Quaternary International 86*, 3–28.
Boulton, G. S., van der Meer, J. J. M., Beets, D. J., Hart, J. & Ruegg, G. H. J. 1999: The sedimentary and structural evolution of a recent push moraine complex: Holmströmbreen, Spitsbergen. *Quaternary Science Reviews 18*, 339–371.
Boulton, G. S., van der Meer, J. J. M., Hart, J., Beets, D., Ruegg, G. H. J., van der Wateren, F. M. & Jarvis, J. 1996: Till and moraine emplacement in a deforming bed surge – an example from a marine environment. *Quaternary Science Reviews 15*, 961–987.
Cassidy, N. J., Russel, A. J., Marren, P. M., Fay, H., Knudsen, Ó., Rushmer, E. L. & van Dijk, T. A. G. P. 2003: GPR derived architecture of November 1996 jökulhlaup deposits, Skeiðarársandur, Iceland. *In* Bristow, C. S. & Jol, H. M. (eds.): *Ground Penetrating Radar in Sediments*, 143–152. *Geological Society of London, Special Publication 211*.
Christiansen, E. A., Gendzwill, D. J. & Menelay, W. A. 1982: Howe Lake: A hydrodynamic blowout structure. *Canadian Journal of Earth Sciences 19*, 1122–1139.
Christoffersen, P., Piotrowski, J. A. & Larsen, N. K. 2005: Basal processes beneath an Arctic glacier and their geomorphic imprint after a surge, Elisebreen, Svalbard. *Quaternary Research 64*, 125–137.
Croot, D. G. 1988: Morphological, structural and mechanical analysis of neoglacial ice-pushed ridges in Iceland. *In* Croot, D. G. (ed.): *Glaciotectonics: Forms and Processes*, 33–47. A. A. Balkema, Rotterdam.
Dreimanis, A. 1989: Tills: Their genetic terminology and classification. *In* Goldwait, R. P. & Matsch, C. L. (eds.): *Genetic Classification of Glacigenic Deposits*, 17–83. A. A. Balkema, Rotterdam.
Etzelmüller, B., Farbrot, H., Guðmundsson, Á., Humlum, O., Tveito, O. E. & Björnsson, H. 2007: The regional distribution of mountain permafrost in Iceland. *Permafrost and Periglacial Processes 18*, 185–199.
Evans, D. J. A. (ed.) 2003: *Glacial Landsystems*. 532 pp. Arnold, London.
Evans, D. J. A. & Benn, D. I. 2004: *A Practical Guide to the Study of Glacial Sediments*. 266 pp. Arnold, London.
Evans, D. J. A. & Rea, B. R. 1999: Geomorphology and sedimentology of surging glaciers: A landsystem approach. *Annals of Glaciology 28*, 75–82.
Evans, D. J. A. & Rea, B. R. 2003: Surging glacier landsystem. *In* Evans, D. J. A. (ed.): *Glacial Landsystems*, 259–288. Arnold, London.
Evans, D. J. A., Lemmen, D. S. & Rea, B. R. 1999: Glacial landsystems of the southwest Laurentide Ice Sheet: Modern Icelandic analogues. *Journal of Quaternary Science 14*, 673–691.
Evans, D. J. A., Philipps, E. R., Hiemstra, J. F. & Auton, C. A. 2006: Subglacial till: Formation, sedimentary characteristics and classification. *Earth-Science Reviews 78*, 115–176.
Evans, D. J. A., Twigg, D. R., Rea, B. R. & Shand, M. 2007: Surficial geology and geomorphology of the Brúarjökull surging glacier landsystem. *Journal of Maps 2007*, 349–367.
Eythorsson, J. 1963: Brúarjökull hlaupinn (A sudden advance of Brúarjökull). *Jökull 13*, 19–21.
Eythorsson, J. 1964: Brúarjökulsleiðangur 1964 (An expedition to Brúarjökull 1964). *Jökull 14*, 104–107.
French, H. M. 1996: *The Periglacial Environment*. 341 pp. Longman, Harlow.
Friedman, J. D., Johanson, C. E., Óskarsson, N., Svenson, H., Thorarinsson, S. & Williams, S. R. Jr. 1971: Observations on Icelandic polygon surfaces and palsa areas. Photo interpretations and field studies. *Geografiska Annaler 53A*, 115–145.
Gripp, K. 1929: Glaciological and geological results of the Hamburg Spitsbergen-expedition of 1927. *In* van der Meer, J. J. M. (ed.): *Spitsbergen Push Moraines*, 3–98 *Developments in Quaternary Science 4*. Elsevier, Amsterdam.
Guðmundsson, M. T., Högnadóttir, P. & Björnsson, H. 1996: Brúarjökull: Framhlaupið 1963–1964 og áhrif þess á rennsli Jökulsár á Brú. *Raunvísindastofnun Háskólans, RH-11-96*, 33 pp.
Hambrey, M. J. & Huddart, D. 1995: Englacial and proglaciotectonic processes at the snout of a thermally complex glacier in Svalbard. *Journal of Quaternary Science 10*, 313–326.
Hambrey, M. J., Dowdeswell, J. A., Murrey, T. & Porter, P. R. 1996: Thrusting and debris-entrainment in a surging glacier: Bakaninbreen, Svalbard. *Annals of Glaciology 22*, 241–248.
Hart, J. K. & Watts, R. 1997: Comparison of the styles of deformation associated with two recent push moraines, south Van Keulenfjorden, Svalbard. *Earth Surface Processes and Landforms 22*, 1089–1107.
Huddart, D. & Hambrey, M. J. 1996: Sedimentary and tectonic development of a high-arctic thrust moraine complex, Comfortlessbreen, Svalbard. *Boreas 6*, 227–243.
Jol, H. M. & Bristow, C. S. 2003: GPR in sediments: Advice on data collection, basic processing and interpretation, a good practice guide. *In* Bristow, C. S. & Jol, H. M. (eds.): *Ground Penetrating Radar in Sediments*, 9–27. *Geological Society of London, Special Publication 211*.
Kälin, M. 1971: The Active Push Moraine of the Thompson Glacier, Axel Heiberg Island, Canadian Arctic Archipelago. *Axel Heiberg Island Research Reports, Glaciology 4*, 68 pp.
Kilfeather, A. A. & van der Meer, J. J. M. 2008: Pore size, shape and connectivity in tills and their relationships to deformation processes. *Quaternary Science Reviews 27*, 250–266.
Kjær, K. H., Sultan, L., Krüger, J. & Schomacker, A. 2004: Architecture and sedimentation of fan-shaped outwash in front of the Mýrdalsjökull ice cap, Iceland. *Sedimentary Geology 172*, 139–163.
Kjær, K. H., Larsen, E., van der Meer, J., Ingólfsson, Ó., Krüger, J., Benediktsson, Í. Ö., Knudsen, C. G. & Schomacker, A. 2006: Subglacial decoupling at the sediment/bedrock interface: A new mechanism for rapid flowing ice. *Quaternary Science Reviews 25*, 2704–2712.
Kjær, K. H., Korsgaard, N. J. & Schomacker, A. 2008: Impact of multiple glacier surges – a geomorphological map from Brúarjökull, East Iceland. *Journal of Maps 2008*, 5–20.
Kjerúlf, þ. 1962: Vatnajökull hlaupinn (Brúarjökull 1890). *Jökull 12*, 47–48.
Krüger, J. 1994: Glacial processes, sediments, landforms, and stratigraphy in the terminus region of Mýrdalsjökull, Iceland. *Folia Geographica Danica 21*, 1–233.
Krüger, J. & Kjær, K. H. 1999: A data chart for field description and genetic interpretation of glacial diamicts and associated sediments –

with examples from Greenland, Iceland, and Denmark. *Boreas 28*, 386–402.
Magnússon, E., Pálsson, F. & Björnsson, H. 2004: Yfirborð Brúar- og Eyjabakkajökuls og vatnasvið Jökulsár á Brú, Kreppu, Kverkár og Jökulsár á Fljótsdal 1946-2000. *Raunvísindastofnun Háskólans, RH-10-2004*, 31 pp.
Maizels, J. 1993: Lithofacies variations within sandur deposits: The role of runoff regime, flow dynamics and sediment supply characteristics. *Sedimentary Geology 85*, 299–325.
Menzies, J. (ed.) 2002: *Modern Glacial Environments. A Revised Student Edition*. 543 pp. Butterworth-Heinemann, Oxford.
Paul, M. A. & Eyles, N. 1990: Constraints on the preservation of diamict facies (melt-out tills) at the margins of stagnant glaciers. *Quaternary Science Reviews 9*, 51–69.
Pedersen, S. A. S. 2005: Structural analysis of the Rubjerg Knude glaciotectonic complex, Vendsyssel, northern Denmark. *Geological Survey of Denmark and Greenland, Bulletin 8*, 192 pp.
Piotrowski, J. A., Larsen, N. K. & Junge, F. W. 2004: Reflections on soft subglacial beds as a mosaic of deforming and stable spots. *Quaternary Science Reviews 23*, 993–1000.
Ravn, L. 2006: *Interaktionen mellem klima og landskab-sedimentjordsystemet i et periglacialt miljø foran Brúarjökull, Island*. M.Sc. thesis, University of Copenhagen, 57 pp.
Schomacker, A. 2007: Dead-ice under different climate conditions: Processes, landforms, sediments and melt rates in Iceland and Svalbard. *LUNDQUA Thesis 59*, 25 pp.
Schomacker, A. & Kjær, K. H. 2007: Origin and de-icing of multiple generations of ice-cored moraines at Brúarjökull, Iceland. *Boreas 36*, 411–425.
Schomacker, A., Krüger, J. & Kjær, K. H. 2006: Ice-cored drumlins at the surge-type glacier Brúarjökull, Iceland: A transitional-state landform. *Journal of Quaternary Science 21*, 85–93.
Sharp, M. 1985a: Sedimentation and stratigraphy at Eyjabakkajökull – an Icelandic surging glacier. *Quaternary Research 24*, 268–284.
Sharp, M. 1985b: Crevasse-fill' ridges – a landform type characteristic of surging glaciers? *Geografiska Annaler 67A*, 213–220.
Swift, D. A., Evans, D. J. A. & Fallick, A. E. 2006: Transverse englacial debris-rich bands at Kvíárjökull, southeast Iceland. *Quaternary Science Reviews 25*, 1708–1718.
Thorarinsson, S. 1964: On the age of the terminal moraines of Brúarjökull and Hálsajökull. *Jökull 14*, 67–75.
Thorarinsson, S. 1969: Glacier surges in Iceland, with special reference to the surges of Brúarjökull. *Canadian Journal of Earth Sciences 6*, 875–882.
Todtmann, E. M. 1955: Übersicht über die Eisrandlagen in Kringilsárrani von 1890–1955. *Jökull 5*, 8–10.
Todtmann, E. M. 1960: Gletcherforschungen auf Island (Vatnajökull). *Universität Hamburg. Abhandlungen aus dem Gebiet der Auslandskunde 65C*, 1–95.
Twiss, R. J. & Moores, E. M. 1992: *Structural Geology*. 532 pp. W. H. Freeman and Company, New York.
van der Meer, J. J. M., Menzies, J. & Rose, J. 2003: Subglacial till: The deforming glacier bed. *Quaternary Science Reviews 22*, 1659–1685.
van der Wateren, D. F. M. 1995a: Structural geology and sedimentology of push moraines: Processes of soft sediment deformation in a glacial environment and the distribution of glaciotectonic styles. *Mededelingen Rijks Geologische Dienst 54*, 168 pp.
van der Wateren, D. F. M. 1995b: Processes of glaciotectonism. *In* Menzies, J. (ed.): *Modern Glacial Environments. A Revised Student Edition*, 417–444. Butterworth-Heineman, London.
van Vliet-Lanoë, B., Bourgeois, O. & Dauteuil, O. 1998: Thufur formation in Northern Iceland and its relation to Holocene climate change. *Permafrost and Periglacial Processes 9*, 347–365.

APPENDIX IV

Quaternary Science Reviews xxx (2009) 1–23

Contents lists available at ScienceDirect

Quaternary Science Reviews

journal homepage: www.elsevier.com/locate/quascirev

The 1890 surge end moraine at Eyjabakkajökull, Iceland: a re-assessment of a classic glaciotectonic locality

Í.Ö. Benediktsson [a,*], A. Schomacker [a], H. Lokrantz [b], Ó. Ingólfsson [a]

[a] University of Iceland, Institute of Earth Sciences, Askja, Sturlugata 7, IS-101 Reykjavík, Iceland
[b] Bergab, Korta gatan 7, S-171 54 Solna, Stockholm, Sweden

ARTICLE INFO

Article history:
Received 4 June 2009
Received in revised form
6 October 2009
Accepted 8 October 2009

ABSTRACT

The glaciotectonic architecture and sequential evolution of the Eyjabakkajökull 1890 surge end moraines in Iceland were studied for understanding better the formation and evolution of glaciotectonic end moraines and their relation to glacier dynamics. Based on morphological, geological and geophysical data from terrain cross-profiles, cross-sections and ground penetrating radar profiles, we demonstrate that three different qualitative and conceptual models are required to explain the genesis of the Eyjabakkajökull moraines. Firstly, a narrow, single-crested moraine ridge at the distal end of a marginal sediment wedge formed in response to decoupling of the subglacial sediment from the bedrock and associated downglacier sediment transport. Secondly, large lobate end moraine ridges with multiple, closely spaced, narrow asymmetric crests formed by proglacial piggy-back thrusting. Thirdly, a new model shows that moraine ridges with different morphologies may reflect different members of an end moraine continuum. This is true for the eastern and western parts of the Eyjabakkajökull moraines as they show similar morphological and structural styles which developed to different degrees. The former represents an intermediate member with décollement at 4–5 m depth and 27–33% shortening through multiple open anticlines that are reflected as moderately spaced symmetric crests on the surface. The latter represents an end member with décollement at about 27 m depth and 39% horizontal shortening through multiple high amplitude, overturned and overthrusted anticlines, appearing as broadly spaced symmetric crests. We propose that the opposite end member would be a moraine of multiple symmetric, wide open anticlinal crests of low amplitude. Our data suggest that the glacier coupled to the foreland to initiate the end moraine formation when it had surged to within 70–190 m of its terminal position. This indicates a time frame of 2–6 days for the formation of the end moraines.

1. Introduction

End moraines form due to deformation of proglacial or submarginal sediments, chiefly as a result of ice pushing and/or gravity spreading, and signify the process of glaciotectonism beneath or in front of ice margins (Aber et al., 1989; van der Wateren, 1995a,b; Benn and Evans, 1998; Bennett, 2001; Aber and Ber, 2007). Glaciotectonism is a significant component of glacier dynamics and consequently, studies of glaciotectonic landforms provide important information on ice flow mechanism, basal drainage, fluctuating water pressure and hydrofracturing, subglacial and ice-marginal stresses, sediment shear strength, thermal regime of the glacier and the foreland, sediment transport, history of deformation events, and the overall interplay of glaciers with their forelands (Boulton and Hindmarsh, 1987; van der Wateren, 1995a; Bennett, 2001; McCarrol and Rijsdijk, 2003; Motyka and Echelmeyer, 2003; Pedersen, 2005; Kjær et al., 2006; Kuriger et al., 2006; Motyka et al., 2006; Benediktsson et al., 2008, 2009; Phillips et al., 2008; Roberts et al., 2009).

End moraine ridges and marginal sediment wedges created by surging glaciers and ice streams are among the most prominent glaciotectonic landforms in both modern and Pleistocene glacial environments. In order to increase our understanding of the dynamics and mechanics of fast flowing ice masses, end moraines of surging glaciers have increasingly been investigated in recent years (Boulton et al., 1999; Bennett et al., 1999, 2004a,b; Bennett, 2001; Benediktsson et al., 2008, 2009; Roberts et al., 2009). However, some uncertainties remain about the conditions under which these end moraines form; e.g. (i) how does thickness and composition of the foreland sediment affect the end moraine formation; (ii) what causes lateral variation in morphology and structural style; (iii) how is the structural style related to the morphology; and (iv) why do

* Corresponding author. Tel.: +354 525 4305; fax: +354 562 9767.
E-mail address: iob2@hi.is (Í.Ö. Benediktsson).

0277-3791/$ – see front matter © 2009 Elsevier Ltd. All rights reserved.
doi:10.1016/j.quascirev.2009.10.004

glaciers couple to their forelands to create end moraines and how long before surge termination does this happen?

This paper presents a study on prominent glaciotectonic end moraine ridges that formed during the 1890 surge of Eyjabakkajökull, Iceland (Fig. 1). Their size and morphology makes them, together with the Brúarjökull surge moraines (Benediktsson et al., 2008, 2009), unique to Icelandic moraines, but with similarity to moraines described from high-Arctic areas (Kälin, 1971; Croot, 1988b; Boulton et al., 1999) and Alaska (Motyka and Echelmeyer, 2003; Kuriger et al., 2006). The Eyjabakkajökull moraines were earlier described by Croot (1987, 1988a) as ridges of two distinct elements: a subglacial extension zone with low-angle normal faults that are linked by a floor thrust to a proglacial compression zone signified by imbricate thrust sheets. In the discussion of glaciotectonics, the Eyjabakkajökull moraines have ever since been referred to as a classic example of the formation and architecture of push moraines (e.g. Croot, 1988b; Aber et al., 1989; Benn and Evans, 1998; Bennett, 2001; Aber and Ber, 2007). However, Croot (1988a) emphasizes that "… the internal structure and evolution of only one [morphological] type [of ridges] have been described" and that "further work along similar lines on the sections available in the other ridges will help fill the gaps in our knowledge of the structure and evolution of neoglacial tectonic features." The aim of our study is to describe the Eyjabakkajökull moraine complex with the main focus on 'the other ridges', and to re-assess Croot's (1987, 1988a) descriptions and model. With modern methods and techniques, we investigate the factors controlling the morphology, architecture and formation of these moraines, and show that Croot's (1987, 1988a) model is only applicable for the central part of the moraine complex. Hitherto, the remaining parts have lacked a genetic explanation and thus, three models, arising from lateral variability in morphology and sedimentary composition, are presented to explain the genesis of the entire end moraine complex.

2. Eyjabakkajökull and its forefield

2.1. Eyjabakkajökull

Eyjabakkajökull is a surge-type outlet glacier draining the NE part of the Vatnajökull ice cap in Iceland. The glacier occupies a 4–6 km wide valley, and is composed of three distinct outlets from the main ice cap that descend from 1200–1500 m a.s.l. and combine to form a glacier tongue which is about 10 km long and 4 km wide where it terminates at around 700 m a.s.l. In the ablation zone, the outlets are separated by two prominent medial moraines that originate from nunataks further upglacier (Fig. 1).

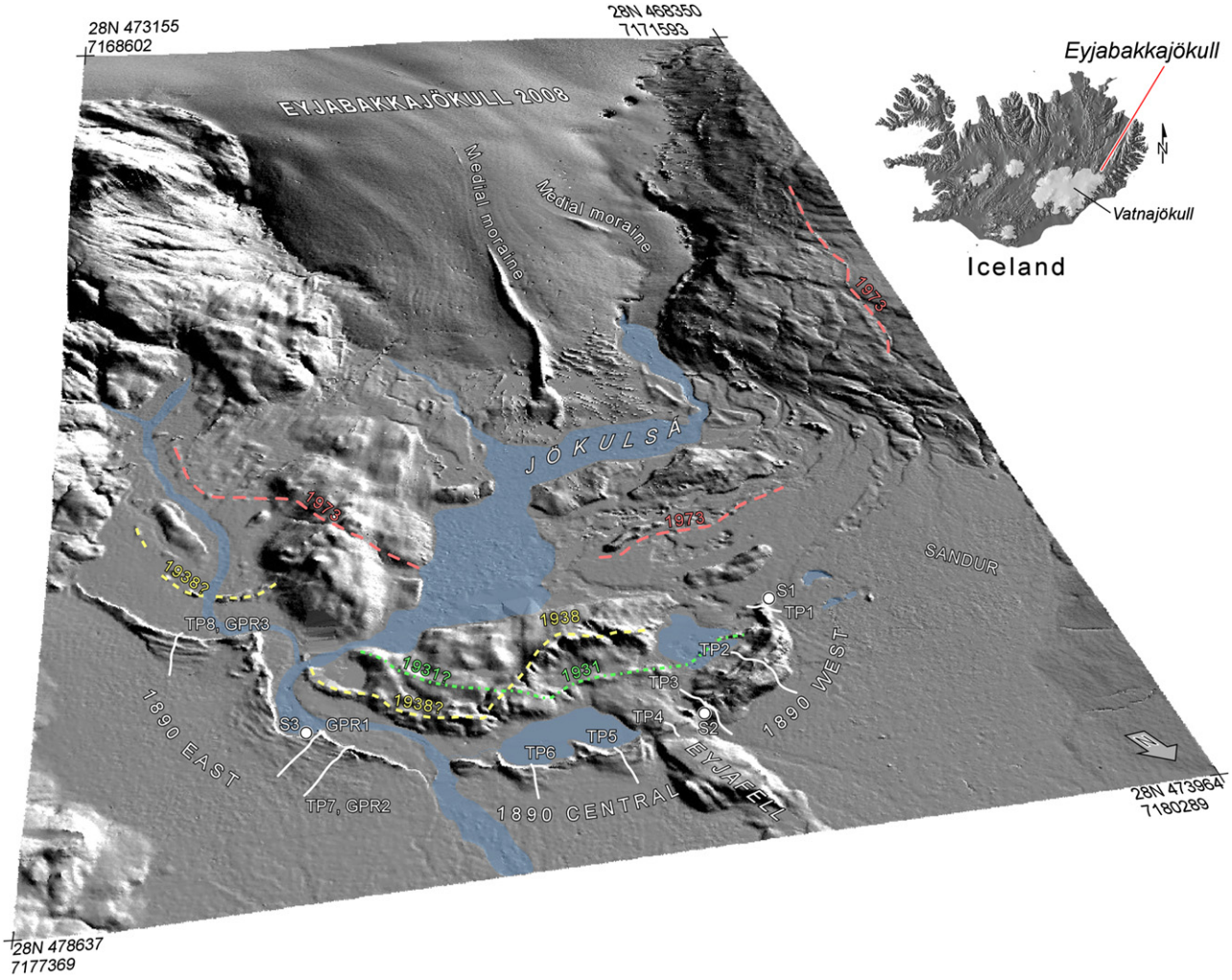

Fig. 1. The forefield of the surge-type glacier Eyjabakkajökull, eastern Iceland. The digital elevation model, generated from aerial photographs recorded in August 2008, is visualized as a hillshade relief model. End moraines from the 1890, 1931, 1938 and 1972–1973 surges are indicated. Rivers and major lakes are in blue. Lines TP1–TP8 and GPR1–GPR3 represent terrain cross-profiles (Fig. 4) and ground penetrating radar profiles (Figs. 12–14), and dots S1–S3 indicate excavated cross-sections (Figs. 5, 7 and 11). The view is approximately 5 km across. UTM coordinates are in metres.

Please cite this article in press as: Benediktsson, Í.Ö., et al., The 1890 surge end moraine at Eyjabakkajökull, Iceland: a re-assessment of a classic..., Quaternary Science Reviews (2009), doi:10.1016/j.quascirev.2009.10.004

The recent surge history of Eyjabakkajökull is well documented with advances recorded in 1890, 1931, 1938 and 1972–1973 (Thoroddsen, 1914; Thorarinsson, 1938, 1943; Todtmann, 1953, 1960; Williams, 1976; Kaldal and Víkingsson, 2000; Björnsson et al., 2003). The most extensive advance (3–4 km) occurred in 1890 when the glacier terminated at the Eyjafell bedrock knob and formed the end moraines described in this paper (Fig. 1). The surges in 1931 and 1938 were probably smaller as they terminated 250 and 750 m upglacier from the 1890 moraines (Kaldal and Víkingsson, 2000), however producing prominent glaciotectonic end moraines. During the 1972–1973 surge, the glacier advanced approximately 2 km between late August 1972 and September 1973 with maximum flow rates of up to 30 m/day (Williams, 1976; Björnsson, 1982; Sharp and Dugmore, 1985). At present, the snout of Eyjabakkajökull has a low profile and is retreating with crevasse-squeeze ridges and debris bands emerging from the ice.

2.2. The forefield

The forefield of Eyjabakkajökull is characterized by sandur plains, end moraines, ice-cored and ice-free hummocky moraines, flutes, crevasse-squeeze ridges and concertina eskers (Fig. 1; Todtmann, 1953; Sharp, 1985a,b; Croot, 1987, 1988a; Evans and Rea, 1999, 2003; Evans et al., 1999; Kaldal and Víkingsson, 2000). Prior to the 1890 surge, the distal part of the proglacial sandur had developed a thick vegetated soil cover of loess, peat and tephra (LPT) (Croot, 1987, 1988a). Known tephra horizons indicate that this LPT sediment accumulated during long periods of low glacial activity, probably during the late Holocene and the Medieval Warm Period. End moraines resulting from the 1890, 1931 and 1938 surges demonstrate glaciotectonic structures and are conspicuous in the proglacial area, whereas end moraines from the 1972 to 1973 surge are indistinct. There is a small end moraine about 1 km upglacier of the 1973 terminal position in the eastern part of the area. The age of this moraine is not known but Kaldal and Víkingsson (2000) speculate that it could result from a minor surge around 1990. They also suggest the possibility that the three glacier outlets that confluence in Eyjabakkajökull do not surge simultaneously.

Indicators of permafrost are rare in the glacier forefield. Indistinct frost-crack polygons were observed on the Eyjafell bedrock knob and circular ponds occur in places in front of the 1890 moraine and in clusters on the Eyjabakkar outwash plain to the north (Fig. 1). Similar ponds observed in the forefield of the adjacent Brúarjökull have been interpreted as collapsed palsas, an indicator of deteriorating permafrost (Todtmann, 1955, 1960; Friedman et al., 1971; Kjær et al., 2006, 2008; Schomacker and Kjær, 2007; Benediktsson et al., 2008). Mean annual air temperature on the Eyjabakkar outwash plain approximately 10 km from the glacier was 0.1 °C between November 1997 and October 2008, indicating that the present climate is too warm for significant permafrost to exist. However, as temperatures in Iceland were 1.5–2 °C lower during the Little Ice Age (LIA; Bergthórsson, 1969; Guðmundsson, 1997; Flowers et al., 2008), it is possible that discontinuous permafrost occurred in the forefield of Eyjabakkajökull at the time of the 1890 surge.

3. Methods

3.1. Aerial photos and geomorphology

The glacier forefield was initially studied on a series of aerial photographs from 1967–1998. End moraine morphology was analysed in geographical information systems (GIS) on the basis of a new aerial photographs from August 2008 and a resultant digital elevation model (DEM). The aerial photographs have a resolution of 20 cm and the DEM has a grid spacing of 3 m.

Eight terrain cross-profiles were measured in the field with a TopCon 236N precision levelling instrument across the 1890 end moraine to demonstrate its morphological and geometrical characteristics. Each profile was surveyed approximately perpendicular to the moraine strike (Fig. 1).

3.2. Sedimentology and structural geology

The sediments and internal architecture of the 1890 end moraine were studied in three natural cross-sections (Figs. 1 and 2). The data chart by Krüger and Kjær (1999) was used as a basis for documentation of sediment lithologies and structures, and glaciotectonic structures were described following the terminology of Marshak and Mitra (1988), Twiss and Moores (1992) and Evans and Benn (2004). Sections 1 and 2 were manually cleaned and studied up close while the steepness of the river-cut section 3 above the river Jökulsá prohibited any close-up studies and cleaning (Fig. 1). Section 3 was therefore mapped, using binoculars, and photographed from *c.* 50 m distance. Subsequently, the high resolution photographs were used to fill in details on the section diagram. The internal architecture was mapped at scales of 1:50 (section 1), 1:100 (sections 2a, 2b and 3) and 1:200 (section 2).

3.3. Cross-section balancing

Cross-section balancing was applied to sections 2 and 3, and GPR profiles 1, 2 and 3 (Fig. 1) following the methodology of Dahlström (1969), Marshak and Mitra (1988) and Pedersen (1996, 2005) (see article Section 5). Despite the simplicity of the method, it has rarely been applied in glacial environments (e.g. Croot, 1987, 1988a; Pedersen, 1996, 2005; Hart and Roberts, 1997; Boulton et al., 1999) to quantify total shortening and depth of décollement surfaces, perhaps because of the general absence of continuous marker horizons that allow one to measure the shortening of the original strata, or because glaciotectonic disturbances are too complex.

3.4. Ground penetrating radar (GPR)

In order to map the internal structure of the end moraine, three transverse ground penetrating radar profiles (Figs. 1 and 2) were recorded with a Sensors & Software Inc. pulseEKKO PRO system using a pulsar voltage of 90 V. The best balance between penetration depth and resolution of the reflectors was obtained with a centre frequency of 100 MHz, a step size of 0.25 m, an antenna separation of 1 m and antennas oriented perpendicular-broadside to the survey line. Data were dewow-corrected and then automatic gain controlled in order to correct for loss of amplitude due to geometrical spreading of the radar waves and signal scattering and attenuation. Common-mid-point (CMP) analysis was used for depth conversion of the recorded two-way-travel time. The CMP analysis gave a velocity of 0.07 m/ns, which corresponds well to table values of 0.06–0.1 m/ns for saturated and damp sand (Jol and Bristow, 2003), and to velocities recorded in other glacial environments in Iceland (e.g. Cassidy et al., 2003; Kjær et al., 2004; Burke et al. 2008; Benediktsson et al., 2009). Data were processed with the Sensors & Software Inc. EKKO_View Deluxe 1.3 software. Topography was added to all GPR data from a GPS directly linked to the GPR data logger as well as from levelled terrain profiles.

4. Geomorphology of the 1890 end moraine

The lateral variation in the morphology of the 1890 end moraine is obvious in the field, and from the 2008 aerial photographs, DEM

Please cite this article in press as: Benediktsson, Í.Ö., et al., The 1890 surge end moraine at Eyjabakkajökull, Iceland: a re-assessment of a classic..., Quaternary Science Reviews (2009), doi:10.1016/j.quascirev.2009.10.004

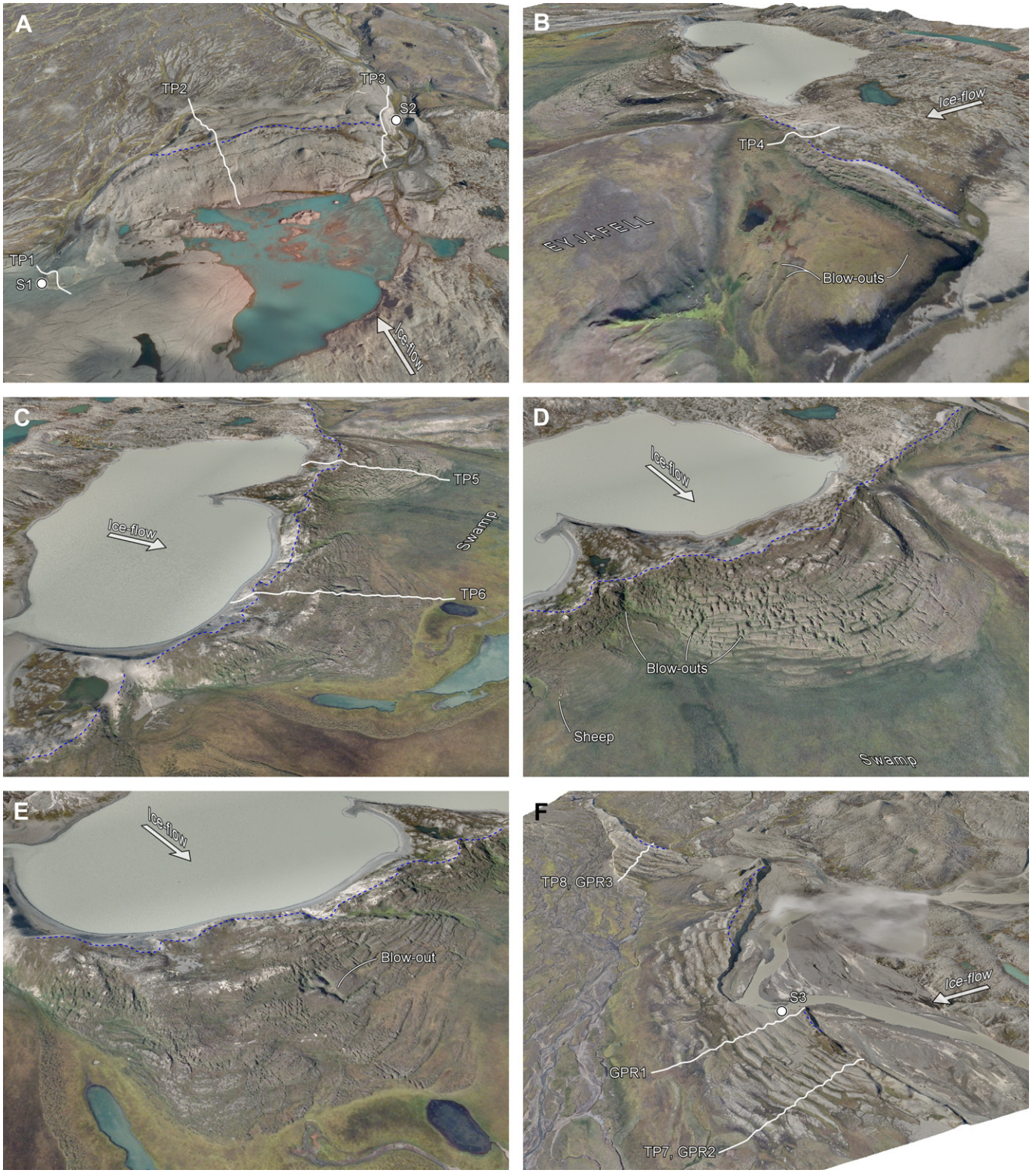

Fig. 2. Views of the 1890 end moraine. Aerial orthophotographs from 2008 draped over a 3 m grid DEM with 1.5× vertical exaggeration. TP1–TP8 and GPR1–GPR3 indicate terrain and ground penetrating radar profiles surveyed across the end moraine. Excavated cross-sections are represented by dots S1–S3. Terminal position of the former ice margin is indicated by a blue dashed line. (A) Large ridge in the western part of the forefield with multiple widely spaced and broad symmetric crests in the central and distal zones of the ridge, but lower asymmetric crests on the proximal slope (see TPs 1–3, Figs. 1 and 4). (B) Small and narrow single-crested ridge in the central part resting on the Eyjafell bedrock knob (see TP4, Figs. 1 and 4). (C) View to the west across two of three distinct moraine lobes in the central part (see TPs 5–6, Figs. 1 and 4). (D) and (E) Close-ups of large ridges in the central part consisting of multiple closely spaced, asymmetric narrow crests (see TPs 5–6, Figs. 1 and 4). Note the number of semi-circular blow-out depressions and associated channels dissecting the foreslope. Sheep are indicated for scale. (F) Large ridge east of Jökulsá with multiple moderately spaced symmetric crests (see TPs 7–8, Figs. 1 and 4).

Please cite this article in press as: Benediktsson, Í.Ö., et al., The 1890 surge end moraine at Eyjabakkajökull, Iceland: a re-assessment of a classic..., Quaternary Science Reviews (2009), doi:10.1016/j.quascirev.2009.10.004

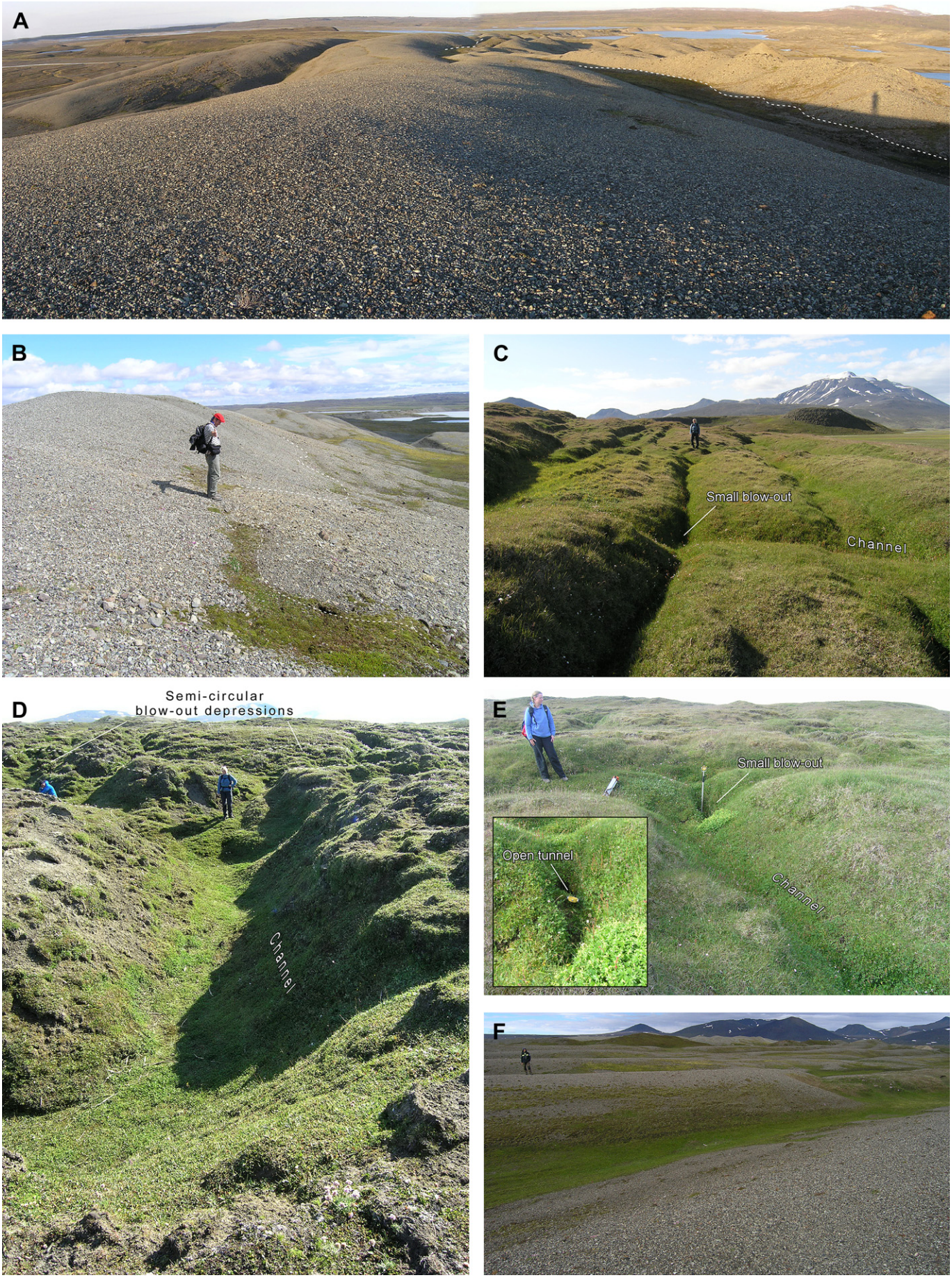

Please cite this article in press as: Benediktsson, Í.Ö., et al., The 1890 surge end moraine at Eyjabakkajökull, Iceland: a re-assessment of a classic..., Quaternary Science Reviews (2009), doi:10.1016/j.quascirev.2009.10.004

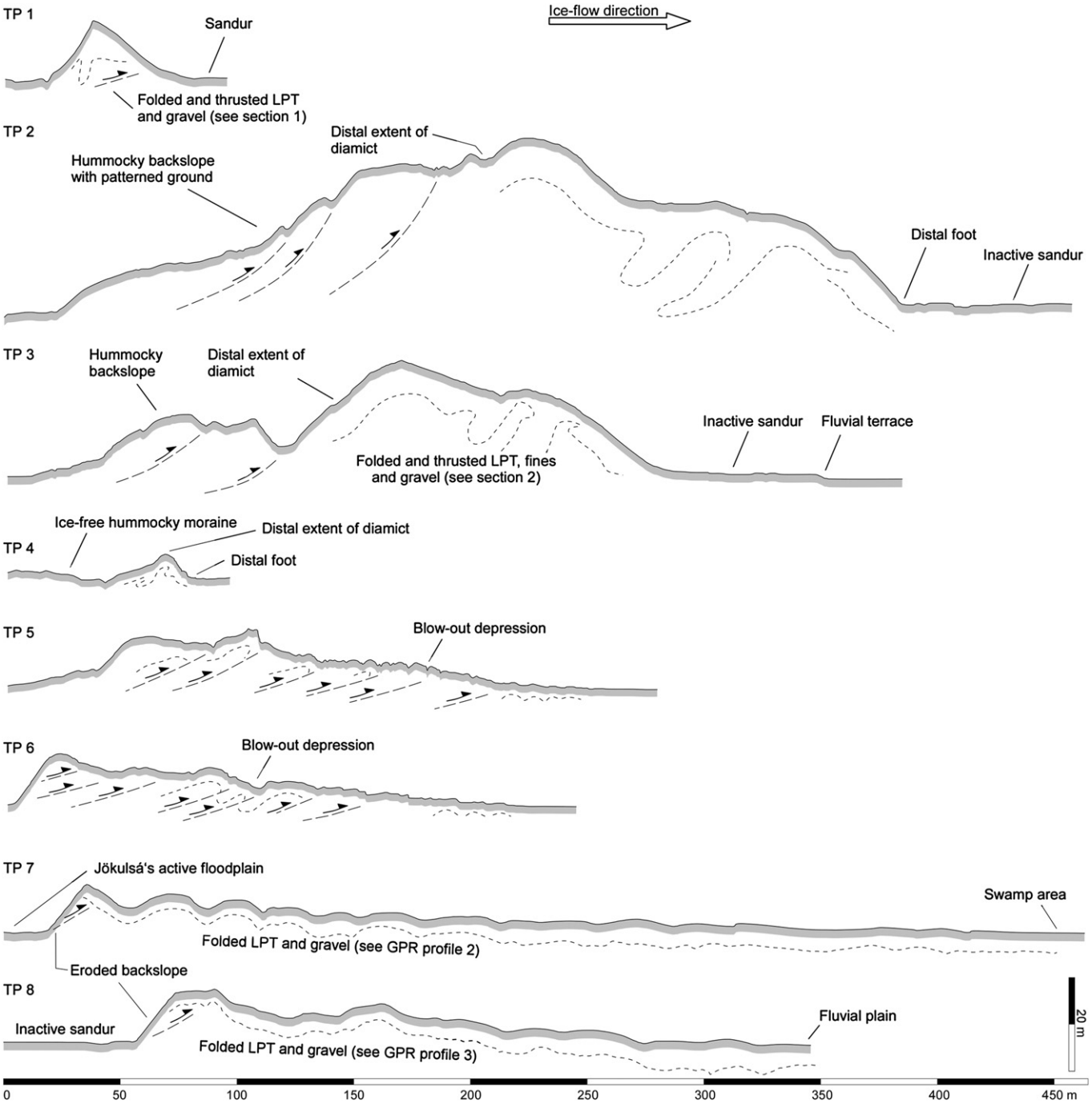

Fig. 4. Terrain profiles (TP) 1–8, measured across the 1890 end moraine. Documented (TPs 1, 3, 7, 8) and inferred (TPs 2, 4, 5, 6) glaciotectonics are indicated. See Fig. 2 for locations of the profiles. Vertical exaggeration is 2×.

and hillshade (Figs. 1–3). The original morphology of the end moraine is well preserved as the ridges do not seem to have degraded much since their formation. However, fluvial erosion has affected the proximal and distal slopes in various degrees, especially in the western part. For demonstrating the diverse morphology of the moraine, 3D-views were extracted from the 2008 aerial imagery draped on the DEM, and eight terrain cross-profiles (TPs) were surveyed to document the morphological characteristics of the end moraine (Figs. 2 and 4). The terrain profiles show that the end moraine can be divided into four

Fig. 3. Ground photographs illustrating the morphology of the 1890 end moraine. (A) View of the multi-crested western part of the end moraine (see Fig. 2A). Note the symmetric ridges to the left and asymmetric hummocky ridges to the right. Dashed line indicates the boundary between till and proglacial outwash gravel and marks the terminal position of the 1890 ice margin. The photo is *c.* 10 m across at the bottom. Ice flow was from right to left. (B) A close-up of the boundary between the till (right) and the outwash gravel (left). (C) The foreslope of a ridge in the central part of the end moraine complex with multiple closely spaced asymmetric crests (see Fig. 2D). Ice flow was from left to right. Eyjafell and Mt. Snæfell (1833 m a.s.l.) in the background. (D) The large blow-out depression and channel marked on Fig. 2E. Ice flow was towards the viewer. (E) One of the numerous small blow-outs and channels on the foreslope of the ridge on Fig. 2D. Ice flow was towards the viewer. The inset photograph shows the 1.2 m long pole lying in an open subsurface tunnel extending upglacier. (F) The moraine ridge in the eastern part with multiple regularly spaced symmetric crests (see Fig. 2F). Ice flow was from upper left to lower right.

Please cite this article in press as: Benediktsson, Í.Ö., et al., The 1890 surge end moraine at Eyjabakkajökull, Iceland: a re-assessment of a classic..., Quaternary Science Reviews (2009), doi:10.1016/j.quascirev.2009.10.004

morphological types, each of which represents a certain style or intensity of glaciotectonic deformation: (A) large ridge consisting of multiple widely spaced and broad symmetric crests in the central and distal zone, and smaller asymmetric crests in the proximal zone; (B) small and narrow single-crested ridge; (C) large ridge of multiple closely spaced, asymmetric narrow crests; and (D) large ridge of multiple moderately spaced symmetric crests.

4.1. Morphological type A

As displayed by TP1, the westernmost tip of the end moraine is ~12 m high and narrow with steep proximal and distal slopes as a result of extensive post-tectonic fluvial erosion (Figs. 1, 2A and 4). The ridge is primarily composed of folded and thrusted loess, peat and tephra (LPT) sequence with a diamict cover on top, thus indicating deformation beneath the ice margin. Elsewhere, the western part of the moraine ridge is up to 40 m high and 470 m wide. It is composed of multiple asymmetric crests on the proximal slope and symmetric crests in the central and distal zone (Fig. 3A). The crests are usually 40–60 m apart. The backslope contains hummocky moraine extending almost to the highest crest in the centre (Figs. 2A and 3B). These morphological characteristics are well demonstrated by TP2 and TP3, the latter lying exactly above section 2 (Figs. 2A and 4). On the upglacier side of the moraine

Table 1
Sedimentary facies identified in the 1890 end moraine.

Sedimentary facies	Location and description	Interpretation	References
1	Sections 1, 2, 3 – 0.2–3 cm thick silt, silty-sand and fine-sand laminae of orange to dark-brown peat, light-gray to yellowish minerogenic loess interbedded with black or dark-gray tephra – Cohesive, firm and difficult to excavate – Sometimes totally mixed by pervasive external deformation	Sequence of loess, peat and tephra (LPT) – Represents palaeosols originally developed on a wetland similar to that north of the end moraine – Frequent loess and tephra deposition favoured transformation of organic matter into peat – Known tephra horizons (e.g. the white rhyolithic Öræfajökull 1362 AD) indicate accumulation during periods of low glacial activity in the late Holocene and the Medieval Warm Period	Brady and Weil, 1999
2	Sections 1, 2, 3 – Angular, well sorted black basaltic or white rhyolithic ash – Thickness ranges from a few millimetres to ~30 cm – Occur as interbeds or lenses and patches in facies 1 and 3	Tephra – Greatest thickness occurs in folds – Lenses and patches result from external deformation	
3	Section 1 (minor facies) and 2 (major facies) – Light brown to blue and greyish and either laminated or massive clay, silt, sandy-silt and fine-sand – Colour change is unsystematic and unrelated to difference in grain-size – Resembles sediments observed in a small stream at the foot of section 2 – Include tephra and peat layers at certain levels	Fluvial fines – Deposited from running water at low flow regime – Laminated components represent loess-deposition without organic material involved; hence the separation from the LPT – Lamination in shear zones is tectonic resulting from high cumulative strain	Maizels, 1993; van der Wateren, 1995a,b
4	Sections 1, 2, 3 – Medium to coarse sand, typically massive but shows horizontal bedding in places	Fluvial sand – Contributing facies of the proglacial sandur reflecting deposition under low and moderate flow regime conditions	Maizels, 1993; Marren, 2005
5	Sections 1, 2, 3, and sandur – Fine to medium-grained, clast supported, and either horizontally laminated or massive gravel – Often interbedded with facies 3 sand – Shows usually fining upwards into a surface sand layer – Clasts are sub-angular to well-rounded and typically 1–5 cm in diameter, although outsized clasts of 10–15 cm occur in the medium-grained parts	Proglacial sandur deposits – Associated with high meltwater discharge – Grain size variations reflect variable flow regimes during the vertical accretion of the sandur	Maizels, 1993; Benn and Evans, 1998; Marren, 2005
6a	Section 1 – 10–40 cm thick, massive, medium-grained, matrix-supported, friable diamict, rich in sub-angular to sub-rounded pebbles and cobbles, which frequently show striations with no preferred orientation	Basal till – Deposited beneath the sole of the surging glacier snout. Consistence, massive appearance and striated clasts indicate active transport in a subglacial environment	Benn and Evans, 1996; Krüger and Kjær, 1999; van der Meer et al., 2003; Evans et al., 2006
6b	Section 2 and hummocky moraine on proximal slope – Massive, medium-grained, matrix-supported and loose diamict, dominated by sub-angular to very angular pebbles and boulders	Supraglacial melt-out till – Deposited from the stagnant snout after the surge	Boulton, 1970, 1972; Paul and Eyles, 1990

Please cite this article in press as: Benediktsson, Í.Ö., et al., The 1890 surge end moraine at Eyjabakkajökull, Iceland: a re-assessment of a classic..., Quaternary Science Reviews (2009), doi:10.1016/j.quascirev.2009.10.004

there is a water-, sediment-, and dead-ice-filled depression indicating the excavation of material during the moraine formation (Fig. 2A).

4.2. Morphological type B

This type of morphology is represented by TP4 which lies across a short segment of the end moraine just east of TP3 (Figs. 1, 2B and 4). Between those two profiles, the morphology and sedimentary composition of the end moraine changes dramatically within a short distance as the terrain rises towards the Eyjafell bedrock knob (Figs. 1 and 2B). TP4 shows a low, 20–50 m wide moraine ridge with a steep frontal slope and a gentle backslope with ice-free hummocky moraine (Fig. 4). The relatively small dimension of this part of the moraine probably owes to an originally thinner sediment cover on the elevated terrain. The moraine consists of LPT sequence with a thin diamict cover on the proximal slope extending up to the crest. The size, morphology and sedimentary composition of this part of the end moraine strongly resemble the end moraines previously described by Benediktsson et al. (2008) from the adjacent Brúarjökull surge-type glacier, thus indicating similar genesis. Two semi-circular depressions at the head of small channels were observed about 50 m in front of this moraine segment, possibly indicating blow-out of overpressurized porewater at the time of the moraine formation (Christiansen et al., 1982; Kjær et al., 2006; Benediktsson et al., 2008).

4.3. Morphological type C

Although the sedimentary composition remains the same, another significant change occurs in the end moraine morphology as the terrain descends off Eyjafell towards the swamp area further east (Figs. 1 and 2C–E). As illustrated by TP5 and TP6, the moraine is $<$12 m high and 250–280 m wide, and composed of multiple narrow and closely spaced asymmetric crests interpreted as imbricate thrust sheets with internal folds (Croot, 1987, 1988a; Fig. 4). The distance between the crests ranges from 3 to 15 m and their amplitude decreases distally before fading into the foreland swamp. The most distal crests are only identified as a change in the vegetation resulting from a slight lift-off from the groundwater table. Numerous abrupt-head channels of various sizes dissect the foreslope of the moraine (Figs. 2D,E). Those are interpreted as structures formed by the blow-out of overpressurized porewater at the end of the surge (Figs. 2C–E, 3C–E and 4; Christiansen et al., 1982; Croot, 1987, 1988a; Kjær et al., 2006; Benediktsson et al., 2008). The channel heads are at places marked by deep, semi-circular depressions originating at the boundary between the crests, probably indicating hydrofracturing along the sole of thrust sheets (Croot, 1987, 1988a; Figs. 2C–E and 3C–E). Open pipes extending upglacier with a diameter of *c.* 10–20 cm were observed in a few of these depressions, indicating running water in subsurface tunnels (Kjær et al., 2006; van der Meer et al., 2009; Fig. 3E).

4.4. Morphological type D

East of the Jökulsá river (Figs. 1, 2F and 4), the moraine consists of LPT overlain by glaciofluvial gravel and thus, the sedimentary composition is different from the central part (TPs 4–6) but resembles the western part of the moraine (TPs 1–3). TP7 and TP8 represent a 300–400 m wide ridge of multiple, regularly spaced symmetric crests with a wavelength of 25–35 m and decreasing amplitude towards the foreland (Figs. 2F, 3F and 4). This morphological type has strong analogies to surge moraines in Svalbard (Croot, 1988b; Hart and Roberts, 1997; Boulton et al., 1999) and Pleistocene moraines in the Netherlands (Bakker and van der Meer, 2003). The river Jökulsá occupies a depression upglacier of the moraine at TP7 and has caused significant erosion of the proximal slope. Likewise, an inactive sandur just proximal to TP8 implies post-tectonic glaciofluvial erosion of the backslope.

5. The sedimentary composition and architecture of the 1890 end moraine

The internal sedimentary composition and architecture of the 1890 end moraine was documented from three cross-sections and three ground penetrating radar (GPR) profiles. Sections 1 and 2 signify the architectural style of the western part of the end moraine complex, while the eastern part is represented by section 3 and GPR profiles 1–3 (Figs. 1 and 2). Six major sediment facies were identified: (1) sequence of loess, peat and tephra; (2) tephra; (3) fluvial fines; (4) fluvial sand; (5) proglacial sandur deposits; and (6) basal till and supraglacial melt-out till. Those are described and interpreted in Table 1.

5.1. Section 1

Section 1 is located at the westernmost tip of the end moraine, approximately at the convergence of two former surge lobes (Figs. 1 and 2A). At section 1, the moraine is $\sim$12 m high and 60 m wide. Both the proximal and distal slopes have been significantly modified by post-tectonic fluvial erosion by the formerly active western branch of the river Jökulsá. The section is 20 m wide and exposes the moraine from about 5 m above the sandur up to the top. The section cuts the moraine at an angle from 0 to 9 m, but is orientated perpendicular to the moraine ridge from 9 to 20 m (Fig. 5).

5.1.1. Architecture of section 1

The lower part of section 1 shows gravel that is unconformably overlain by deformed LPT. This is marked by a set of high strain thrust planes along which the cumulative displacement is probably several metres, as judged by the offset of black tephra layers around 12 and 18 m (Figs. 5 and 6B,C). The LPT above the gravel shows both brittle and ductile deformation as exemplified by a tight chevron fold with sheared limbs in the proximal part (*c.* 3–7 m). The distal limb of the fold develops into a zone of asymmetric box folds, some of which are overturned (Figs. 5 and 6A). In the upper part of the LPT, thrust planes denote brittle deformation of both the LPT and the overlying gravel. The moraine ridge is capped by a 40 cm thick diamict that is interpreted as basal till (Fig. 5B).

5.1.2. Structural evolution of section 1

The general stratigraphy in the area consists of LPT overlain by gravels and sands (Fig. 7E). The architecture of section 1 suggests a major thrust zone where stacking of the sedimentary sequence has occurred, as indicated by the appearance of the gravel both below and above the LPT. The till on the top of the moraine ridge indicates that the thrusting and stacking occurred under the glacier snout. Thus, section 1 represents the proximal part of the end moraine with a significant amount of horizontal shortening.

Analyses of eigenvectors of shear planes, fold limbs and fold axes indicate a glaciotectonic stress application from the south (Fig. 5A). This corresponds to the east-west trend of the moraine ridge and, although the general ice flow direction of Eyjabakkajökull is to the north-east, implies localized ice flow to the north owing to lateral spreading of the ice lobe.

Please cite this article in press as: Benediktsson, Í.Ö., et al., The 1890 surge end moraine at Eyjabakkajökull, Iceland: a re-assessment of a classic..., Quaternary Science Reviews (2009), doi:10.1016/j.quascirev.2009.10.004

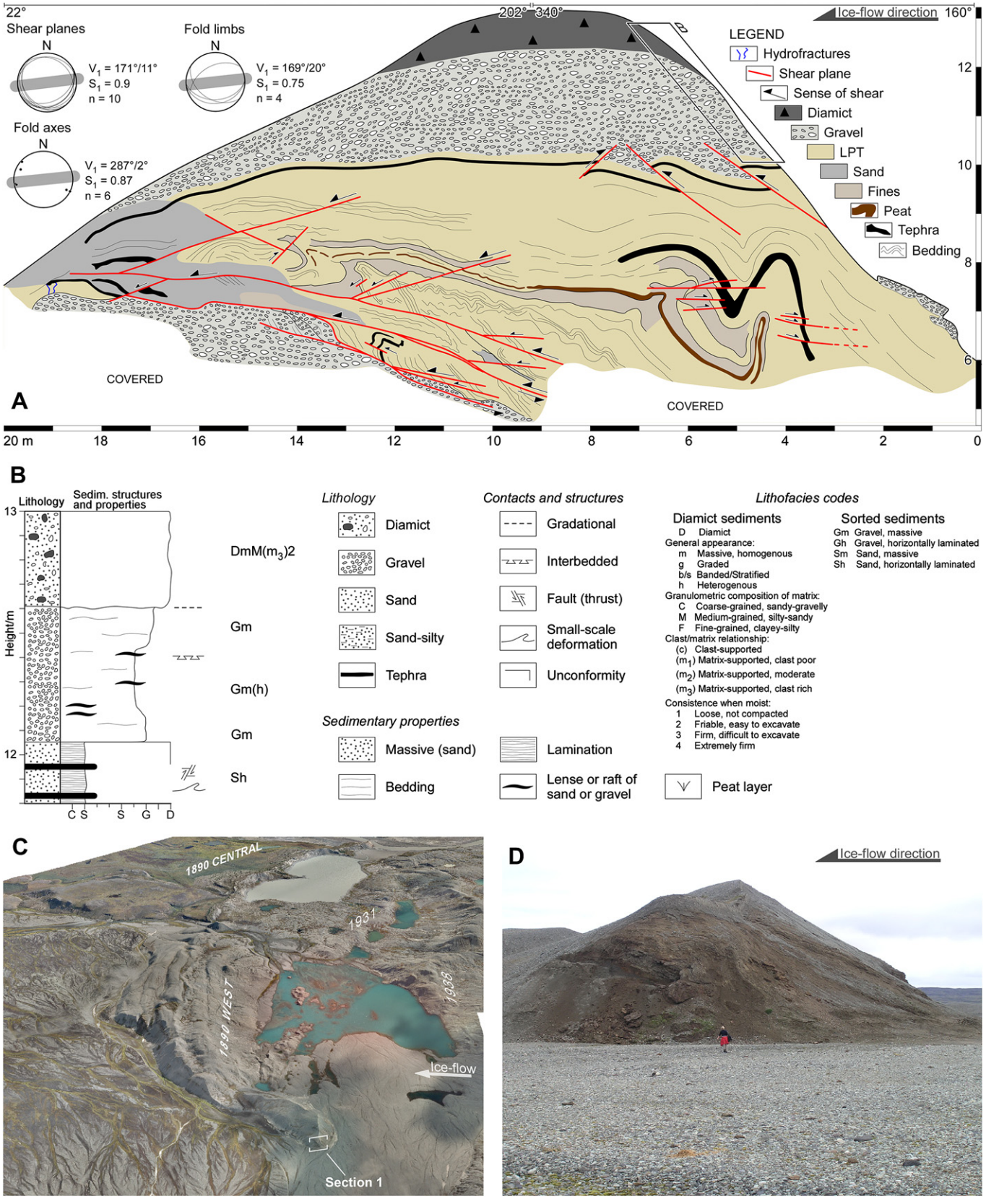

Fig. 5. Section 1. (A) Diagram of the section including structural data. Gray bars on the stereonets indicate the orientation of the moraine ridge. (B) Stratigraphical log from the top of the section with symbols and lithofacies codes according to Krüger and Kjær (1999). The location of the log is indicated in A. (C) Overview of the western part of the 1890 end moraine with the location of section 1. The terminal position of the 1890 ice margin can be identified on the top of the moraine ridge. (D) Photograph of the section.

Please cite this article in press as: Benediktsson, Í.Ö., et al., The 1890 surge end moraine at Eyjabakkajökull, Iceland: a re-assessment of a classic..., Quaternary Science Reviews (2009), doi:10.1016/j.quascirev.2009.10.004

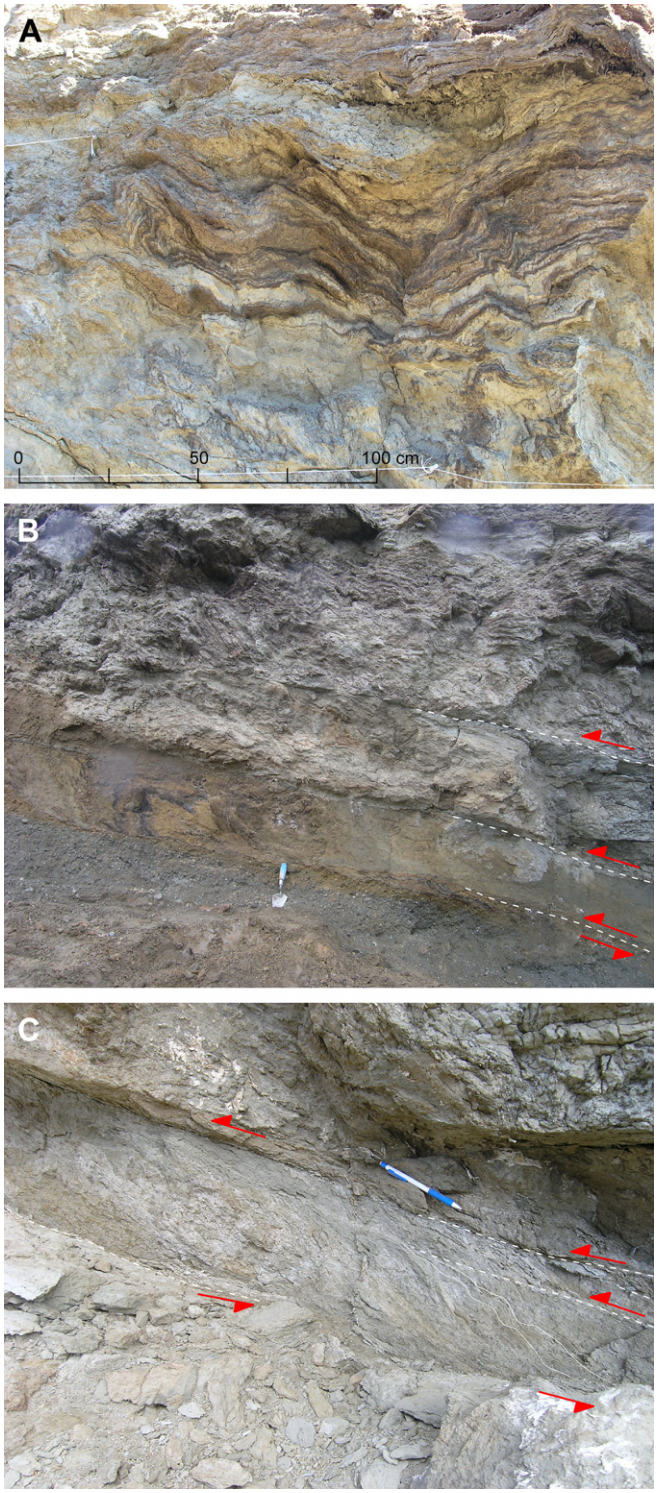

Fig. 6. Sediments and tectonic structures in section 1. Tectonic stress from right to left. (A) Minor folds in laminated LPT in the upper centre. (B) Series of thrusts in LPT at the base. The lowermost thrust occurs at the gravel/LPT interface. (C) Close-up of a high strain shear zone at the base of the section. Note the sigmoidal foliation between the thrusts determining the relative sense of movement.

5.2. Section 2

Section 2 is situated in a gully just west of the Eyjafell bedrock knob (Figs. 1 and 2A). The gully probably was a meltwater outlet during the maximum of the 1890 surge but is now occupied by a small stream that drains a dead-ice lake immediately proximal to the moraine (Fig. 7). Here, the moraine is multi-crested, approximately 280 m wide and 25 m high. Section 2 covers the distal most 116 m and is orientated perpendicular to the moraine ridge (Figs. 7 and 8A).

5.2.1. Architecture of section 2

All six sediment facies were identified in section 2 (Table 1). Black tephras that are traceable throughout the section served as marker horizons during the mapping of the facies architecture. The architecture reveals both ductile and brittle deformation but is characterized by large-scale folding with intensive shearing in high strain areas. The section is divided in two structural zones, i.e. (i) the central crest zone at 0–65 m; and (ii) the distal crest zone at 65–112 m (Fig. 7).

5.2.1.1. The central crest zone, 0–65 m. This part of the section reveals the lowest strain and thus reflects the general stratigraphy in the area before the time of moraine formation (Figs. 7A,E). The backslope of the central crest is draped by a veneer of diamict indicating the position of the ice front when the moraine was being formed. The architecture of the central crest zone is dominated by an open anticline, as outlined by the tephra markers and sand layers in the overlying gravel (Fig. 7A). Minor deformation structures, such as a small recumbent fold on the distal part of the hinge zone (at *c.* 38 m), are observed on the limbs of the anticline. The distal limb is overturned and frequently broken by a number of thrust planes, along which the displacement varies from several centimetres up to two metres (Fig. 7B). Despite the different lithology and shear strength between the gravel and the underlying fines, the two facies were folded and thrusted together.

5.2.1.2. The distal crest zone, 65–112 m. The distal crest zone signifies much higher strain than the central crest zone with a large overturned anticline proximal to an overthrusted anticline in the distal part, and a narrow syncline separating the two (Fig. 7). The high strain is moreover emphasized by a number of small and large shears and sigmoidal structures in the lower limb of the proximal anticline (Figs. 7C and 8E).

The overturned anticline at 66–83 m (Fig. 7C), contains continuous tephra markers from the proximal (upper) limb and throughout the hinge zone. Some backthrusting occurs in the proximal limb which otherwise has been subjected to relatively low strain. Tectonic foliation in the fines appears towards the hinge of the anticline, indicating increased strain. The highest strain is, however, observed in the distal (lower) limb of the anticline where a number of small, *en echelon*-orientated thrust planes were observed, with a displacement ranging from a few cm to ~2 m (Fig. 7C). In places these thrust planes have developed sigma structures (Fig. 8E). Although the tephra markers are not visible in the lower part of the section, the facies 4 sand shows that the distal (lower) limb of the overturned anticline continues as the proximal limb of a narrow syncline. This is also indicated by bedding in the stratigraphically underlying gravel, which dominates the syncline (Fig. 7C). Although the tephra markers are not visible in the syncline hinge, the sand in the core illustrates the geometry of the syncline and indicates that the hinge zone is buried at shallow depth.

The most distal crest of section 2 (*c.* 85–112 m) is formed by an open anticline with an overthrusted distal limb. There is an inconsistency in the strain between the upper and lower tephra markers of the proximal limb. The upper tephra markers indicate relatively low strain in the proximal limb with occasional small fore- and backthrusts, while the lower tephra markers seem to have

Please cite this article in press as: Benediktsson, Í.Ö., et al., The 1890 surge end moraine at Eyjabakkajökull, Iceland: a re-assessment of a classic..., Quaternary Science Reviews (2009), doi:10.1016/j.quascirev.2009.10.004

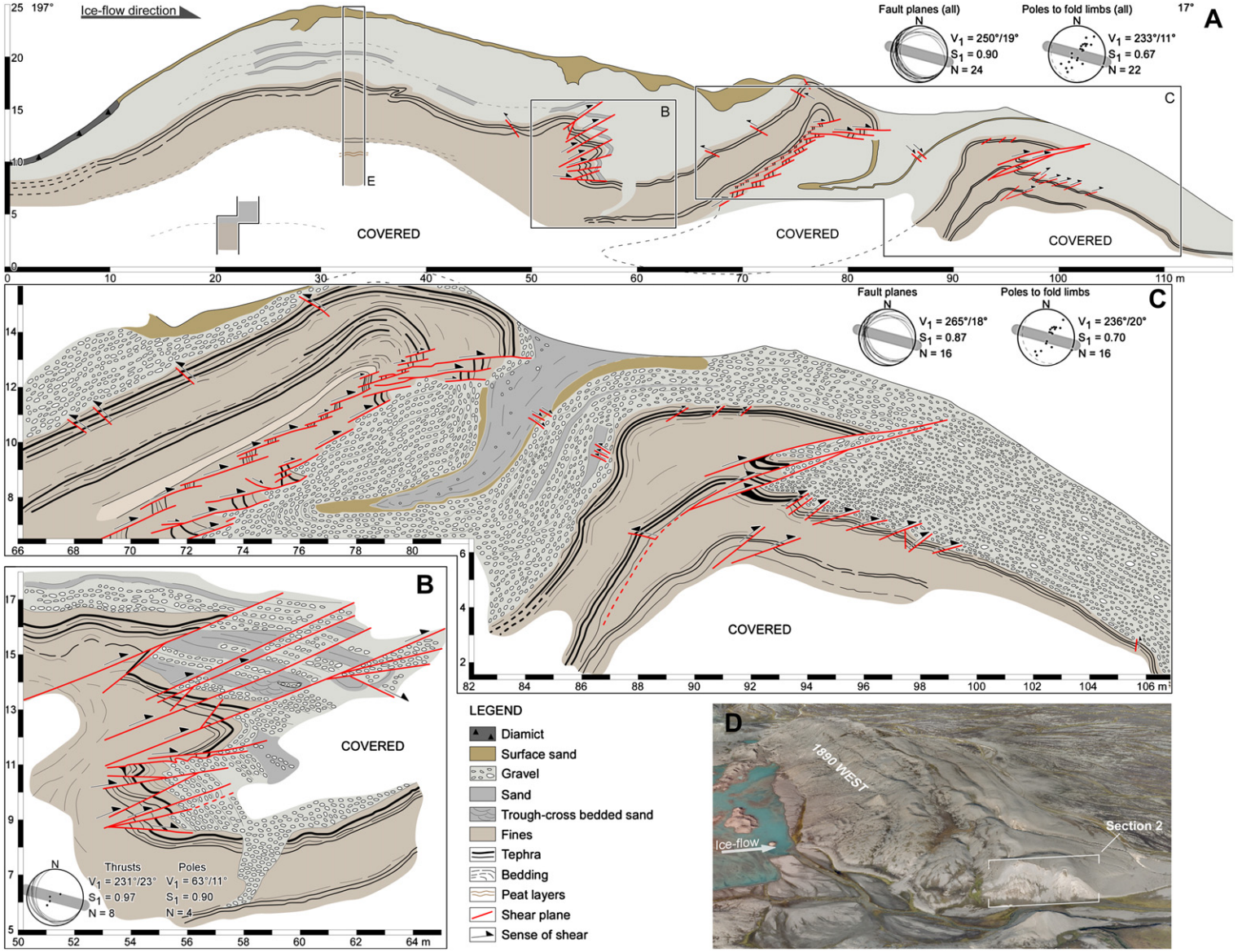

Fig. 7. Section 2. (A) Diagram of the section with structural data. Gray bars on the stereonets indicate the orientation of the moraine ridge. (B) Detailed diagram and structural data of the overturned distal limb of the anticline at 55–65 m in the central crest zone. (C) Detailed diagram of the distal crest zone with structural data. (D) Overview of the western part of the 1890 end moraine with the location of section 2 indicated. Note the sharp boundary between the submarginal and proglacial parts of the moraine ridge. (E) Stratigraphical log of the central crest zone. The location of the log is indicated in A. Legend is provided in Fig. 5B.

Please cite this article in press as: Benediktsson, Í.Ö., et al., The 1890 surge end moraine at Eyjabakkajökull, Iceland: a re-assessment of a classic..., Quaternary Science Reviews (2009), doi:10.1016/j.quascirev.2009.10.004

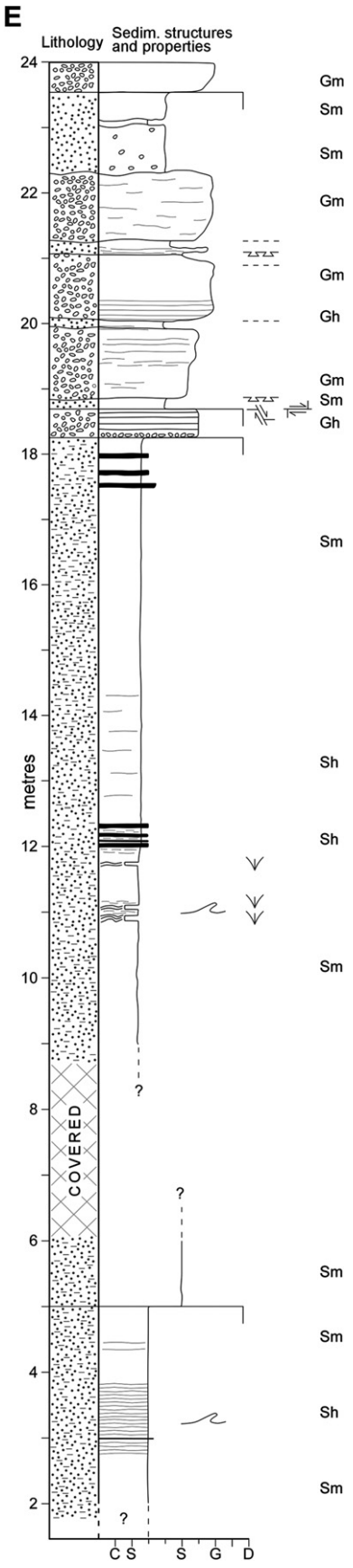

Fig. 7. (*continued*).

been displaced by several metres along an unidentifiable overthrust. A series of large thrusts occurs with up to ~4 m displacement. Below these thrusts, drag folds appear with significant thickening of tephra, box folding and tectonic foliation (Figs. 7C and 8D). Moreover, numerous thrusts were observed on the distal limb of the anticline, however, with a much smaller displacement and lower strain than the thrusts above.

5.2.2. Balancing and structural evolution of section 2

By applying line and area balancing to section 2, the total shortening and depth to décollement have been calculated (Fig. 9A). The line balancing gives the difference (ΔL) between the length of the marker bed in the undeformed (L_u) and deformed (L_d) states, so that

$$\Delta L = L_d - L_u$$

where L_u is measured by tracing the marker between the proximal and distal ends of the section, and (L_d) is the horizontal (shortening) distance occupied by the deformed markers. Note that to measure the length of the tephra markers in section 2, the hinge of a syncline between 60 and 90 m had to be inferred. The total shortening (s) can be described as:

$$s = \frac{L_d - L_u}{L_u}$$

The area balancing assumes that the area of the body subjected to stress remained constant before (A_u) and after (A_d) the deformation, meaning that $A_d = A_u$, and that a décollement plane demarcates the lower boundary of the displaced sequence. For simplification, internal displacement through simple shear deformation along minor shear planes is not accounted for in the calculations as it is difficult to identify all minor shear planes and quantify the displacement along them. Thus, a slight uncertainty remains in the calculations and the numbers obtained from the calculations on total shortening can be regarded as minimum numbers, while numbers on the décollement depth denote maximum depth. However, because folding is the principal style of deformation in the balanced sections, the calculations give a good estimate of the total shortening and the depth to the décollement surface.

By calculating the total area (A) of the deformed section, the depth to the décollement surface (h) has been estimated by:

$$h = \frac{A}{\Delta L}$$

The total shortening of the uppermost tephra marker within section 2 is 39% and the depth to the décollement is 26.7 m, which most likely coincides with the bedrock surface, as indicated by its presence at or close to the surface just 70 m east of the section (Fig. 1).

As section 2 only covers the distal half of the moraine ridge, an uncertainty remains about the shortening within the proximal half. By measuring the area of a potential cross-section extending between the proximal and distal extremities of the moraine ridge, and by using the depth to the décollement as calculated from section 2, the total shortening (ΔL) within the entire moraine ridge was calculated from

$$\Delta L = \frac{A}{h}$$

Then the length of the tephra markers within the moraine ridge were derived by

$$L_u = L_d - \Delta L,$$

Please cite this article in press as: Benediktsson, Í.Ö., et al., The 1890 surge end moraine at Eyjabakkajökull, Iceland: a re-assessment of a classic..., Quaternary Science Reviews (2009), doi:10.1016/j.quascirev.2009.10.004

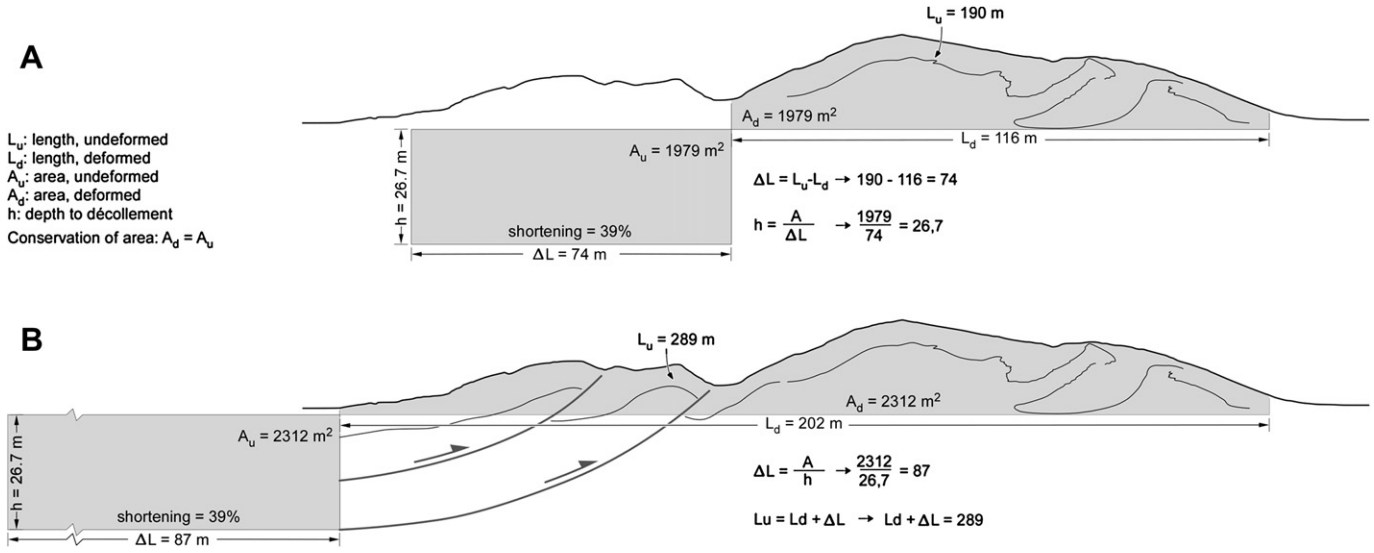

Fig. 9. Cross-section balancing of the western part of the 1890 end moraine. (A) Balancing of section 2. (B) The proximal part of the ridge is balanced on the basis of the décollement depth derived from balancing of section 2. Glaciotectonic structures are inferred with reference to section 1 and the morphology of the proximal slope.

providing a basis for inferring the glaciotectonics within the proximal half of the moraine ridge.

The high strain in the distal crests compared to the central crest shows that most of the shortening within section 2 took place in the distal part. Nevertheless, this need not be the area of maximum strain and shortening within the moraine ridge as its proximal part is not exposed in the section. Given that the depth to the décollement (26.7 m) and the amount of shortening (39%) remained constant across the moraine ridge, the length of the deformed tephra markers in the proximal part (not exposed in section 2) can be calculated and subsequently used to infer the glaciotectonics (Fig. 9B). Based on the morphology of the moraine ridge, the architecture of section 1 implying thrusting, and the structural style of section 2, we assume that the structural style within the proximal part of the moraine was dominated by two anticlinal folds with listric thrusts cutting through the hinges (Fig. 9B).

It seems that large-scale folding and thrusting were the primary and secondary styles of deformation, respectively, meaning that when folding could not compensate for the shortening anymore, thrusting took over in the distal limbs of the anticlines (Fig. 10). It is most probable that the central crest formed immediately in front of the ice before submarginal sediments began to be thrust up on the proximal part of the moraine. The construction of the central crest probably preceded the formation of the distal crests with open anticlinal folding of the fines and gravel. However, the next anticline in front had probably begun to form before the first anticline had been fully developed. For example, the frequent thrusting in the overturned distal limb of the anticline in the central crest zone suggests an obstruction in front that prevented its forward movement. This obstruction also provided a support for the loose gravel when it turned over with the underlying fines, as the gravel would otherwise have collapsed

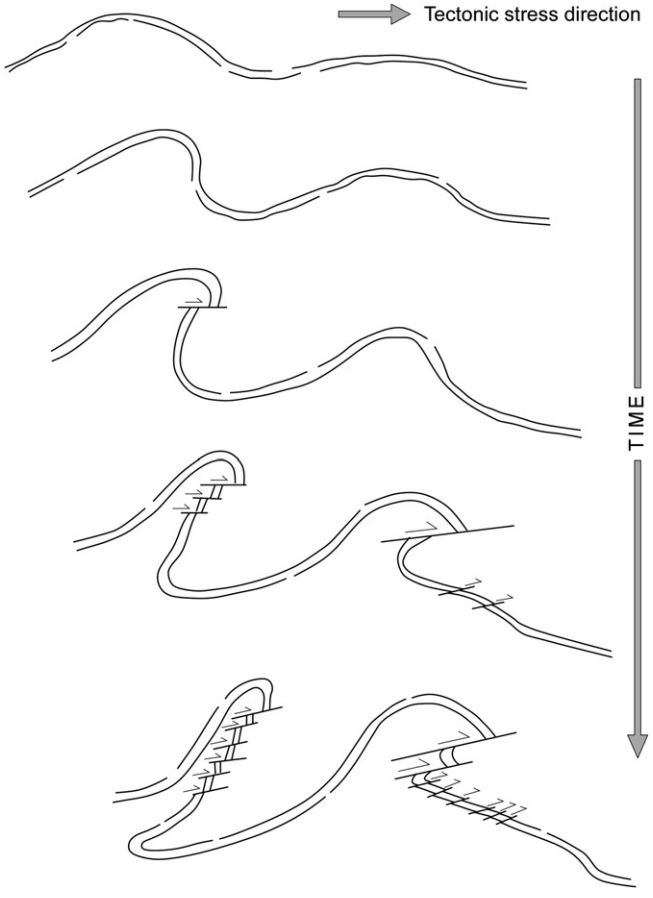

Fig. 10. Simple model of the evolution of the overturned and sheared anticlines in the distal crest zone of section 2.

Fig. 8. Sediments and tectonic structures in section 2. Tectonic stress from left to right. (A) Photograph of the section. Pile of rucksacks in the foreground for scale. Mt. Snæfell (1833 m a.s.l.) in the background. (B) Facies 3 fines in the central crest zone. Note the light brown and blue silty fine-sand interbedded with layers of peat and tephra. A 60 cm long scraper for scale. (C) Overview of the two anticlines in the distal crest zone. Person for scale. (D) Tectonically foliated tephra in the overthrusted fold in the distal crest zone. (E) σ-type rotation structure of competent gravel within ductile plasma of fines, indicating clockwise shear vergence in the lower (distal) limb of the overturned anticline in the distal crest zone. (F) The overturned distal limb of the anticline in the central crest zone. Note the thrusts and the black tephra markers. A 1 m long ruler for scale. Dashed line indicates the axial plane of the fold. (G) Normal and thrust faults in the distal limb of the overthrusted anticline in the distal crest zone. Trowel for scale.

Please cite this article in press as: Benediktsson, Í.Ö., et al., The 1890 surge end moraine at Eyjabakkajökull, Iceland: a re-assessment of a classic..., Quaternary Science Reviews (2009), doi:10.1016/j.quascirev.2009.10.004

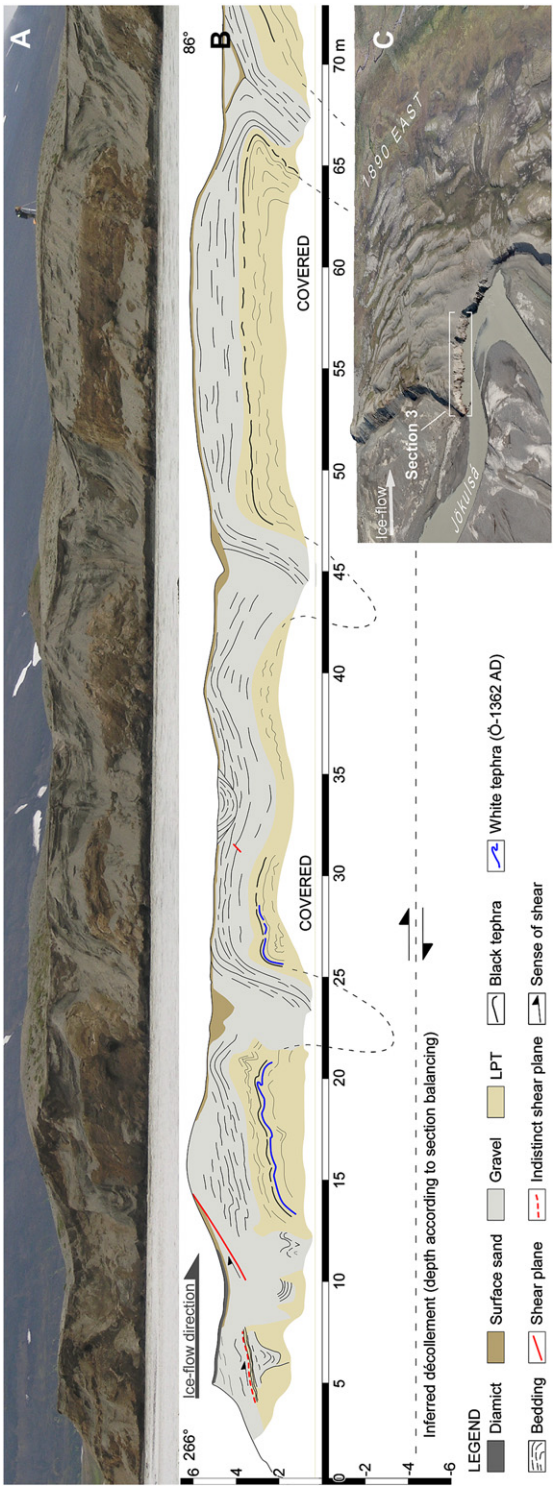

Fig. 11. Section 3. (A) Photograph of the section. Person for scale to the right. (B) Diagram of the section with inferred synclines and décollement. (C) Overview of the section and its surroundings.

and lost its original sedimentary properties (Figs. 7A,B). If deformation had continued, thrusting in the distal limb of the central crest probably would have developed in the same manner as in the next anticline in front (Figs. 7A,C).

The structural data are consistent throughout the section and correspond to stress from the south west. Fault planes primarily incline upglacier (thrusts) although occasional downglacier inclining faults (normal) are observed (Fig. 7A). Fold limbs incline both towards the hinterland and the foreland, indicating the proximal and distal limbs of the three anticlines. When the structural data of the two sub-sections are separated, stronger consistency appears (Figs. 7B,C). Faults dipping upglacier are exclusively thrust faults while downglacier dipping faults represent both backthrusts and low-angle normal faults. Reconstructed fold limbs correspond to a direct measurement of the fold axis of the overturned anticline in the distal crest zone, as it appears on the surface of the moraine above the section (Figs. 7C and 8A).

5.3. Section 3

Section 3 is a 73 m long and 6 m high river-cut section developed by erosion and undercutting of the eastern bank of river Jökulsá (Figs. 1 and 11A,B). The section covers the most proximal part of the multi-crested moraine (Fig. 11C) and the proximal ~60 m of GPR profile 1 (Fig. 12); hence, it serves as a basis for the interpretation of the stratigraphy and architecture of GPR profiles 1–3 (Figs. 12–14).

5.3.1. Architecture of section 3

All sediment facies, except facies 3 fines, were observed in section 3 (Table 1). A veneer of diamict was observed on the surface between 5 and 12 m, indicating that the glacier snout overrode the backslope of the moraine (Fig. 11).

The glaciotectonics in section 3 reflect the characteristic multi-crested morphology of the end moraine east of Jökulsá (Figs. 1 and 2F). Tephra layers in the LPT and bedding in the gravel outline the section architecture, which is dominated by wide open anticlines with narrow synclines in between (Fig. 11). The hinge zones of the synclines are located beneath the river level and are thus not visible in the section. However, the narrow appearance of the synclines indicates that their hinges are buried at shallow depths. The anticlines comprise a simple architecture with little internal deformation although occasional multiple asymmetric chevron and box folding is found on the limbs of the anticlines, as evident in the LPT at 11–28 m (Fig. 11). Around 65 m, the distal limb of the most distal anticline is overturned, and notably, the gravel follows the LPT through the overturning, indicating that the LPT is the controlling facies in the deformation. The geometry and architecture of the anticline–syncline pairs is consistent throughout the section, suggesting a simple structural style of the end moraine reflected by the morphology with three distinct ridges on the surface (Fig. 11).

5.4. GPR profiles 1–3

GPR profiles 1–3 were surveyed across the multi-crested end moraine east of Jökulsá (Fig. 2F). They show remarkable similarity in reflection pattern and architecture and are thus described together below. Correlation between reflectors allowed estimation of the total shortening within the moraine. To test the quality of the balancing of the GPR profiles, the shortening derived from the reflectors was compared to the shortening of the surface, which should give the minimum possible shortening within the end moraine. The proximal part of GPR profile 1 runs directly across

Please cite this article in press as: Benediktsson, Í.Ö., et al., The 1890 surge end moraine at Eyjabakkajökull, Iceland: a re-assessment of a classic..., Quaternary Science Reviews (2009), doi:10.1016/j.quascirev.2009.10.004

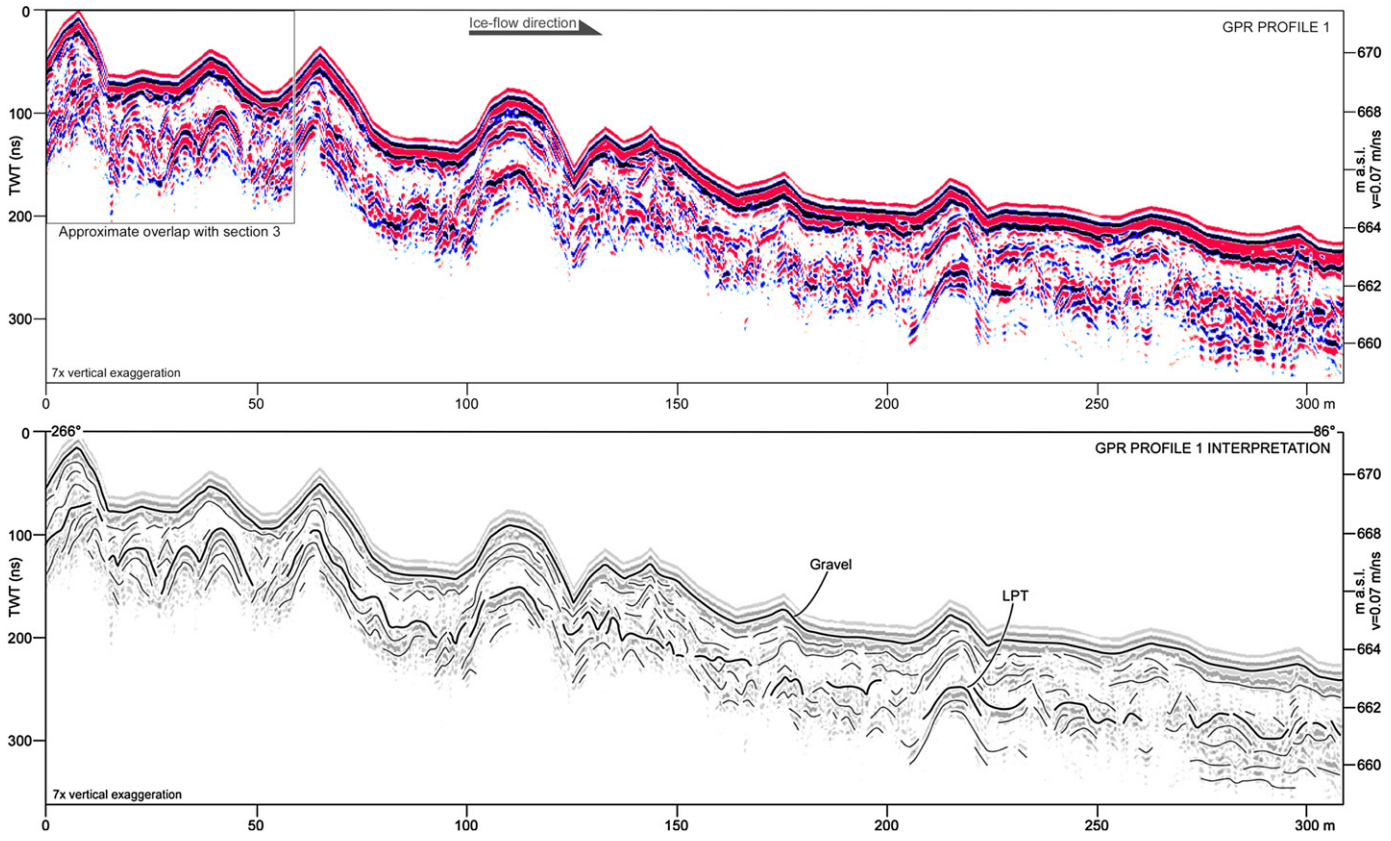

Fig. 12. GPR profile 1 (100 MHz) and structural interpretation. Note how well the architecture of the end moraine is reflected by its surface morphology although small anticline–syncline pairs are buried, e.g. at *c*. 20–50 m. See Fig. 2 for location of the profile.

section 3, which, therefore, provides the basis for interpretation of the stratigraphy and architecture of the GPR profiles. The profiles are 255–410 m long, extending from the backslope of the moraine beyond its distal extremity (Figs. 2F and 12–14).

The reflection pattern of GPR profiles 1–3 indicates stratigraphy similar to that of section 3, i.e. with LPT at the base and glaciofluvial gravel on top (Table 1). The homogeneity of the gravel body results in very weak or no reflection appearing as a void in the upper half of the profiles. However, occasional strong reflectors are detected in this area, probably indicating interbedded layers or lenses of facies 4 sand (Figs. 12–14). Usually at 2–3 m depth, strong reflectors indicate the transition from the gravel to the LPT below. Due to interbedded tephra layers, the LPT has a strong reflection pattern in the profiles with up to 50 m long reflector segments (Figs. 12–14). Thus, the LPT outlines the glaciotectonics, which are dominated by upright anticline–syncline pairs with decreasing amplitude in distal direction. The hinges of the anticlines are typically well reflected while their limbs together with the synclines hinges are less distinct. The anticlines usually correspond with the ridges on the surface while tight synclines correspond with the troughs (Figs. 12–14).

Although no single horizon can be followed through the entire profiles, the widespread continuity of the LPT reflectors allows correlation of one reflector with another and thereby tracing of the LPT bedding through the profiles. The tracing allows calculation of the total shortening within the LPT, which appears to be 27–33%, indicating the true shortening within the end moraine. Although this number includes uncertainties rising from discontinuity of the LPT reflectors, it seems reasonable when compared to a 16–24% total shortening of the surface, which indicates the minimum possible shortening within the moraine. The discrepancy between the calculated surface and LPT shortening owes to occasional overturned anticlines and small-scale anticline–syncline pairs that are buried.

5.5. Structural evolution of section 3 and GPR profiles 1–3

Section 3 and GPR profiles 1–3 represent the architecture of the end moraine in the eastern part of the forefield where the moraine morphology is characterized by multiple crests that successively decrease from the proximal side towards the foreland. The similarity between the GPR profiles allows for common interpretation based on the architecture of section 3 which overlaps with the proximal part of GPR profile 1.

Line and area balancing of section 3 suggests that the horizontal shortening within the moraine is 32% and the depth to the décollement is 4–5 m, which probably coincides with the base of the LPT or some weak layer within it. The LPT at the base is the controlling facies in the deformation as the overlying gravel completely follows the large-scale structure of the LPT. Only small-scale deformation structures within the LPT, such as chevron and box folds, are not visible in the gravel. Brittle deformation solely occurs in the proximal extremity where a till cover was also observed on the surface. This indicates that the maximum strain occurred through thrusting in the proximal slope beneath the glacier snout. The formation of the end moraine was initiated by an open anticlinal folding of the foreland immediately in front of the ice. As the surge advance progressed, the proximal limb of the initial anticline was overthrusted beneath the ice front, sometimes forming a fault-propagation fold, while multiple anticline–syncline pairs formed sequentially in front of the ice from proximal to distal direction.

Please cite this article in press as: Benediktsson, Í.Ö., et al., The 1890 surge end moraine at Eyjabakkajökull, Iceland: a re-assessment of a classic..., Quaternary Science Reviews (2009), doi:10.1016/j.quascirev.2009.10.004

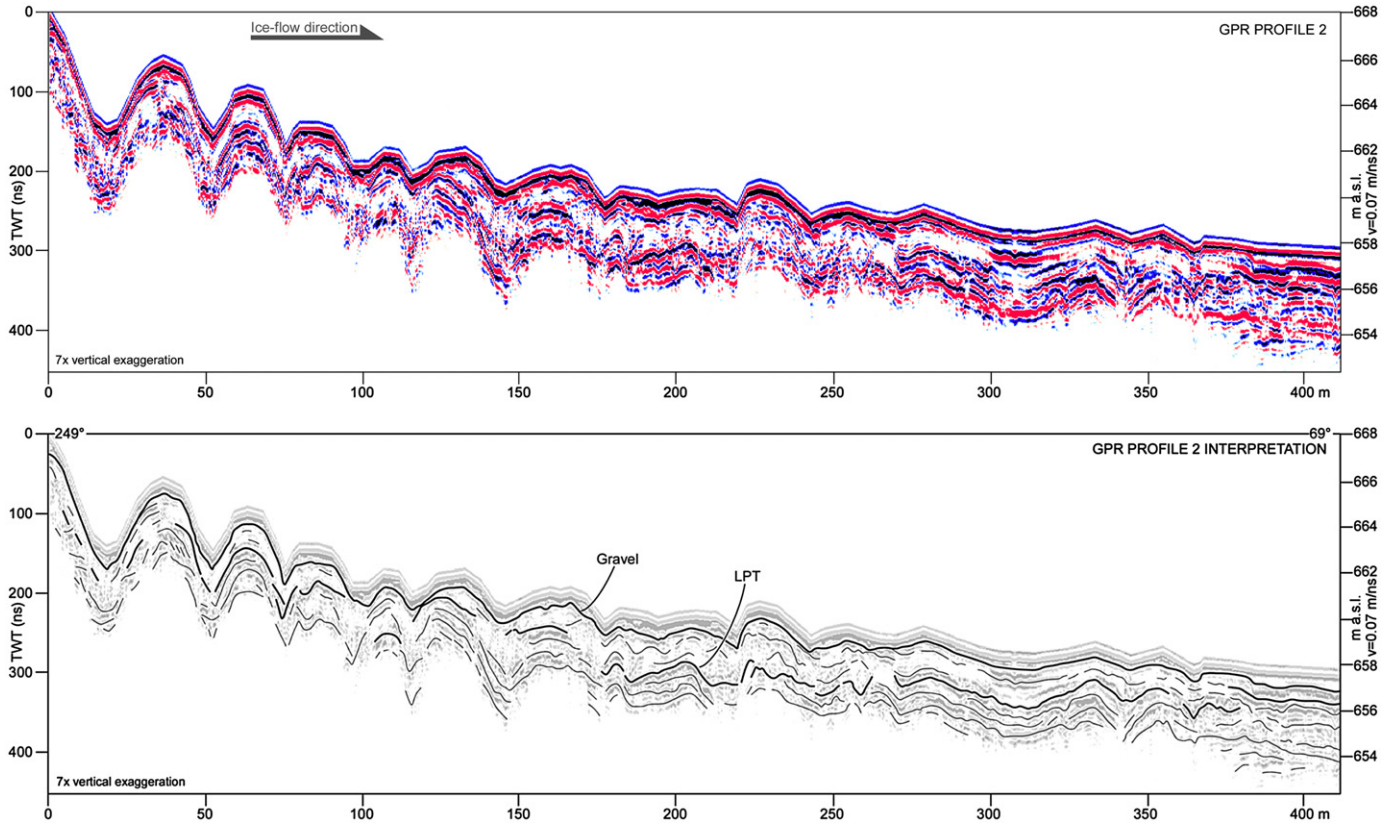

Fig. 13. GPR profile 2 (100 MHz) and structural interpretation. Note the remarkable harmony between the surface morphology and the underlying glaciotectonics, as emphasized by the small difference between the amount of shortening of the surface (24%) and the LPT (29%). The general strengthening of the reflection pattern at around 275 m is interpreted to result from the thinning of the gravel, making the majority of the reflectors originate from the underlying LPT. Possibly, groundwater at shallow depth favours the reflection in the distal part. Between 300 and 325 m, a layer of fine-grained sediments that were deposited in a shallow pond in the syncline trough absorbs almost all the GPR signal in the upper part forming a shadow of very weak or no reflection beneath. See Fig. 2 for location of the profile.

However, the formation of one crest needed not be completed before the next one in front began to form.

6. Evolution of the 1890 end moraine

The morphology and architecture of the 1890 end moraine varies considerably along its length. The variations primarily result from specific conditions in the forefield, out of which the composition and thickness of the sediment sequence seem to be most important. The largest segments of the end moraine have developed where thick sequences of LPT, sand and gravel have been deformed both under the snout of the ice and in front of it. In contrast, the moraine is smaller where it occurs on the swamp area and consists almost solely of LPT. The smallest segments of the moraine ridge, however, are found on the Eyjafell bedrock knob where the sediment cover is thin. These three morphological and structural types of moraine ridges require three different models to explain their formation. Firstly, the model by Benediktsson et al. (2008) from Brúarjökull is modified to explain the formation of the narrow ridge segment on the Eyjafell bedrock knob. Secondly, a slight modification of the model by Croot (1987, 1988a) illustrates the formation of multi-crested thrust-dominated ridges in the central part. Thirdly, a new model is erected for the fold-dominated western and eastern parts of the moraine.

6.1. Model 1 – narrow, single-crested ridge

Benediktsson et al. (2008) demonstrated that the 40–80 m wide and 5–20 m high 1890 surge end moraines of Brúarjökull were a morphological expression of a ~500 m long marginal sediment wedge. The wedge resulted from sediment/bedrock decoupling and associated downglacier sediment transport and compression. The sediment/bedrock decoupling was facilitated by overpressurized subglacial porewater that blew-out at the very end of the surge, as evident by circular blow-out depressions at the abrupt-head of channels in front of the end moraine (Kjær et al., 2006). The narrow, single-crested ridge in the central part of the 1890 Eyjabakkajökull end moraine complex has a strong resemblance to the Brúarjökull moraines; for example bedrock at a shallow depth (<10 m), a similar geometry (~40 m wide and ~5 m high), sedimentary composition (LPT), and morphological characteristics such as a gentle hummocky backslope and steep foreslope, and blow-out depressions a few tens of metres in front of the moraine. Although we neither have data on a submarginal sediment wedge nor the internal architecture of the moraine ridge, its strong geometrical, sedimentological and morphological resemblance to the Brúarjökull moraines suggests a similar genesis. At this particular locality in the Eyjabakkajökull forefield, the Eyjafell bedrock knob sticks up in the landscape (Fig. 1) capped by a thin cover of fine-grained sediments and till. Following Benediktsson et al. (2008), we suggest that fine-grained subglacial sediment was coupled to the ice but decoupled from the bedrock beneath due to overpressurized porewater. The friction between the ice and the bed caused ductile deformation of the sediment while it was displaced downglacier due to the decoupling at the bedrock. This mode of deformation and downglacier transport of subglacial sediment resulted in a gradual thickening of sediment towards the end moraine crest. When the glacier was close to its terminal position, the

Please cite this article in press as: Benediktsson, Í.Ö., et al., The 1890 surge end moraine at Eyjabakkajökull, Iceland: a re-assessment of a classic..., Quaternary Science Reviews (2009), doi:10.1016/j.quascirev.2009.10.004

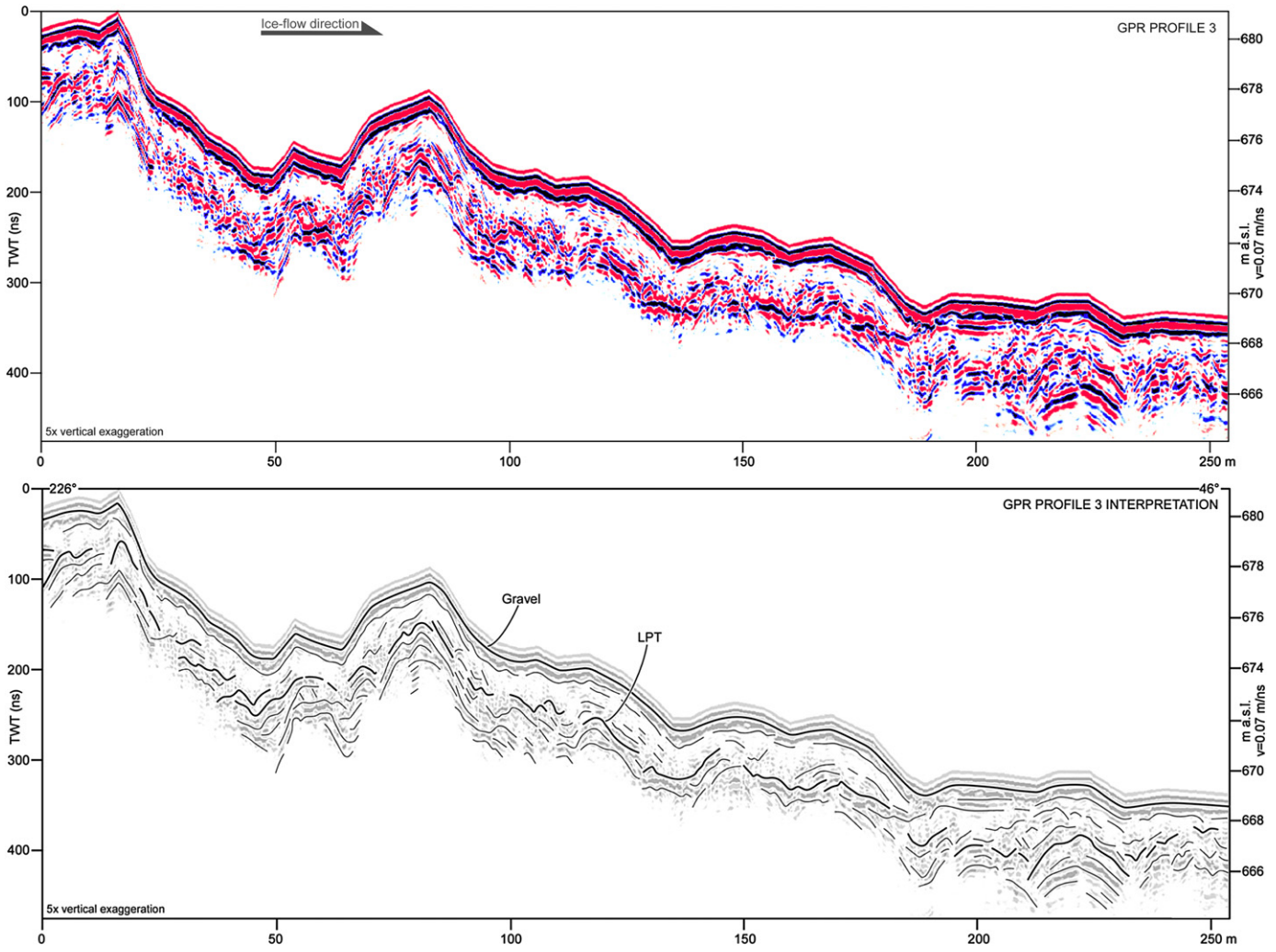

Fig. 14. GPR profile 3 (100 MHz) and structural interpretation. Note the two relatively narrow anticlines associated with the two largest crests at *c.* 0–25 and 65–90 m, and a small crest in between formed by the hinge of a box fold. The most distal anticline occurs beneath a relatively thin layer of gravel; hence, the strong reflection of the LPT below. Discrepancy between shortening within the LPT (27%) and the surface (16%) suggests that some important deformation structures detected by the GPR are not reflected by the surface morphology. This applies to a number of small-scale folds rather than thrusts, such as at 25–40 m, 90–130 m and in the most distal ~60 m. See Fig. 2 for location of the profile.

overpressurized porewater blew-out in front of the moraine causing subglacial porewater pressures to drop and brittle deformation to set in as the final phase of the moraine construction (Fig. 15).

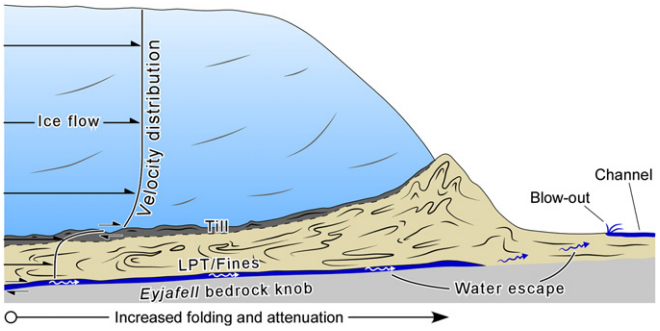

Fig. 15. Model 1. Conceptual model illustrating the formation of a narrow, single-crested moraine ridge and a marginal sediment wedge. The wedge formed in response to downglacier subglacial sediment transport and associated compressive deformation as a result of a decoupling between the sediment and bedrock at shallow depth. When subglacial porewater pressures dropped at the end of the surge, brittle deformation commenced to complete the moraine ridge formation on the distal top of the wedge. Modified after Benediktsson et al. (2008).

Compared to the Brúarjökull moraines, the potential submarginal sediment wedge at Eyjabakkajökull is probably much smaller owing to the upglacier dip of the Eyjafell bedrock knob and thus a shorter distance within which conditions favourable for decoupling at the bedrock and associated downglacier sediment transport may have occurred. Typically, bedrock knobs with thin or no sediment cover tend to obstruct glacier flow due to increased basal friction, often resulting in division of the ice margin into lobes. The moraine ridges around the Eyjafell bedrock knob indicate no such division of the former ice margin (Fig. 1), suggesting that basal friction did not increase when the glacier advanced across Eyjafell. We hypothesize that friction between the ice and the sediment was relatively high, resulting in subglacial deformation, but that decoupling at the sediment/bedrock interface maintained high ice flow velocity, thus inhibiting lobate division of the ice margin.

6.2. Model 2 – a large ridge of multiple, closely spaced asymmetric crests

This model is applicable only for the three distinct lobes in the central part of the 1890 end moraine (Fig. 1). In the present study, morphological data were collected on this part of the moraine but

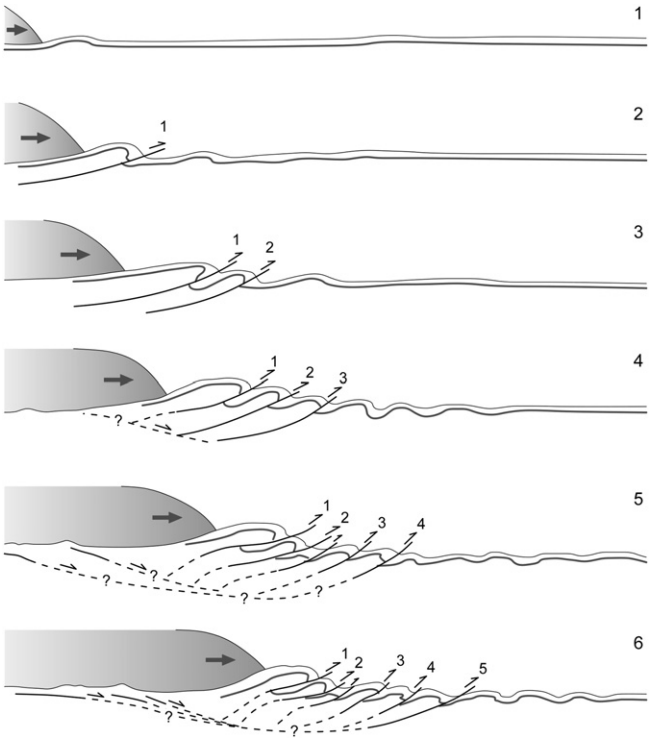

Fig. 16. Model 2. A sequential model showing the formation of a large ridge of multiple, closely spaced asymmetric crests (i.e. the central part of the 1890 end moraine). Each crest represents a thrust sheet within which folds indicate the initial style of deformation. However, minor open anticlines form the small ridges in the very distal part. The glaciotectonic stress was absorbed within a moderately narrow zone (200–300 m) due to short-lived lubrication along thrusts; hence, the moraine is composed of imbricate thrust sheets rather than, e.g. nappes. Modified after Croot (1987).

no data could be obtained on the internal architecture. Therefore, we mainly follow the previous model by Croot (1987, 1988a), however, with our modifications included (Fig. 16).

High porewater pressures generated within the LPT, the uppermost facies of the subglacial succession, lowered its shear strength and facilitated folding as the initial phase of deformation beneath and in front of the snout (Fig. 16, stage 1). Folds were usually rooted on a gravel surface below as a result of high friction at the LPT/gravel interface. As porewater pressures within the LPT became too high, the water blew-out in front of the moraine, probably along hydrofractures, leading to a drop in the LPT porewater pressure. This is suggested by a number of blow-out structures and channels on the foreslope of the moraine (Christiansen et al., 1982; Croot, 1987, 1988a; Kjær et al., 2006; Kuriger et al., 2006; Benediktsson et al., 2008; van der Meer et al., 2009; Figs. 2D,E and 3C–E). However, these blow-outs were relatively short-lived events because the water pressure dropped as soon as the water drained from the sediment. Owing to the pressure drop, the sediment stiffened and the glaciotectonic stress could no longer be released through folding only. Thus, thrusting set in and sheets of gravel and LPT became imbricated (Fig. 16, stages 2–3). The forward movement of the thrusts was encouraged by lubrication of the overpressurized porewater along the base of each thrust sheet. Prolonged lubrication of thrust planes often leads to the formation of nappes (e.g. van der Wateren, 1995a, b), but because the hydrofracturing was a sudden event and the lubrication short-lived, the glaciotectonic stress was absorbed within a moderately narrow zone (200–300 m) resulting in a moraine composed of imbricate thrust sheets (Motyka and Echelmeyer, 2003; Kuriger et al., 2006). The order in which the thrust sheets evolved is uncertain, but most likely they evolved in a piggy-back manner, such that younger thrusts developed below the older ones, which consequently were carried forward by the more recent thrusts below (Croot, 1987, 1988a; Fig. 16, stages 3–6). As the movement of each thrust ceased, further movement was initially taken up by folding in front before continued along a new thrust below. The most distal ridges of the moraine were formed by symmetric open folds, some of which may be associated with blind thrusts (Croot, 1987, 1988a; Fig. 16, stage 6).

This mode of moraine formation resembles recently observed, active moraine formation at Taku Glacier, Alaska (Motyka and Echelmeyer, 2003; Kuriger et al., 2006) where fine-grained sediments were deformed within 200–300 from the ice margin during episodic events. Distinct bulges developed through water-lubricated thrusting, indicated by upwelling of water at the toe of the bulges, and folding in their snouts. This supports our conclusion for the formation of the three lobes in the central part of the 1890 Eyjabakkajökull moraine complex.

6.3. Model 3 – a large ridge of multiple, widely spaced and broad symmetric crests

In order to summarize the formation of the western and eastern parts of the end moraine, a new model must be erected on the basis of observational data from morphological surveys, geological sections 1–3 and GPR profiles 1–3 (Fig. 2). The model illustrates the formation and structural evolution of an end moraine continuum, from the time before changes occurred in the glacier-foreland coupling to initiate the moraine formation at the end of the surge, to the last phase in the formation of the moraine ridge.

Although there is little left of the subglacial bed of the 1890 surge due to post-surge glaciofluvial erosion, and thus evidence for the ice flow mechanism is rare, we suggest that deformation of the bed, favoured by high porewater pressure (Boulton and Hindmarsh, 1987; Alley et al., 1989), was the dominating process of ice flow during the surge, rather than, e.g. decoupling at the bed (Björnsson, 1998; Engelhardt and Kamb, 1998) or at the bedrock (Kjær et al., 2006; Fig. 17, stage 1). This is based on the presence of flutes in the area upglacier from the end moraine. Flutes are formed during deformation of the glacier bed (e.g. Benn, 1994; Hart, 1998; van der Meer et al., 2003), and often show a strong clast fabric indicating coupling to the glacier sole (Kjær et al., 2006). Decoupling at the ice/bed interface would, therefore, result in negligible deformation of the bed and poorly or non-fluted till surfaces. Similarly, decoupling at the sediment/bedrock interface would cause substantial transport of subglacial sediment in downglacier direction resulting in the formation of marginal sediment wedges (Benediktsson et al., 2008). This is an unlikely scenario at Eyjabakkajökull as there are no indicators of substantial subglacial sediment transport and marginal sediment wedges. During the course of the surge, the glacier mainly advanced across sandur without deforming the proglacial sediment significantly (Fig. 17, stage 1).

Water pressures fluctuate during surges and usually decrease considerably during surge cessation in association with minor flooding or blow-out of water that was stored behind the surge front, leading to coupling of the glacier to the foreland and deformation of submarginal and proglacial sediments (e.g. Kamb et al., 1985; Raymond et al., 1987; Humphrey and Raymond, 1994; Björnsson, 1998; Fuller and Murrey, 2000; Bennett, 2001; Bennett et al., 2004b; Christoffersen et al., 2005; Nelson et al., 2005; Kjær et al., 2006; Benediktsson et al., 2008, 2009). Balancing of sections 2 and 3, and GPR profiles 1–3, suggests that Eyjabakkajökull coupled to the foreland as it had surged to within 70–190 m of its terminal position. This probably took place due to meltwater discharge

Please cite this article in press as: Benediktsson, Í.Ö., et al., The 1890 surge end moraine at Eyjabakkajökull, Iceland: a re-assessment of a classic..., Quaternary Science Reviews (2009), doi:10.1016/j.quascirev.2009.10.004

events and associated lowering of submarginal porewater pressures at the end of the surge, when the surge front was passing through the ice-marginal zone (Raymond et al., 1987; Humphrey and Raymond, 1994). Assuming that the maximum ice flow velocity of the 1890 surge was similar to the 1972–1973 surge, i.e. ~30 m/day, the coupling to the foreland occurred 2–6 days before surge termination, thus indicating the time frame within which the end moraine complex was formed. However, this time frame might be slightly longer because of a potential ice slow-down towards the surge cessation (Raymond, 1987; Humphrey and Raymond, 1994). As the glacier coupled to the foreland, it pushed the proglacial sediments, which, in response, released the applied stress by detaching from a plane of décollement and deforming into multiple symmetric, low amplitude anticlinal ridges representing one end member of the end moraine continuum (Fig. 17, stage 2). As the surge progressed, the anticlines evolved, usually such that the most proximal ones became higher and narrower whilst new anticlines developed on the distal side. This resulted in a multi-crested ridge with a successively diminishing crest height in distal direction. This is evident from the eastern part of the 1890 end moraine (section 3 and GPR profiles 1–3), where the total shortening is 27–33% representing an intermediate stage in the end moraine continuum (Fig. 17, stage 3). Continued push by the glacier led to overturning of the most proximal anticlines while the more distal ones rose and narrowed, however, without overturning. When the stress applied by the glacier could no more be released through folding, the fold hinges and distal limbs became subject to shearing (Fig. 17, stages 4–5). As the ridge became too large for the glacier to push forward, it obstructed the forward motion of the ice and exerted a counter-stress towards the ice front. This likely resulted in substantial compression and thrusting in the crevassed snout, as indicated by hummocky moraine resulting from sediment that was brought up into the ice along thrust planes. The large end moraine in front of the ice also prevented submarginal material from being transported forward. However, the stress applied by the ice forced the submarginal material to deform and dislocate in direction towards the least resistance, which was upwards. This resulted in imbricate thrust sheets appearing as asymmetric ridges on the proximal slope of the end moraine (Fig. 17, stage 5). The submarginal thrusting and imbricate thrust sheets are evident from sections 1 and 2 in the western part of the 1890 end moraine, which represents the most developed stage of the moraine formation with a total shortening of at least 39% (Fig. 17, stage 6). The stagnation and downwasting of the glacier snout after the surge left an ice-cored moraine on the surface of each thrust sheet, giving the proximal slope a hummocky appearance (Figs. 2A, 3A and 4).

The morphological and architectural characteristics and the horizontal shortening of the end moraine have strong analogies to surge end moraines on Svalbard (van der Wateren, 1995a; Hart and Roberts, 1997; Boulton et al., 1999) and Pleistocene moraines in The Netherlands (van der Wateren, 1995a; Bakker and van der Meer, 2003). These occur in modern and ancient permafrost areas, respectively, and developed with the décollement plane located at the permafrost base. Studies of active moraine formation at a non-surging glacier in Alaska have shown that large end moraines, partly similar to the Eyjabakkajökull moraines, may also develop in non-permafrost areas (Motyka and Echelmeyer, 2003; Kuriger et al., 2006). The question therefore arises whether permafrost affected the formation of the Eyjabakkajökull moraines to some extent. Since they were formed around the time of the Little Ice Age maximum, it is possible that relatively thin, discontinuous permafrost affected the end moraine formation, perhaps by transmitting the applied stress for a few hundreds of metres away from the ice margin and through a thickness of several metres, thereby extending the zone of glaciotectonic deformation. We doubt, however, that the décollement at 26.7 m depth in the western part coincides with the base of the frozen sediment mass as this would probably require continuous and thicker permafrost. The décollement at 4–5 m depth in the eastern part most likely coincides with the LPT/gravel interface, although it cannot be excluded that the décollement developed at the base of the frozen sediment.

7. Summary and conclusions

This study on the 1890 surge end moraines of Eyjabakkajökull demonstrates that a single sequential model should not be applied because of significant lateral variations in morphology, sedimentology and internal architecture. Instead, three models are required to explain the genesis of four morphological types of end moraines, each of which reflects a specific type or intensity of deformation:

- During the surge, subglacial porewater pressures were high favouring the forward motion of the glacier through deformation of the bed. As a result of decreased submarginal porewater pressure and increased effective pressure at the end of the surge, the glacier coupled to the foreland to initiate the end moraine formation when it had surged to within 70–190 m of its terminal position. This corresponds to 2–6 days before surge termination, thus indicating the time frame for the end moraine formation.
- A relatively small moraine ridge on the Eyjafell bedrock knob formed in response to decoupling of a thin sediment cover from the bedrock, resulting in subglacial deformation and downglacier sediment transport. This led to the formation of a small marginal wedge or ramp with the end moraine on the distal end.
- A wide moraine ridge of multiple narrow and asymmetric crests in the central part of the forefield comprises of a number of imbricate thrust sheets with internal folds. Numerous blow-out structures dissecting the foreslope are evident of rapid release of overpressurized water at the end of the surge. This is in agreement with the classic model of Croot (1987, 1988a) which is, however, only applicable for the central part of the end moraine complex.
- The eastern and western parts of the end moraine signify the intermediate and extreme stages in an end moraine continuum, respectively. The eastern part has a net horizontal compressive strain of 27–33%, visible in the form of open anticline–syncline pairs that are rooted at 4–5 m depth. The net horizontal compressive strain in the western part is 39%, and appears as thrusts in the proximal zone and overturned and overthrusted anticlines in the central and distal zones of the ridge. Here, the décollement plane is located at ~27 m depth, which probably coincides with the bedrock surface. We propose that the opposite end member of the continuum would be a moraine of multiple symmetric, open anticlinal ridges of low amplitude.
- Soft fine-grained sediment facies (LPT) with high porewater pressure are the controlling facies in the deformation, which is principally ductile. Rigid gravel that usually overlies the fine-grained facies simply follows the structure of the underlying facies, but may have been important in favouring thrusting when folding could not accommodate for the stress release anymore.
- Modelling of the moraines could help with identifying and isolating the different parameters affecting the end moraine formation and thus increase our understanding of the

Please cite this article in press as: Benediktsson, Í.Ö., et al., The 1890 surge end moraine at Eyjabakkajökull, Iceland: a re-assessment of a classic..., Quaternary Science Reviews (2009), doi:10.1016/j.quascirev.2009.10.004

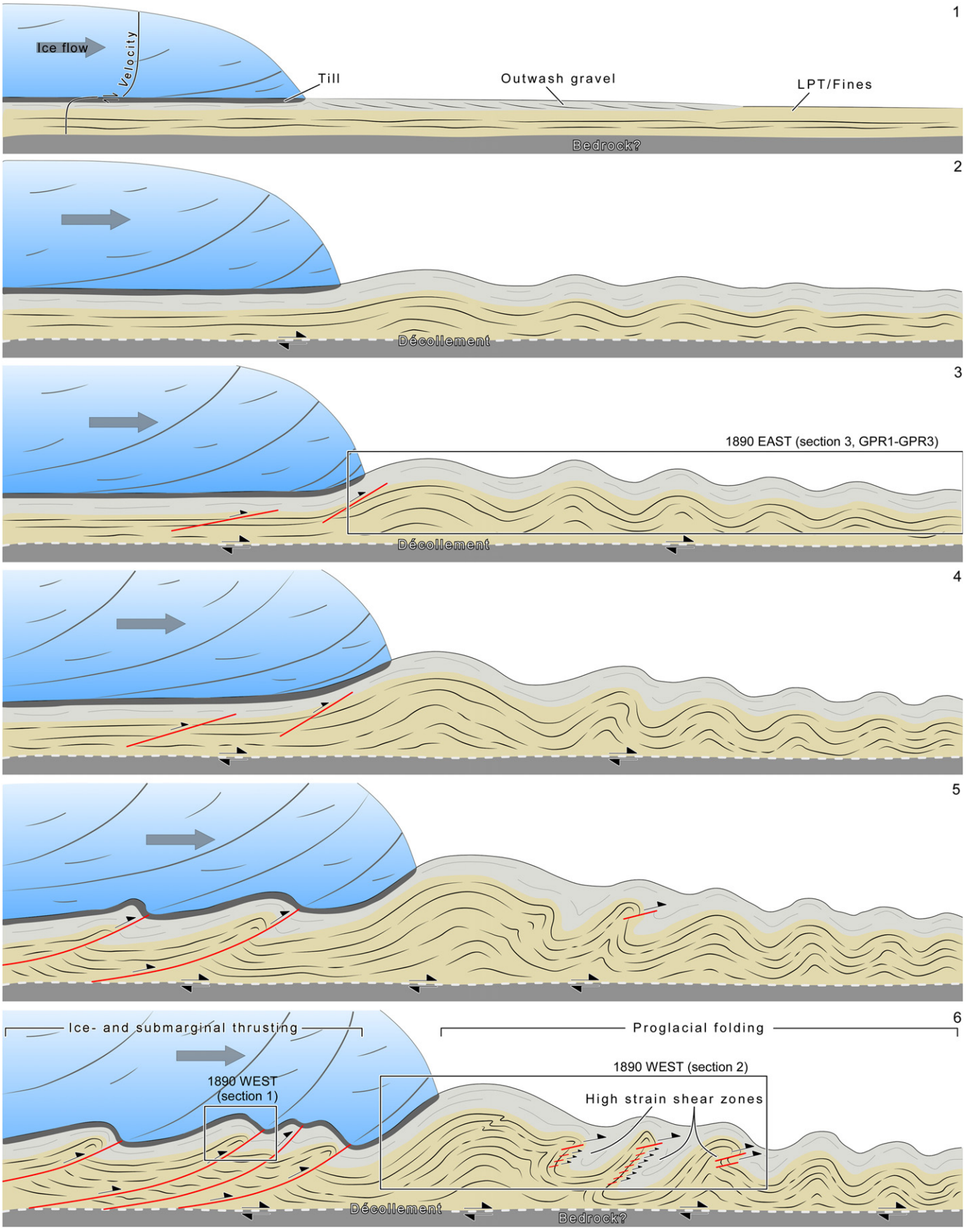

Please cite this article in press as: Benediktsson, Í.Ö., et al., The 1890 surge end moraine at Eyjabakkajökull, Iceland: a re-assessment of a classic..., Quaternary Science Reviews (2009), doi:10.1016/j.quascirev.2009.10.004

formation and evolution of glaciotectonic end moraines and their relation to glacier dynamics.

Acknowledgements

The Eyjabakkajökull Project was funded by the University of Iceland Research Fund, Energy Research Fund of Landsvirkjun, Verkefna- og rannsóknarsjóður Fljótsdalshrepps (grants to ÍÖB and ÓI). Additional funding was provided to AS by the Royal Swedish Academy of Sciences and Christian og Ottilia Brorsons Rejselegat for yngre videnskabsmænd og -kvinder. ÍÖB acknowledges support from the Icelandic Research Fund for Graduate Students, the University of Iceland Research Fund and Landsvirkjun. Thanks are due to Mark Johnson, Jaap van der Meer, Torbjörn Andersson, Amanda Ferguson, Eygló Ólafsdóttir, Skafti Brynjólfsson, Susi Ebmeier, Antje Herbrich and Jón Björn Ólafsson for invaluable assistance, discussions and company during the 2006–2008 Eyjabakkajökull field campaigns. Rúnar Ingi Hjartarson and Björn Oddson are thanked for logistical assistance. Jaap van der Meer is specially thanked for fruitful discussions about the 1890 end moraine in the field and for constructive comments on an earlier version of this paper. Thanks are furthermore due to Kurt H. Kjær for providing the ground penetrating radar and for discussions and comments that improved the paper. Constructive comments by Roman Motyka and one anonymous reviewer are gratefully acknowledged.

References

Aber, J.S., Ber, A., 2007. Glaciotectonism. Elsevier, Amsterdam. Developments in Quaternary Science 6, 1-246.

Aber, J., Croot, D.G., Fenton, M.M., 1989. Glaciotectonic Landforms and Structures. Kluwer, Dordrecht.

Alley, R.B., Blankenship, D.D., Rooney, S.T., Bentley, C.R., 1989. Water-pressure coupling of sliding and bed deformation: III. Application to ice stream B, Antarctica. Journal of Glaciology 35, 130–139.

Bakker, M.A.J., van der Meer, J.J.M., 2003. Structure of a Pleistocene push moraine revealed by GPR: the eastern Veluwe Ridge, The Netherlands. In: Bristow, C.S., Jol, H.M. (Eds.), Ground Penetrating Radar in Sediments, vol. 211. Geological Society, London, pp. 143–152. Special Publications.

Benediktsson, Í.Ö., Möller, P., Ingólfsson, Ó., van der Meer, J.J.M., Kjær, K.H., Krüger, J., 2008. Instantaneous end moraine and sediment wedge formation during the 1890 surge of Brúarjökull. Iceland. Quaternary Science Reviews 27, 209–234.

Benediktsson, Í.Ö., Ingólfsson, Ó., Schomacker, A., Kjær, K.H., 2009. Formation of submarginal and proglacial end moraines: implications of ice-flow mechanism during the 1963–64 surge of Brúarjökull. Iceland. Boreas 38, 440–457. doi:10.1111/j.1502-3885.2008.00077.x.

Benn, D.I., 1994. Fluted moraine formation and till genesis below a temperate valley glacier: Slettmarkbreen, Jotunheimen, southern Norway. Sedimentology 41, 279–292.

Benn, D.I., Evans, D.J.A., 1996. The interpretation and classification of subglacially-deformed materials. Quaternary Science Reviews 15, 23–52.

Benn, D.I., Evans, D.J.A., 1998. Glaciers and Glaciation. Arnold, London, 734 p.

Bennett, M.R., 2001. The morphology, structural evolution and significance of push moraines. Earth-Science Reviews 53, 197–236.

Bennett, M.R., Hambrey, M.J., Huddart, D., Glasser, N.F., Crawford, K., 1999. The landform and sediment assemblage produced by a tidewater glacier surge in Kongsfjorden, Svalbard. Quaternary Science Reviews 18, 1213–1246.

Bennett, M.R., Huddart, D., Waller, R.I., Midgley, N.G., Gonzalez, S., Tomio, A., 2004a. Styles of ice-marginal deformation at Hagafellsjökull-Eystri, Iceland, during the 1998/99 winter-spring surge. Boreas 33, 97–107.

Bennett, M.R., Huddart, D., Waller, R.I., Cassidy, N., Tomio, A., Zukowskyj, P., Midgley, N.G., Cook, S.J., Gonzalez, S., Glasser, N.F., 2004b. Sedimentary and tectonic architecture of a large push moraine: a case study from Hagafellsjökull-Eystri, Iceland. Sedimentary Geology 172, 269–292.

Bergthórsson, P., 1969. An estimate of drift ice and temperature in Iceland in 1000 years. Jökull 19, 94–101.

Björnsson, H., 1982. Drainage basins on Vatnajökull mapped by radio echo soundings. Nordic Hydrology 1982, 213–232.

Björnsson, H., 1998. Hydrological characteristics of the drainage system beneath a surging glacier. Nature 395, 771–774.

Björnsson, H., Pálsson, F., Sigurðsson, O., 2003. Surges of glaciers in Iceland. Annals of Glaciology 36, 82–90.

Boulton, G.S., 1970. On the deposition of subglacial and melt-out tills at the margins of certain Svalbard glaciers. Journal of Glaciology 9, 231–245.

Boulton, G.S., 1972. Modern Arctic glaciers as depositional models for former ice sheets. Journal of the Geological Society of London 128, 361–393.

Boulton, G.S., Hindmarsh, C.A., 1987. Sediment deformation beneath glaciers: rheology and geological consequences. Journal of Geophysical Research 92, 9059–9082.

Boulton, G.S., van der Meer, J.J.M., Beets, D.J., Hart, J., Ruegg, G.H.J., 1999. The sedimentary and structural evolution of a recent push moraine complex: Holmstrømbreen, Spitsbergen. Quaternary Science Reviews 18, 339–371.

Brady, N.C., Weil, R.R., 1999. The Nature and Properties of Soils. Twelfth ed. Prentice Hall, New Jersey, 881 p.

Burke, M.J., Woodward, J., Russell, A.J., Fleisher, P.J., Bailey, P.K., 2008. Controls on the sedimentary architecture of a single event englacial esker: Skeiðarárjökull. Iceland. Quaternary Science Reviews 27, 1829–1847.

Cassidy, N.J., Russell, A.J., Marren, P.M., Fay, H., Knudsen, Ó., Rushmer, E.L., van Dijk, T.A.G.P., 2003. In: Bristow, C.S., Jol, H.M. (Eds.), Ground Penetrating Radar in Sediments. GPR derived architecture of November 1996 jökulhlaup deposits, Skeiðarársandur, Iceland, vol. 211. Geological Society, London, pp. 153–166. Special Publications.

Christiansen, E.A., Gendzwill, D.J., Meneley, W.A., 1982. Howe Lake: a hydrodynamic blowout structure. Canadian Journal of Earth Sciences 19, 1122–1139.

Christoffersen, P., Piotrowski, J.A., Larsen, N.K., 2005. Basal processes beneath an Arctic glacier and their geomorphic imprint after a surge, Elisebreen, Svalbard. Quaternary Research 64, 125–137.

Croot, D.G., 1987. Glacio-tectonic structures: a mesoscale model of thin-skinned thrust sheets? Journal of Structural Geology 9, 797–808.

Croot, D.G., 1988a. Morphological, structural and mechanical analysis of neoglacial ice-pushed ridges in Iceland. In: Croot, D.G. (Ed.), Glaciotectonics: Forms and Processes. Balkema, Rotterdam, pp. 33–47.

Croot, D.G., 1988b. Glaciotectonics: Forms and Processes. Balkema, Rotterdam, 212 p.

Dahlström, C.D.A., 1969. Balanced cross sections. Canadian Journal of Earth Sciences 6, 743–757.

Engelhardt, H., Kamb, B., 1998. Basal sliding of ice stream B, West Antarctica. Journal of Glaciology 44, 223–230.

Evans, D.J.A., Benn, D.I., 2004. A Practical Guide to the Study of Glacial Sediments. Arnold, London, 266 p.

Evans, D.J.A., Rea, B.R., 1999. Geomorphology and sedimentology of surging glaciers: a landsystem approach. Annals of Glaciology 28, 75–82.

Evans, D.J.A., Rea, B.R., 2003. Surging glacier landsystem. In: Evans, D.J.A. (Ed.), Glacial Landsystems. Arnold, London, pp. 259–288.

Evans, D.J.A., Lemmen, D.S., Rea, B.R., 1999. Glacial landsystems of the southwest Laurentide Ice Sheet: modern Icelandic analogues. Journal of Quaternary Science 14, 673–691.

Evans, D.J.A., Phillips, E.R., Hiemstra, J.F., Auton, C.A., 2006. Subglacial till: Formation, sedimentary characteristics and classification. Earth-Science Reviews 78, 115–176.

Flowers, G.E., Björnsson, H., Geirsdóttir, Á., Miller, G.H., Black, J.L., Clarke, G.K.C., 2008. Holocene climate conditions and glacier variation in central Iceland from physical modelling and empirical evidence. Quaternary Science Reviews 27, 797–813.

Friedman, J.D., Johanson, C.E., Óskarsson, N., Svanson, H., Thorarinsson, S., Williams Jr., S.R., 1971. Observations on Icelandic polygon surfaces and palsa areas. Photo interpretations and field studies. Geografiska Annaler 53A, 115–145.

Fuller, S., Murrey, T., 2000. Evidence against pervasive bed deformation during the surge of an Icelandic glacier. In: Maltman, A.J., Hubbard, B., Hambrey, M.J. (Eds.), Deformation of Glacial Materials, vol. 176. Geological Society of London Special Publication, London, pp. 203–216.

Guðmundsson, H., 1997. A review of the Holocene environmental history of Iceland. Quaternary Science Reviews 16, 81–92.

Hart, J.K., 1998. The deforming bed/debris-rich basal ice continuum and its implications for the formation of glacial landforms (flutes) and sediments (melt-out till). Quaternary Science Reviews 17, 737–754.

Hart, J.K., Roberts, W.J., 1997. A comparison of the styles of deformation associated with two recent push moraines, south Van Keulenfjorden, Svalbard. Earth Surface Processes and Landforms 22, 1089–1107.

Humphrey, N.F., Raymond, C.F., 1994. Hydrology, erosion and sediment production in a surging glacier: Variegated Glacier, Alaska, 1982–83. Journal of Glaciology 40, 539–552.

Jol, H.M., Bristow, C.S., 2003. GPR in sediments: advice on data collection, basic processing and interpretation, a good practice guide. In: Bristow, C.S., Jol, H.M. (Eds.), Ground Penetrating Radar in Sediments, vol. 211. Geological Society, London, pp. 9–27. Special Publications.

Kaldal, I., Víkingsson, S., 2000. Jarðgrunnskort af Eyjabökkum. Orkustofnun, OS-2000/068, 10 p.

Fig. 17. Model 3. A sequential model illustrating the formation of a continuum of large end moraine ridges with multiple, widely spaced symmetric crests. The third stage of the model represents the eastern part of the 1890 end moraine with intermediate strain whilst the last stage indicates extreme deformation with intense folding and shearing as observed in the western part.

Please cite this article in press as: Benediktsson, Í.Ö., et al., The 1890 surge end moraine at Eyjabakkajökull, Iceland: a re-assessment of a classic..., Quaternary Science Reviews (2009), doi:10.1016/j.quascirev.2009.10.004

Kälin, M., 1971. The active push moraine of the Thompson Glacier, Axel Heiberg Island, Canadian Arctic Archipelago. Axel Heiberg Island Research Reports, Glaciology No. 4, McGill University, Montreal. PhD thesis, ETH Zurich.
Kamb, B., Raymond, C.F., Harrison, W.D., Engelhardt, H., Echelmeyer, K.A., Humphrey, N., Brugman, M.M., Pfeffer, T., 1985. Glacier surge mechanism: 1982–1983 surge of Variegated glacier, Alaska. Science 227 (4686), 469–479.
Kjær, K.H., Sultan, L., Krüger, J., Schomacker, A., 2004. Architecture and sedimentation of fan-shaped outwash in front of the Mýrdalsjökull ice cap. Iceland. Sedimentary Geology 172, 139–163.
Kjær, K.H., Larsen, E., van der Meer, J.J.M., IngólfssonÓ., Benediktsson, Í.Ö., Knudsen, C.G., Schomacker, A., 2006. Subglacial decoupling at the sediment/bedrock interface: a new mechanism for rapid flowing ice. Quaternary Science Reviews 25, 2704–2712.
Kjær, K.H., Korsgaard, N.J., Schomacker, A., 2008. Impact of multiple glacier surges – a geomorphological map from Brúarjökull, East Iceland. Journal of Maps 2008, 5–20.
Krüger, J., Kjær, K.H., 1999. A data chart for field description and genetic interpretation of glacial diamicts and associated sediments – with examples from Greenland, Iceland, and Denmark. Boreas 28, 386–402.
Kuriger, E.M., Truffer, M., Motyka, R.J., Bucki, A.K., 2006. Episodic reactivation of large-scale push moraines in front of the advancing Taku Glacier, Alaska. Journal of Geophysical Research 111, F01009. doi:10.1029/2005JF000385.
Maizels, J., 1993. Lithofacies variations within sandur deposits: the role of runoff regime, flow dynamics and sediment supply characteristics. Sedimentary Geology 85, 299–325.
Marren, P.M., 2005. Magnitude and frequency in proglacial rivers: a geomorphological and sedimentological perspective. Earth-Science Reviews 70, 203–251.
Marshak, S., Mitra, G., 1988. Basic Methods of Structural Geology. Prentice Hall, New Jersey, 446 p.
McCarrol, D., Rijsdijk, K.F., 2003. Deformation styles as a key for interpreting glacial depositional environments. Journal of Quaternary Science 9, 209–233.
Motyka, R.J., Echelmeyer, K.Á., 2003. Taku Glacier (Alaska, U.S.A.) on the move again: active deformation of proglacial sediments. Journal of Glaciology 49, 50–58.
Motyka, R.J., Truffer, M., Kuriger, E.M., Bucki, A.K., 2006. Rapid erosion of soft sediment by tidewater glacier advance: Taku Glacier, Alaska. USA. Geophysical Research Letters 33, L24504. doi:10.1029/2006GL028467.
Nelson, A.E., Willis, I.C., Cofaigh, C.Ó., 2005. Till genesis and glacier motion inferred from sedimentological evidence associated with the surge-type glacier, Brúarjökull. Iceland. Annals of Glaciology 42, 14–22.
Paul, M.A., Eyles, N., 1990. Constraints on the preservation of diamict facies (melt-out tills) at the margins of stagnant glaciers. Quaternary Science Reviews 9, 51–69.
Pedersen, S.A.S., 1996. Progressive glaciotectonic deformation in Weichselian and Palaeogene deposits at Feggeklit, northern Denmark. Bulletin of the Geological Society of Denmark 42, 153–174.
Pedersen, S.A.S., 2005. Structural analysis of the Rubjerg Knude Glaciotectonic Complex, Vendsyssel, northern Denmark. Geological Survey of Denmark and Greenland Bulletin 8, 1–192.
Phillips, E., Lee, J.R., Burke, H., 2008. Progressive proglacial to subglacial deformation and syntectonic sedimentation at the margins of Mid-Pleistocene British Ice Sheet: evidence from north Norfolk. UK. Quaternary Science Reviews 27, 1848–1871.
Raymond, C.F., 1987. How do glaciers surge? A review. Journal of Geophysical Research 92 (B9), 9121–9134.
Raymond, C.F., Johannesson, T., Pfeffer, T., 1987. Propagation of a glacier surge into stagnant ice. Journal of Geophysical Research 92 (B9), 9037–9049.
Roberts, D.H., Yde, J.C., Knudsen, N.T., Long, A.J., Lloyd, J.M., 2009. Ice marginal dynamics during surge activity, Kuannersuit Glacier, Disko Island, West Greenland. Quaternary Science Reviews 28, 209–222.
Schomacker, A., Kjær, K.H., 2007. Origin and de-icing of multiple generations of ice-cored moraines at Brúarjökull. Iceland. Boreas 36, 411–425.
Sharp, M., 1985a. Sedimentation and stratigraphy at Eyjabakkajökull – an Icelandic surging glacier. Quaternary Research 24, 268–284.
Sharp, M., 1985b. "Creveasse-fill" ridges – a landform type characteristic of surging glaciers? Geografiska Annaler 67A, 213–220.
Sharp, M., Dugmore, A., 1985. Holocene glacier fluctuations in Eastern Iceland. Zeitschrift für Gletcherkunde und Glazialgeologie 21, 341–349.
Thorarinsson, S., 1938. Über anomale Gletcherswankungen mit besonderer Berücksichtigung des Vatnajökullgebietes. Geologiska föreningen i Stockholms förhandlingar 60 (3), 490–506. Maj-oktober.
Thorarinsson, S., 1943. Oscillations of the Icelandic glaciers in the last 250 years. Geografiska Annaler 25, 1–54.
Thoroddsen, Th, 1914. Ferdabók. Skýrslur um rannsóknir á Íslandi 1882–1898. Þriðja bindi. Kaupmannahöfn. Hið íslenzka fræðafélag 1914, 1–360.
Todtmann, E.M., 1953. Am Rand des Eyjabakkagletchers, Sommer 1953. Jökull 3, 34–36.
Todtmann, E.M., 1955. Übersicht über die Eisrandlagen in Kringilsárrani von 1890–1955. Jökull 5, 8–10.
Todtmann, E.M., 1960. Gletcherforschungen auf Island (Vatnajökull). Universität Hamburg. Abhandlungen aus dem Gebiet des Auslandskunde 65C, 1–95.
Twiss, R.J., Moores, E.M., 1992. Structural Geology. W.H. Freeman and Company, New York, 532 p.
van der Meer, J.J.M., Menzies, J., Rose, J., 2003. Subglacial till: the deforming glacier bed. Quaternary Science Reviews 22, 1659–1685.
van der Meer, J.J.M., Kjær, K.H., Krüger, J., Rabassa, J., Kilfeather, A.A., 2009. Under pressure: clastic dykes in glacial settings. Quaternary Science Reviews 28, 708–720.
van der Wateren, D.F.M., 1995a. Structural geology and sedimentology of push moraines: processes of soft sediment deformation in a glacial environment and the distribution of glaciotectonic styles. Mededelingen Rijks Geologische Dienst 54, 1–168.
van der Wateren, D.F.M., 1995b. Processes of glaciotectonism. In: Menzies, J. (Ed.), Modern Glacial Environments: Processes, Dynamics and Sediments. Glacial Environments, vol. 1. Butterworth-Heineman, London, pp. 309–335.
Williams Jr., R.S., 1976. Vatnajökull ice cap, Iceland. USGS Prof. Paper 929, 188–193.

Please cite this article in press as: Benediktsson, Í.Ö., et al., The 1890 surge end moraine at Eyjabakkajökull, Iceland: a re-assessment of a classic..., Quaternary Science Reviews (2009), doi:10.1016/j.quascirev.2009.10.004